uOttawa

L'Université canadienne
Canada's university

FACULTÉ DES ÉTUDES SUPÉRIEURES ET POSTOCTORALES

uOttawa

L'Université canadienne
Canada's university

FACULTY OF GRADUATE AND POSDOCTORAL STUDIES

Ami Jun-Yee Chin

AUTEUR DE LA THÈSE / AUTHOR OF THESIS

M.Sc. (Chemistry)

GRADE / DEGREE

Department of Chemistry

FACULTÉ, ÉCOLE, DÉPARTEMENT / FACULTY, SCHOOL, DEPARTMENT

Part A: Development of a Fluorescence Resonance Energy Transfer Assay for High Throughput Screening for Catalysts in the Desymmetrization of Meso Substrates
Part B: Application of Hydrazide Based Catalyst in Friedel-Crafts Alkylation

TITRE DE LA THÈSE / TITLE OF THESIS

W. Ogilvie

DIRECTEUR (DIRECTRICE) DE LA THÈSE / THESIS SUPERVISOR

CO-DIRECTEUR (CO-DIRECTRICE) DE LA THÈSE / THESIS CO-SUPERVISOR

EXAMINATEURS (EXAMINATRICES) DE LA THÈSE / THESIS EXAMINERS

T. Durst

K. Fagnou

Gary W. Slater

LE DOYEN DE LA FACULTÉ DES ÉTUDES SUPÉRIEURES ET POSTDOCTORALES /
DEAN OF THE FACULTY OF GRADUATE AND POSTDOCORAL STUDIES

PART A
DEVELOPMENT OF A FLUORESCENCE RESONANCE ENERGY TRANSFER ASSAY FOR HIGH THROUGHPUT SCREENING FOR CATALYSTS IN THE DESYMMETRIZATION OF MESO SUBSTRATES

PART B
APPLICATION OF HYDRAZIDE BASED CATALYST IN FRIEDEL-CRAFTS ALKYLATION

By

Ami Jun-Yee Chin

B.Sc. University of Ottawa, 2002

A Thesis Submitted to the School of Graduate Studies and Research
In Partial Fulfillment of the Requirements for the Degree of
Master of Science

Ottawa-Carleton Chemistry Institute
Department of Chemistry
University of Ottawa
Ottawa, Ontario
Canada

Candidate **Supervisor**

Ami Jun-Yee Chin **Dr. William W. Ogilvie**

Your file Votre référence
ISBN: 0-494-14891-8
Our file Notre référence
ISBN: 0-494-14891-8

TABLE OF CONTENTS

LIST OF FIGURES

LIST OF SCHEMES

LIST OF TABLES

ACKNOWLEDGMENTS

I saved the best page to write last, it's also the most important page as I am ever so grateful to many, many people.

Bill, your guidance and your patience have been much appreciated. Thank you for always being so generous with your time and knowledge. I truly value what I have learned over the past two years, lessons in chemistry and life alike.

Dr. Durst, sir, you have always been so kind; I will definitely miss your stories most. I promise to drop by your office some time to hear more!

I must also give thanks to all my colleagues who have made my experience here memorable. Livia, for the words of encouragement that we have shared between us, yes, even Sharpless had bad days! Alison, who could ask for a better bench buddy? You're such a great teacher; I'm glad that you were close by! Mathieu, for always making me laugh with your imitations of others (even when they were of me!). Josée, ma prof de français, my project would have indeed seen more obstacles had it not been for the work you that you have accomplished. Other past and present students also deserve a big hug for their kindness and friendship; Matt, Liz, Natalie, Kelly, Pat, Joe #1and #2 you guys have been great! I must also give a special thanks to Melissa for her help with the HLPC!

Last but not least, I want to thank all my family and friends for their unconditional love and support since the very beginning. I am grateful to my parents and my godparents for always being there for me. I especially want to thank Connie, who has not only fulfilled the role of a big sister but also that of an alarm clock, chauffer, compass, financial advisor, therapist and god knows what else!!!

Much love to all of you – ton Ami

For my Parents Jack and Nancy,
my Godparents Albert and Theresa,
my Sister Connie,
and last but not least,
for Me...

" I beg of you ... to have patience with everything unresolved in your heart and try to love the questions themselves as if they were locked rooms or books written in a foreign language. Don't search for the answers, which could not be given to you now, because you would not be able to live them. And the point is, to live everything. Live the questions now. Perhaps then, someday far in the future, you will gradually, without ever noticing it, live your way into the answer..."

- Ranier Maria Rilke

LIST OF ABBREVIATIONS

AUC	area under the curve
Bn	benzyl
br	broad
cm	centimeter
d	doublet
dd	doublet of doublet
DMF	*N,N*-dimethylformamide
DNS	Dansyl
DIPEA	*N,N*-diisopropylethylamine
EDC	1-(3-dimethylaminopropyl)-3-ethylcarbodiimide hydrochloride
ee	Enantiomeric excess
EI	electron impact
eqv	equivalent
ESI	electrospray ionization
Et	ethyl
EtOAc	ethyl acetate
HBTU	*O*- Benzotriazol-1-yl-*N,N,N',N*,'-tetramethyluronium hexafluoro-phosphate
HOBT	1-hydroxybenzotriazole
HPLC	High performance liquid chromatography
Hz	hertz
λ	wavelength
*i*Pr	isopropyl
IR	infrared spectrometry
m	multiplet
M	molar
Me	methyl
MeOH	methanol
MHz	megaherzt

mmol	millimoles
M.P.	Melting point
MS	mass spectrometry
nm	nanometer
NMR	nuclear magnetic resonance
Ph	phenyl
ppm	parts per million
PYR	Pyrene
q	quartet
s	singlet
soln	solution
t	triplet
TFA	trifluoroacetic acid
THF	tetrahydrofuran
TLC	thin layer chromatography

PART A

ABSTRACT

Highthroughput methods have been increasingly applied to catalyst screening, however, efforts to use these for enantioselective measures are still lacking. We propose to apply Fluorescence Resonance Energy Transfer (FRET) as a highthroughput screening method to fulfill such a purpose. This concept is applied to the desymmetrization of *meso* substrates. The *meso* compound will be equipped with a recognition element for catalyst binding, two different fluorescence donor molecules to distinguish between the chiral centres and also a fluorescence acceptor molecule to suppress fluorescence. Upon catalytic hydrolysis, the fluorescence acceptor molecules will be discharged into solution and thus can be detected by use of a spectrophotometer. As each donor molecule has a characteristic fluorescence emission wavelength, measuring the respective fluorescence intensities will ultimately allow for one to rapidly determine the enantiomeric excess. Efforts towards establishing this FRET based assay are discussed herein.

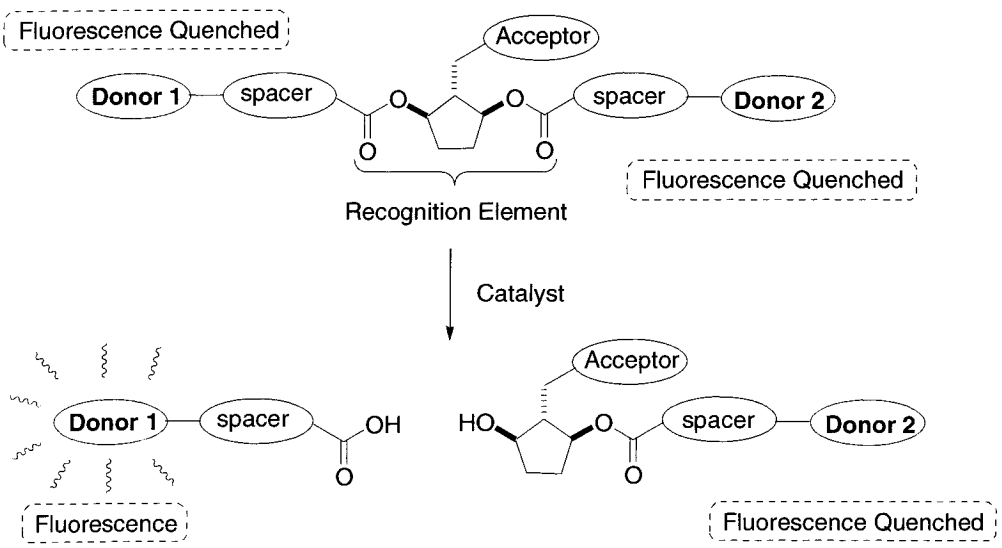

CHAPTER 1
HIGH THROUGHPUT METHODS

1.1 Combinatorial Chemistry

1.1.1 History

The Nobel Prize for Chemistry in 1984 was awarded to Robert B. Merrifield for his pioneering work on solid-phase peptide synthesis[1]. In this work, polystyrene was used as a solid support to anchor a growing polypeptide chain. A protected amino acid was first attached by its C-terminus to the polystyrene support, followed by deprotection of the corresponding amino group. A second amino acid, once again protected at the N-terminus, was then coupled to the first amino acid forming a dipeptide. Sequential deprotection and coupling of amino acids, as shown in Figure 1, resulted in the synthesis of a polypeptide chain. Since the growing peptide product was anchored to a polymeric support, separating the product from the reagents of each step was done so with ease by simply filtering. This cycle of synthesis was terminated by simple cleavage of the first amino acid from the solid support to eject a polypeptide.

Merrifeld's work in solid phase synthesis laid the foundation for other scientists to build upon. His method saw further developments in the 1980's by Houghten[2] who envisioned that several different peptides could be synthesized within the same reaction vessel. This in fact, was the birth of combinatorial chemistry.

Combinatorial chemistry seeks to synthesize the maximum number of compounds in a minimal amount of time. This unorthodox scientific method was initially met with much skeptism by critics.

---

[1] Merrifield R.B., *J. Am. Chem. Soc.* **1963**, *85*, 2149.

[2] Houghten R.A., *Proc. Natl Sci. USA* **1985**, *82*, 5131.

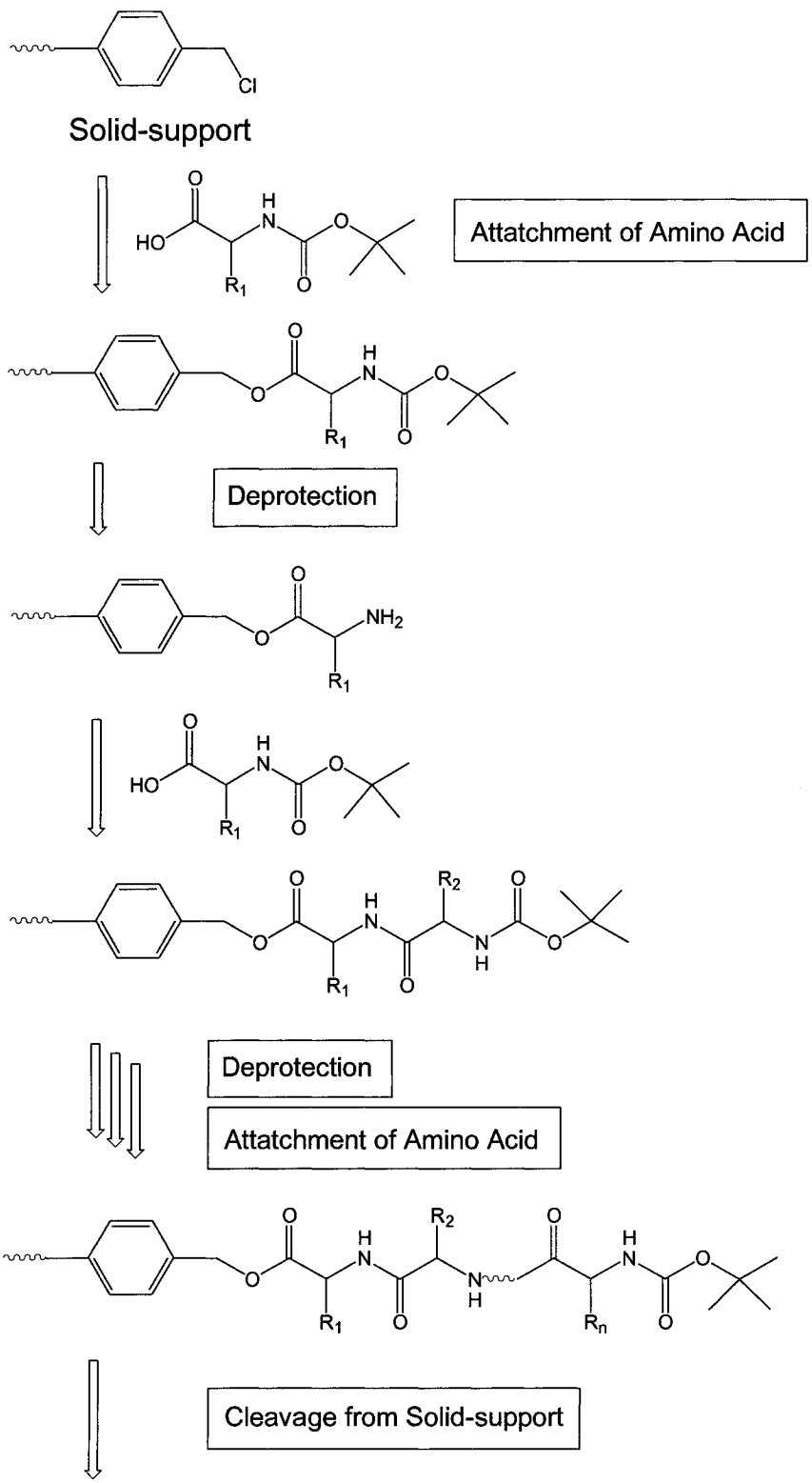

Figure 1. Merrifield's Automated Synthesis of Polypetides on Solid-support.

Many chemists still embraced a more conventional means of chemical synthesis: one reaction to give a single product. Indeed, generating a fully characterized product in high purity is a source of pride for the skilled chemist, but the time lost in doing so is a costly factor. Despite the initial reluctance by the chemical community to put combinatorial chemistry to practice, the method has created many advances in the pharmaceutical industry.

1.1.2 Combinatorial Chemistry in Drug Discovery

Traditional drug discovery rests on the isolation and identification of active pharmaceutical agents from natural products, a process that is demanding both in time and manpower. Advances in computational chemistry coupled with methods of determining the 3-dimensional structure and chemical nature of biological targets, allow for rational drug design. An element of serendipity also plays a role in drug discovery. The accidental finding of penicillin and the uncovering of new activity in an old drug are just two of the many examples of chance discovery.

It takes several years from the time a drug target is conceived in the boardroom to when potential leads are discovered and further developed to drug candidates that can be admitted into clinical trials. Much labour is invested to individually synthesize compounds, submit them to biological assays to test for activity and to identify promising leads for yet further investigation. Drug discovery requires a significant investment in manpower, time and money.

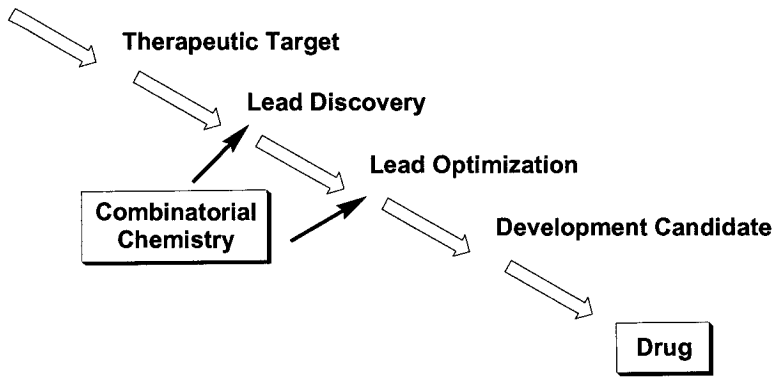

Figure 2. The Area of Impact of Combinatorial Chemistry on Drug Discovery Process.

As mentioned previously, combinational chemistry provides a rapid route to a large number of chemical variants. The idea of integrating this method of synthesis to the drug discovery process is thus an attractive one. The process of performing a reaction, working it up and purifying it to yield a single product is simply too time consuming for industry. Combinatorial chemistry would allow one to generate a large library of compounds at once, which could then be screened for activity. Once a drug lead is identified, combinatorial methods can again be applied to its optimization. This will facilitate structure activity relationship (SAR) studies by generating a more diverse set of analogues. Incorporating combinatorial chemistry to the science of drug discovery attempts to reduce the amount of time it takes to identify a drug candidate and for the competitive pharmaceutical industry, time saved translates ultimately to gained revenue.

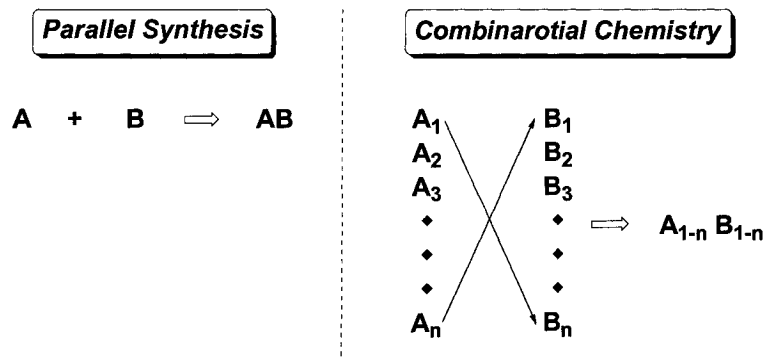

Figure 3. A Comparison Between Traditional Synthesis and Combinatorial Chemistry.

1.1.3 Principles of Combinatorial Chemistry.

Combinatorial chemistry allows one to create a large number of compounds in a short amount of time. The process is faster than traditional one-reaction-at-a-time chemistry as it does not require products to be fully purified and characterized at each stage of the synthesis.

There are two major strategies in the science of combinatorial chemistry: the "pool and spilt" method and the "parallel synthesis" method. The latter strategy is not "combinatorial" in the strictest sense, but as it also gives rise to a large library of compounds through automated synthesis, it will be considered here as a method in "combichem".

The pool and spit strategy was initially conceived by Furka[3] and applied to polypeptide synthesis. First, resin beads are divided equally into separate reaction vessels before coupling them to a different designated protected amino acid for each reaction vessel. The products obtained are then pooled to undergo collective washing and deprotection steps. The mixture of beads is then divided

---

[3] Furka, A.; Sebestyen, F.; Asgedom, M; Dibo, Abstr. 14th Int. Conr. Biochem. 5,1988, 47.

once again to a given number of reaction vessels, in which each is coupled with a different building block. The result, in this example with peptide synthesis, is a mixture of dimers, synthesized to give all possible combinations for the number of different monomers that were used. Following this idea, a total of "x^n" products can be synthesized by starting out with "*x*" number of monomers and repeating the coupling sequence "*n*" amount of times.

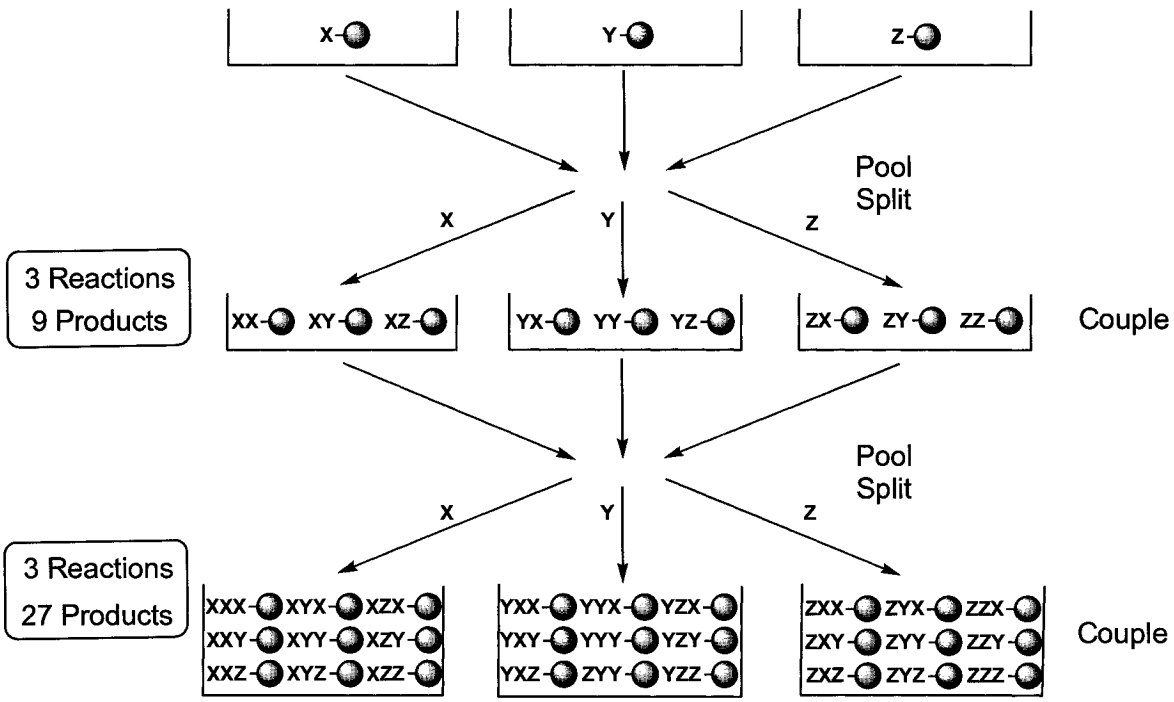

Figure 4. Mix and Split Method Using 3 Monomeric Building Blocks.

With parallel synthesis, compounds are prepared separately in a parallel automated fashion. As illustrated in Figure 5, a defined array of synthesis is employed such that the identity of a given compound can be easily deduced by its position in the array. Parallel synthesis, unlike the split and pool method, can be done on solid phase or in solution. However, for the same number of steps, parallel synthesis does not generate as many compounds as the split and pool method.

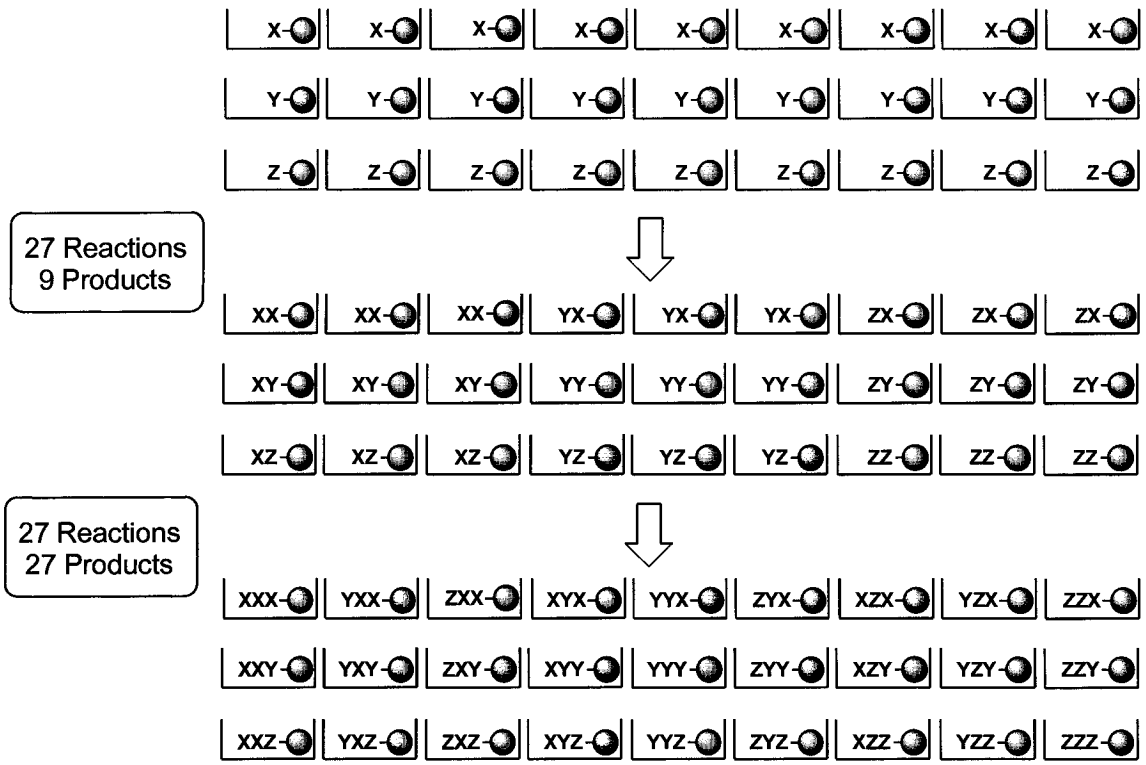

Figure 5. Parallel Synthesis Using 3 Monomeric Building Blocks.

1.2 Asymmetric Catalysis

1.2.1 The Importance of Asymmetric Reactions

As much as one third of currently prescribed pharmaceutical agents are chiral. It has long been known that enantiomers of a chiral drug can exhibit different biological activities. Given that the biological receptors themselves have a specific 3-dimensional arrangement in space, it makes sense that they will interact better, if not only, with one enantiomer of a drug. A classic example of this can be found with Thalidomide, a drug prescribed to pregnant women in the 1960's for morning sickness. Produced and sold as a racemate, tragedy befell the mothers taking Thalidomide as many gave birth to babies with birth defects. Further investigation suggested that the R isomer of the drug provided relief of

nausea symptoms while the S isomer was responsible for teratogenic defects. However, it was discovered that even when the R isomer is used in enantiopure form, the tetragenic effects persisted, as the drug was racemerized within the body.

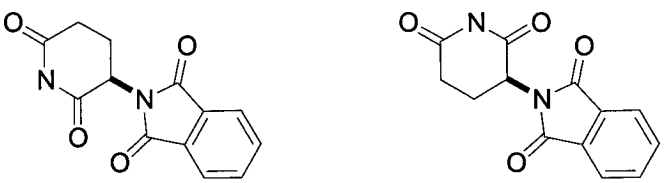

R - Thalidomide

⇩

Alleviates morning sickness

S - Thalidomide

⇩

Teratogen

Figure 6. Isomers of Thalidomide.

Learning a valuable and costly lesson from Thalidomide, current regulations require that drug candidates bearing chirality must have both enantiomers evaluated in detail.

Examining the top 10 selling drugs for the year 2003, we see that 9 of the drugs contain chiral active ingredients[4].

[4] Rouhi, M. *Chem. Eng. News.* **2004**, *82*, 47.

DRUG	Sales (Billions)	Active Ingredient	Form of Active Ingredient
Lipitor	10.3	Atrovastatin	Single Enantiomer
Zocor	6.1	Simvastatin	Single Enantiomer
Zyprexa	4.8	Olanzapine	Achiral
Norvasc	4.5	Amlodipine	Racemate
Procrit	4.0	Epoetina	Protein
Prevacid	4.0	Lansoprazole	Racemate
Nexium	3.8	Esmoeprazole	Single Enantiomer
Plavix	3.7	Clopidogrel	Single Enantiomer
Advair	3.7	Salmeteral	Racemate
		Fluticasone	Single Enantiomer
Zoloft	3.4	Sertraline	Single Enantiomer

Table 1. Top 10 Selling Drugs for 2003.

Further to this, the growth in the chiral drug market is reflected by the global drug sales for 1998 - 2000, where chiral drugs represent for over 100 billion dollars in revenue for the year 2000[5].

[5] Stinson, S.C. *Chem. Eng. News.* **2000**, *78*, 55.

Drug Type	1998	1999	2000
Cardiovascular	$21,906	$24,805	$26,012
Antibiotics / Antifungals	$19,756	$20,907	$26,265
Hormones / Endocrinology	$12,297	$13,760	$17,345
Cancer	$8,006	$9,420	$13,360
Central Nervous System	$7,027	$8,592	$13,720
Hematology	$6,730	$8,580	$11,445
Antiviral	$6,131	$7,540	$13,446
Respiratory	$4,305	$5,087	$8,795
Gastrointestinal	$1,718	$2,998	$5,335
Ophthalmic	$1,482	$1,794	$2,070
Dermatological	$1,124	$1,270	$1,540
Analgesics	$842	$1,045	$1,135
Vaccines	$568	$676	$1,100
Others	$7,947	$8,527	$7,425
TOTAL	$99,389	$115,001	$146,013

Table 2. Chiral Drug Sales in Millions.

The importance of producing enantiopure chiral compounds is clear and it necessitates the chemical industry to develop methods for asymmetric reactions.

1.2.3 Enantioselective Catalysis

Enantioselective catalysis is an ideal route to introduce chirality into a substrate. Surprisingly, most pharmaceutical companies still resort to conventional methods to resolve enantiomers. Finding the right catalyst for a given reaction can be a challenging task and incorporating combinatorial chemistry to catalyst discovery would be ideal. The hurdle in this area of chemistry is finding the appropriate high

throughput method to screen for enantioselectivity. Traditional enantioselectivity screening methods such as high performance liquid chromatography (HPLC) or gas chromatography (GC) are reliable but lengthy processes. Although methods have been developed to test for catalyst activity since the 1990's, it was not until 1997 that a method was designed for the enantioselective catalyst. A few examples of colourimetric screening methods for such applications will be discussed here.

1.2.4. UV /Vis Screening Technique

The first example of a high throughput screening method employing UV/vis techniques was demonstrated by Reetz[6] and coworkers in 1997. The project aimed to discover an enzyme that could selectivity hydrolyze a racemic mixture of 2-methyl decanoate. By selecting p-nitrophenol esters as test substrates ***(S)* - 1** and ***(R)* – 1** (Scheme 1), Reetz took advantage of the fact the p-nitrophenol moiety **3** that was discharged after hydrolysis, produced a yellow colour. The progress of reaction could then be monitored by measuring the absorbance of the reaction mixture over time. The *(S)* and *(R)* enantiomers were evaluated separately according to this screening technique and the absorbance values were compared to give a measure of the enantiomeric excess (ee).

Drawbacks plagued this initial effort towards high throughput screening for ee. Firstly, the method necessitated the incorporation of a chromophore, in this case p-nitrophenol. This modified the substrate for which the catalyst was originally intended and its effects on catalyst activity were unknown. Another shortcoming is that a racemic mixture could not be analyzed by this method, as any

---

[6] Reetz, M.T.; Zonta, A.;Schimossek, K.; Liebeton, K.; Jaeger, K.E. *Angew. Chem.* **1997**, *109*, 2961.

absorbance measurement would only be a reflection of the reaction rate and not of enantioselectivity.

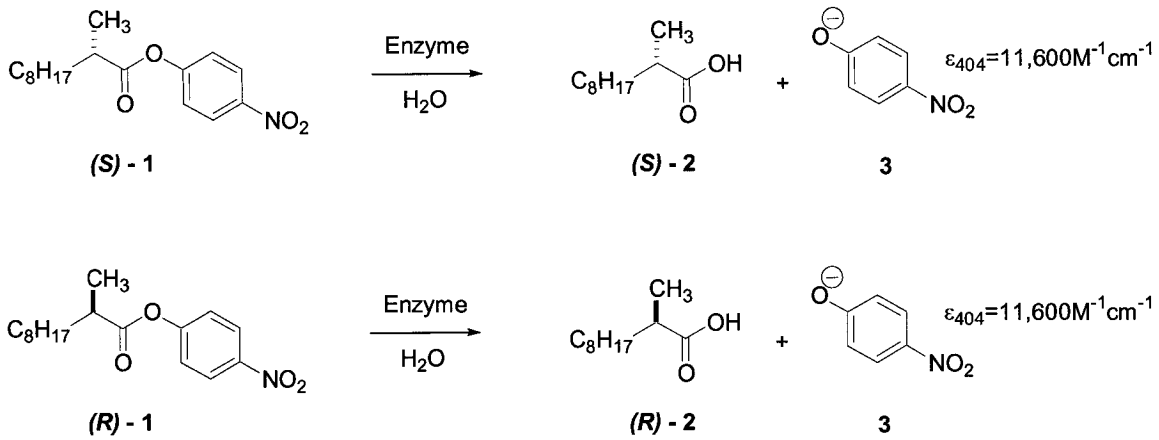

Scheme 1. Enantiomeric Excess Determined by Absorbance Measurement of Each Enantiomer Separately.

Since both enantiomers were subjected to the enzymatic hydrolysis in different reaction vessels, the ee values did not reflect the true selectivity in which competition for the enzyme between substrates came into play.
To addressed this latter problem, Janes and Kazluaskas developed the Quick E test[7].

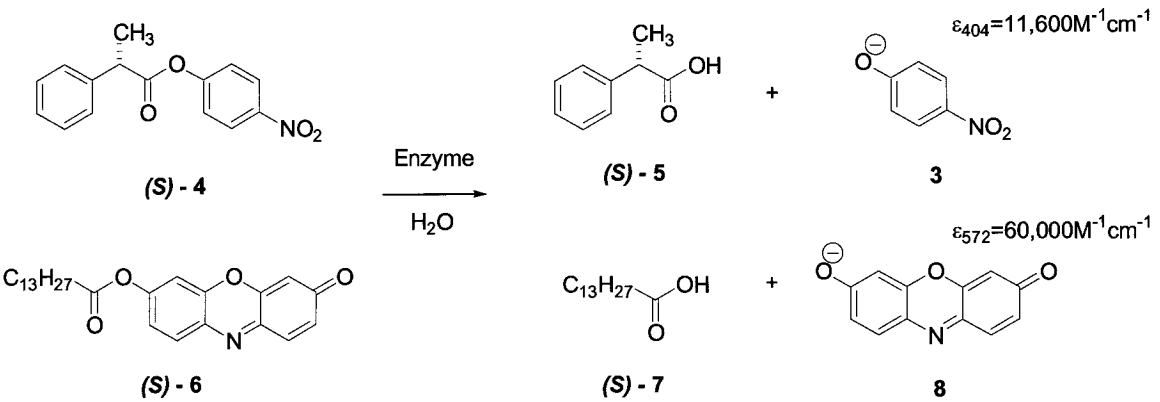

Scheme 2. Quick E Test Using the *(S)* – Enantiomer as an Example.

---

[7] Janes, L.E. and Kazlauskas. *J. Org. Chem.* **1997**, *62*, 4560.

Similar to the previously discussed method by Reetz, each enantiomer of a chiral p-nitrophenol ester was subjected to catalysis conditions separately. This time a resorufin ester **6** was added to the reaction to represent the opposite enantiomer in solution. Hydrolysis of the true substrate and the pseudo enantiomer **6**, released a different chromophore that was detected under different wavelengths. This permitted the derivation of ee values under the conditions of substrate competition for enzyme binding.

Again the method was hampered by the fact that enantiomers were evaluated separately. Nonetheless, this colourimetric based technique allowed for a quick determination of mutant enzymes that showed the greatest potential for selectivity.

1.2.5 Fluorescence Techniques

Fluorescence has also been adapted for high throughput screening. An example can be found in the work of Klein and Reymond[8] who studied the enzymatic resolution of chiral acetates by transformation to the corresponding alcohol products **10**. The alcohols were then oxidized with horse-liver alcohol dehydrogenase and the resulting ketones were reacted with Bovine Serum Albumin (BSA) to release the attached chromophore **12**. By comparing the relative fluorescence between reactions, each starting with a pure enantiomer of the substrate, an ee value could be established. Since this could be done in a 96 microtiter wellplate, results could be accumulated quickly. Yet it must be noted that the ee was measured in an indirect manner, as additional transformations to the immediate catalysis product **10** were necessary to produce the necessary chromophore.

---

[8] Klein, G. and Reymond, J.-L. *Helv. Chim. Acta*. **1999**, *82*, 400.

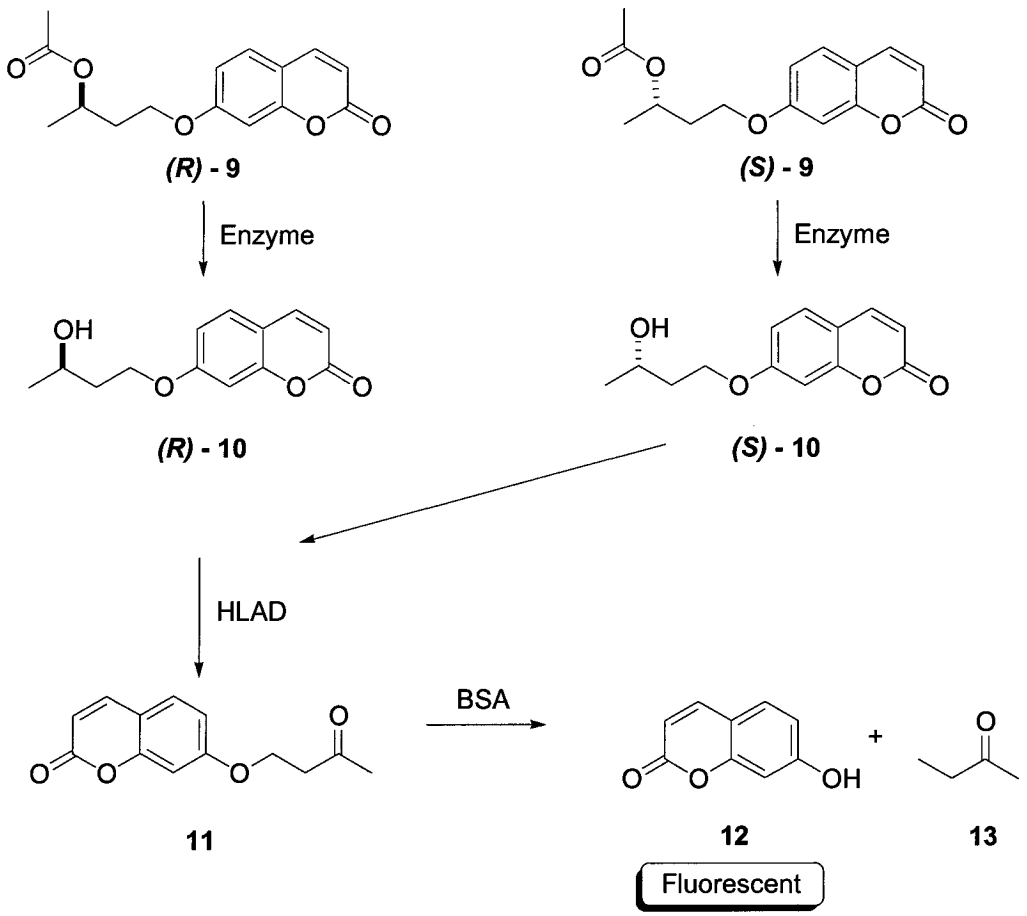

Scheme 3. Determination of Enantioselectivity by Fluorescence Method.

Fluorescence is a highly sensitive technique that permits one to work with small quantities of reagents. This is ideal for combinatorial chemistry and high throughput screening. Unfortunately, fluorescent screening methods to date still resort to the separate analysis of enantiomers. Indeed, there is still great potential to further develop this technique so as to encompass the screening of racemic mixtures for quick and reliable ee determination. Fluorescence resonance energy transfer (FRET), is a fluorescence technique that can be adapted for this very application. A more detailed discussion regarding FRET is to follow.

CHAPTER 2
FLUORESCENCE RESONCANCE ENERGY TRANSFER

Fluorescence resonance energy transfer is a technique that has already been established several years ago. It has proven to be a valuable tool in the field of biochemistry and more recently its applications in chemistry are noted.

2.1 Principles of Fluorescence Resonance Energy Transfer

2.1.1 The Fluorescence Process

Before exploring the subject of Fluorescence Resonance Energy Transfer, we must first understand the fundamentals of fluorescence. When a molecule in the ground state absorbs a photon, it quickly achieves an excited state. It can relax back to the ground state via several different processes. These include fluorescence, phosphorescence, conversion to heat energy and transfer of energy to an acceptor as depicted in Figure 7.

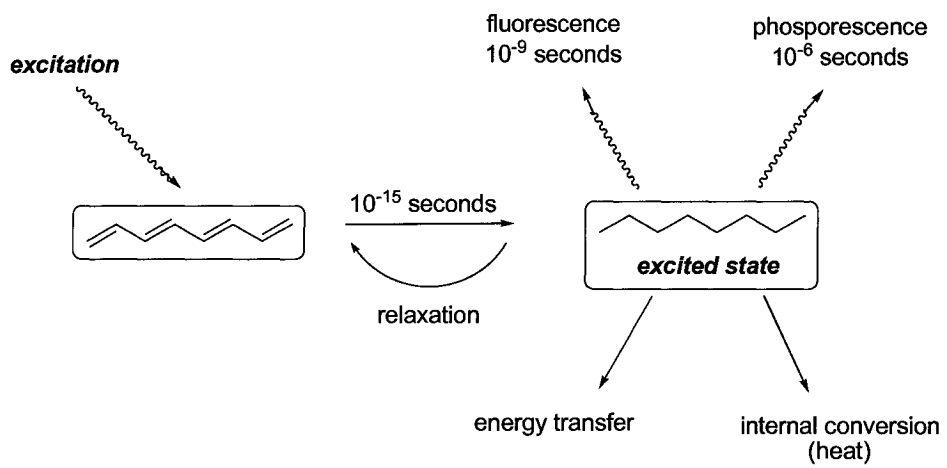

Figure 7. Possible Pathways for Relaxation from Photon Excited State.

The fluorescence phenomenon is more specifically described as a three stage process unique to certain chemical compounds called fluorophores. After a photon of energy $h\nu_{ex}$ from a light source is absorbed by the fluorophore, an excited electron singlet state S2 is produced as shown in the Jablonski diagram below (Figure 8). This excited state is short-lived and lasts for only 1-10 nanoseconds. The energy in the excited singlet state S2 is partially dissipated by random events, such as interaction between the fluorophore and its environment, to bring the molecule to a relaxed singlet state S1. In the last stage of the fluorescence process, relaxation of the fluorophore from S1 to the initial ground state S_o by emission of photons, results in fluorescence. As photons are emitted from a relaxed singlet state S1, which is lower in energy then the initial excited singlet state S2, the wavelength of the emitted photon is longer than that which initiated photon excitation.

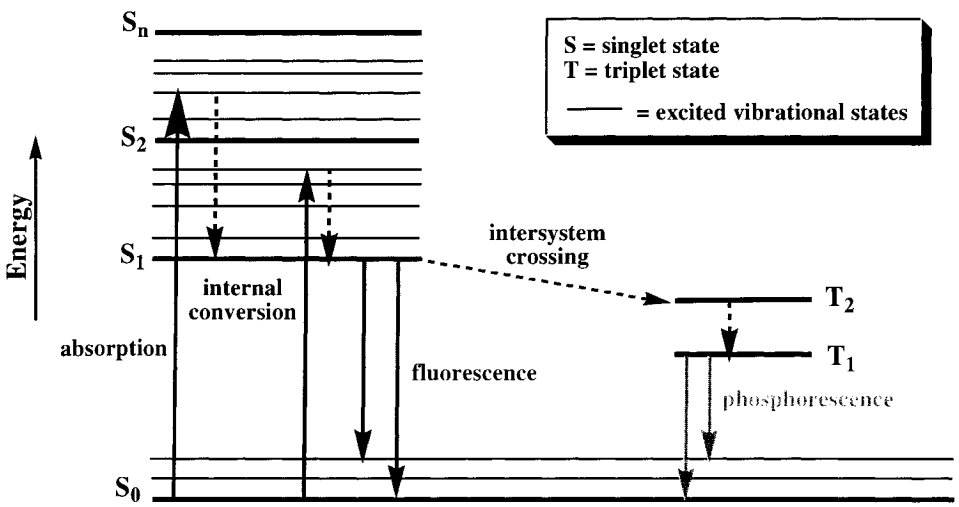

Figure. 8. Jablonski Diagram.

2.1.2 Principles of Fluorescence Resonance Energy Transfer

Fluorescence resonance energy transfer, frequently referred to by its acronym FRET, is a distance dependant interaction between two fluorophores. Taking into consideration the fluorescence process, FRET interrupts it at the photon emission stage. As previously mentioned, excited electrons populating the relaxed singlet state can relax to the ground state by photon emission resulting in fluorescence. It has also been pointed out that there are several ways by which excited electrons can return to the ground state S_o. FRET is one such method.

FRET occurs in the case where a second fluorophore, coined the acceptor, is present in the same molecule as the excited fluorophore, the donor. Energy from the excited donor can be transferred to the acceptor molecule, eliminating the donor's need for photon emission and thus suppressing donor fluorescence. The acceptor molecule now bears additional energy that decays by one of the relaxation processes noted earlier.

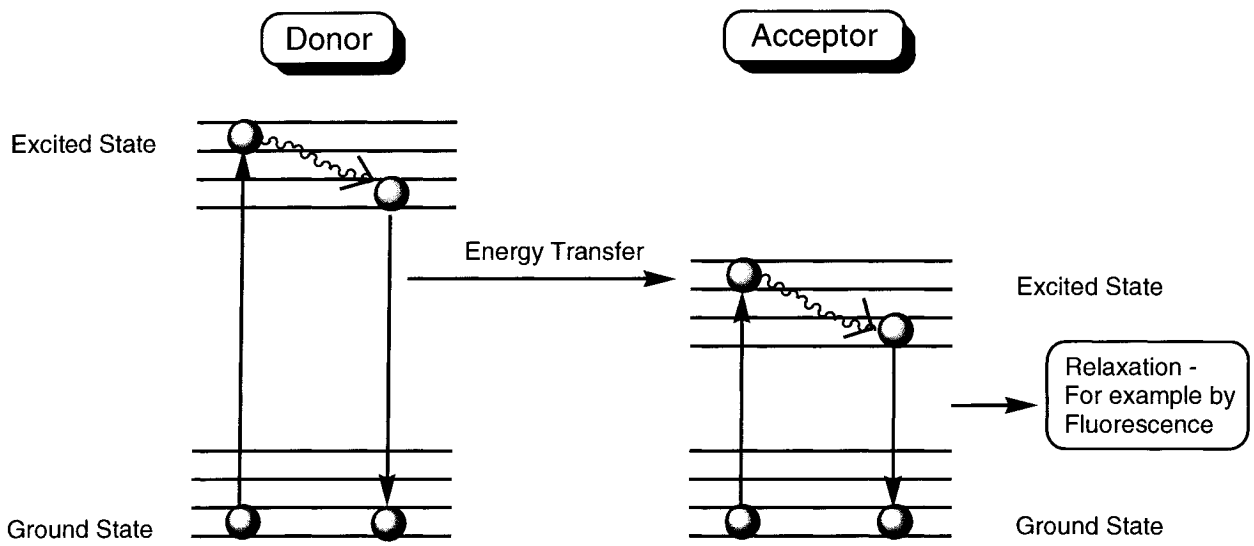

Figure 9. Suppression of Donor Fluorescence by Transfer of Energy to Acceptor.

Certain criteria must be taken into consideration when searching for a compatible donor -acceptor pair. As FRET relies on the intramolecular transfer of energy between donor and acceptor molecules, the dipole moments of the donor and acceptor must be aligned and the distance between the two should be in the range of 10 to 100 Angstroms. The absorption spectrum of the acceptor needs also to overlap with the emission spectrum of the donor to ensure the energy can be transferred and fluorescence quenched.

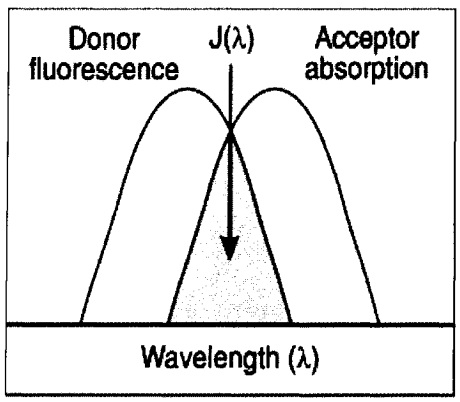

Figure 10. Overlapping Donor and Acceptor Emission Bands as a Criterion for FRET.

2.2. Applications of FRET

FRET has impacted the field of biochemistry for decades already. However, it was only recently that this technology was introduced to the area of chemical research. The prospects for exploiting FRET as a research tool in chemistry is without a doubt a new and exciting concept.

2.2.1 Applications in Chemistry

Hartwig and co-workers have succeeded in demonstrating the utility of FRET as a high throughput screening method[9,10,11]. Hartwig was able to monitor cross-coupling reactions, the linking of a substrate A to a substrate B, by exploiting the principles of FRET. He envisioned that one component of the coupling reaction could be linked to a dye that would fluoresce at a characteristic wavelength when free in solution. The substrate B, a second component in the cross-coupling reaction, in turn would be linked with a fluorescence quencher molecule. If coupling between substrates A and B is achieved, then the fluorescence of the donor molecule attached to substrate A should be successfully suppressed by the quencher molecule on substrate B.

---

[9] Stauffer, S. R.; Beare, N. F.; Stambuli, J. P.; Hartwig, J. F. *J. Am. Chem. Soc.* **2001**, *123*, 4641.

[10] Stambuli, J. P.; Stauffer, S. R.; Shaughnessy, K. H.; Hartwig, J. F. *J. Am. Chem. Soc.* **2001**, *123*, 2677.

[11] Stauffer, S. R. and Hartwig, J. F. *J. Am. Chem. Soc.* **2003**, *125*, 6977.

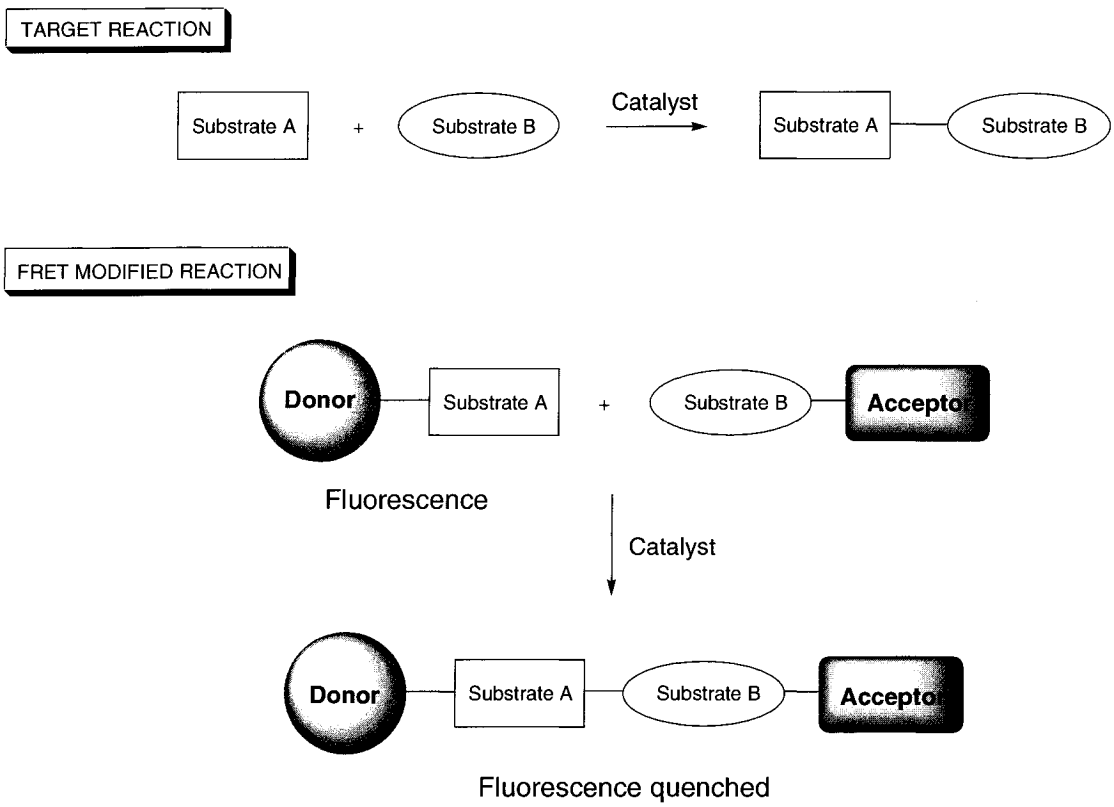

Figure 11. Application of FRET to Cross-coupling Reactions.

Dansyl **14** was selected as the fluorescent donor for this assay. This donor molecule offered an ideal situation for the coupling reactions to which it was applied. It possessed relatively inert functional groups but the sulfonyl group still allowed for the attachment of substrates to the donor molecule. Since dansyl has a characteristic emission wavelength at 490 nm, a compatible quencher molecule must absorb at this wavelength. The azo dye **15** fit the criteria in this case.

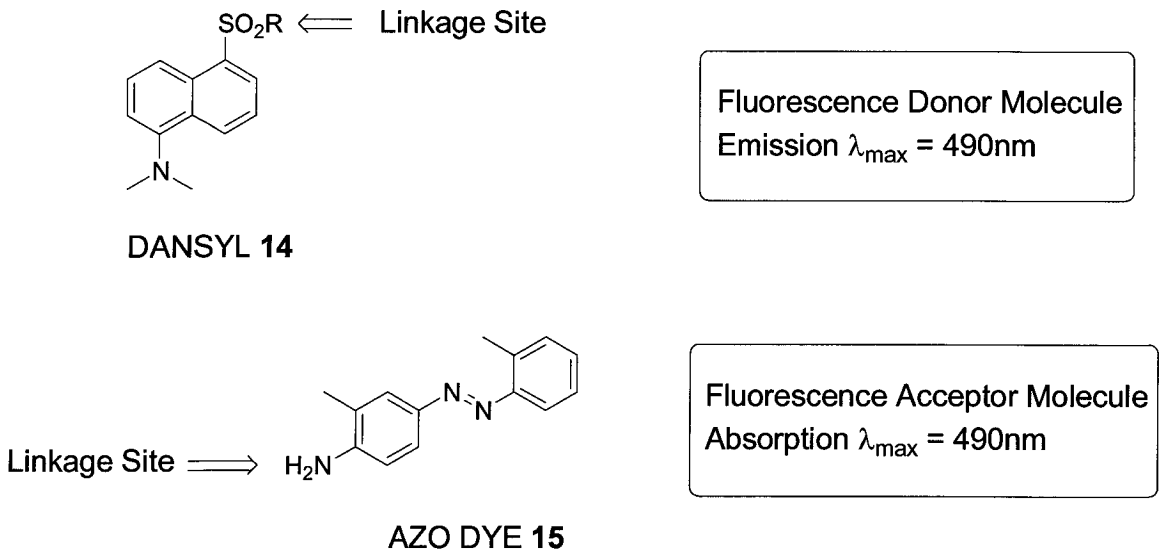

Figure 12. Compatible FRET Donor and Acceptor Pair.

With this innovative strategy in hand, Hartwig and his research group first applied FRET to the discovery of new reaction conditions for room-temperature Heck reactions[12]. In this case, dansyl, the donor molecule, was tethered to a styrenyl group and the azo dye **15**, the acceptor molecule, was tethered to an aryl bromide. As depicted in Figure 13, covalent bonding between the styrenyl and aryl groups would bring the donor and acceptor moieties close enough to quench fluorescence output.

---

[12] Stambuli, J. P.; Stauffer, S. R.; Shaughnessy, K. H.; Hartwig, J. F. *J. Am. Chem. Soc.* **2001**, *123*, 2677.

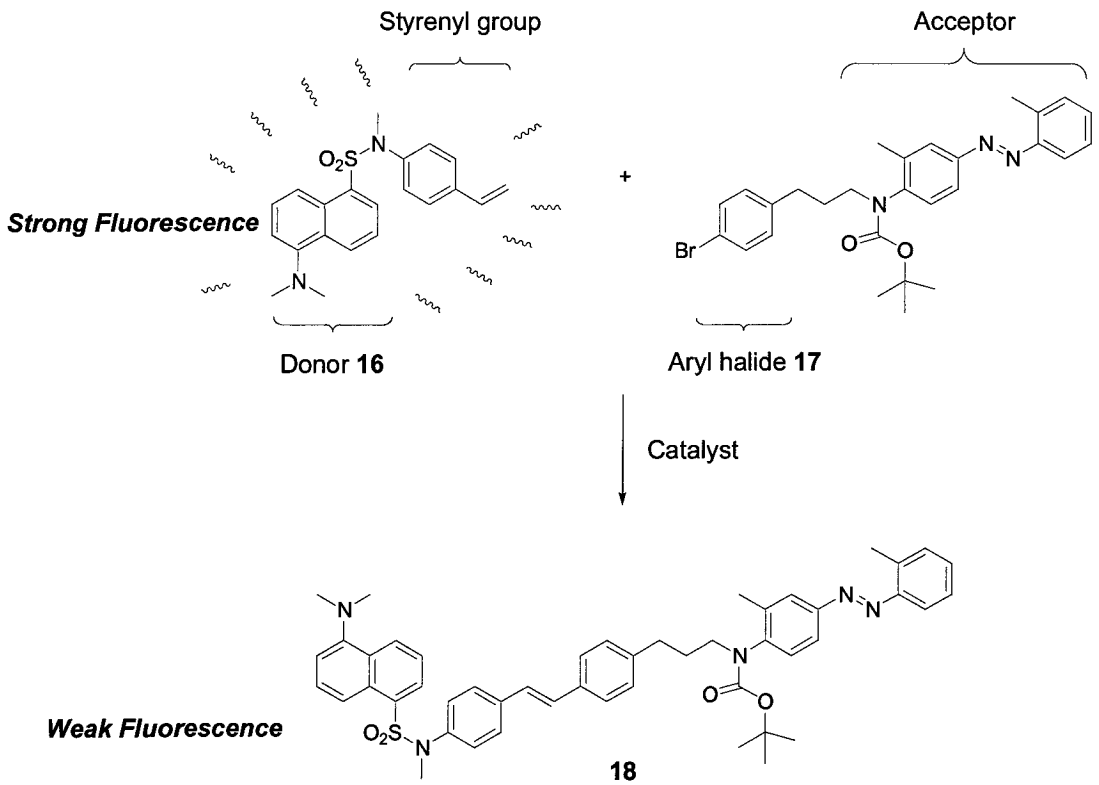

Figure 13. Fluorescence Quenching by Uniting Donor and Acceptor Molecules Through a Cross Coupling Reaction.

After synthesizing the coupling substrates, 96 different ligands were evaluated in the palladium cross-coupling reaction on a wellplate. The reactions were first conducted at 70 °C by sealing the wellplate and heating it on an aluminum block. Aliquots were taken from each well after 15 hours and diluted before fluorescence measurements were performed on an automated plate reader. The fluorescence measurements were then compared to a calibration curve that correlated the fluorescence intensity to the mole fraction of the product to derive the reaction yield. Repeated experiments showed the FRET technique used here had good reproducibility. The 15 most promising leads from this first set of experiments were then subjected to solvent studies with the same experimental method as previously described. Experimental yields derived from the FRET technique were also compared to yields obtained from conventional HPLC methodology using an internal standard. A deviation of greater than 10% was

noted for only one case. This discrepancy was rectified after repeating the experiment in question and subjecting it to FRET analysis again. The two most active ligands from the solvent scan experiment were then put forward in a room-temperature Heck reaction which proceeded in excellent yields. Hartwig's group has also successfully applied their innovative assay to the discovery of new reactions conditions for the cross-coupling of aryl halides with ethyl cyanoacetate as well as with amines.

2.2 Novel Assay Development

Hartwig's chemistry has shown the utility of FRET as a high throughput screening method. Indeed there is still potential to expand its applications, namely to the screening of catalyst enantioselectivity where efforts are still lacking.

Given that many donor-acceptors pairs exist, we envisioned that each enantiomer of a chiral substrate could be tagged by a different FRET pair. In this way, each enantiomer could be detected by measuring the fluorescence of the racemic mixture at the wavelength characteristic of its designated donor. As fluorescence intensity is proportional to the concentration of the donor, the progress of reaction could be monitored.

2.2.1 Application of FRET to Amide Bond Formation.

Initial efforts in our lab focused on asymmetric amide bond formation. This effort was largely motivated by the desire to improve on the industrial synthesis of Indinavir (Crixivan) **19**, a drug used to treat patients affected by the HIV virus.

Scheme 4 depicts an efficient but rather linear sequence to manufacture a key fragment of this HIV protease inhibitor[13].

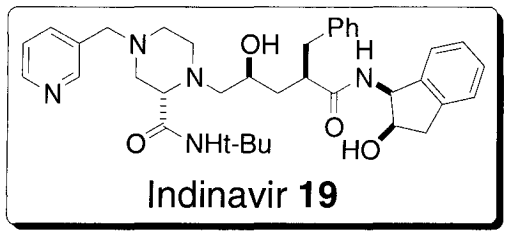

Indinavir **19**

Key Amide Fromation Step

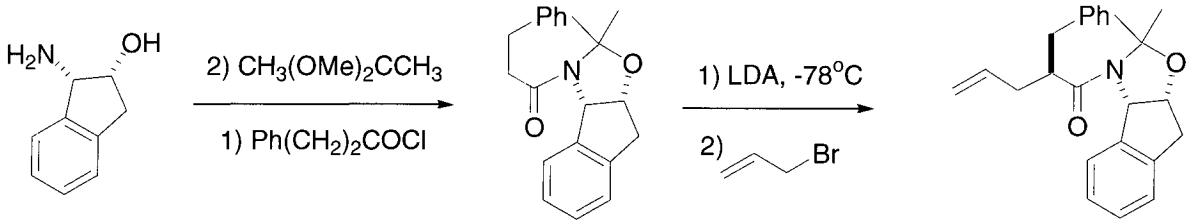

20 **21** **22**

Scheme 4. Key Amide Formation Step in Industrial Synthesis of Indinavir.

Traditional methodology for amide bond formation (Scheme 5) is not deemed suitable for substrates bearing a chiral center alpha to the amide functionality as in the case of Indinavir. Conversions of esters or acid chlorides to amides in the presence of amines, as outlined in route A and B, would epimerize the chiral centre alpha to the amide group and produce a racemate. Coupling agents (route C) are a reliable way to preserve chiral information in amide bond construction,

---

[13] (a) Rossen, K.; Pye, P.J.; DiMichele, L.M.; Volante, R.P.; Reider P.J. *Tetrahedron Lett.*, **1998**, *39*, 6823; (b) Rossen, K.; Reamer, R.A.; Volante, R.P.; Reider, P.J., *Terahedron. Lett.*, **1996**, *37*, 6843; (c) Maligres, P.E.; Weissman, S.A.; Upadhyay, V.; Cianciosi, S.J.; Reamer, R.A.; Purick, R.M.; Sager, J.; (d) Rossen, K.; Eng, K.K. *Tetrahedron*, **1996**, *52*, 3327; (e) Maligres P.E.; Upadhyay, V.; Rossen, K.; Cianciosi, S.J.; Purick, R.M.; Eng, K.K.; Reamer, R.A.; Askin, D.; Volante, R.P.;Reider, P.J. *Tetrahedron. Lett.*, **1995**, *36*, 2195; (f) Askin, D.; Eng, K.K.; Rossen, K.; Purick, R.M.; Wells, M.T.; Volante, R.P.; Reider, P.J. *Tetrahedron. Lett.*, **1994**, *35*, 673

but the cost of doing so on a large scale industrial process makes the strategy unappealing.

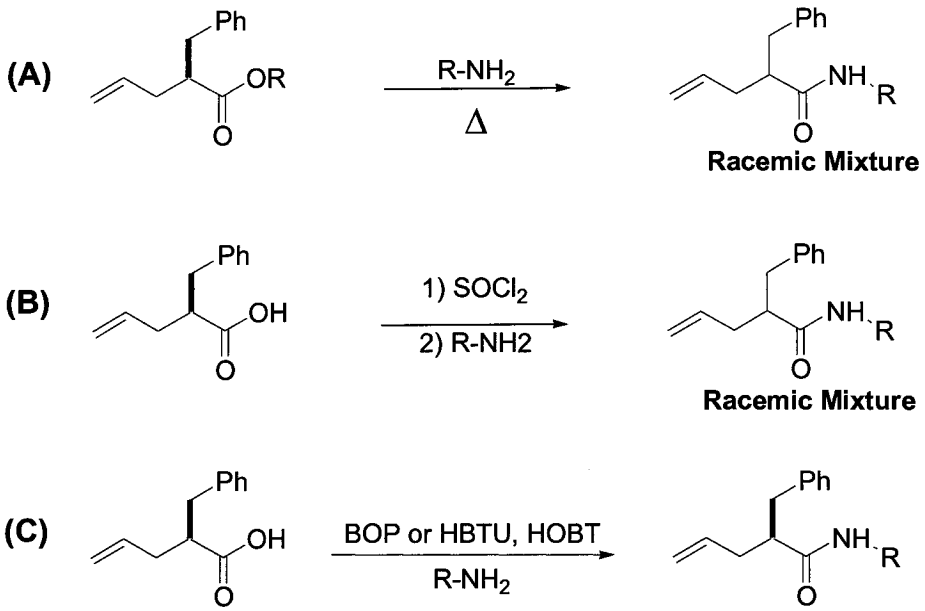

Scheme 5. Strategies for Amide Bond Formation.

This is the reason why Indinavir is made by its current method instead of a more convergent route involving the coupling of chiral subunits. We therefore propose to proceed via a catalytic route towards amide bond construction in the synthesis of Indinivir.

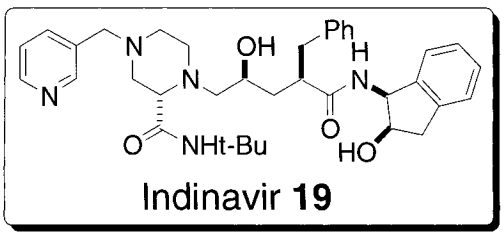

Indinavir **19**

Proposed Amide Formation Step

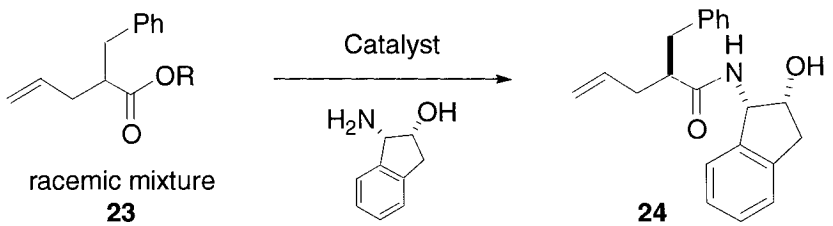

racemic mixture
23

24

Scheme 6. Proposed Catalyst Application to Amide Bond Formation Towards the Synthesis of Indinavir

Asymmetric catalysis would be ideal in this case, as this will permit the use of the racemic ester **23**. The leftover ester isomer from the catalytic resolution can then be recycled. Not only is this a cost effective strategy but catalysis also offers a more convergent route towards the synthesis of Indinivir.

As stated before, our objective was to develop a FRET based assay to accurately and rapidly screen for enantioselectivity. The coupling reaction in Figure **14**, became a model reaction to test our concept.

Each enantiomer of the chiral ester is tagged with a different donor-acceptor pair, resulting in pseudoenantiomers. Since the donor and acceptor molecules are linked covalently to one another, fluorescence is suppressed. It must be noted that a spacer unit separates the ester recognition element and the FRET moieties. This is an important feature in our substrate design as the spacer ensures that the donor and acceptor moieties do not interfere with the catalyst's interaction with the reaction center.

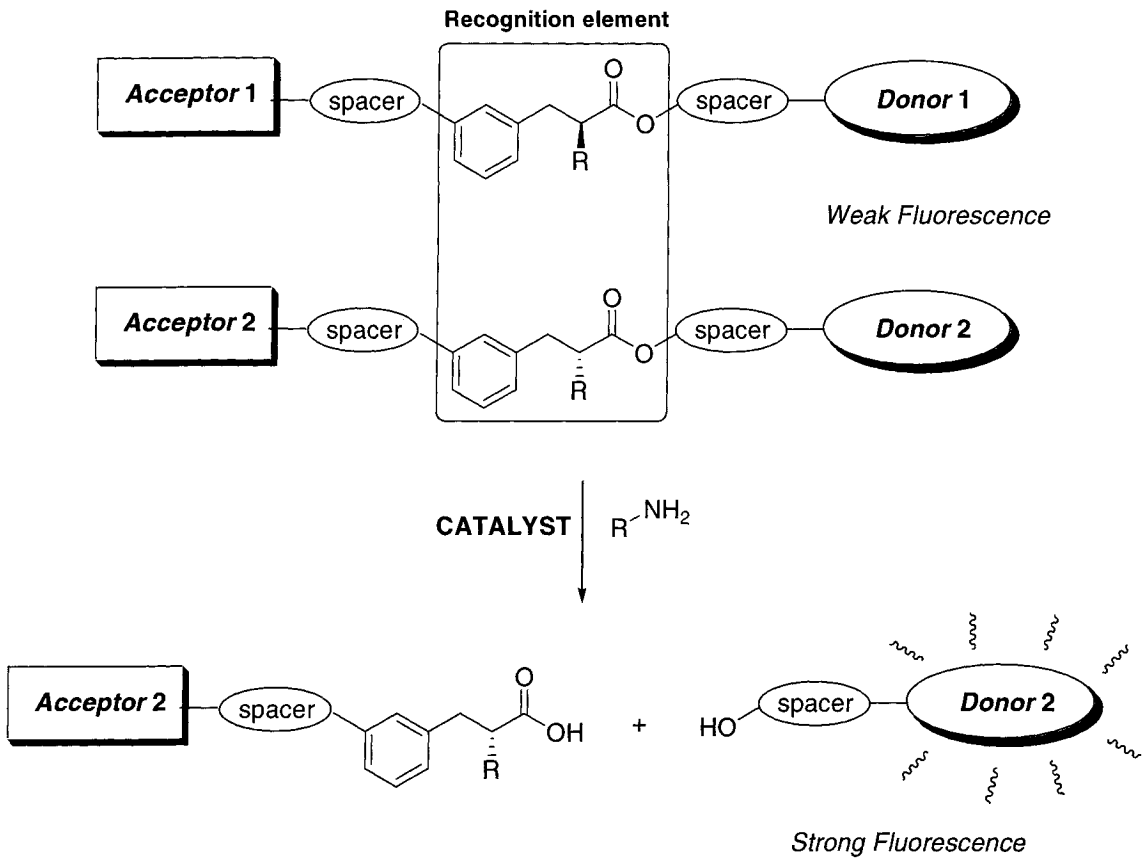

Figure 14. Proposed Model Reaction to Test FRET Based Assay.

When hydrolysis of the ester occurs, the acceptor molecule would be released from the substrate, and fluorescence will no longer be quenched. By observing the intensity and the wavelength of the fluorescence emission, one could account for the selectivity of the reaction.

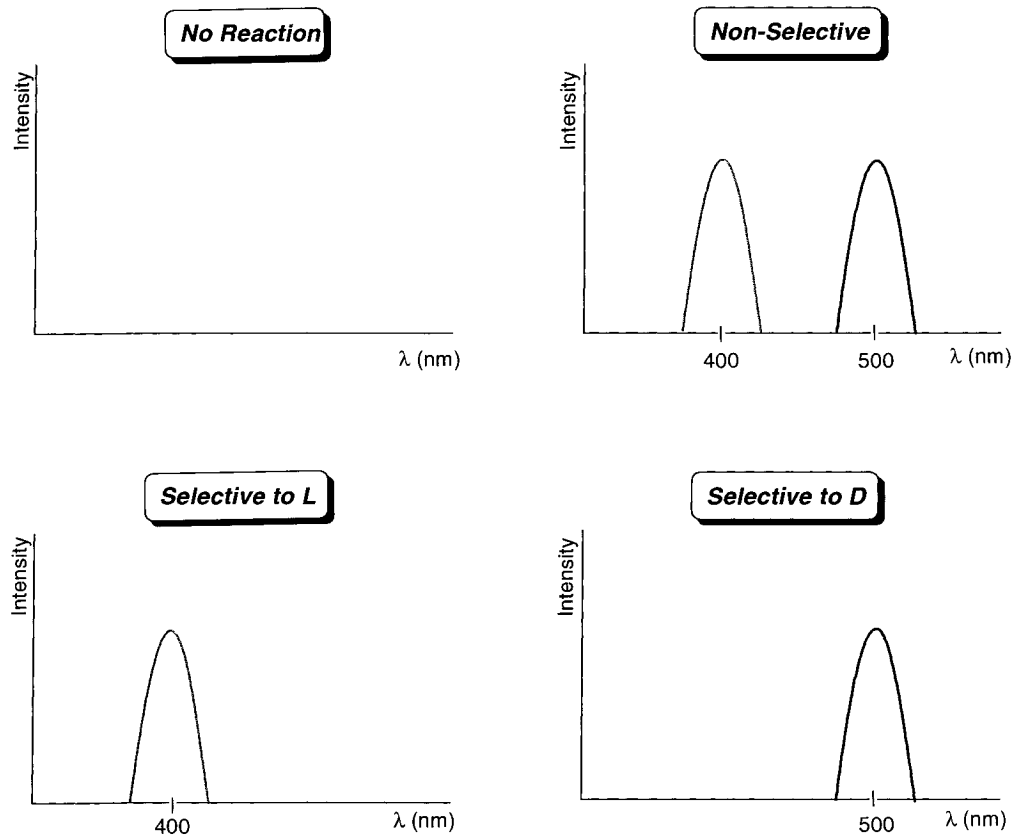

Figure 15. Possible Results for the FRET Based Assay.

Four different scenarios can arise from the catalytic hydrolysis of our chiral substrate (Figure 15). Remembering that the donor molecule of each enatiomeric substrate fluoresces at a characteristic wavelength, a selective reaction will produce an emission spectrum with a single peak. On the other hand if two peaks are observed then a non-selective reaction has occurred.

Josée Cloutier has successfully completed the proof of principle described above. We proposed to expand the research to include *meso* compounds as potential substrates for the FRET assay. Since, technically, both enantiomers are found within the same substrate, this will require the substrate to be equipped with two donors units so as to differentiate between the two chiral centres in question. We will also attempt to use a single acceptor molecule to act as the fluorescence quencher for both donor units.

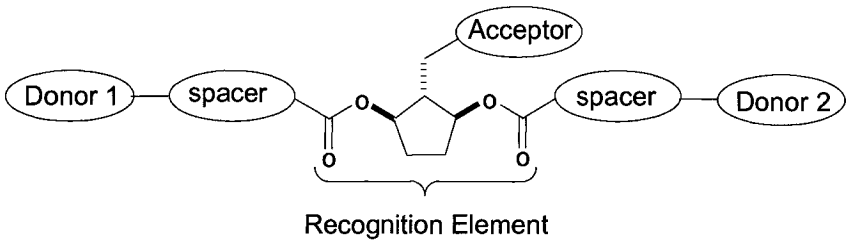

Figure 16. Applying FRET to a *Meso* Substrate.

Results from such an assay will be similar to that described for a FRET assay based on two separate enantiomers (Figure 15). With much eagerness, we commenced our investigation towards developing a reliable FRET based methodology, the results of which are discussed in the following chapters.

CHAPTER 3
PROOF OF PRINCIPLE

Equipped with a better understanding of how FRET works, we wanted to validate our vision to adapt this technology as a high throughput screening method for asymmetric catalysis. It was indeed necessary to design a reliable method of analysis before applying the assay to the discovery of novel catalysts.

3.1 FRET Donor and Acceptor Pairs

It was outlined previously that certain criteria must be met in the search of a compatible donor and acceptor FRET pair. Josée Cloutier was successful in accomplishing this task.

3.1.1 Selection of FRET Donor and Acceptor Pairs

Taking a lead from Hartwig's[12] experiments, which have already identified a reliable FRET pairing, Dansyl **14** was selected as the acceptor while the azo dye, for which we shall assign the name GBC **15**, served as the fluorescence acceptor molecule. As Hartwig had noted, the simplicity and chemical inertness of the Dansyl structure was appealing. This donor molecule was characterized by an excitation maximum at 340 nm and an emission maximum at 520 nm. The pairing was ideal as the acceptor GBC could absorb light at the same wavelength at which the donor, Dansyl, fluoresces. Furthermore, GBC had the added advantage that it was a non-fluorescence acceptor. This would simplify the detection method, as background signal from the acceptor component would be absent.

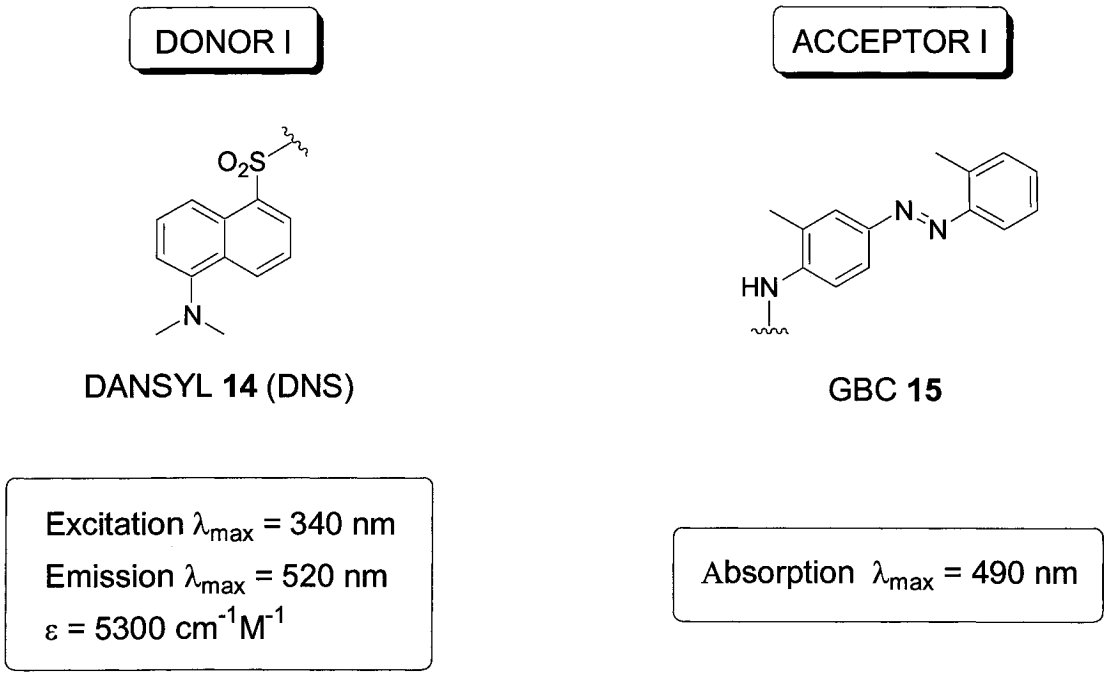

Figure 17. The First Identified FRET Donor-Acceptor Pair.

The search for the second donor acceptor pair proved to be more challenging than expected. Not only must this second pairing obey the criteria for FRET, but the second donor must have a distinguishable fluorescence emission from the first donor, Dansyl. The two donor molecules must also not fluoresce at the excitation wavelength of the other donor as this would result in high background fluorescence. These conditions limited the scope of donor-acceptor pairs that were available for our purpose.

Many systems were investigated before a refined literature search revealed that pyrene **25** would potentially be a good acceptor candidate. PYR has an excitation maximum at 360 nm and fluoresces at 380 nm, both of which can be differentiated from the excitation and emission of the DNS donor. The well-separated emission wavelengths would present a definite advantage in our assay by eliminating ambiguity during spectral analysis.

Finding a suitable acceptor molecule for PYR was not an immediate success. Either quenching of PYR was incomplete or the fluorescence spectrum of the quencher overlapped with that of the DNS moiety, thereby interfering with its proper detection. To resolve the latter problem, the quencher would ideally be one that did not emit light, such as GBC, the acceptor in our first FRET pair. It then occurred to us that perhaps GBC could also be paired up with PYR. GBC, at first glance, might appear to be an incompatible acceptor for PYR as it has an absorption maximum at 490 nm, whereas PYR emits light at 380 nm. The quenching range and not solely the maximum quenching wavelength must be considered here. Fortunately, the emission spectrum of PYR is within the absorption range of GBC.

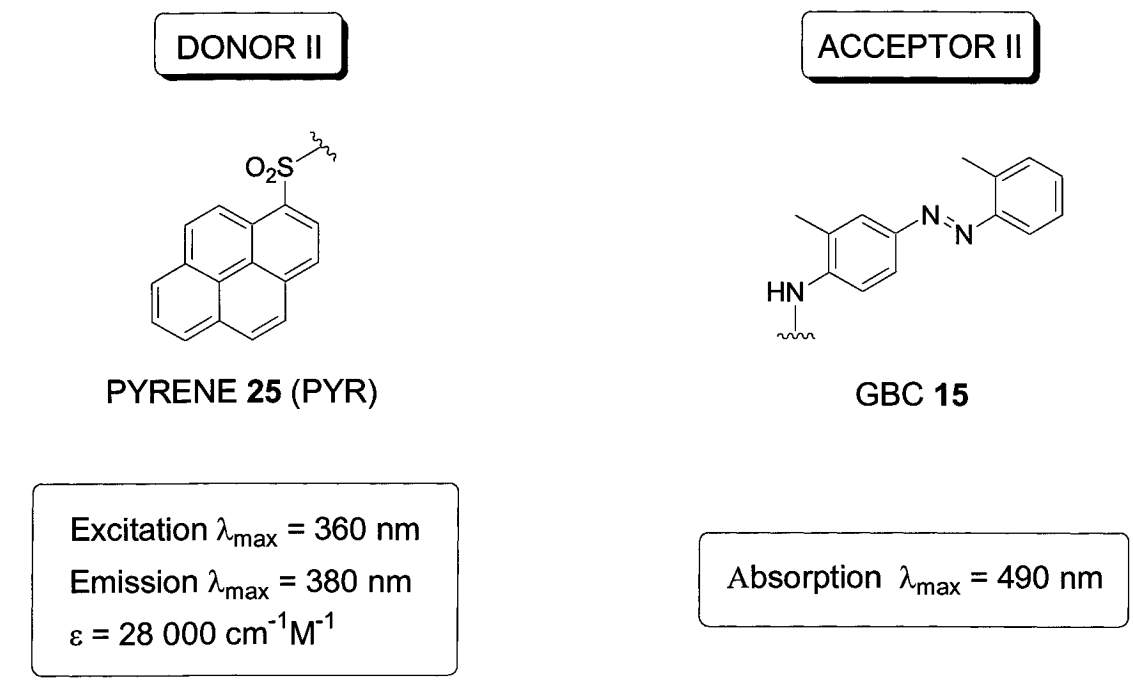

Figure 18. The Second FRET Donor-Acceptor Pair.

The characteristics of the two FRET donor-acceptor pairs appeared to be compatible in every respect, with the exception to the extinction coefficients of the donors. The extinction coefficient is relative to the ratio of how much light is emitted and how much is absorbed by a fluorophore. This describes the efficiency of the fluorophore to fluoresce. Concerns were raised since the extinction coefficient of PYR is more then four times that of DNS. We needed to apply PYR and DNS in equimolar concentrations, and if PYR fluoresces more intensity than the latter, we run the risk of having the fluorescence data out of the detection range. A possible solution was to change the excitation/emission slit width of the spectrophotometer when detecting for PYR. This however, would be at the cost of lengthening the scanning process.

3.1.2 Calibration Curves

Our first efforts in establishing calibration curves with our newly found FRET pairs made use of available substrates synthesized by Josée Cloutier in accordance with her project as shown in Figure 19, along with their respective excitation and emission spectra. From this figure, we can see that the emission band of each donor molecule is easily distinguishable from one another, thus, confirming that we had made a sound selection of fluorescence donors for our experiments.

A

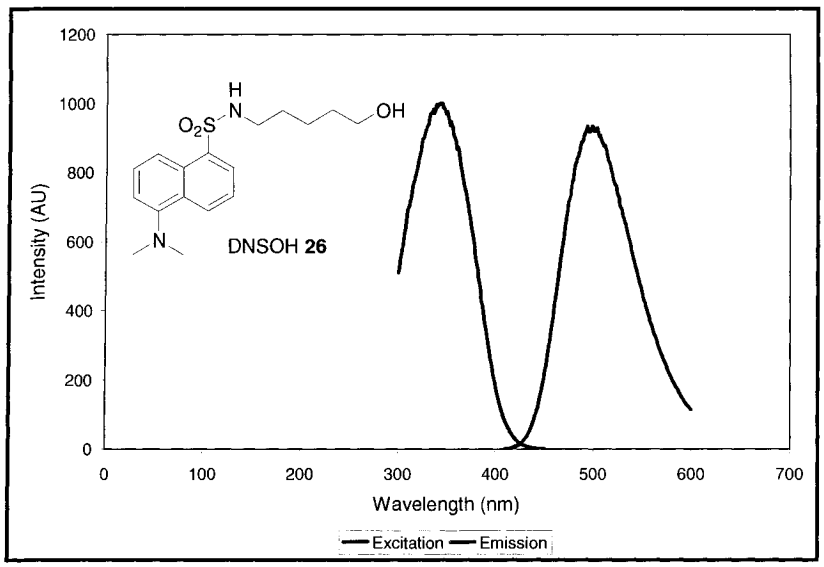

B

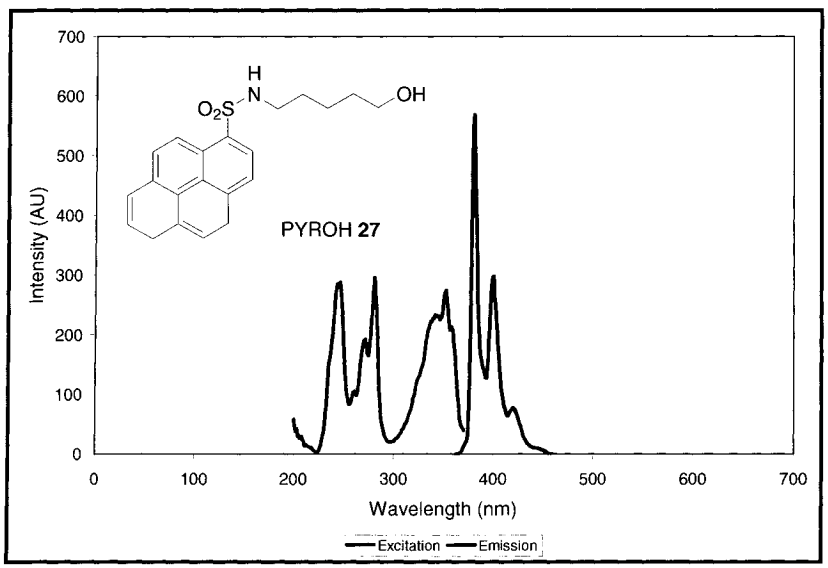

Figure 19. Excitation and Emission Spectra of A) Dansyl B) Pyrene.

Initial scanning experiments of a mixture of **26** and **27** found that one need not excite the donors at a wavelength corresponding to their absorption maxima. Using an excitation wavelength of 370 nm resulted in a fluorescence spectrum in which the emission intensity of each donor was within a similar range. Being able to use a single wavelength to detect for both PYR and DNS would also serve to simplify our method.

It was important to understand the interaction between the PYR and DNS donors in solution and to assure that the concentration of each donor moiety correlates to their respective emission intensity. A series of solutions were made, using dichloromethane as a solvent, with varying amounts of the two donors to verify a linear fluorescence response with respect to concentration.

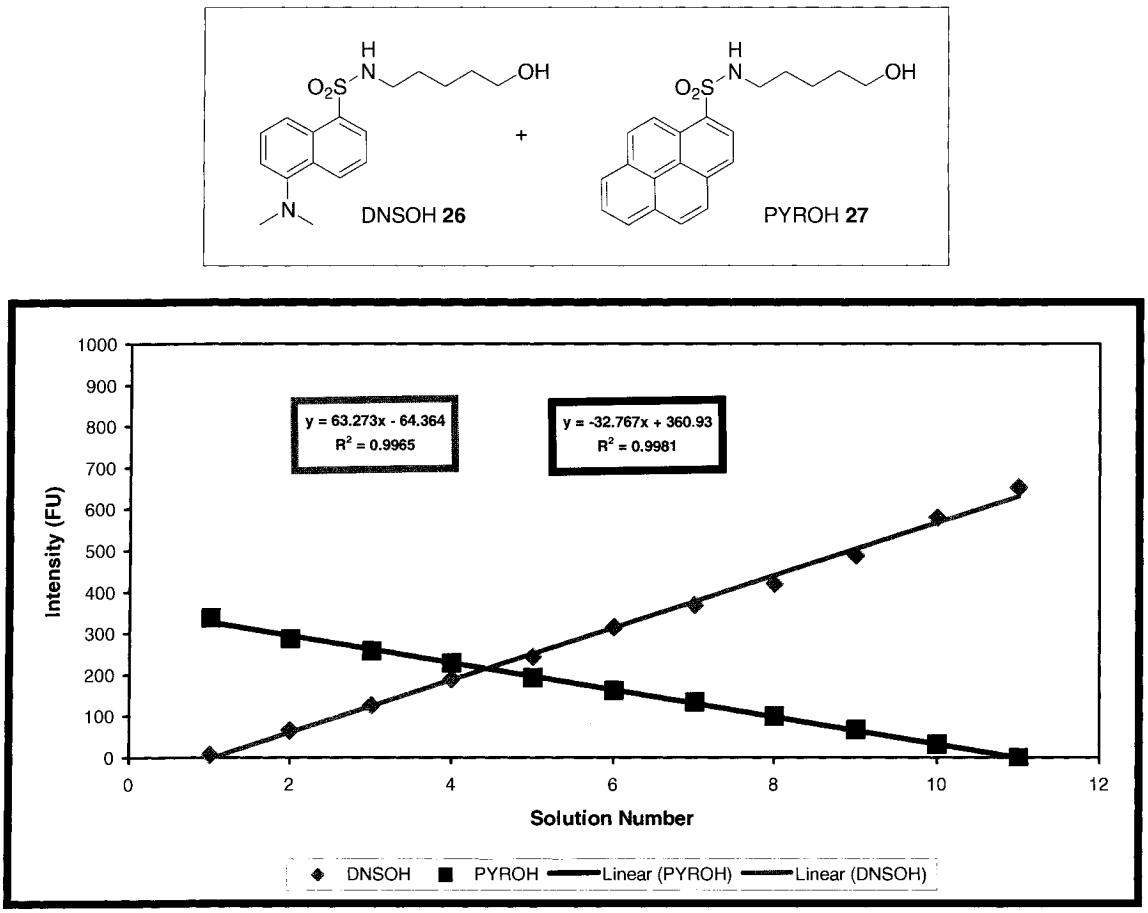

Figure 20. Calibration Curve of Solutions with Varying Ratios of **26** and **27**.

Solution	[DNSOH] (X10E-5M)	[PYROH] (X10E-5M)
1	0	10
2	1	9
3	2	8
4	3	7
5	4	6
6	5	5
7	6	4
8	7	3
9	8	2
10	9	1
11	10	0

Table 3. Concentration of DNSOH and PYROH in Solutions.

We were pleased to see that the fluorescence of both DNSOH (**26**) and PYROH (**27**) displayed a linear response with increasing donor concentrations (Figure 20). It must also be noted that the presence of a second donor in solution did not interfere with the linearity of the calibration curve.

The next logical step was to see if the presence of any acceptor, GBC, free in solution would affect the detection of the donor molecules. The methyl ester **28** was used to represent the acceptor in solution for solubility reasons.

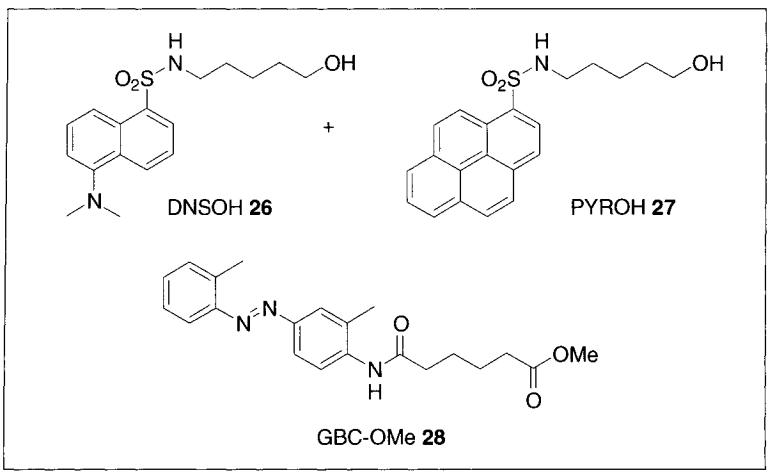

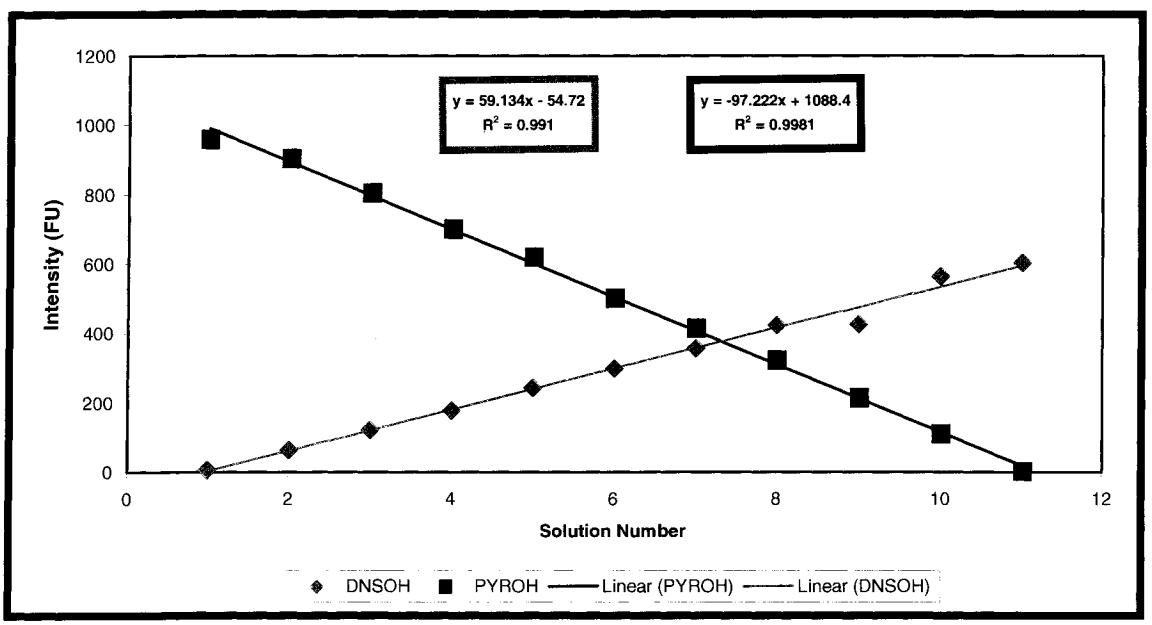

Figure 21. Calibration Curve Showing Influences of GBC on Donor Fluorescence.

Solutions used for Figure 20 were spiked with the acceptor **28** in an amount that was equimolar to the total amount of donor moieties in solution and subjected to analysis.

Once again, a linear trend line was observed for both DNSOH **26** and PYROH **27** (Figure 21). The calibration curves provided us with encouraging results and helped us to establish a reliable set of experimental parameters (concentrations, excitation wavelength, etc.) for our future studies.

3.2. Mimic of Enantioselective Hydrolysis

We have confirmed that the fluorescence of a donor molecule is correlated to its concentration. The observed linear dependence was not impaired by the presence of a second FRET donor-acceptor pair nor was intermolecular quenching by free acceptor molecules an issue. Armed with a better knowledge of the compatibility between the two sets of donors, DNS and PYR, and the acceptor molecule GBC in practice, we were now at a position to extend the relevance of this technology to *meso* substrates.

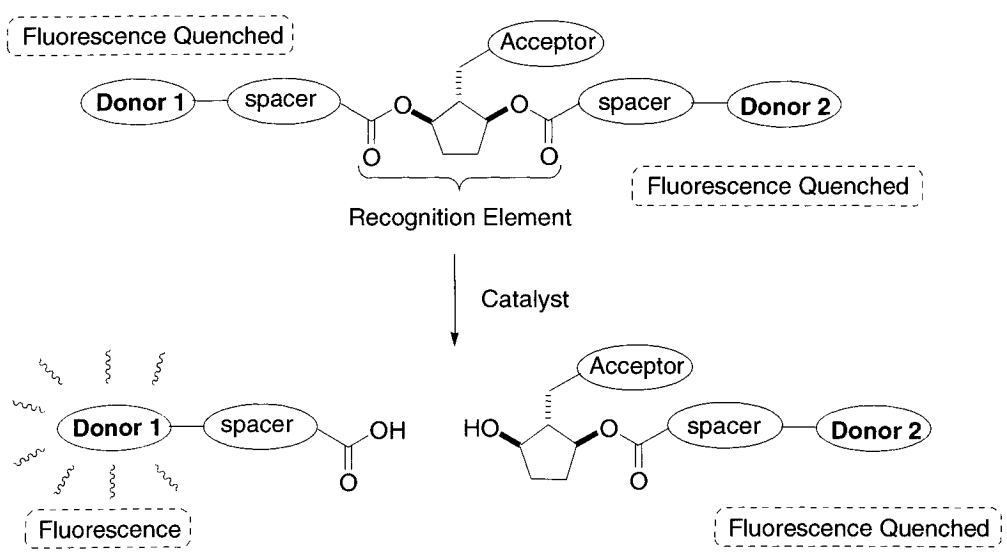

Figure 22. Enantioselective Hydrolysis of a FRET Labeled *Meso* Substrate.

Before finding a known model reaction to test our FRET method with, it was necessary to complete one more experiment. The basis of our assay, for the detection of desymmetry in *meso* substrates, rests heavily on the hypothesis that a single acceptor molecule can simultaneously quench two different donor molecules to which it is covalently linked. To verify this, we sought to covalently join DNS, PYR and GBC together to give a single substrate. This substrate would be subject to scanning experiments where the fluorescence output would be monitored. Furthermore, the substrate will be used to simulate a hydrolysis reaction, for which a calibration curve would be generated to represent a variety of situations with respect to selectivity.

3.2.1 Aspartic Acid as a Building Block: Amide Series.

The structure of aspartic acid (Figure 23), posed an ideal building block for our purpose of uniting the FRET moieties together. The two carboxylic acids and the amino functionality provided the possibility of coupling with three different groups: the two donors and the acceptor molecules. Each of these must first be tethered to a spacer molecule before coupling to the amino acid.

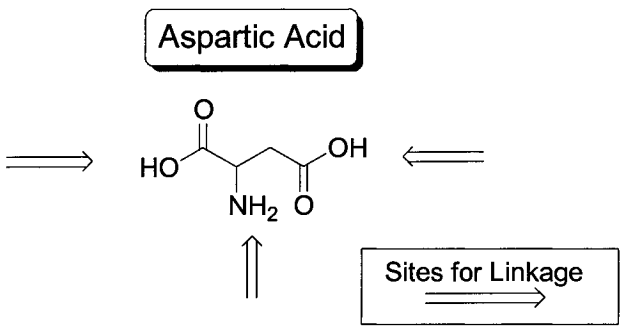

Figure 23. Linkage Sites of Aspartic Acid.

The spacer consisted of an aliphatic unit of 4 carbons long. An aliphatic system was our first choice, as its simplicity and chemical inertness would not interfere with substrate synthesis and more importantly catalyst action. Its main purpose is to assure a good separation between the FRET moieties and the recognition element of the substrate, so as to prevent any interference from the former. This will be particularly important when are ready to use the assay on true substrates. Aliphatic spacers were selected over a more rigid system to avoid problems such as solubility. Although the flexibility of an aliphatic system might allow the spacer to fold over the recognition element, and thereby hinder catalyst binding, it was still the best choice for our initial work. Our synthesis towards our targeted FRET substrate began with installing the spacer unit to the Dansyl donor.

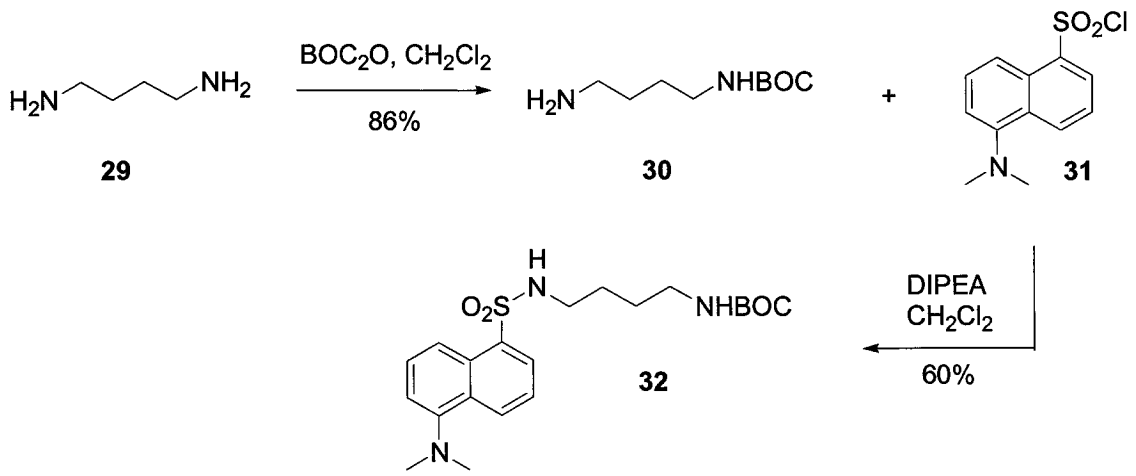

Scheme 7. Tethering of Dansyl to Spacer Unit.

1,4-Diaminobutane **29**, allowed for linkage to other groups via its two amino terminals and thus, was selected to be our spacer unit. To avoid double coupling of the same group, the diamino reagent was first protected by a BOC group at one of its amine functionalities. As **29** is a relatively inexpensive reagent, it was used in excess with the more costly BOC anhydride to give **32** in good yield. The amine spacer was then successfully installed by reacting the commercially available Dansyl chloride with the amine spacer **30**.

Standard coupling conditions using EDC and HOBT were employed to incorporate the Dansyl probe to our protected aspartic acid by a robust amide linkage.

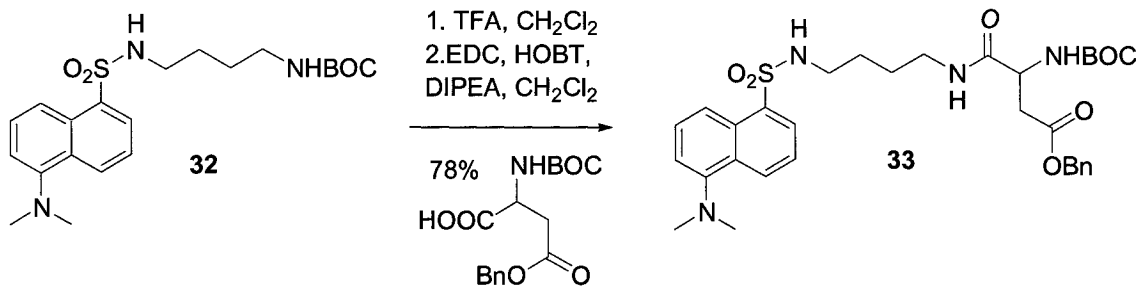

Scheme 8. Coupling of Dansyl Donor to Aspartic Acid.

Preparation of the pyrene and GBC pieces were also underway in this convergent synthesis. The second donor probe, **35**, was synthesized with a similar strategy as previously shown with the Dansyl donor. Pyrene sulfonyl chloride was generated with oxalyl chloride before reacting it with the amine linker **30**.

The GBC acceptor **39** was made by refluxing the commercially available azo dye **37** with adipic anhydride. Heat was required in this case to promote condensation between the amine and carboxylic acid functionalities, as the former was poorly nucleophillc.

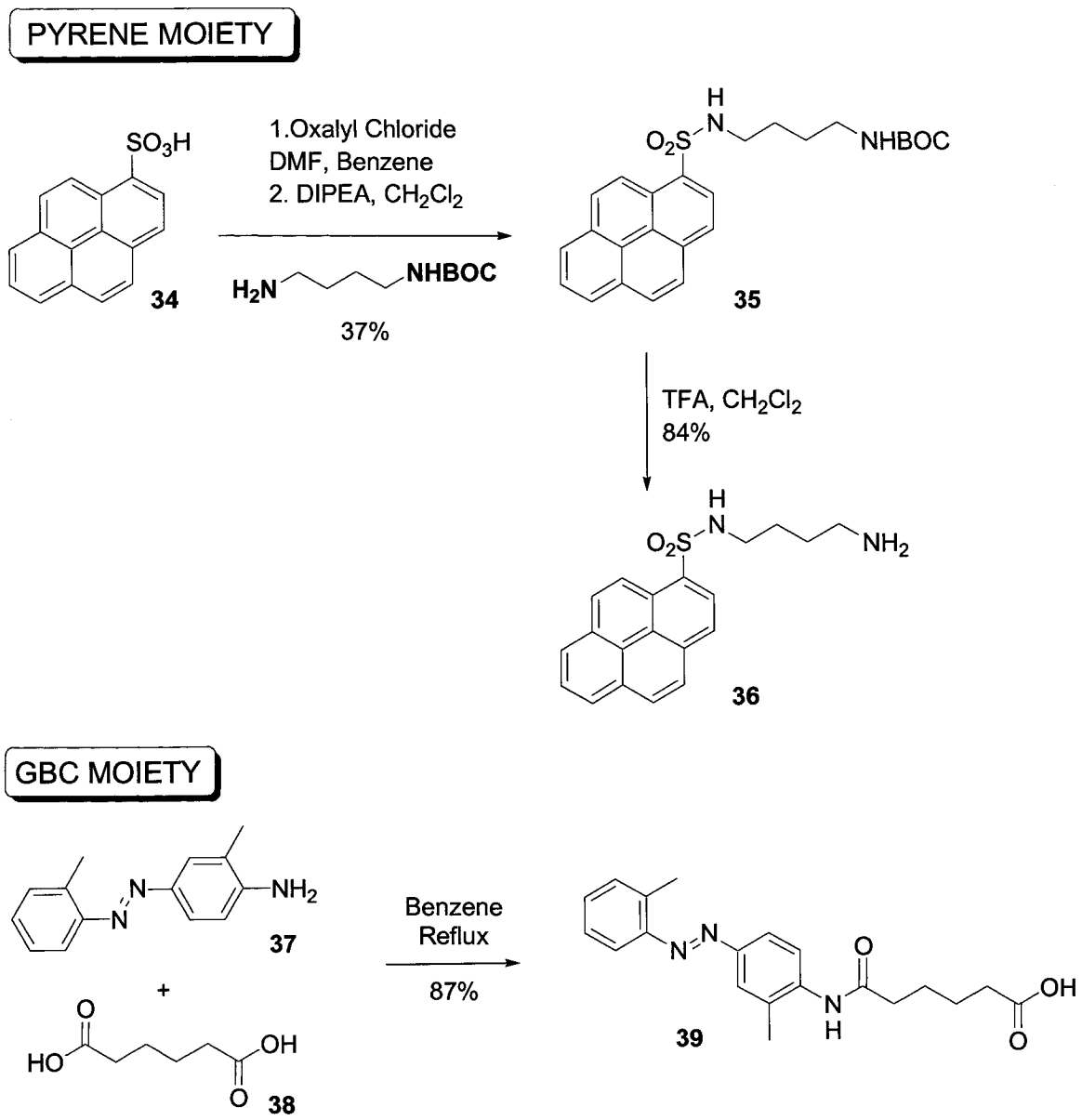

Scheme 9. Synthesis of Pyrene Donor and GBC Acceptor Moieties.

Before combining the second donor **36** to the aspartic acid substrate **33**, the benzyl ester protecting group needed to be removed. Hydrogenation with palladium on carbon, a typical method for the removal of a benzyl protecting group, was not successful. The majority of the starting material was still apparent

by TLC despite long reaction times and catalyst refreshing. Thus, hydrolysis mediated by LiOH was evaluated for benzyl removal to unveil the carboxy group.

The acid intermediate was coupled with the Pyrene donor to give **41** in modest yield. With both donors installed on the same molecule, the acceptor was the missing piece that needed to be added to complete our synthesis of **42**. Deprotection of the compound **41** proceeded with TFA before the GBC component could be added through an amide linkage. Performing this reaction with the usual coupling reagents gave a highly insoluble product mixture that proved difficult to purify. The reaction was repeated using HBTU as a coupling agent in hopes that it would give a cleaner reaction, however, this was not the case. Multiple columns were needed before finally subjecting the mixture to preparative HPLC. As much material was lost in each purification attempt, the product was finally isolated in 12% yield. Since there was sufficient material for our experimental needs, avenues to optimize the synthetic scheme were not pursued.

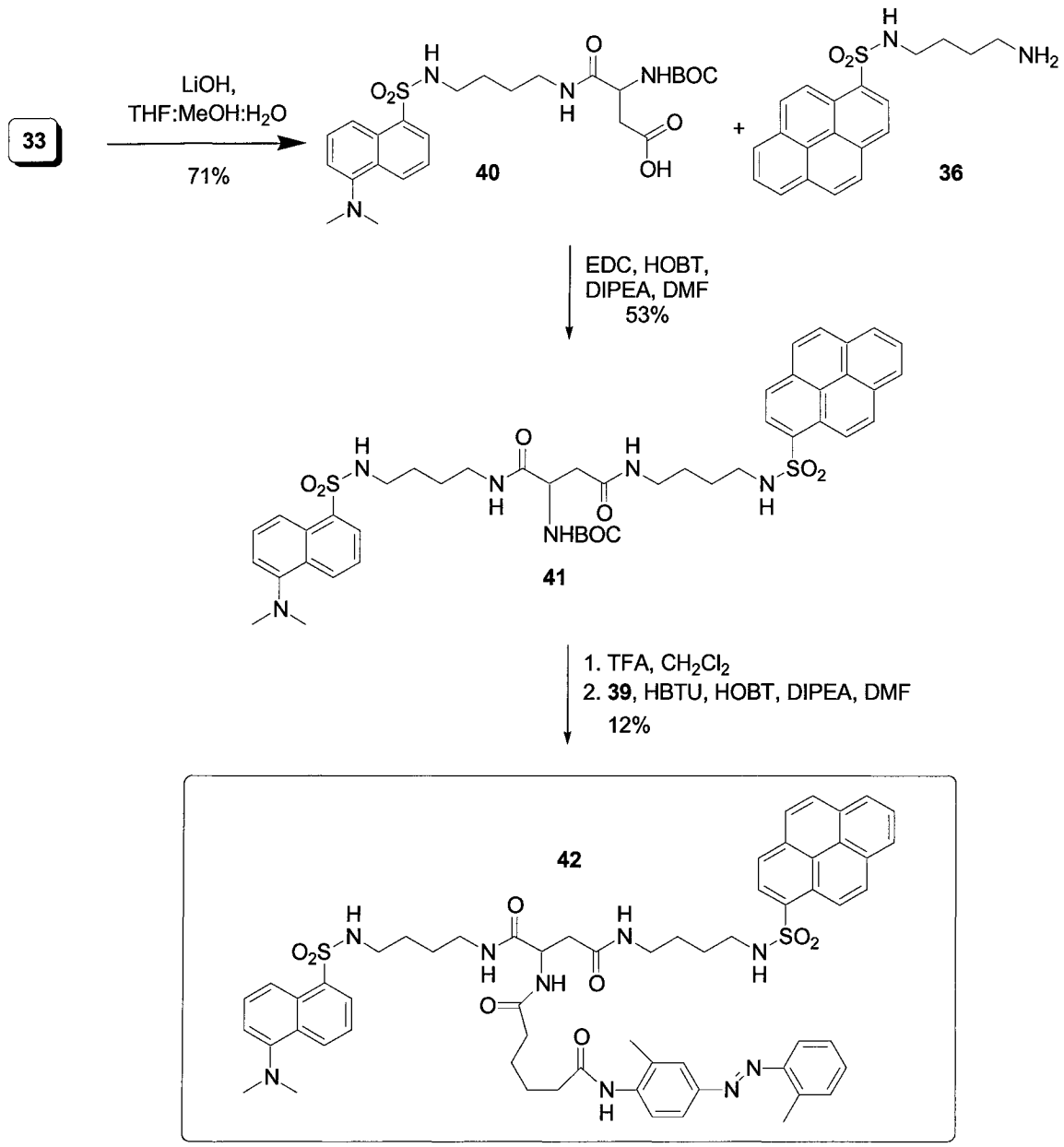

Scheme 10. Incorporation of PYR and GBC Moieties to Target Substrate.

With the DNS, PYR and GBC moieties all coupled to the same substrate, we could now evaluate whether the latter could simultaneously suppress the fluorescence of two donors. The emission spectra of DNSBOC **32** and PYRBOC **35** shown below, generated from an excitation wavelength of 370nm, will act as a reference for comparing the quenching ability of GBC in **42**.

A)

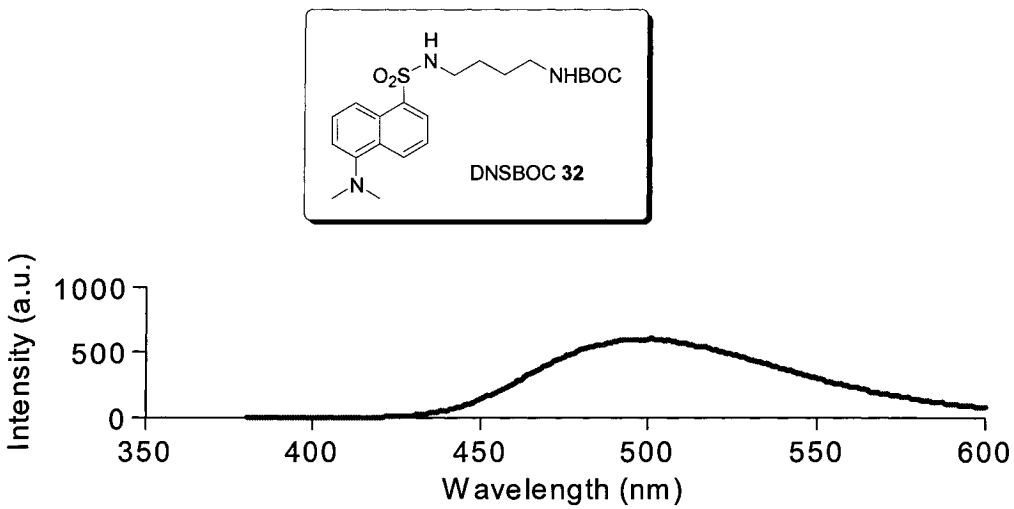

B)

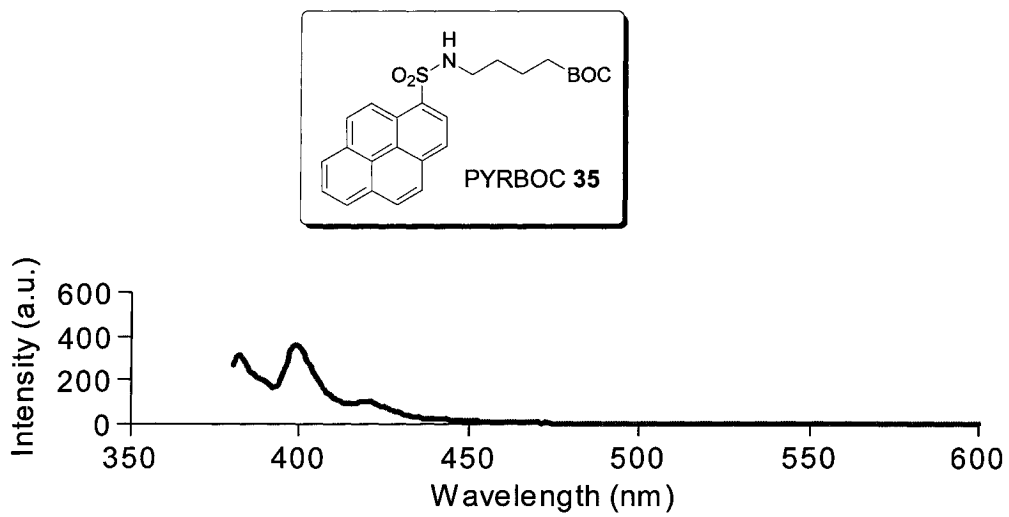

Figure 24. A) Emission Spectrum of DNSBOC **32** (ex/em slits = 5 nm/2.5 nm).
B) Emission Spectrum of PYRBOC **35** (ex/em slits = 2.5 nm/ 2.5 nm).

As mentioned in the previous section, Pyrene has a higher extinction coefficient than Dansyl and thus, the slit widths on the spectrophotometer had to be adjusted accordingly. Figure 24 clearly shows that DNSBOC has an emission maximum at approximately 500nm while that of PYRBOC was at 400nm.

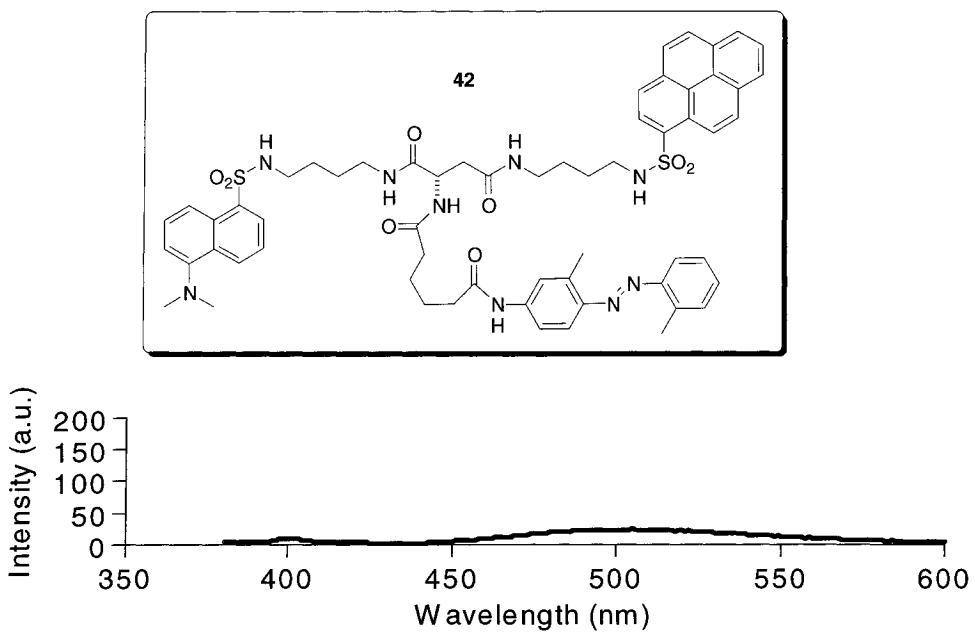

Figure 25. Emission Spectrum of DPG Amide **42**. (ex/em slits = 5 nm/ 5nm)

Subjecting DPG amide **42** to fluorescence scanning at an excitation wavelength of 370 nm, revealed that emissions at 500 nm and 400 nm, characteristic of DNS and PYR respectively, were effectively suppressed. This was indeed great news! We therefore strategized to generate a calibration curve for the hypothetical hydrolysis of DPG Amide **42** as further evidence that FRET could be a measure of enantioselectivity.

3.2.1.1 Calibration Curve: Mimic of Hydrolysis.

To imitate the hydrolysis of DPG Amide **42**, components to represent hydrolysis products had to be synthesized. In addition to the DPG Amide itself, necessary substrates for this experiment include a component bearing a) DNS and GBC (DG Amide), b) PYR and GBC (PG amide), as well as c) DNSBOC and d) PYRBOC.

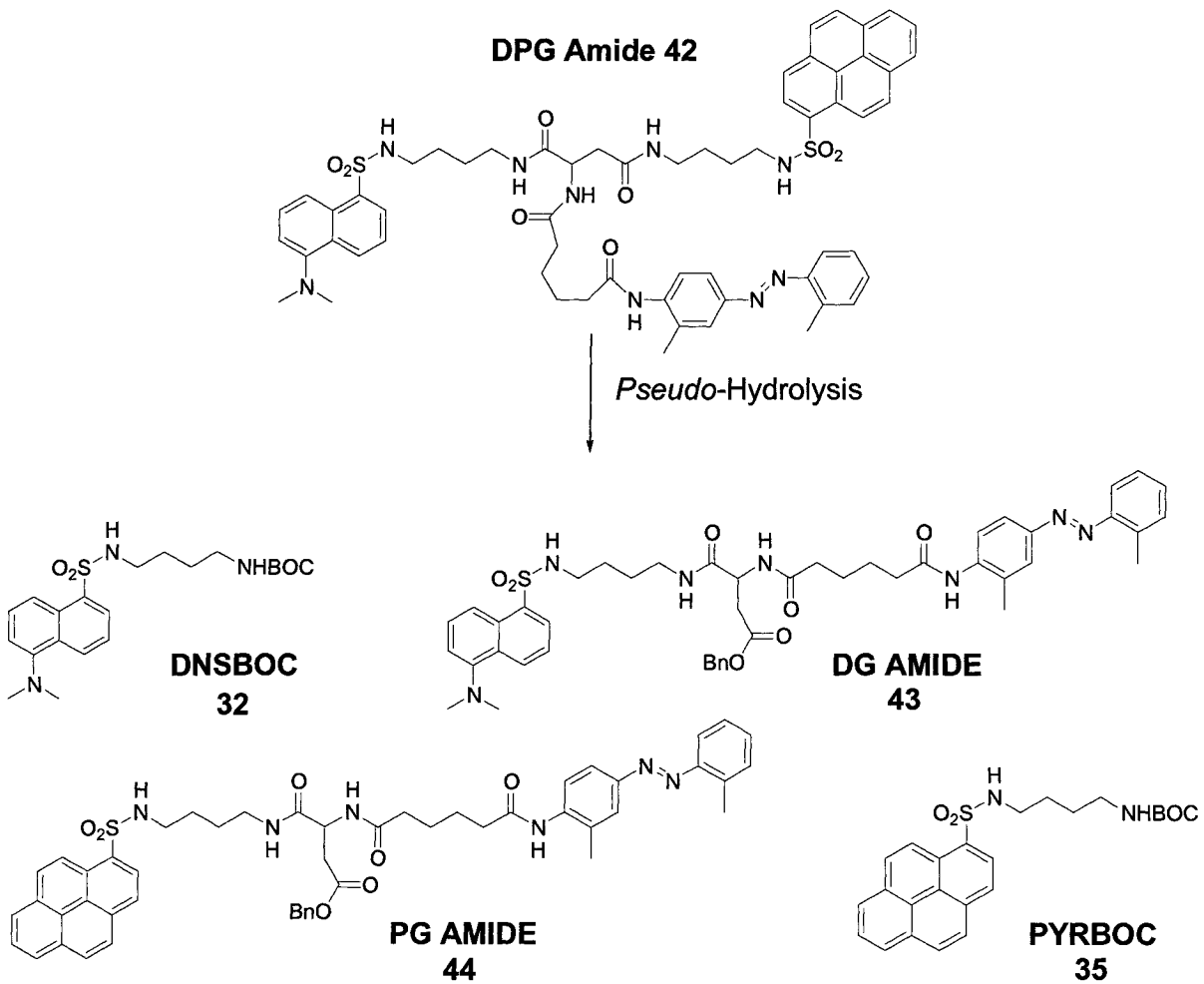

Figure 26. *Pseudo*-Hydrolysis of DPG Amide.

The synthesis of DG Amide and PG Amide was straightforward. The former was made by a reaction between the previously synthesized **32** and **39**.

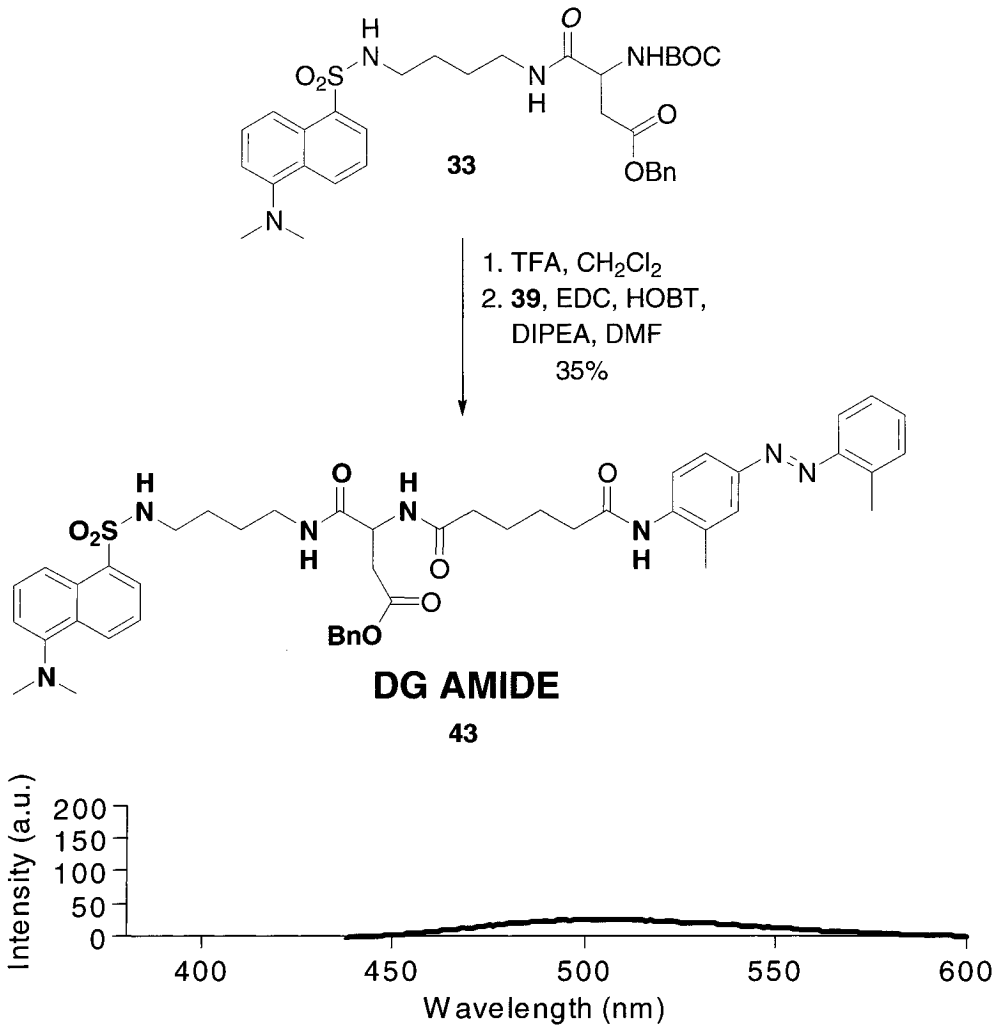

Scheme 11. Synthesis and Emission Spectrum of DG Amide (ex/em slits 5nm/5nm).

The fluorescence spectrum above shows that the fluorescence signal was close to the baseline. This indicated that the acceptor molecule, GBC, effectively suppressed DNS emission at 500nm.

Preparation of PG Amide **44** proceeded with the coupling of the amine **36** with the commercially available aspartic acid component to give **45**. Deprotection of the amino group, followed by formation of a peptide bond to tether the GBC component, generated the PG Amide product.

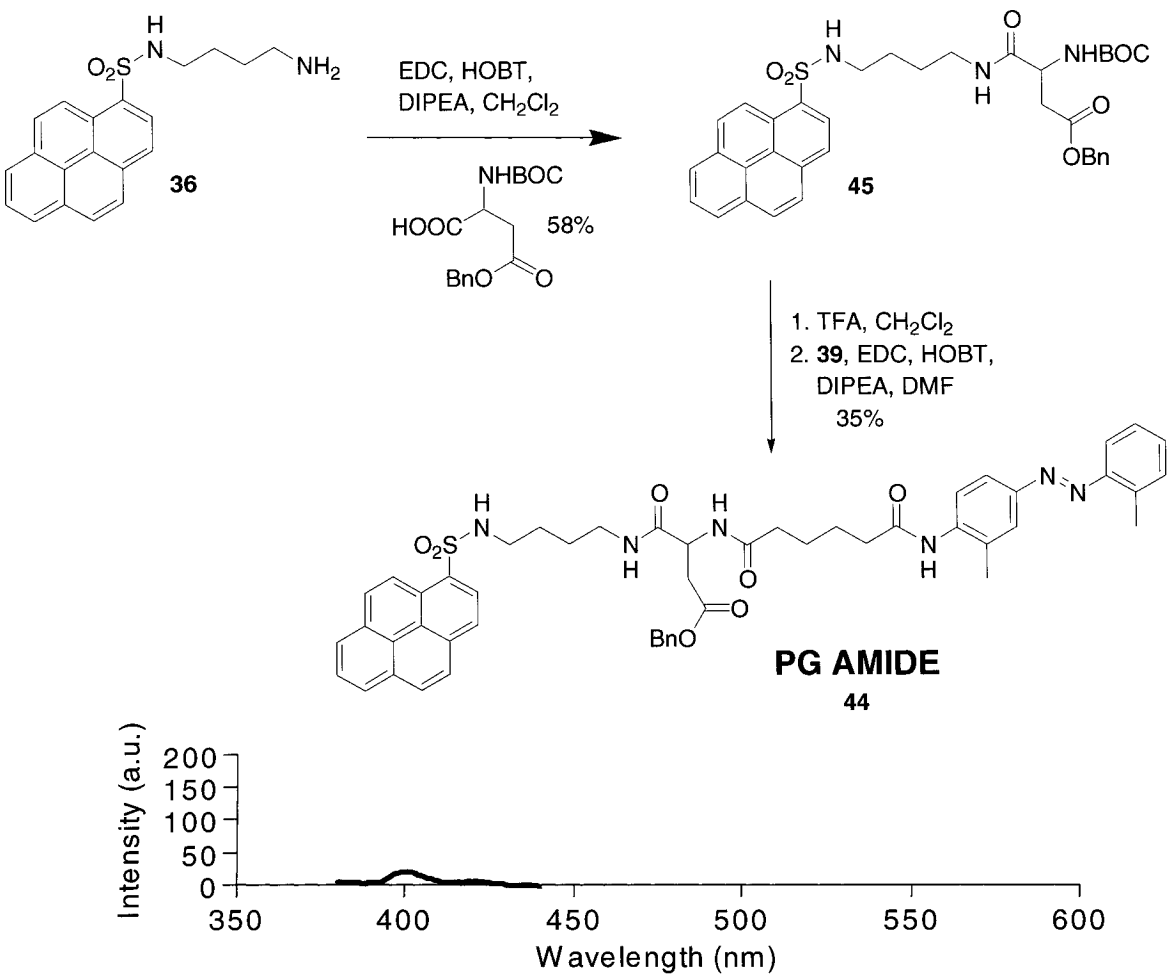

Scheme 12. Synthesis and Emission Spectrum of PG Amide (ex/em slits= 5nm/5nm).

Once again, the covalently bonded GBC was able to prevent fluorescence of the donor, in this case, PYR, which emits light at 400 nm.

With the desired substrates in hand, a *pseudo*-hydrolysis experiment was devised to establish the relationship between the concentration of free donor molecules (hydrolysis products) and their emission intensity. Since each donor molecule fluoresced at a characteristic wavelength, product conversion and product ratio could be determined from a calibration curve.

Stock solutions (1.54×10^{-3}M) were prepared in dichloromethane and from these, 34 solutions containing specific amounts of each substrate were formulated to mimic different hydrolysis situations starting from 1.54×10^{-4}M of the DPG amide. Hydrolysis that was selective for the release of the Dansyl moiety (solutions 1-11) was simulated by a set of 11 equimolar solutions with increasing concentration of DNSBOC **32**. To accurately represent the reaction, the amounts of the starting material, DPG Amide, and of the possible hydrolysis products, were adjusted accordingly for each solution. Thus, for the hydrolysis of **42** that had proceeded to an extent of 40%, a solution with 6 part **42**, 4 part **32** and 4 part **44** was created (Solution 5, Table 4).

Selective to DNS	**Volume (X 10^{-1}mL)**				
Solutions	**DPG AMIDE**	**DNSBOC**	**PG AMIDE**	**PYRBOC**	**DG AMIDE**
1	10	0	0	0	0
2	9	1	9	0	0
3	8	2	8	0	0
4	7	3	7	0	0
5	6	4	6	0	0
6	5	5	5	0	0
7	4	6	4	0	0
8	3	7	3	0	0
9	2	8	2	0	0
10	1	9	1	0	0
11	0	10	0	0	0

Table 4. Relative Amounts of Substrates for *Pseudo*-Hydrolysis of 42 that is Selective for the Release of Dansyl. Prepared from 1.54×10^{-3}M Stock Solutions.

A similar set of solutions for selective hydrolysis with respect to Pyrene (solutions 12-22) was also prepared. In the case where non-selective hydrolysis occurs, solutions with one donor held at a constant concentration (corresponding to 50% hydrolysis) and the other donor varied were formulated (solutions 23-34).

Selective to PYR	Volume (X 10^{-1}mL)				
Solutions	**DPG AMIDE**	**DNSBOC**	**PG AMIDE**	**PYRBOC**	**DG AMIDE**
12	10	0	0	0	0
13	9	0	0	1	9
14	8	0	0	2	8
15	7	0	0	3	7
16	6	0	0	4	6
17	5	0	0	5	5
18	4	0	0	6	4
19	3	0	0	7	3
20	2	0	0	8	2
21	1	0	0	9	1
22	0	0	0	10	0

Table 5. Relative Amounts of Substrates for *Pseudo*-Hydrolysis of **42** that is Selective for the Release of Pyrene. Prepared from 1.54 x 10^{-3}M Stock Solutions.

Non-Selective	Volume (X 10^{-1}mL)				
Solutions	DPG AMIDE	DNSBOC	PG AMIDE	PYRBOC	DG AMIDE
DNSBOC Varied PYRBOC Held Constant at 50%					
23	5	0	0	5	5
24	4	1	1	5	5
25	3	2	2	5	5
26	2	3	3	5	5
27	1	4	4	5	5
28	0	5	5	5	5
PYRBOC Varied DNSBOC Held Constant at 50%					
29	5	5	5	0	0
30	4	5	5	1	1
31	3	5	5	2	2
32	2	5	5	3	3
33	1	5	5	4	4
34	0	5	5	5	5

Table 6. Relative Amounts of Substrates for *Pseudo*-Hydrolysis of **42** that is Non-selective. Prepared from 1.54 x 10^{-3}M Stock Solutions.

Table 4-6 documents the relative amounts of each reaction components in each solution. Each solution was scanned with the usual excitation wavelength of 370nm as well as at 315 nm and 340 nm for sake of comparison (5 nm/5 nm slit widths). The emission intensity at 500 nm and 400 nm for DNS and PYR were recorded and translated to a set of graphs (Figures 28-31). As previous data (Figure 25) had proven that intramolecular quenching is mediated superbly by GBC, we were confidant that any fluorescence was a direct result of free donor molecules in solution.

To correct for any errors in concentration, each solution was spiked with an internal standard and analyzed by HLPC. The following graphs compare the theoretical concentration of the donors in each solution with the calculated value obtained by HPLC.

A) Selective for Dansyl: Solutions 1-11.

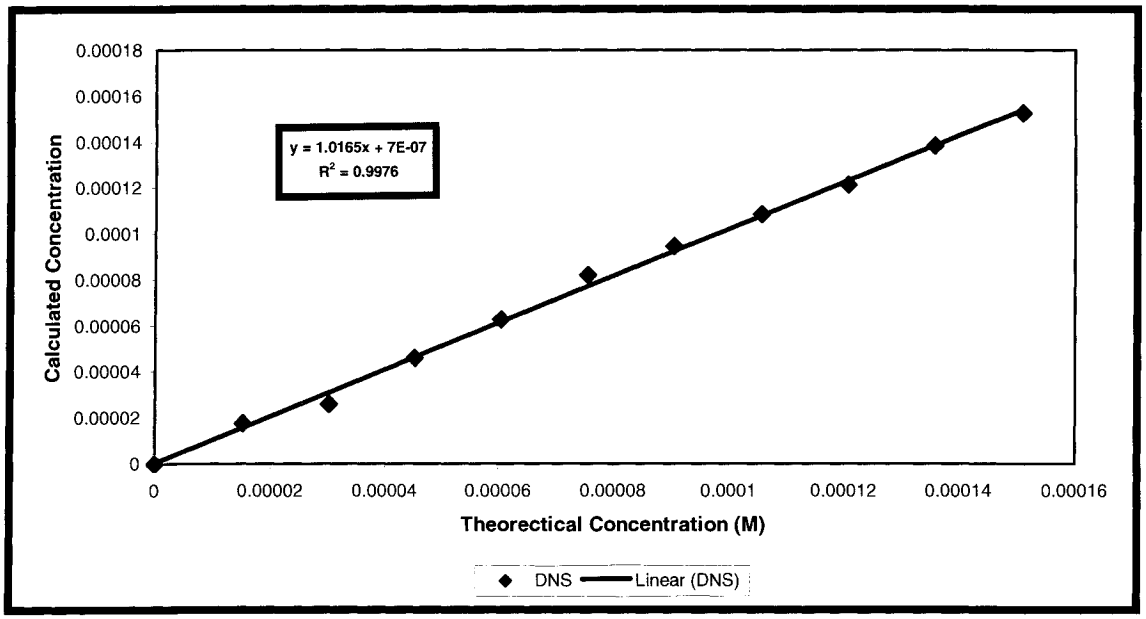

B) Selective for Pyrene: Solutions 12-22.

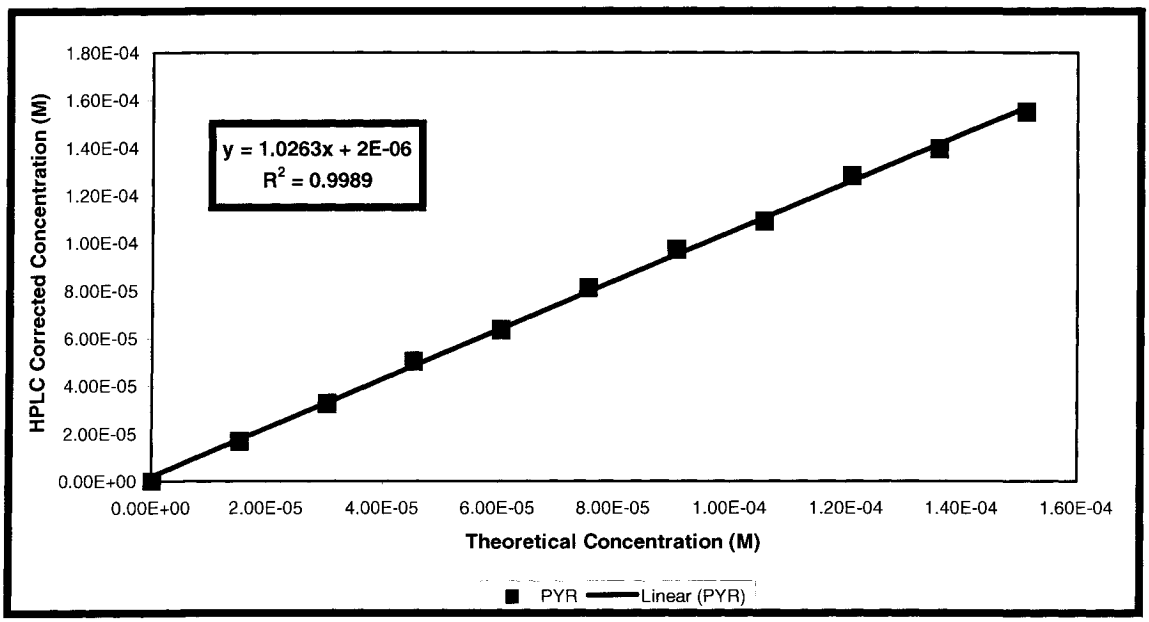

C) Nonselctive Reaction - Dansyl Varied, Pyrene Held Constant at 7.55 X 10^{-5}M (50% Hydrolyzed): Solutions 23-28.

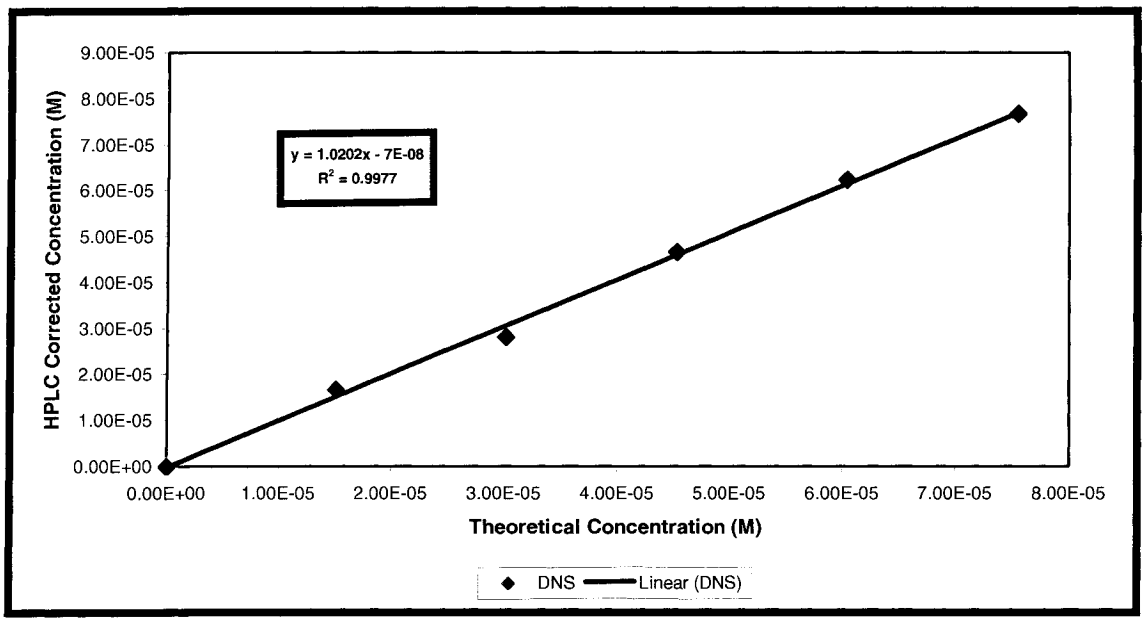

D) Nonselective Reaction - Pyrene Varied, Dansyl Held Constant at 7.55 X 10^{-5}M (50% Hydrolyzed): Solutions 29-34.

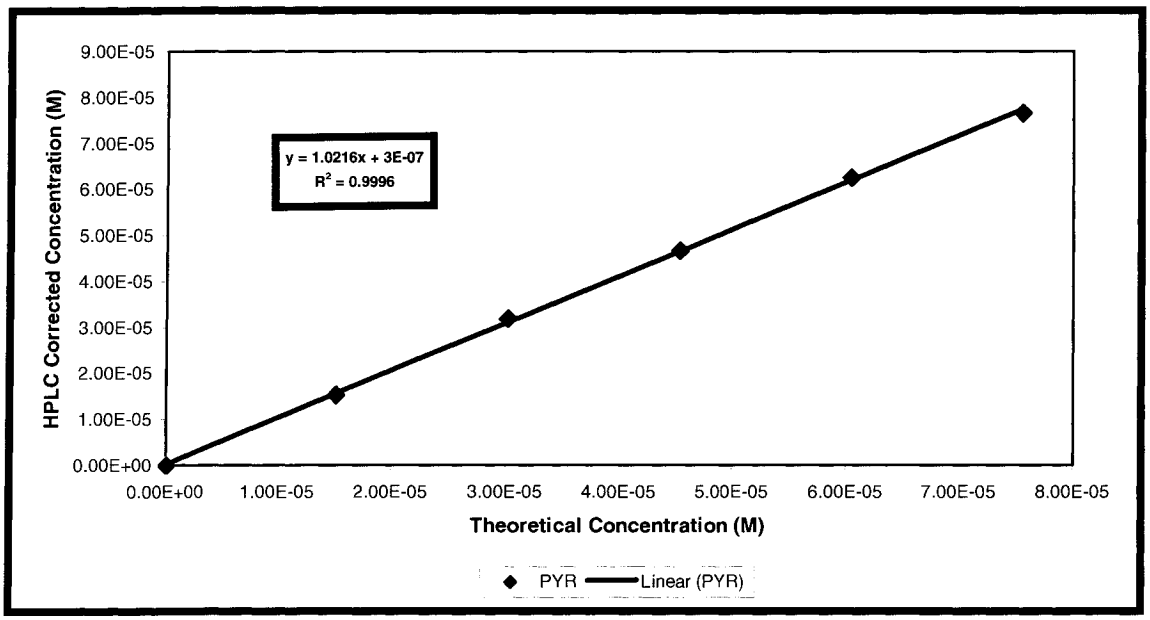

Figure 27. Comparison Between Theoretical and HPLC Corrected Concentrations of Solution Sets for Pseudo-Hydrolysis Study.

As a linear trend was observed for each case, accuracy in the preparation of the solution sets was confirmed. Charts associating the emission intensity and the corrected concentration of the each donor were then plotted (Figures 28-31).

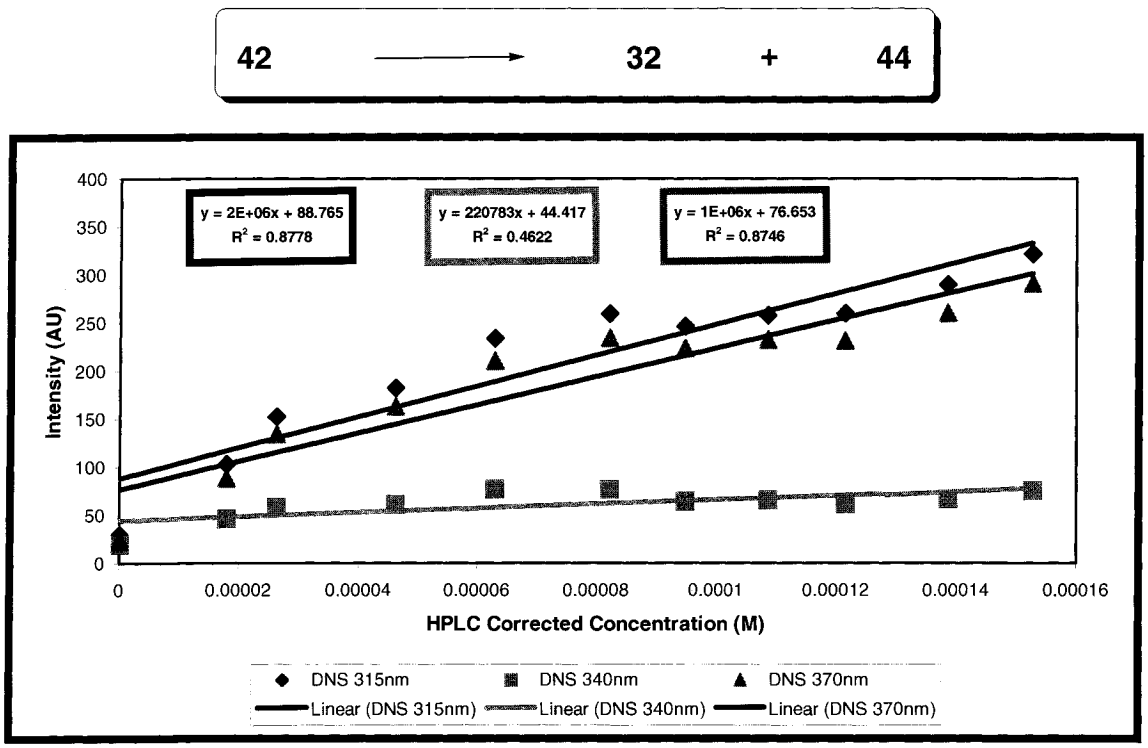

Figure 28. Correlation Between Donor Intensity and HPLC Corrected Concentrations of Solutions 1-11 (Selective for Dansyl) for *Pseudo*-Hydrolysis Study.

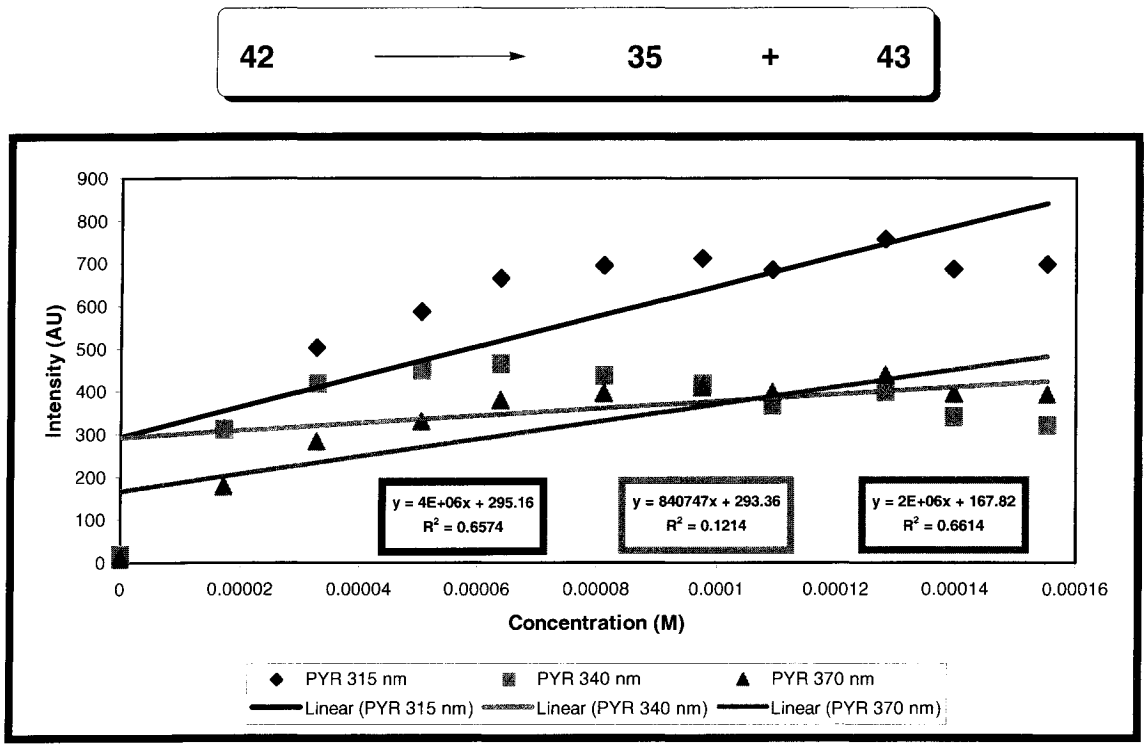

Figure 29. Correlation Between Donor Intensity and HPLC Corrected Concentrations of Solutions 12-22 (Selective for Pyrene) for *Pseudo*-Hydrolysis Study.

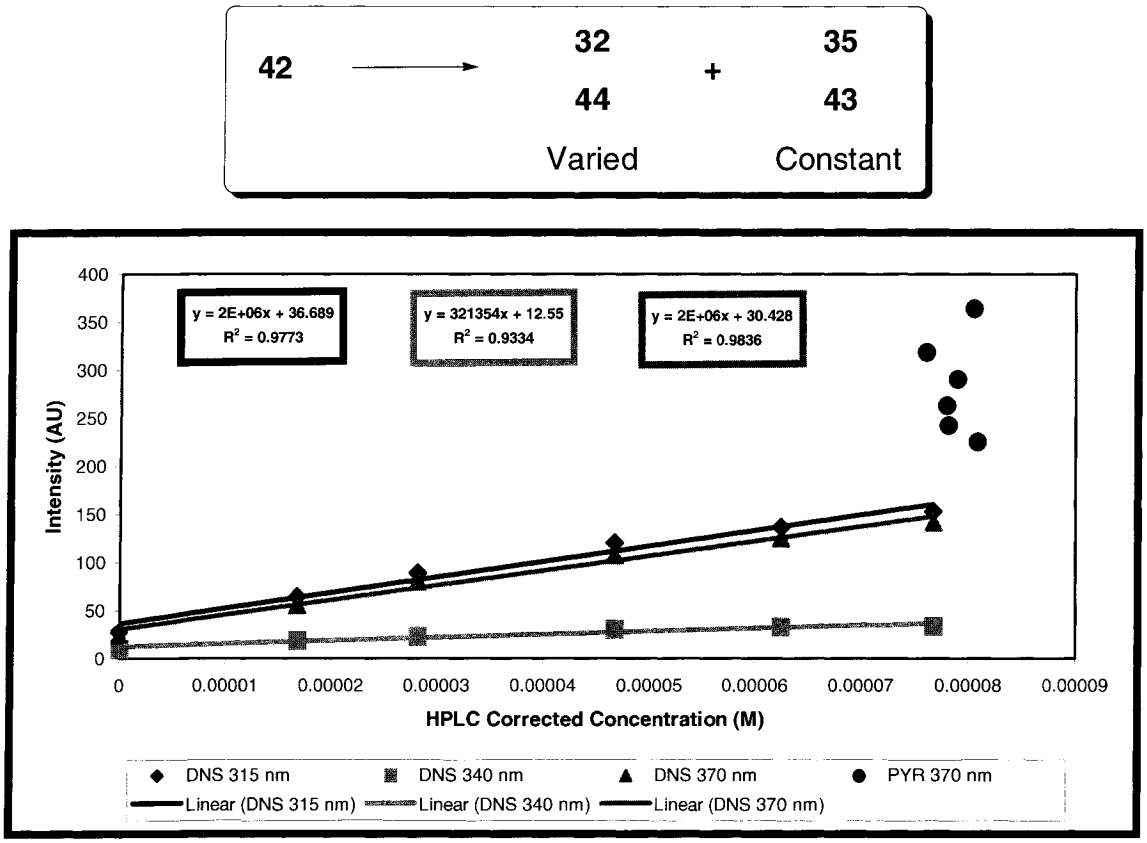

Figure 30. Correlation Between Donor Intensity and HPLC Corrected Concentrations of Solutions 23-28 (Non-selective Reaction) for *Pseudo*-Hydrolysis Study. Dansyl Varied, Pyrene Held Constant at 7.55 X 10^{-5}M (50% Hydrolyzed).

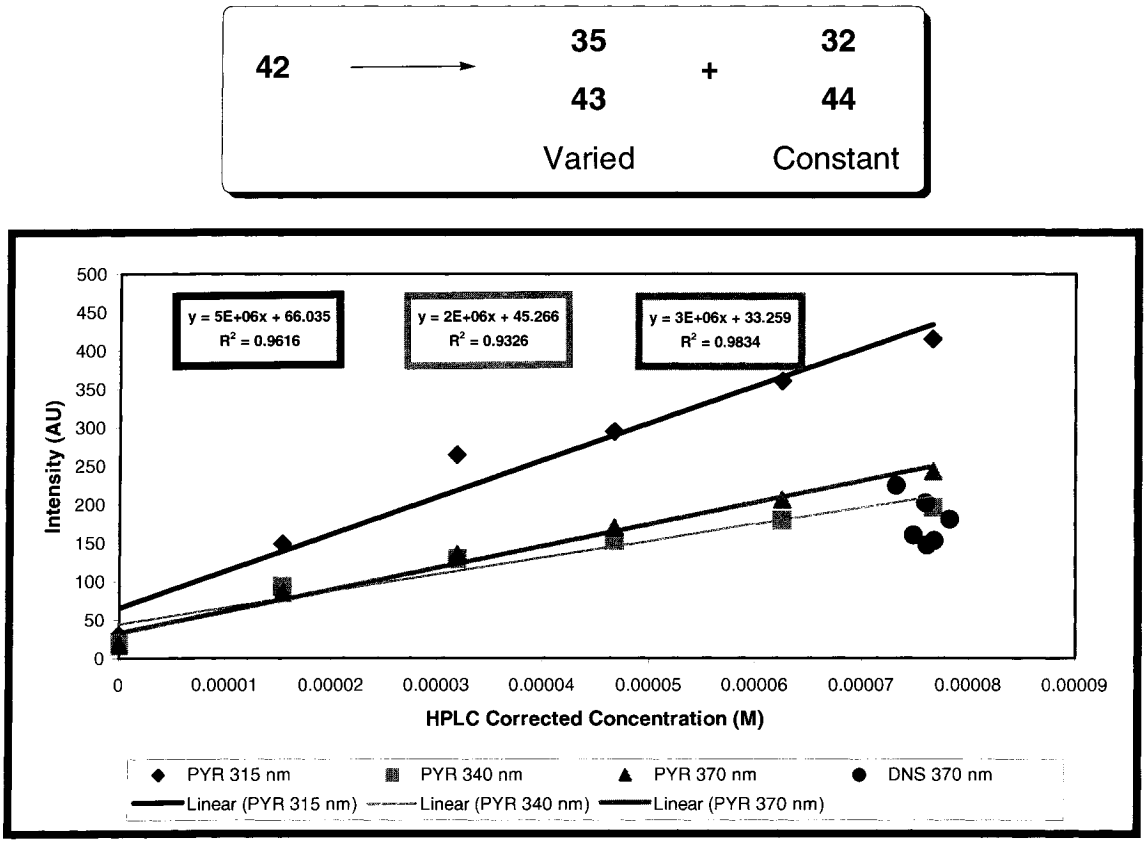

Figure 31. Correlation Between Donor Intensity and HPLC Corrected Concentrations of Solutions 29-34 (Nonselective Reaction) for *Pseudo*-Hydrolysis Study. Pyrene Varied, Dansyl Held Constant at 7.55 X 10^{-5}M (50% Hydrolyzed).

Ideally, the plots should show that the donor emission intensity varies linearly with its concentration. In the non-selective experiment (Figures 30-31), one donor molecule's concentration was varied while the second one was always kept at a constant. As such, plotting the results of the latter should give a single point. Although this was not the case in Figures 30-31, the graph points corresponding to the donor whose concentration was held constant in the different solutions, were clustered in the same area. This slight variation in results was regarded to be quite acceptable.

Observing Figures 28-31, we were disappointed to see that linearity was not consistent for each hydrolysis situation. However, we could not clearly attribute this as a disproof of our hypothesis that FRET could be applied as a technique to measure yield and selectivity. Concerns regarding the validity of the experimental results were raised due to the poor solubility of the starting material DPG Amide **42**. Indeed, examination of the stock solution of DPG Amide showed that the compound had precipitated out, despite having been prepared in low concentration. This indicated that the dissolved concentration is different from the calculated concentration. The presence of precipitate in solution can affect how much light is absorbed by the solution (in other words quantum yield) and therefore negatively affect fluorescence output. This reasoning was further supported by the fact that better correlation was observed in situations where solutions contained lesser amounts of **42**, such as in the cases of non-selective hydrolysis (Figures 30-31). The poor solubility of **42**, can explain in part the non – linearity of the plots in Figures 28-31, although other unidentified factors were also likely to be contributing.

We felt that the limited solubility of DPG Amide was partly due to the numerous amide bonds present in the molecule. Two conceivable options for resolving this problem included changing the solvent or changing the substrate. The latter, although more cumbersome, was pursued because in future applications, it would be best to have a substrate that exhibited solubility in a variety of solvents. Good solvent compatibility would definitely expand the scope of the assay for eventual catalyst scanning.

3.2.2 Hydrolysis Mimic: Esters Series.

To address the issue of substrate solubility, we decided to replace two of the amide linkages in DPG Amide **42** with esters functionalities. This would be a simple modification to our original synthetic scheme for the amides series, in

which 5-aminopentanol would replace the 1,4-diaminobutane linker. The following scheme shows how this ester series would be implemented in our *pseudo*-hydrolysis reaction.

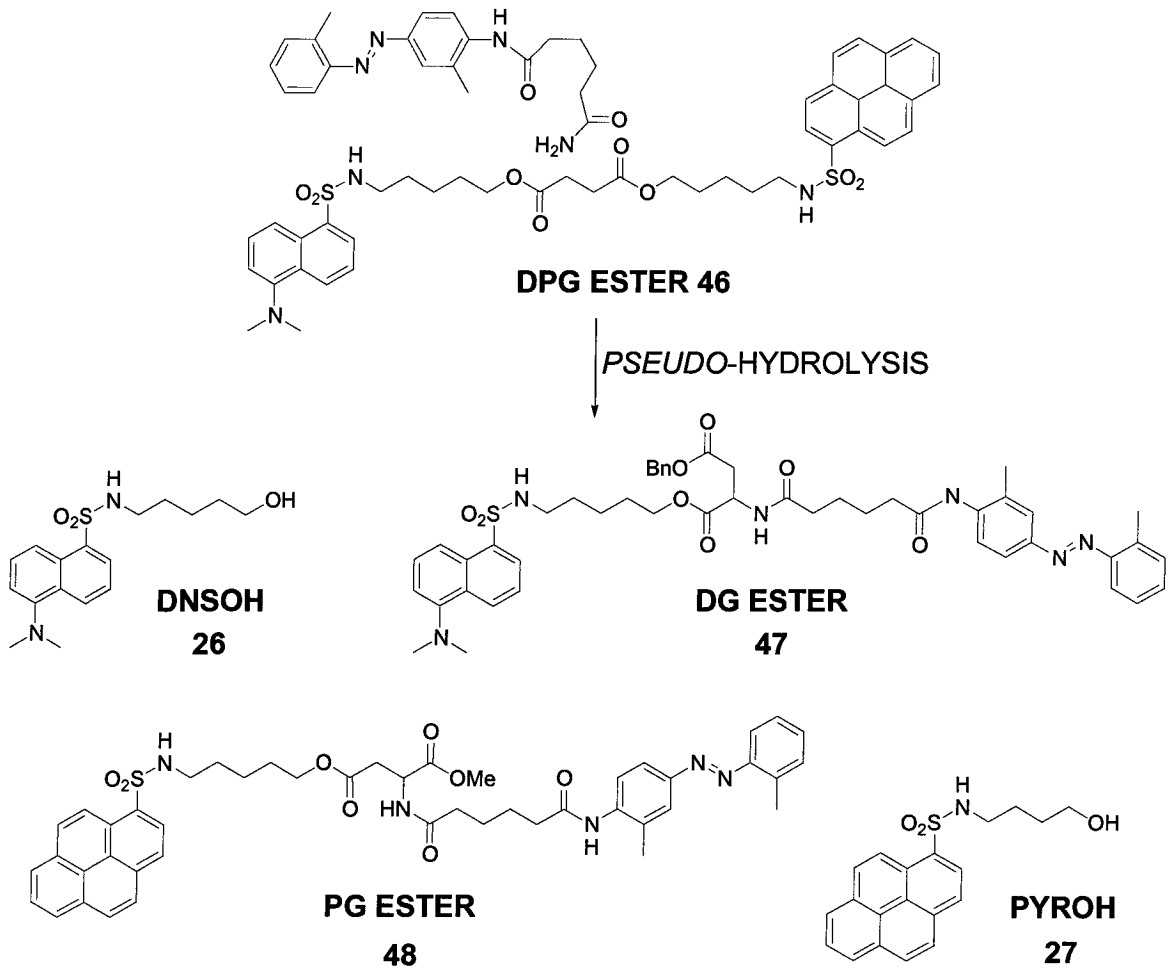

Figure 32. Mimic of Hydrolysis with Ester Series.

Preparation of the donors proceeded in a straightforward manner. Dansyl chloride reacted cleanly with the amino alcohol **49** in a S_N2 reaction to deliver the alcohol product **26** in 96% yield. The primary amino group, being more nucleophillic then the alcohol functionality, eliminated the need for protection of the latter. Pyrene sulfonyl chloride, whose synthesis has already been discussed, was reacted similarly to give **27**. Fluorescence spectra, taken in dichloroethane, produced the expected peaks for the Dansyl and Pyrene moieties.

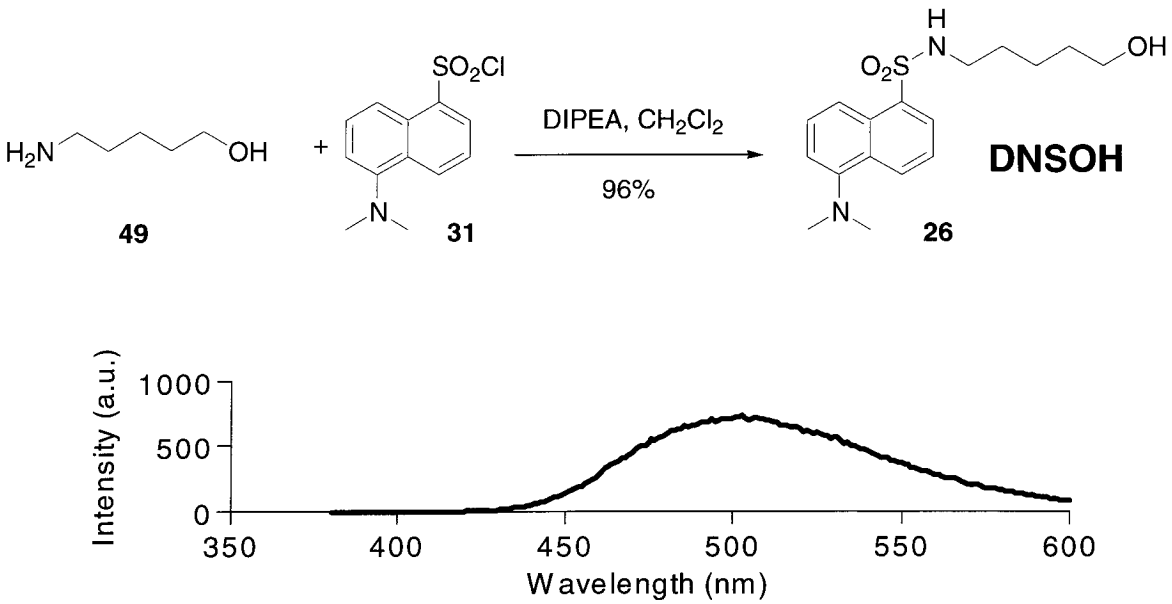

Scheme 13. Synthesis and Emission Spectrum of DNSOH.

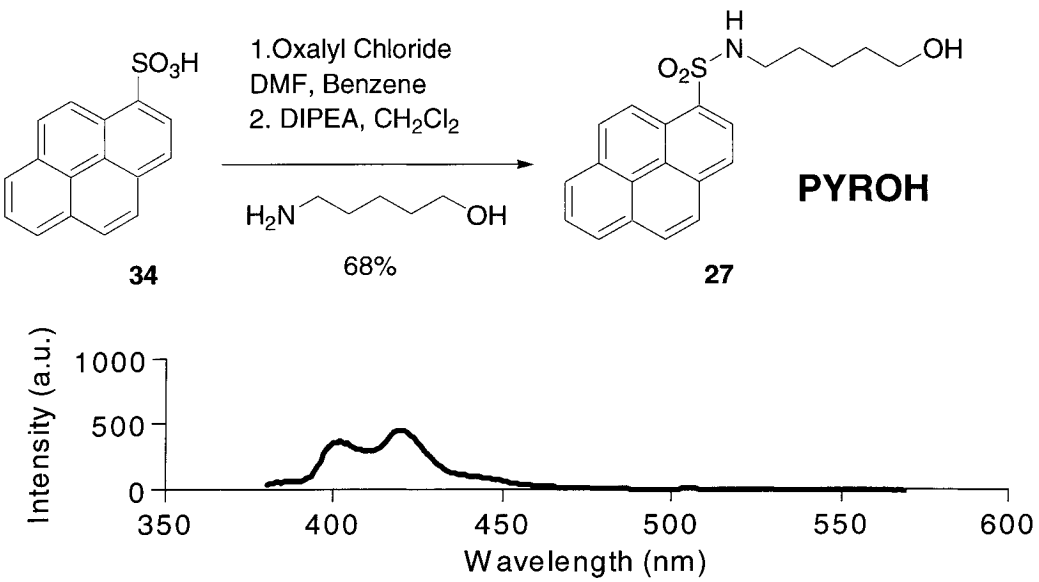

Scheme 14. Synthesis and Emission Spectrum of PYROH **27**.

This change in solvent choice was motivated by the desire to find a solvent that was less volatile then the original dichloromethane. We ultimately would like to pursue this assay in a wellplate format and a less volatile solvent would be better suited for such a purpose. Dichloroethane (b.p. 80 °C) seemed to be a wise replacement for the dichloromethane (b.p. 40°C) since both solvents have similar properties with the exception of volatility.

Aspartic acid served as a building block once again to unite PYR, DNS and GBC in the same molecule. The preparation of the target structure **46** was similar to that of DPG Amide.

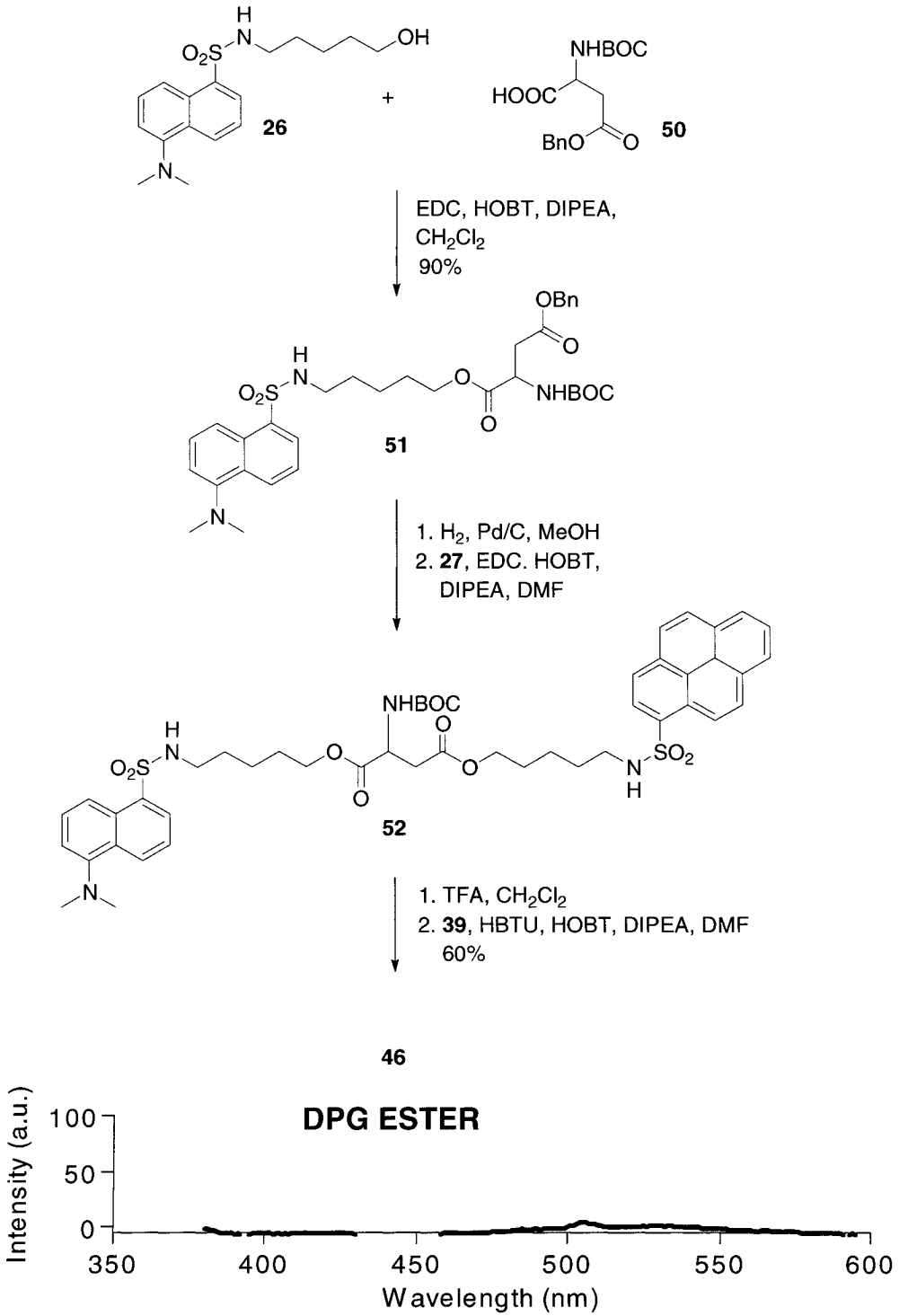

Scheme 15. Synthesis and Emission Spectrum of DPG Ester **46**.

Fluorescence at 500 nm for DNS and 400 nm for PYR was not observed for the DPG Ester as quenching was mediated by the GBC acceptor molecule. DG Ester and PG Ester were also prepared in a manner much analogous to their amide counterparts.

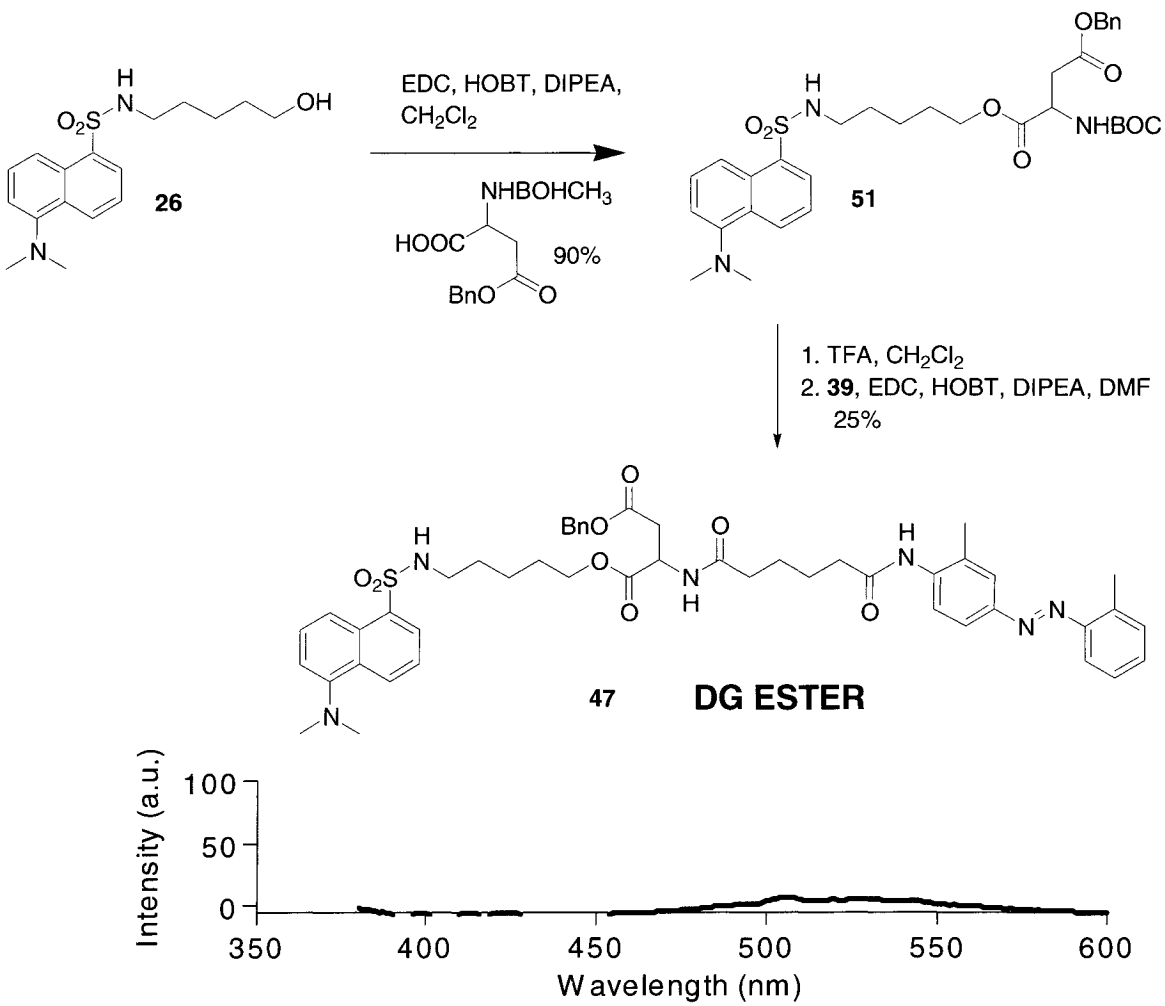

Scheme 16. Synthesis and Emission Spectrum of DG Ester 47.

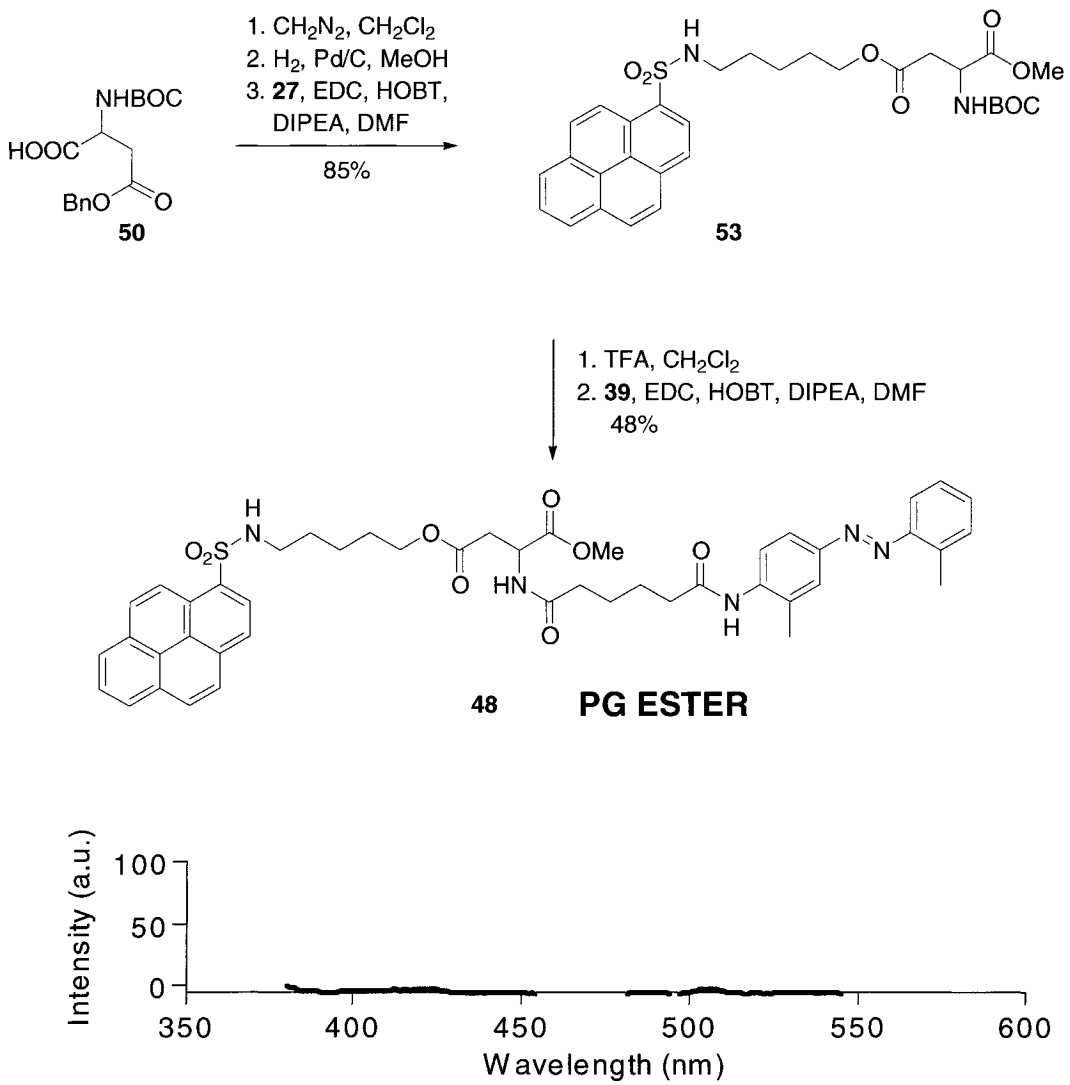

Scheme 17. Synthesis and Emission Spectrum of PG Ester **48**.

Three differences were noteworthy in this reaction scheme. The first being that benzyl deprotection mediated by hydrogen gas and palladium catalyst proceeded smoothly with the ester substrates. PYROH was installed to beta carboxy group to be consistent with the DPG Ester product. In addition to this, the yield for each step of the synthesis, although not always ideal, was usually superior to that of the amide series.

The ester components were used to create 1.54 X 10^{-3} M stock solutions using dichloroethane as a solvent. From these, as in the case of the amide series, a set of solutions was prepared to mimic the hydrolysis of the DPG Ester **46**. The experimental setup was such that each solution would represent the hydrolysis of **46** with a starting concentration of 1.54 X 10^{-4} M. Depending on the extent and selectivity of hydrolysis, the amounts of DPG ester and the hydrolysis products (DNSOH, PG Ester, PYROH, DG Ester) were adjusted accordingly for each individual solution. Eleven solutions (Table 7) were fabricated to represent hydrolysis that was selective for releasing the Dansyl moiety. Similarly, a second set of solutions was also created to represent the hydrolysis that was selective to the Pyrene donor (Table 8).

Selective to DNS	**Volume (X 10^{-1} mL)**				
Solutions	**DPG ESTER**	**DNSOH**	**PG ESTER**	**PYROH**	**DG ESTER**
1	10	0	0	0	0
2	9	1	9	0	0
3	8	2	8	0	0
4	7	3	7	0	0
5	6	4	6	0	0
6	5	5	5	0	0
7	4	6	4	0	0
8	3	7	3	0	0
9	2	8	2	0	0
10	1	9	1	0	0
11	0	10	0	0	0

Table 7. Relative Amounts of Substrates for *Pseudo*-Hydrolysis of **46** that is Selective for the Release of Dansyl. Prepared from 1.54 x 10^{-3}M Stock Solutions.

Selective to PYR	Volume (X 10^{-1} mL)				
Solutions	**DPG ESTER**	**DNSOH**	**PG ESTER**	**PYROH**	**DG ESTER**
12	10	0	0	0	0
13	9	0	0	1	9
14	8	0	0	2	8
15	7	0	0	3	7
16	6	0	0	4	6
17	5	0	0	5	5
18	4	0	0	6	4
19	3	0	0	7	3
20	2	0	0	8	2
21	1	0	0	9	1
22	0	0	0	10	0

Table 8. Relative Amounts of Substrates for *Pseudo*-Hydrolysis of 46 that is Selective for the Release of Pyrene. Prepared from 1.54 x 10^{-3}M Stock Solutions.

Hydrolysis that was non-selective was also simulated. A set of solutions were prepared such that one fluorescence donor was always present at a concentration that was equivalent to being 50% hydrolyzed, while the concentration of the second donor was varied.

Non-Selective	Volume (X 10^{-1} mL)				
Solutions	DPG ESTER	DNSOH	PG ESTER	PYROH	DG ESTER
DNSBOC Varied PYRBOC Held Constant at 50%					
23	5	0	0	5	5
24	4.5	0.5	0.5	5	5
25	4	1	1	5	5
26	3.5	1.5	1.5	5	5
27	3	2	2	5	5
28	2.5	2.5	2.5	5	5
29	2	3	3	5	5
30	1.5	3.5	3.5	5	5
31	1	4	4	5	5
32	0.5	4.5	4.5	5	5
33	0	5	5	5	5
PYRBOC Varied DNSBOC Held Constant at 50%					
34	5	5	5	0	0
35	4.5	5	5	0.5	0.5
36	4	5	5	1	1
37	3.5	5	5	1.5	1.5
38	3	5	5	2	2
39	2.5	5	5	2.5	2.5
40	2	5	5	3	3
41	1.5	5	5	3.5	3.5
42	1	5	5	4	4
43	0.5	5	5	4.5	4.5
44	0	5	5	5	5

Table 9. Relative Amounts of Substrates for *Pseudo*-Hydrolysis of **46** that is Non-selective. Prepared from 1.54 x 10^{-3}M Stock Solutions.

We also wanted to study a case where hydrolysis was random as oppose to the idealist situations represented by Tables 7-9. The donor concentrations of the solutions in Table 10 were arbitrarily chosen to illustrate such a case.

Random	Volume (X 10^{-1} mL)				
Solutions	DPG ESTER	DNSOH	PG ESTER	PYROH	DG ESTER
45	8	1	1	2	2
46	3	4	4	3	3
47	1	8	8	1	1
48	0	7	7	3	3
49	3	1	1	6	6
50	7	2	2	1	1
51	5	3	3	2	2
52	6	1	1	3	3
53	8	1	1	1	1
54	5	4	4	1	1
55	1	3	3	6	6

Table 10. Relative Amounts of Substrates for the Random *Pseudo*-Hydrolysis of **46**. Prepared from 1.54 x 10^{-3}M Stock Solutions.

Each of the 55 solutions was evaluated by a fluorescence spectrophotometer using a quartz cuvette (path length = 1 cm). The excitation/emission slit widths were set to 5nm/10nm and an excitation wavelength of 370 nm was applied. The emission intensity for Dansyl and Pyrene were recorded at 500 nm and 400 nm respectively. To further attest to the feasibility of applying FRET as a high throughput screening method, the 55 solutions were also loaded on a 96 wellplate and evaluated. The fluorescence screening parameters for the analysis by cuvette, were also used for the wellplate study with the exception that 10nm/10nm slit widths were applied. Before relating the emission intensity to the donor concentrations in a plot, HPLC analysis of each solution to verify the actual concentration of the donors was pursued. This was made possible by including an internal standard in each solution.

A) Selective for DND: Solutions 1-11

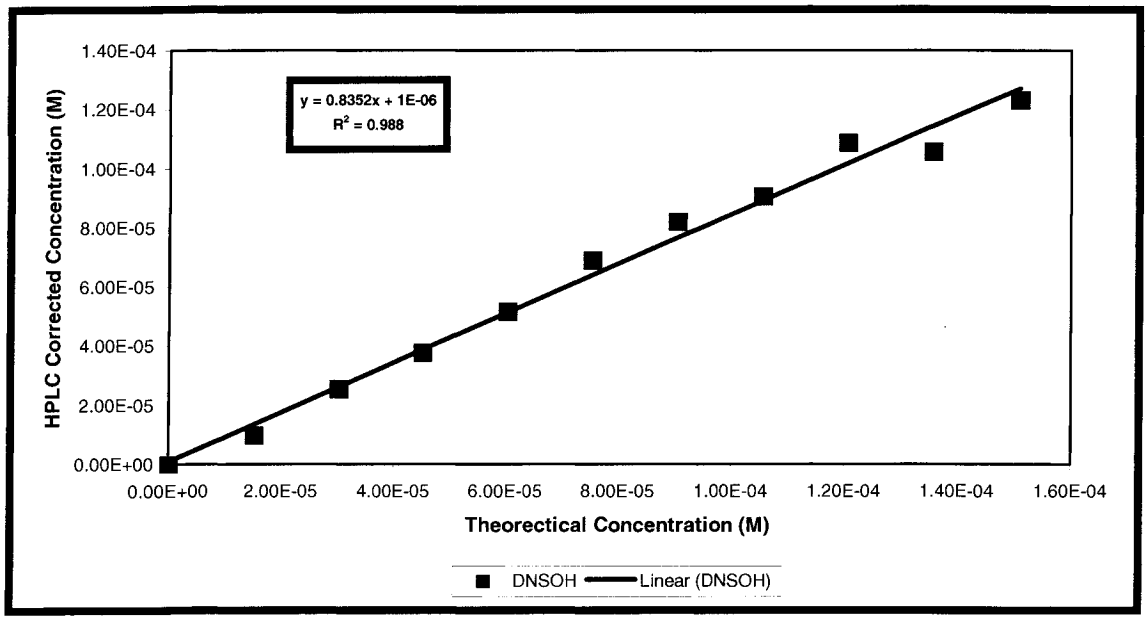

B) Selective for PYR: Solutions 12-22

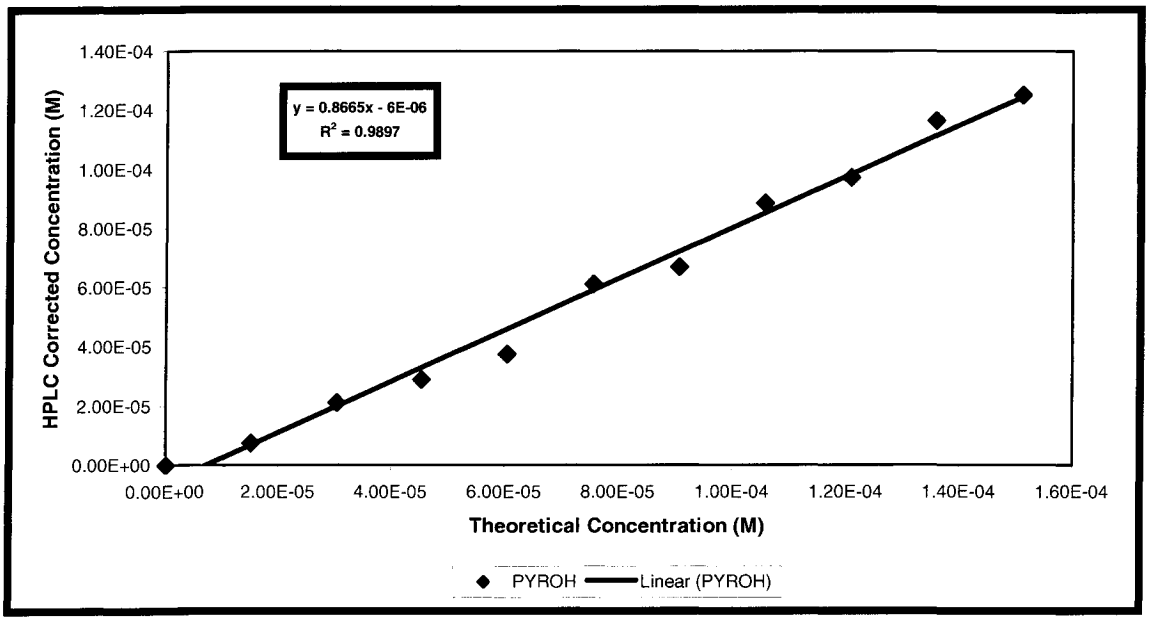

C) Non-selective Reaction – DNS varied, PYR Held Constant at 7.55 X 10^{-5} M (50%) Hydrolyzed: Solutions 23-33.

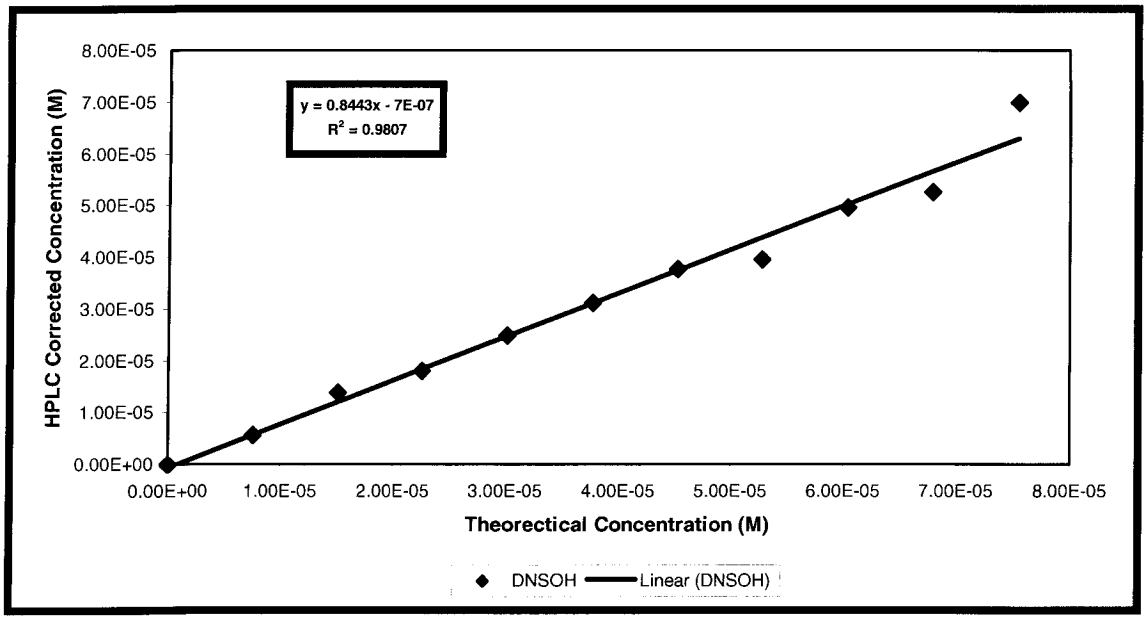

D) Non-selective Reaction – PYR varied, DNS Held Constant at 7.55 X 10^{-5} M (50%) Hydrolyzed: Solutions 34-44.

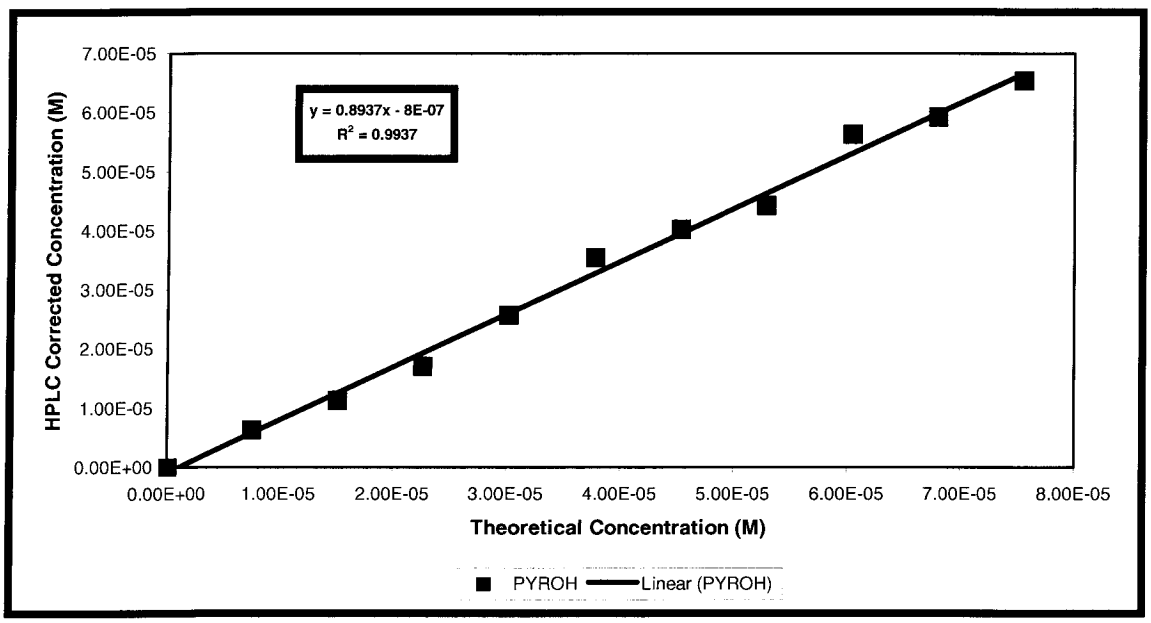

E) Random Hydrolysis: Solutions 34-44.

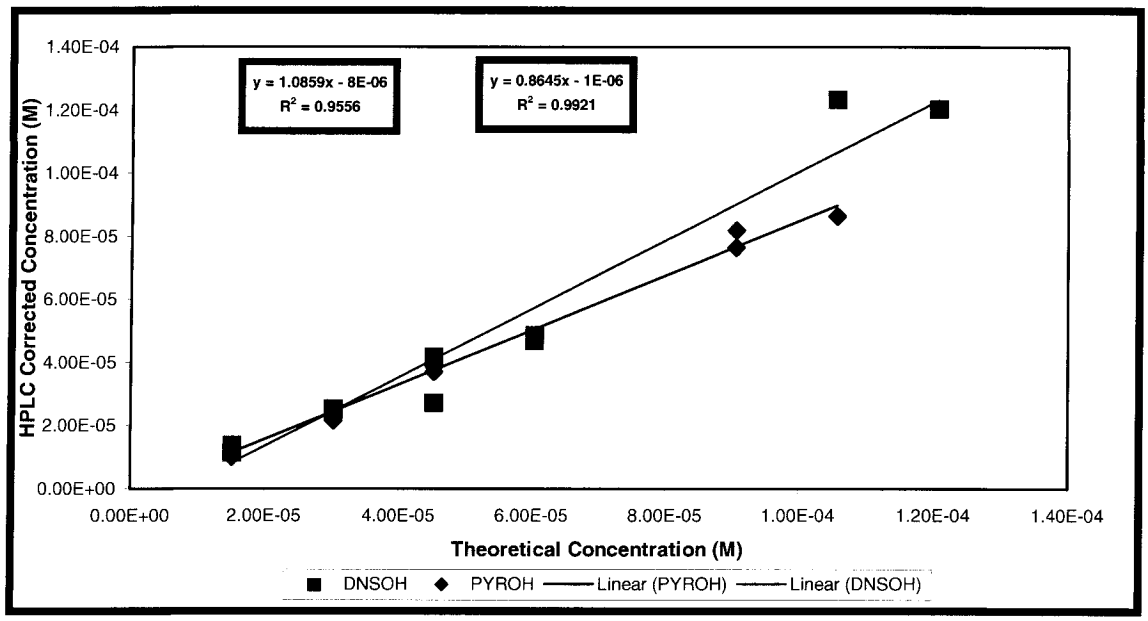

Figure 33. Comparison between the Theoretical and HPLC Corrected Concentraton of Solution Sets for *Pseudo*-Hydrolysis Study.

A comparison between the theoretical and HPLC corrected concentrations of the DNSOH and PYROH donors showed that indeed the solutions were prepared consistently. The corrected concentrations were plotted to emission intensities of the two donor molecules to determine the relationship between the two.

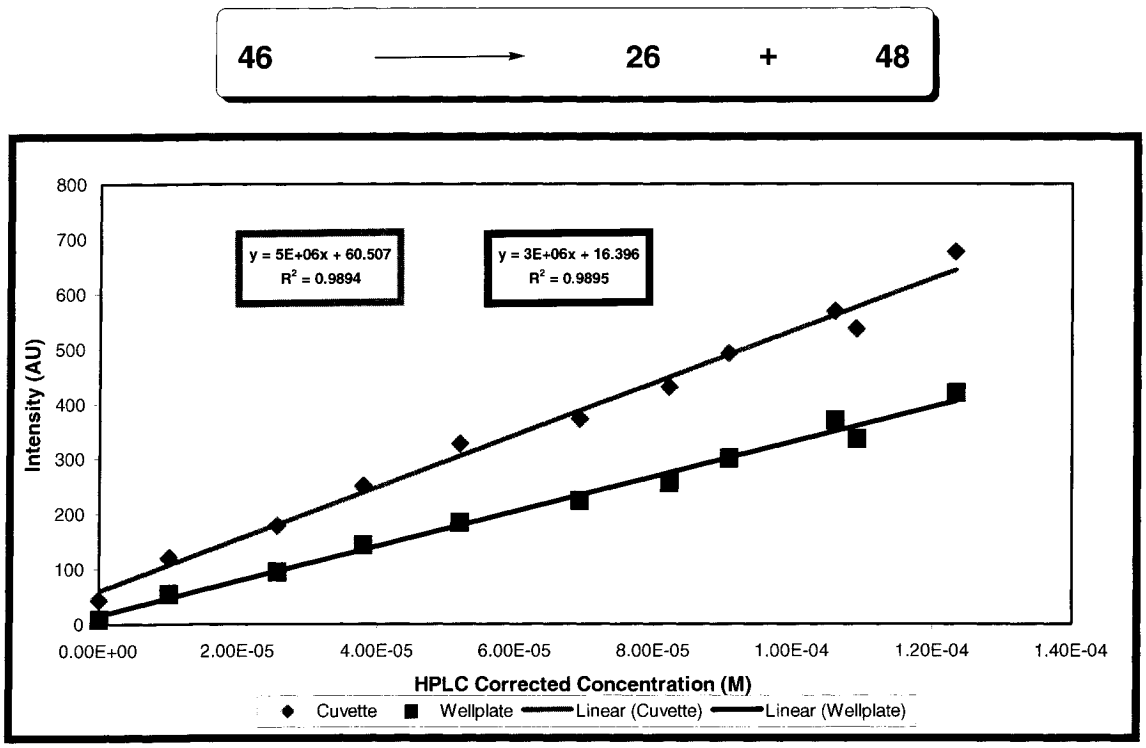

Figure 34. Correlation Between Donor Intensity and HPLC Corrected Concentrations of Solutions 1-11 (Selective for Dansyl) for *Pseudo*-Hydrolysis Study.

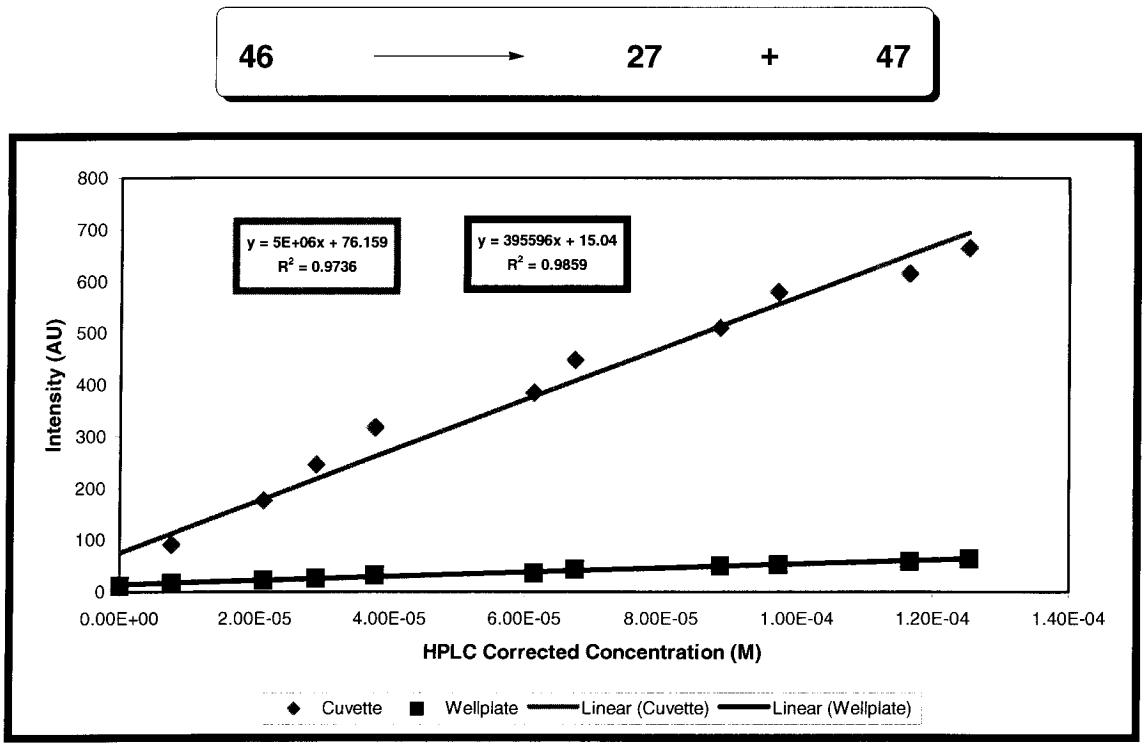

Figure 35. Correlation Between Donor Intensity and HPLC Corrected Concentrations of Solutions 12-22 (Selective for Pyrene) for *Pseudo*-Hydrolysis Study.

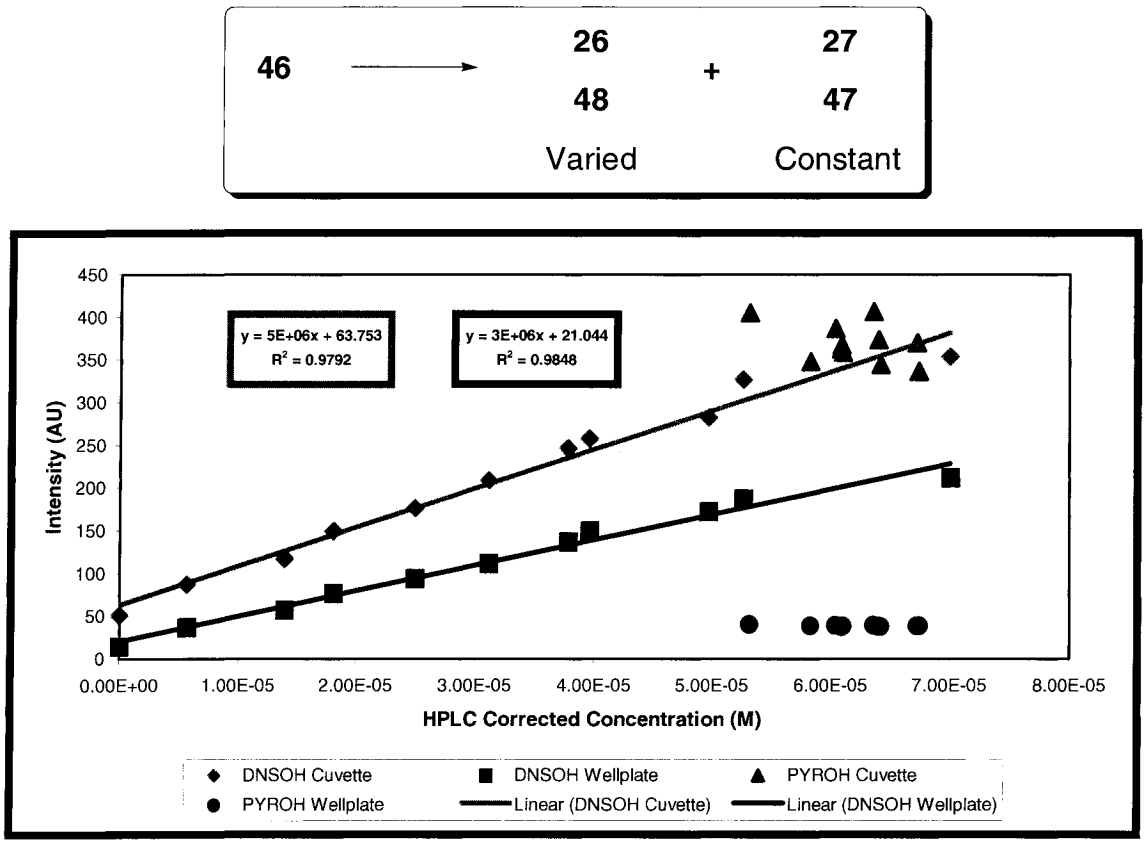

Figure 36. Correlation Between Donor Intensity and HPLC Corrected Concentrations of Solutions 23-33 (Nonselective Reaction) for *Pseudo*-Hydrolysis Study. Dansyl Varied, Pyrene Held Constant at 7.55 X 10^{-5}M (50% Hydrolyzed).

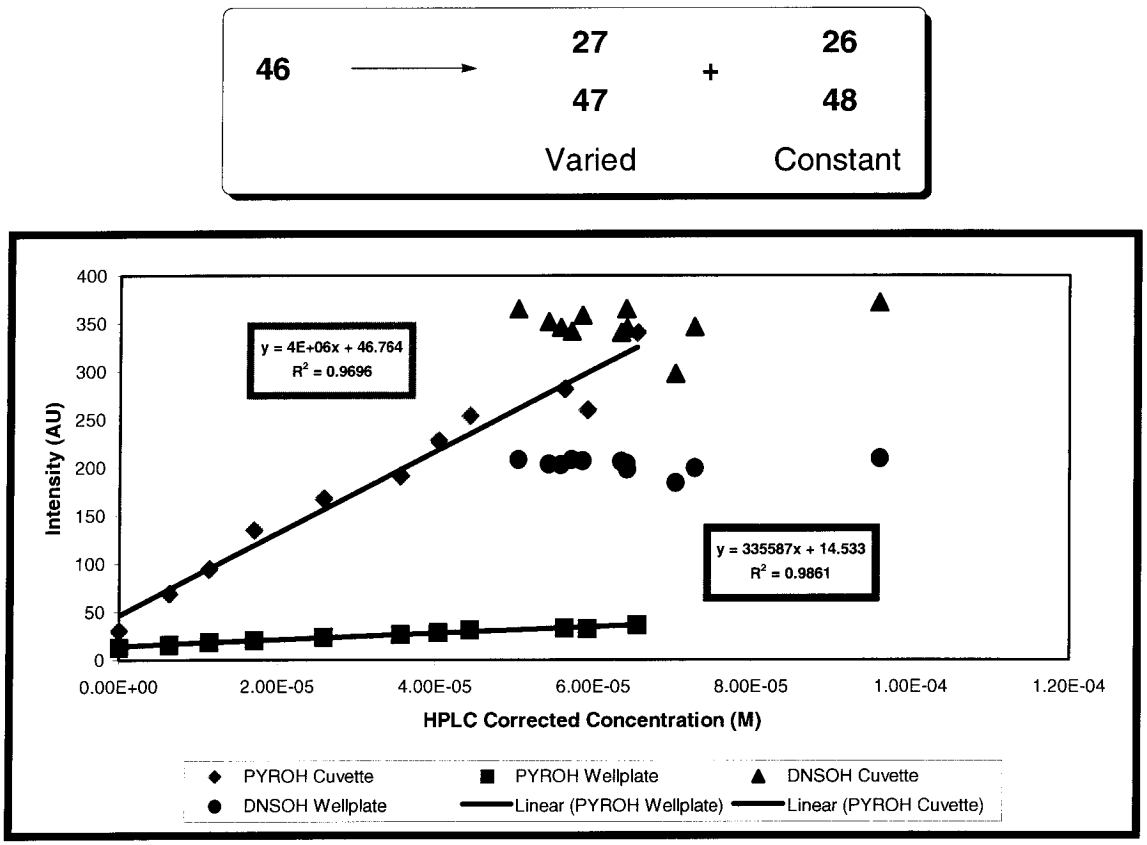

Figure 37. Correlation Between Donor Intensity and HPLC Corrected Concentrations of Solutions 34-44 (Nonselective Reaction) for *Pseudo*-Hydrolysis Study. Pyrene Varied, Dansyl Held Constant at 7.55 X 10^{-5}M (50% Hydrolyzed).

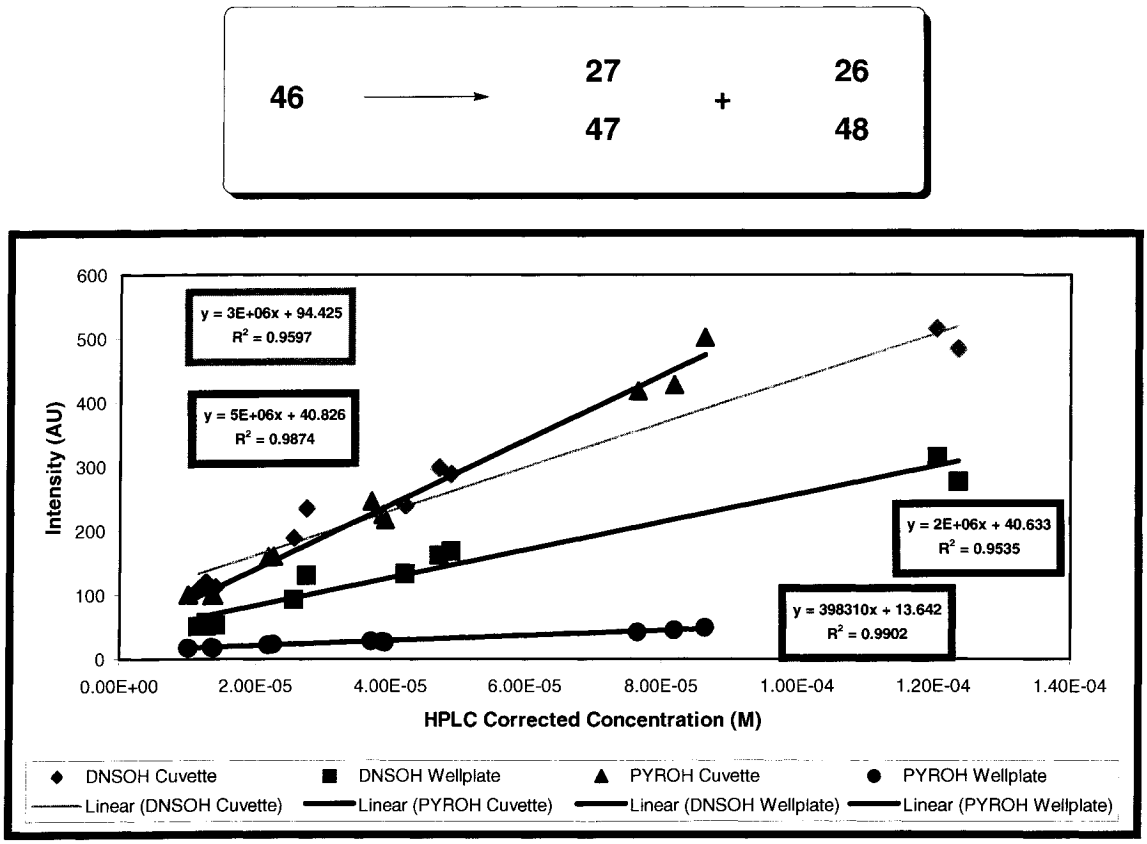

Figure 38. Correlation Between Donor Intensity and HPLC Corrected Concentrations of Solutions 45-55 (Random Reaction) for *Pseudo*-Hydrolysis Study.

Much to our satisfaction, the different hydrolysis situations represented by Figures 34-38, confirmed that indeed the concentration of the fluorescence donor molecule was proportional to its emission intensity. In the case of non-selective hydrolysis (Figure 36-37) the cluster of spots represents the donor that was held at a constant concentration although in an idea situation this would be characterized by a single spot. Despite this, regardless of whether the hydrolysis was selective for a particular donor, non-selective or random, good linearity was observed in the corresponding plots. The linear dependence between the fluorescence intensity and concentration of the donors meant that one could easily determine the concentration of a donor in a given sample by means of a simple fluorescence measurement. We were also delighted to see that our FRET

method could be extended to a wellplate format. Switching to the dichloroethane solvent, minimized discrepancies in the fluorescence readings brought on by solvent evaporation. Indeed, good correlation was found between donor concentration and emission intensity using the wellplate method.

3.3 Conclusions

Our FRET experiments have demonstrated that the DNS/GBC and PYR/GBC FRET pairs are well behaved when evaluated together in the same sample. Applying this to the *pseudo-meso* substrate **46**, allowed us to set up a model hydrolysis reaction to test the possibility of using FRET as a high throughput method to screen for enantioselectivity. Results from our *pseudo*-hydrolysis experiments were promising, as a linear trend could be established between the concentration and fluorescence intensity of the donor probe for a variety of reaction situations. This suggested that the concentration of a product, tagged with a fluorescence donor, could be readily determined by measuring its fluorescence output and relating the data to a calibration curve. When two enantiomeric products are labeled by a different fluorescence donor, the enantiomeric excess can be derived from the concentration of each in solution by using the FRET method. We were also able to demonstrate that applying FRET to a more efficient wellplate format was just as reliable as using a cuvette to analyze samples one at a time.

CHAPTER 4
APPLYING FRET TO THE DESYMMETRIZATION OF *MESO* COMPOUNDS

In the previous chapter were described experiments than successfully demonstrated that a single acceptor molecule could quench the fluorescence of two donor molecules in a FRET process. When testing the system in a hydrolysis mimic, the reaction yield and selectivity could be accurately determined by measuring the fluorescence intensity of each donor. The positive results from this proof of principle encouraged the pursuit of the next course of action towards the development of a FRET based assay for screening enatiomeric excess. It would be a further testament to the reliability of the assay to have the results of a known desymmetrization process involving *meso* compounds comparable to that of a FRET modified system. The following are two examples from literature with which the FRET method could be tested.

4.1 Enzymatic Desymmetrization

The asymmetrization of *meso*-2-cycloalken-1,4-diacetates by different enzymes has already been well established in literature.[14, 15, 16] The five membered ring system, in particular, has received much attention. The work of Johnson and Bis[17] focused on the enantioselective hydrolysis of *meso*-2-cyclopenten-1,4-

---

[14] Schneider, M and Laumen, K. *Tetrahedron Lett.* **1984**, *25*, 5875.

[15]. Schneider, M and Laumen, K. *J. Chem. Soc., Chem. Commun.* **1986**, *26*, 407.

[16] Deardorff, D.R.; Matthews, A.J.; McMeekin, D.S.; Craney, C.L. *Tetrahedron Lett.* **1986**, *27*, 1255

[17] Johnson, C.R. and Bis, S.J. *Tetrahedron Lett.* **1992**, *48*, 7287.

diacetate. The enzyme of interest in their studies was *Candida Antarctica* Lipase B (CAL-B) which afforded the mono acetate product **55** in 90% yield and greater than 99% ee.

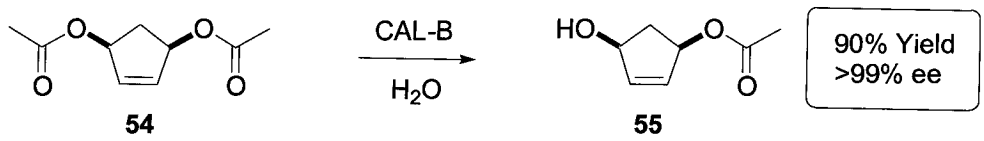

54 **55**

Scheme 15. Enzyme Mediate Enantioselective Hydrolysis.

Supplied as an acrylic supported catalyst, the enzyme was easily recoverable and could be also applied to the corresponding seven membered ring system, again in excellent yield and selectivity. Unfortunately, several disadvantages were associated with biocatalysts, as they usually require buffered solutions and had limited stability. More importantly access to the opposite enantiomer product generated by the natural enzyme is not always possible. In light of this, we were encouraged to search for a non-enzymatic method to break the symmetry of *meso* compounds.

4.2 Palladium Catalyst Mediated Desymmetrization

Non-enzymatic routes to asymmetric induction of prochiral substrates have been investigated by Trost[18] and coworkers. An asset to discovering a non enzymatic route is that both antipodal forms of the catalyst could be synthesized to give access to either enantiomeric versions of the product.

[18] Trost, B.M., Van Vranken, D.L. and Bingel, C. *J. Am. Chem. Soc.* **2003**, *125*, 2410.

Initial efforts, employed ligands derived from 2-(diphenylphosphino) benzoic acid, such as **56,** in a palladium catalyzed synthesis of oxazolidin-2-ones from the prochiral bis-carbamate **57**.

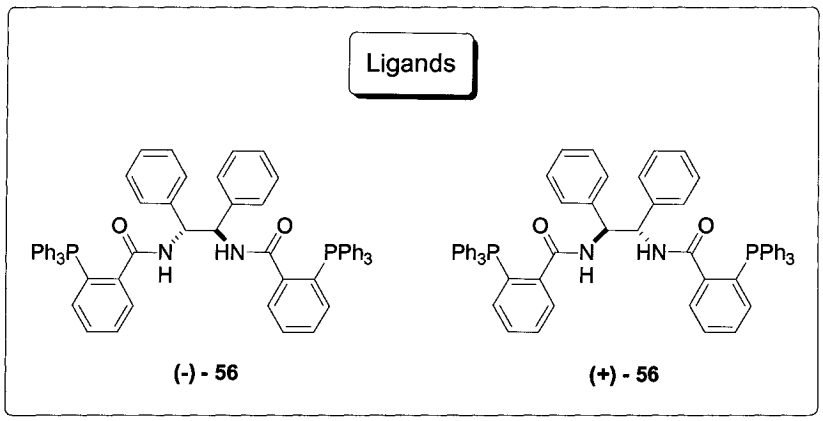

Figure 39. Ligands Based on 2-(diphenylphosphino) Benzoic Acid.

Complexation of the palladium catalyst to the olefin **57** arises on the face that is *anti* to the leaving group. Nevertheless, in the ionization step where enantiodiscrimination occurs, the asymmetric environment imposed by the ligands is translated to the opposite face of the substrate where bond breaking

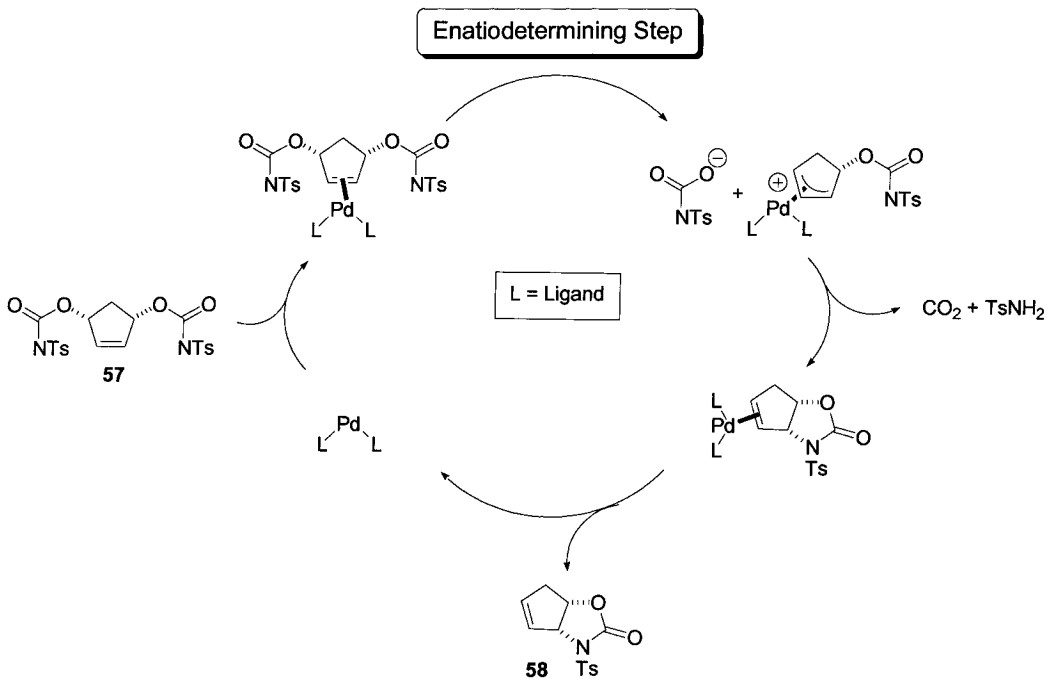

Scheme 19. Oxazolidin-2-one Synthesis by Pd-catalyzed Desymmetrization.

and bond making takes place. As such, one leaving group is favoured over the other to generate an allyl anion that is trapped intramolecularly to give the oxazolidinone **58**, in 91% yield and 79% ee.

Further investigation on the scope of Trost's palladium catalyst to the formation of oxazolidinones, included the case where a substituent was installed *trans* to the leaving groups in the cyclopentene framework. Since the catalyst approaches the *meso* substrate *anti* to the leaving groups, it was reasoned that the added substituent would hinder catalyst binding. Although the effort saw a decrease in both yield and selectivity, the results were still a respectable 75% for yield and 70% for ee.

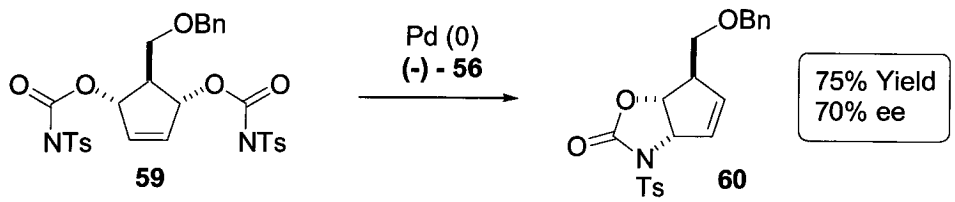

Scheme 20. Pd-Catalyzed Synthesis of Oxazolidin-2-ones from Substituted *Meso* Substrates.

Intermolecular alkylations were also subjected to study in the Trost group. If ionization of the *meso* substrate was the enantiodiscriminating step, then the selectivity of the reaction should not be adversely affected by the change to an intermolecular nucleophile. It was noted that the product of an intermolecular alkylation could also be a substrate for the catalyst, which would thereby produce a doubly alkylated product. However, the very factors that determine the selectivity of the ionization of the initial substrate should sustain and therefore disfavour the likelihood of a double alkylation.

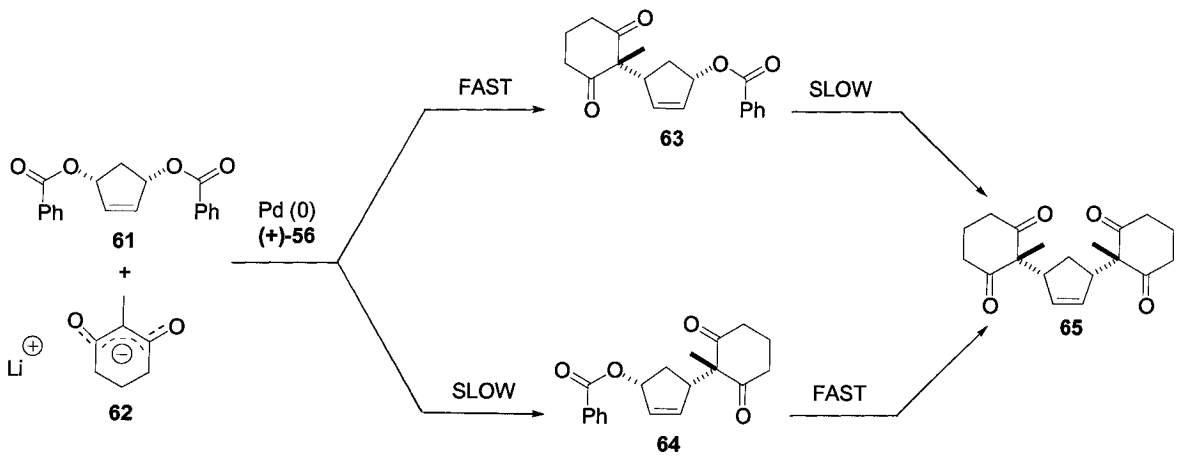

Scheme 21. Pd-Catalyzed Intermolecular Alkylation of a *Meso* Substrate.

Using the lithium enolate of 2-methylcylclohexane-1,3-dione as the nucleophile produced the corresponding mono-alkylated product **63** in 86% yield. The product mixture compose of 95.5% of the compound **63** and 4.5% of its enantiomer **64** to give an ee value of 91%.

4.3 Building a *Meso* Substrate for FRET Applications

Structures analogous to **59** would be ideal to use as a test substrate for our FRET based assay, because the addition of 3 substituents about the cyclopentene core could be accommodated (Figure 40).

Although Trost has yet to attempt the intermolecular alkylation of substituted *meso* substrates such as **59**, we were optimistic that the reaction would be feasible, although the C5 substituent would compromise the yield and selectivity slightly as in the case depicted in Scheme 20.

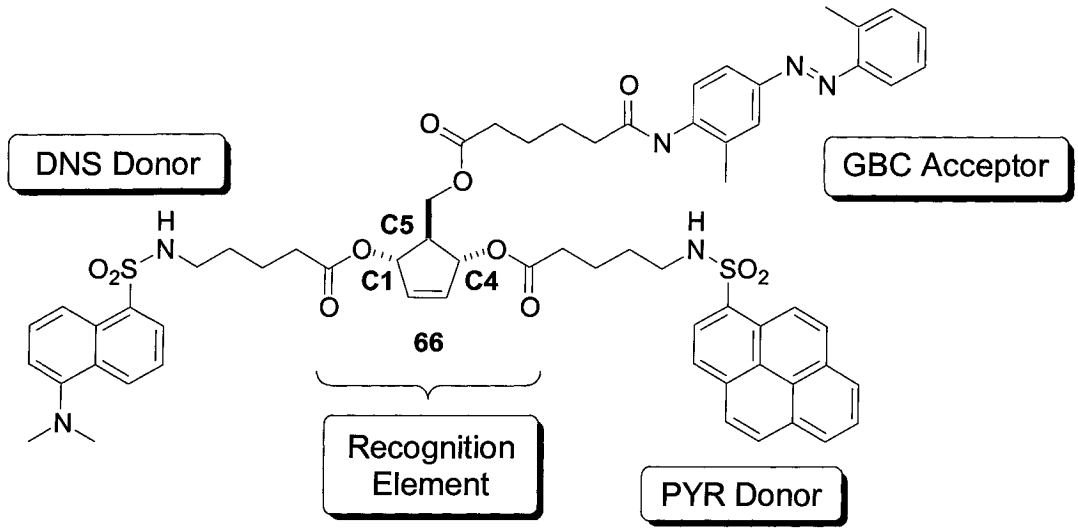

Figure 40. Proposed *Pseudo-Meso* Substrate for Testing with Trost's Pd-Catalyst.

The Dansyl and Pyrene donors could be joined to the cyclopentene ring at C1 and C4 through ester functionalities. The esters, much akin to the carbamates (**56**) that Trost employed, could act as the leaving group in the desymmetrization process. Selective displacement would eject a specific donor molecule as a carboxylate anion that could be detected by its characteristic emission wavelength to give a measure of the reaction yield and enantioselectivity.

As shown in Figure 40, the GBC moiety would be installed as a substituent at the C5 position to satisfy the requirements for FRET to occur. GBC would serve to quench the fluorescence of both donors as it has already been proven to do so by our experiments in the previous section.

We envisioned that the *pseudo-meso* substrate **66**, could be derived from a compound such as **67**, where the differentially protected hydroxyl groups would serve as a point of tether. Selective deprotection of the alcohol functions would allow for the respective donors and acceptor molecules to be sequentially coupled. Generation of the key cyclopentene framework could arise from a ring-

closing metathesis (RCM) of the acyclic diene **68**. The two alkene moieties necessary for RCM could be introduced by an aldol reaction with *(E)*-cinnamaldehyde followed by a Grignard addition with vinyl magnesium bromide on the Weinreb amide **69**. Finally, the Weinreb amide in turn, could be easily generated in a few simple steps from the diol **71**.

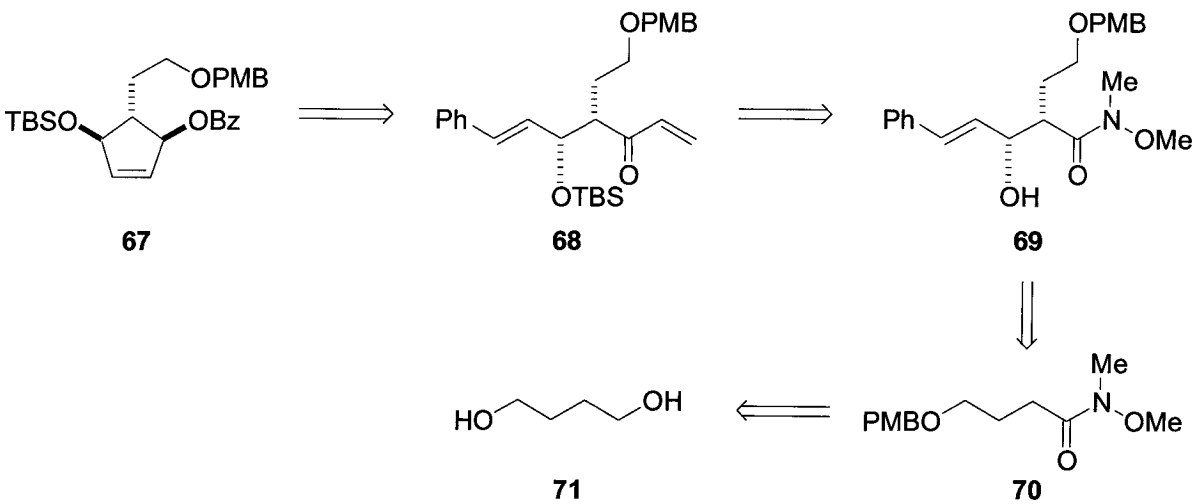

Scheme 22. Retrosynthetic Analysis of *Pseudo-Meso* Substrate.

Starting from the inexpensive 1,4-butandiol, monoprotection was effected with *p*-methoxybenzyl chloride (PMBCl) in excellent yield[19]. Fresh Jones's Reagent was prepared from chromium trioxide to oxidize the primary alcohol **71** to its corresponding carboxylic acid derivative. From this, a Weinreb amide was generated in good yield from coupling the acid with commercially available *N,O* - dimethyl hydroxylamino hydrochloride.

[19] Hirai, K.; Ooi, H.; Esumi, T.; Iwabuchi, Y.; and Hatakeyama, S. *Org. Lett.* **2003**, *5*, 857.

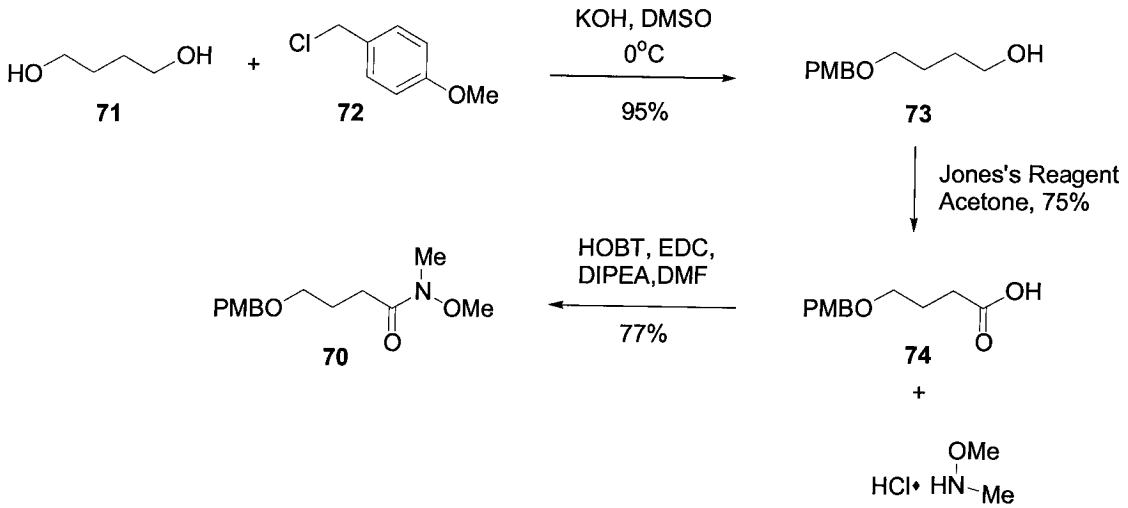

Scheme 23. Synthesis of the Weinreb Amide **70**.

The Weinreb amide was a necessary intermediate as we anticipated a Grignard reaction to the amide carbonyl later in the synthesis. Weinreb amides are typically employed to alleviate the formation of a double addition product. Upon addition of the Grignard reagent, the free metal cation will chelate to the enolate anion and *N*-methoxy group to form a stable tetrahedral intermediate (Figure 41) that would otherwise collapse in solution to give the ketone product. Bearing an electrophilic center, the ketone product could undergo a second Grignard addition to form a tertiary alcohol.

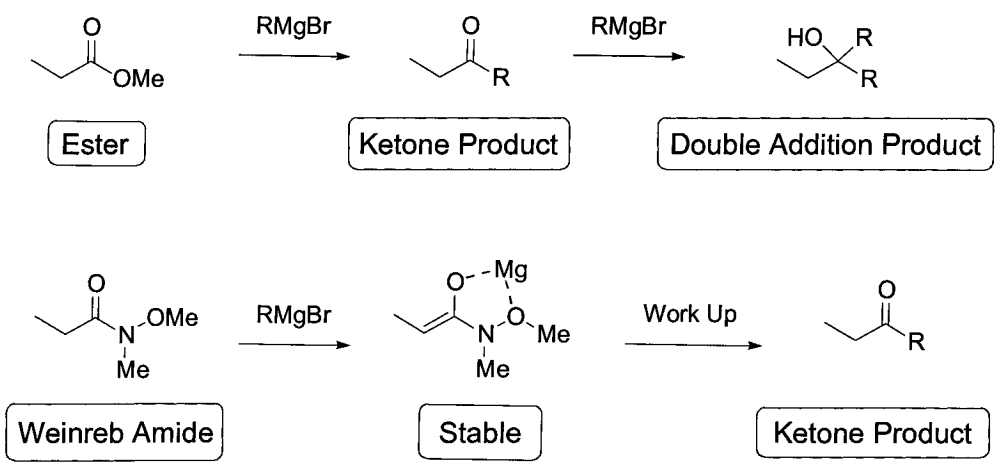

Figure 41. Weinreb Amides in Ketone Synthesis.

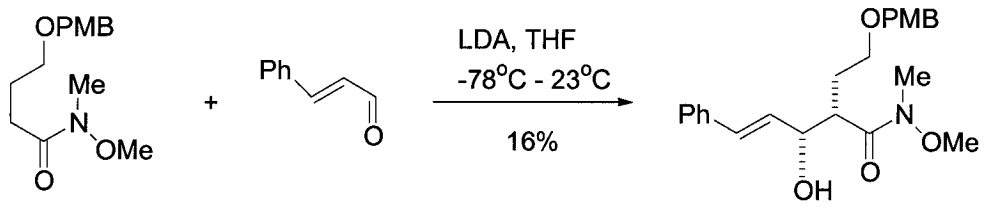

70 **75** **69**

Scheme 24. Aldol Reaction with Weinreb Amide.

With the Weinreb amide in hand, we proceeded to incorporate the first alkene moiety by means of an aldol reaction with *(E)*-cinnamaldehyde (Scheme 24). Despite numerous attempts to alter reaction conditions, the aldol product **69** was isolated in only 16% with recovery of the starting material.

In light of this, we though it would be wise to carry on with the Grignard reaction first to discharge the Weinreb amide before advancing to the Aldol condensation. However, our efforts towards **66** were temporarily abandoned to pursue new developments in our research group. The following Scheme 26 includes the proposed steps to complete the synthesis of our targeted substrate.

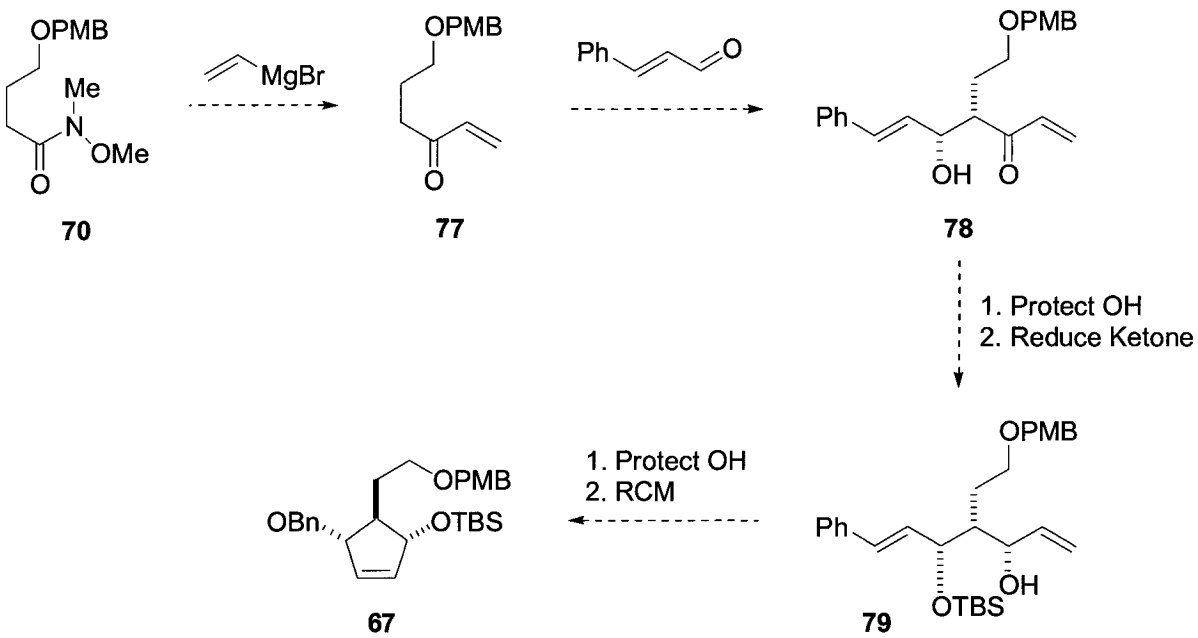

Scheme 26. Proposed Route For the Synthesis of **67**.

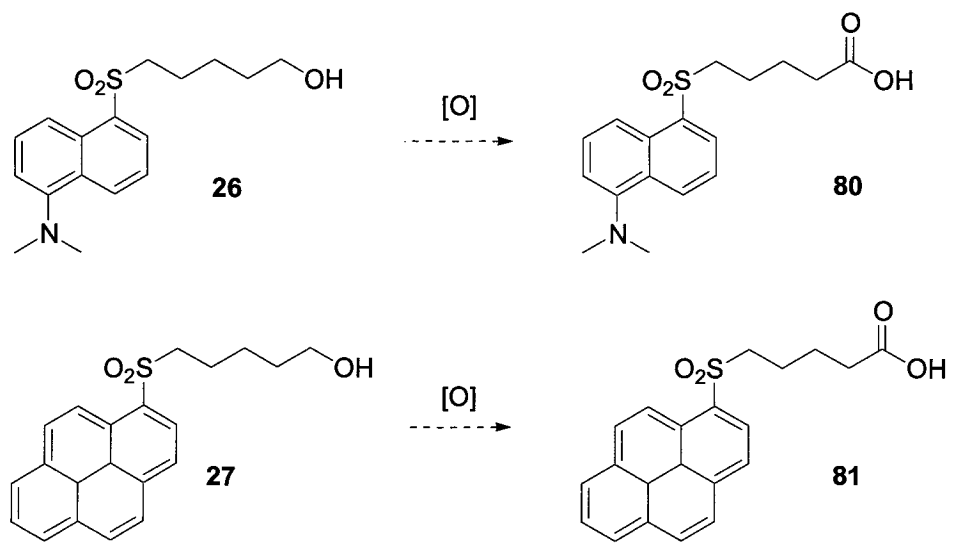

Figure 42. Acid Derivatives of Dansyl and Pyrene Probes.

Once **67** becomes available, the DNS, PYR and GBC pieces can be incorporated through their acid derivatives (Figure 42) to produce the *pseudo-meso* substrate **66**. This compound could then be subjected to desymmetrization using Trost's

chemistry. The reaction yield and enantiomeric excess will then be evaluated by FRET assay to test to our methodology.

4.3 Conclusions

In summary, we were please to see that FRET could be extended to *meso* substrates where a single acceptor molecule (GBC) could successfully suppress the fluorescence of both the DNS and PYR donors. Preliminary results from the hydrolysis mimic experiments were encouraging, as we have confirmed a predictable relationship between donor intensity and its concentration. This information could ultimately be translated to the yield and selectivity of the reaction. In addition to this, our experiments were reproducible in a wellplate format that is essential to our vision of creating a high throughput screening method based on FRET technology.

We have yet to test the feasibility of proposed FRET based assay with a known desymmetrization process such as that developed by the Trost group. This will be a necessary avenue to pursue, as further evidence to support that FRET can be a reliable method for determination of enantiomeric excess is required. We are optimistic that this can be achieved in due time and that FRET will be a powerful tool in the discovery of novel catalysts.

PART B

ABSTRACT

Organocatalysis is a vast growing field in synthetic organic chemistry. In particular, organocatalysts that can impart enantioselectivity to a reaction is of great value. A study on camphor based hydrazide catalysts for applications to the Diels-Alder reaction of α,β-aldehydes has been successfully launched in our group. Formation of a reactive iminium species between the hydrazide catalyst and aldehyde effectively lowers the LUMO energy of the latter to accelerate the reaction. The reaction scope of this catalyst is investigated in this project with the Friedel-Crafts Alkylation of heteroaromatic substrates. Further to this, the design and synthesis of second-generation hydrazide catalysts will be discussed.

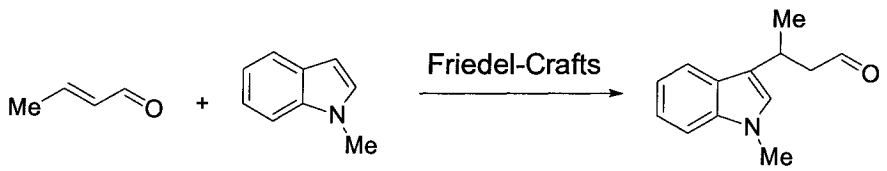

1st Generation Catalyst

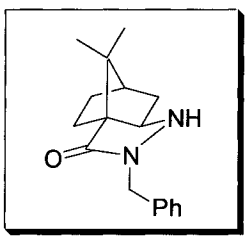

2nd Generation Catalysts

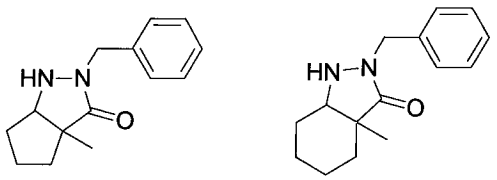

CHAPTER 5
ORGANOCATALYSIS

Catalysts are often employed to accelerate a reaction as well as to induce chirality in a product. Recent developments in catalysis have seen organic compounds become an increasingly relevant player in enantioselective catalysis, a field that has long been dominated by transition metal catalysts and biocatalysts

Organocatalysts display several features that make them attractive for use in synthetic chemistry. Unlike metal catalysts, organic based catalysts can generally tolerate a broader spectrum of reaction conditions including aerobic and wet environments. Compared to their enzyme counterparts, organic catalysts exhibit better solvent compatibility. Further to this, the latter can be synthesized in either antipodal form to give access to the desired enantiomer of a product, whereas enzymes are limited to their naturally occurring structure.

Different types of organic compounds have been evaluated for organocatalytic applications. Chiral amines in particular have shown great utility for such purposes and thus account for a large proportion of the field.

5.1. Proline Catalyst

It is difficult to examine the field of organocatalysis without discussing the pioneering role that proline has played. This small organic molecule possesses several features that make it an ideal catalyst.

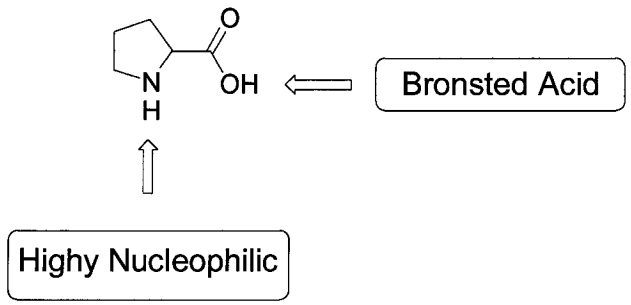

Figure 43. The Bifunctional Feature of Proline.

Available in both antipodes, proline is the only amino acid that bears a secondary amine functionality, being part of a pyrrolidine structure. This imparts proline with an amino group that displays a higher pK_a value and greater nucleophilicity when compared to the other amino acids. The highly nucleophilic nitrogen electron lone pair acts as a Lewis base that readily reacts with carbonyls to generate an enamine or iminium ion. Proline, being an amino acid, also has a carboxylic acid group that could participate in catalysis as a H-bond donor/acceptor, giving proline a bifunctional character.

Proline's earliest example as an enantioselective organocatalyst came independently from two industrial groups[20, 21] that saw its utility in the Robinson annulation reaction.

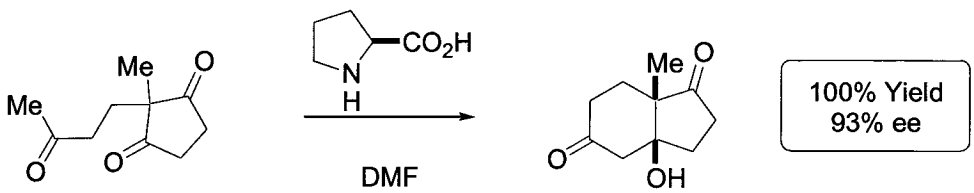

82 **83**

Scheme 27. Proline-Catalyzed Robinson Annulation.

---

[20] Hajos, J. and Parrish, D. *J. Org. Chem.* **1974**, *39*, 1615.

[21] Eder, U.; Sauer, G.; Weichert, R. *Angew. Chem. Int. Ed.* **1971**, *10*, 496.

Using conditions set by Hajos and Parrish[20], we see that 3 mol% of proline was enough to catalyze the intramolecular aldol in Scheme 27 to provide the bicyclic condensation product in 100% yield and 93% ee. This aldol cyclization is often referred to as the Hajos-Parrish-Eder-Sauer-Weichert reaction and has been applied to the synthesis of several natural products.[22, 23]

List and co-workers explored an intermolecular version of this asymmetric aldol reaction. In 2000, the group reported the first proline catalyzed direct asymmetric aldol reaction[24]. In a mixture of ketone and aldehyde, proline preferentially reacted with the former to generate an enamine that was the platform for enantioselectivity. Thus, the reaction shown here does not rely on a preformed enolate as typically required.

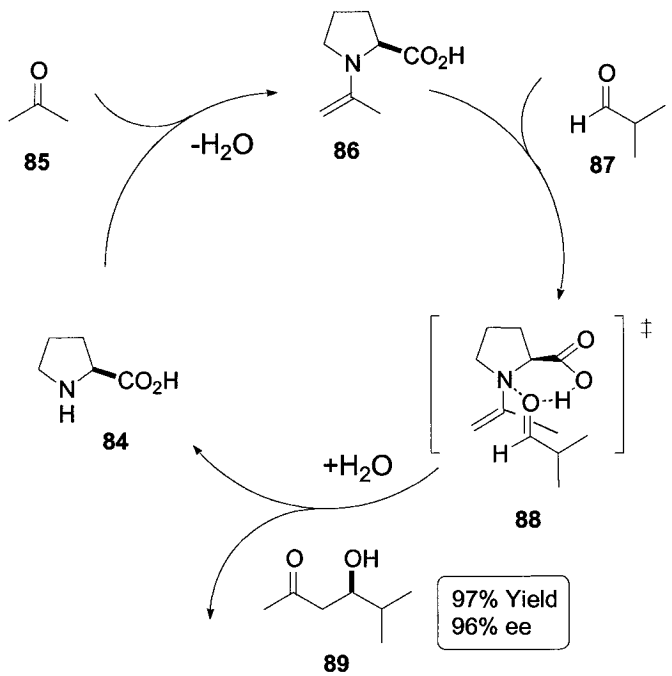

Scheme 28. Proline Mediated Enantioselective Intermolecular Aldol.

---

[22] Danishefsky, S. J.; Masters, J. J.; Young, W. B.; Link, J. T.; Snyder, L. B.; Magee, T. V.; Jung, D. K.; Isaacs, R. C. A.; Bornmann, W. G.; Alaimo, C. A.; Coburn, C. A.; Grandi, M. J. D. *J. Am. Chem. Soc.* **1996**, *118*, 2843.

[23] Mickos, D.E. *J. Am. Chem. Soc.* **1992**, *57*,2732.

[24] List, B. Lerner, R.A., Barbas, C.E. III. *J. Am. Chem. Soc.* **2000**, *122*, 2395.

The cross condensation between the ketone **85** and the branched aldehyde **87** was catalyzed by proline with excellent yield and selectivity.

Although the first proline-catalyzed reaction was invented over 30 years ago, we are only just beginning to understand it's true mechanism of action. Houk and List[25] proposed that a single proline molecule forms the enamine structure and participates in the stabilization of the transition state. The extensive hydrogen-bonding network, mediated through the proline amino and carboxylic acid group, created a highly organized and stable transition state (**88**) that conveyed asymmetry to the product.

The applications of proline are not limited to aldol reactions. It is a catalyst with incredible scope, introducing chirality to a great many synthetic transformations including the Mannich reaction and Michael addition to name a few. It is astounding to observe such diversity arise from such a simple molecule. For certain, many more asymmetric discoveries will originate from proline and proline based catalysts in the near future.

5.2. Iminium Based Catalysis

Our brief discussion of proline has provided us with an example of how chiral amines could catalyze a reaction through the formation of an enamine. Another method for amines to participate in catalysis is by generation of an iminium intermediate. The basis of our project is to discover novel catalysts by exploiting the reactivity of iminium intermediates to accelerate and to impart enantioselectivity to organic reactions. As such, a more detailed investigation of iminium-based catalysis will follow.

---

[25] Houk, K. *J. Am. Chem. Soc.* **2002**, *124*, 7163.

5.2.1 Imidazolidinone Catalysts.

In 2000, the MacMillan group introduced a new organocatalyst that has proven to be remarkable in its application to numerous synthetic transformations. The structure of this catalyst was derived from yet another amino acid. Phenylalanine was incorporated in a cyclic structure to produce the chiral imidazolidinone catalyst **90**, which serves as the catalytic platform for asymmetric carbon-carbon bond forming events. Whereas most of the accomplishments in this field of organocatalysis were centered on the Aldol and Mannich reaction as well as conjugate additions, MacMillan's catalyst offered activity to different reaction scaffolds.

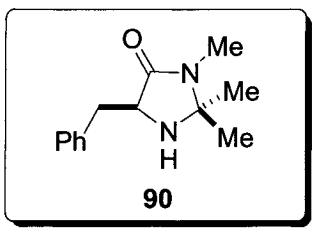

90

Figure 44. MacMillan's Imidazolidinone Catalyst.

5.2.1.1 Applications to Diels Alder Reaction.

The first, in a series of MacMillan publications with regards to their work on imidazolidinone mediated catalysis, focused on the Diels-Alder reaction. Since its introduction almost 8 decades ago, this powerful method of making six membered rings continues to be an important reaction in synthetic construction.

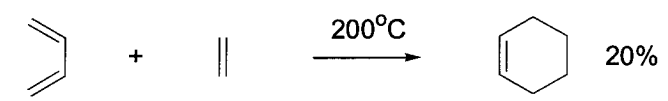

Diene Dienophile Cyclohexene

Scheme 29. Cyclohexene Formation by Diels-Alder Cycloaddition.

The Diels-Alder Reaction is a cycloaddition reaction in which an alkene (a 2 π-electron system), also called a dienophile, reacts with a conjugated *cis*-diene (a 4 π-electron system) to furnish a cyclohexene product. The transformation results in the creation of two σ bonds at the expense of two π bonds. This is an energetically favourable process since σ bonds are more stable than π bonds. The most basic example of the Diels-Alder reaction is provided by the cycloaddition between ethylene and 1,4-butadiene (Scheme 29). However, the given example is poor yielding despite high reaction temperatures. In practice, the process is favoured by the presence of electron-withdrawing groups on the dienophile component and by electron-releasing groups on the diene.

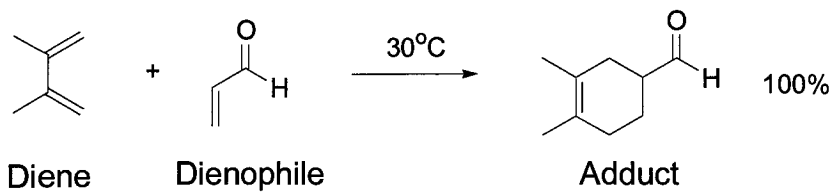

Scheme 30. Diels-Alder Reaction with Substituted Diene and Dienophile.

In this second example shown in Scheme 30, methyl groups were added to the diene as electron donating groups and an aldehyde served as an electron-withdrawing group for the dienophile. The corresponding Diels-Alder adduct was produced quantitatively at a moderate temperature. This increased reactivity can be better accounted for by referring to frontier molecular orbital theory.

Frontier molecular orbital theory describes bond formation by studying the highest occupied molecular orbital (HOMO) and lowest occupied molecular orbital (LUMO) of the reactants involved. In bond formation, a filled molecular orbital of one reagent overlaps with an unfilled molecular orbital of a second reactive specie. The process could only occur if the overlapping orbitals have complementing symmetry and if they have similar energies.

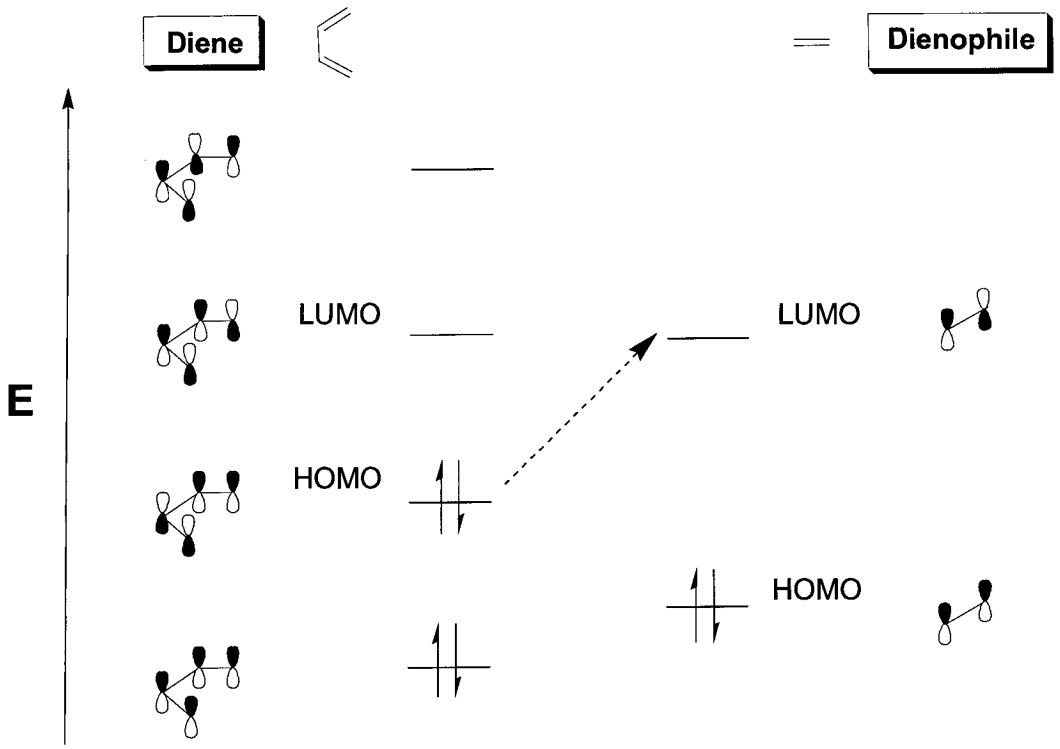

Figure 45. Molecular Orbital Diagram Description of Ethylene and 1,4-Butadiene in the Diels-Alder Reaction.

The strongest bonding interaction will occur between orbitals with similar energies. Hence, the important orbitals to consider here are the HOMO and LUMO of the reagents in question as they exhibit the smallest energy difference. In the case of the Diels-Alder reaction, depicted by the molecular orbital diagram in Figure 45, the smallest energy gap is between the HOMO of the diene and the LUMO of the dienophile. As they also have the appropriate orbital symmetry, the diene HOMO and dienophile LUMO will overlap to allow for bond formation. To further favour bonding interaction, the energy gap between the HOMO and LUMO can be minimized by the addition of appropriate substituents to the reacting substrates. In general, installing an electron-withdrawing group to the dienophile component will result in lowering the LUMO energy. The diene can be coupled to an electron releasing to moiety achieve a higher energy HOMO. With

these two modifications, the HOMO-LUMO energy gap of the diene and dienophile respectively, could be effectively reduced so as to enhance reactivity.

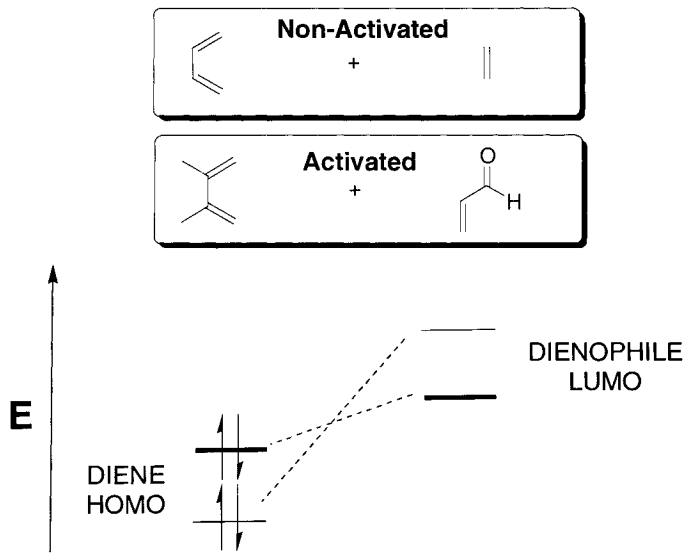

Figure 46. Comparison of the Orbital Energies between Non-Activated and Activated Diels-Alder Substrates.

Another approach to promoting the Diels-Alder reaction relies on the use of Lewis acids. Similar to how electron-withdrawing groups initiate the lowering of dienophile LUMO energy, Lewis acids can chelate to carbonyl dienophiles to produce the same effect. In fact, many enantioselective Diels-Alder reactions are a result of chiral Lewis acid catalysis[26]. MacMillan's group reasoned that the use of organic molecules could affect a similar transformation through catalyst generation of an iminium species. Thus, the chiral oxazolidinone catalyst **90** was introduced.

The MacMillan group investigated α,β-unsaturated aldehydes as substrates for their imidazolidinone catalyzed Diels-Alder reaction[27]. The chiral amine reversibly

---

[26] Engler, T.A.; Letavic,M.A.; Lynch K.O.; Takusagawa, F. *J. Org. Chem.* **1994**, *59*, 1179.

[27] Ahrendt, K.A.; Borths, C.J., MacMillan, D.W.C. *J. Am. Chem. Soc.* **2000**, *122*, 4243.

forms an iminium intermediate with the aldehydic dienophile to effectively lower its LUMO energy, much akin to the situation depicted in Figure 46. Two possible iminiums, corresponding to the *Z* and *E* isomer, could be generated. The preferred conformation was the iminium displaying a *trans* conformation about the N-C double bond. This iminium isomer was determined to be the lower energy conformer as the alkene is located away from the gem-dimethyl group of the catalyst to avoid steric interactions between the two.

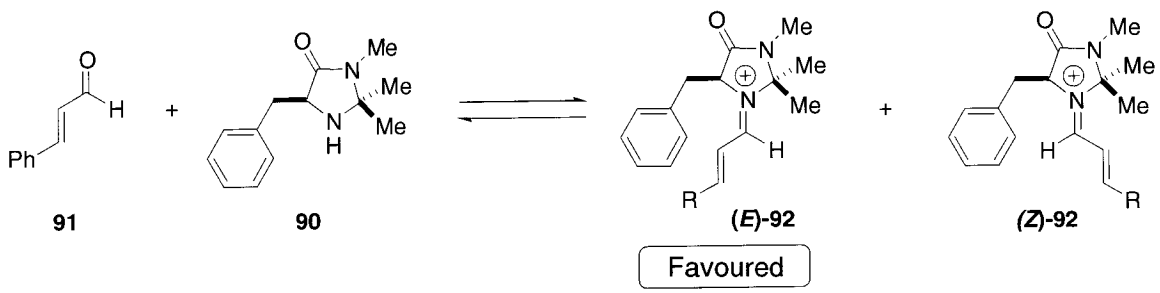

Scheme 31. Reversible Iminium Ion Generation by Chiral Oxazolidinone Catalyst **90**.

A second control for enantioselectivity was imposed by the benzyl substituent of catalyst **90**. Referring to Figure 47, the benzyl group effectively shields the top face (*Re*-face) of the aldehydic system. The diene therefore approaches the activated dienophile from the exposed bottom face for cycloaddition to occur.

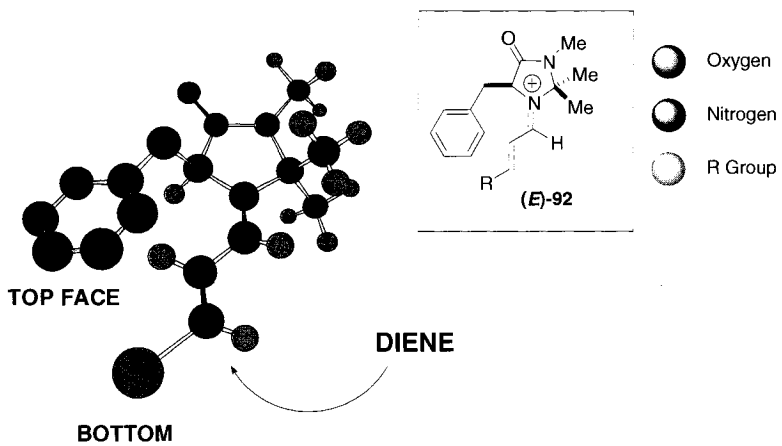

Figure 47. 3-Dimensional Representation of *E*-Iminium. Selected Hydrogen Atoms were Eliminated for Clarity.

The general Scheme 32 summarizes the reaction in three phases. After the iminium ion **95** is formed from the aldehyde and the chiral amine catalyst, it participates in the cycloaddition with the dienophile to furnish **97**. Subsequent hydrolysis ejects the Diels-Alder adduct **98** and restores the starting catalyst.

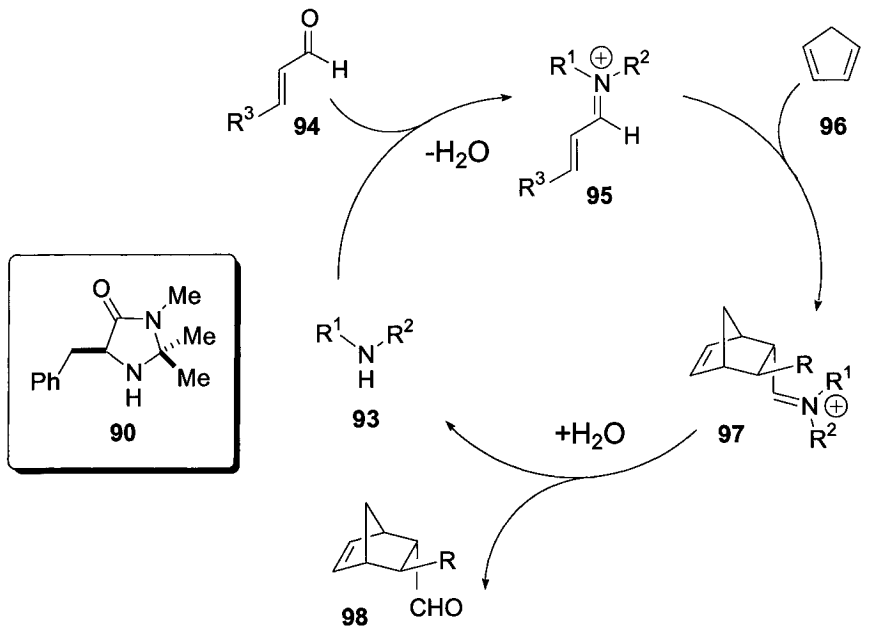

Scheme32. Catalytic Cycle for Iminium Mediated Diels-Alder.

Using (*E*)-cinnamaldehyde and cyclopentadiene as Diels-Alder reaction partners, MacMillan demonstrated the utility of his iminium catalyzed process. Under aerobic and wet conditions, the reaction proceeded with excellent yield and enantioselectivity.

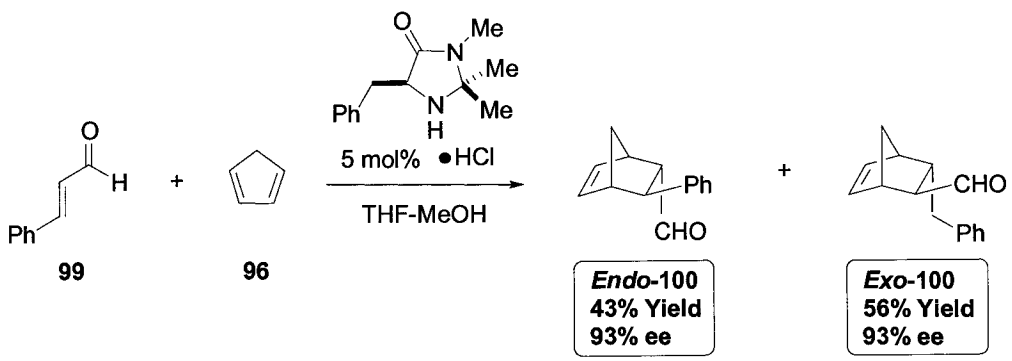

Scheme 33. Iminium Catalyzed Diels-Alder Reaction.

The catalyst, used as its hydrochloride salt, was tolerant to a variety of substrates and diastereoselectivity was improved with dienes other than **96**. Overall, the measures of enantiocontrol that were used have proven to be successful in conveying asymmetry to the Diels-Alder reaction.

5.2.1.2 Friedel-Crafts Alkylation

The Friedel-Crafts reaction describes the alkylation or acylation of aromatic compounds. Traditionally, this is achieved by Lewis acid complexation to an alkyl halide to generate a carbocation species. This carbocation then acts as an electrophile for aromatic substitution to occur.

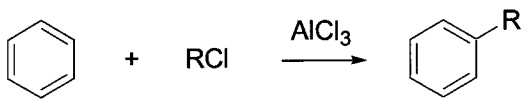

Scheme 35. General Friedel-Crafts Alkylation.

MacMillan's chiral amine catalyst was used to further develop this powerful carbon-carbon bond forming reaction. Pyrroles were the first aromatic heterocycles evaluated for this iminium ion catalyst strategy, which proved to be a rewarding study. In 2001, the MacMillan group published[28] the first enantioselective organocatalytic Friedel-Crafts alkylation. In fact, their work also constituted the primary example of conjugated pyrrole addition regardless of catalyst type. This was unprecedented as reactions between pyrroles and α,β-unsaturated aldehydes were typically observed to undergo acid catalyzed 1,2 addition to the carbonyl group. Examining the 3-dimesional framework of the

---

[28] Parras, N.; MacMillan, D. *J. Am. Chem. Soc.* **2001**, *123*, 4370.

iminium generated from the α,β-unsaturated aldehyde and chiral catalyst **90**, it was suggested that the steric constraints imposed by the catalyst could prevent 1,2-carbonyl addition from occurring. Instead, a less sterically challenging pathway that would lead to the conjugate addition product was envisioned for the pyrrole nucleophile (Figure 48).

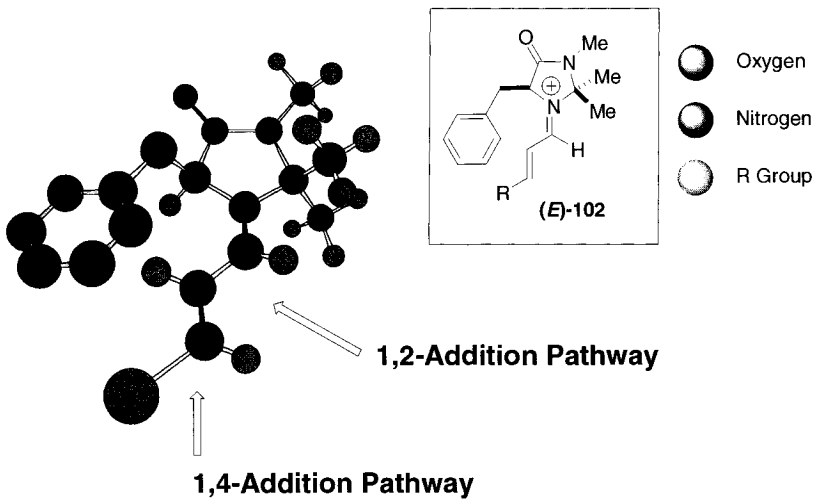

Figure 48. Pathways for Nucleophilic Attack on Iminium Catalyst Framework.

The MacMillan strategy rested on the fact that the LUMO-lowering affect of the catalyst would activate the aldehyde towards conjugated addition by means of an iminium intermediate. Previously described features of this phenylalanine derived catalyst will continue be important in attributing enantiocontrol over the reaction. The following Table 11 documents the success of the iminium mediated Friedel-Crafts Reaction.

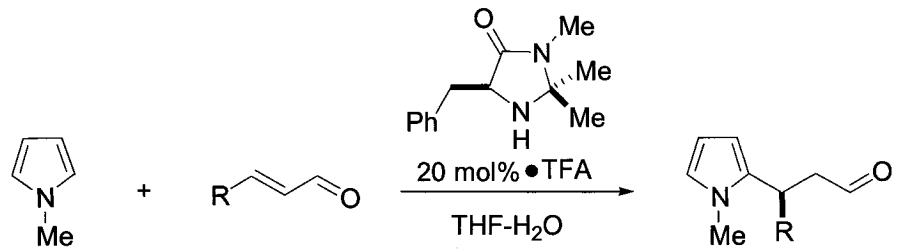

101 102 103

Entry	R	Temp. (°C)	Time (h)	% Yield	% ee
1	Me	-60	72	83	91
2	Pr	-50	72	81	90
3	*i*-Pr	-50	72	80	91
4	Ph	-30	42	87	93
5	4-MeOPh	-30	104	79	91
6	CH_2OBn	-60	72	90	87
7	CO_2Me	-50	104	72	90

Table 11. Organocatalyzed Friedel-Crafts Alkylation Using *N*-Methyl Pyrrole and α,β-Unsaturated Aldehydes.

Indoles, deemed as privileged structures of pharmacological value, were the next aromatic heterocycles targeted by MacMillan's enantioselective strategy. The method was first evaluated using *N*-methyl indole and crotonaldehyde as substrates for the Friedel-Crafts reaction.

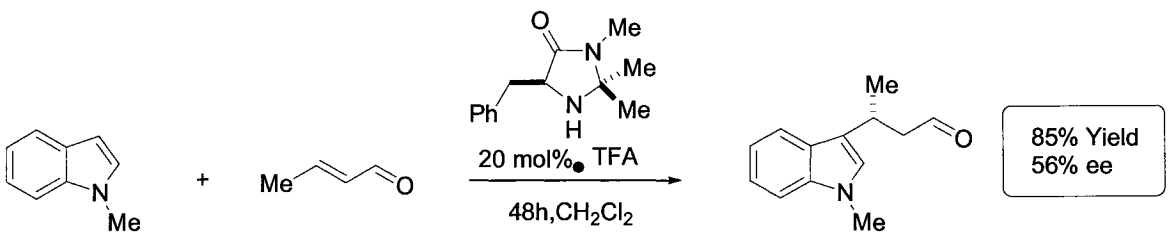

104 105 106

Scheme 36. Organocatalyzed Friedel-Crafts Alkylation Using *N*-Methyl Indole and Crotonaldehyde.

The results unfortunately did not mirror the same success as with the pyrrole substrates (Table 11). The alkylation exhibited poor reaction kinetics and enantioselectivity. It was noted that difference in reactivity might be due to the fact that indoles were less nucleophillic then pyrroles. To address the situation, a new catalyst was proposed by MacMillan and coworkers[29].

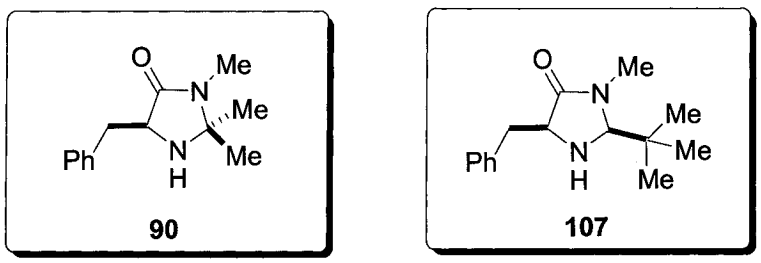

First Generation Second Generation

Figure 49. First and Second Generation of MacMillan's Imidazolidinone Catalyst.

Since iminium formation between the catalyst and aldehyde was hypothesized to be the rate-limiting step in the reaction, the new catalyst design necessitated a more nucleophillic amine group. In an effort to promote iminium formation, structural constraints about the amine moiety needed to be relieved to better exposed the nitrogen lone pair in question. This was achieved by replacing the gem-dimethyl group of the first generation catalyst with a *tert* -butyl group. The change was done to alleviate the eclipsing interaction between the nitrogen lone pair of the amine and the neighboring methyl group (Figure 50).

[29] Austin, J.F.; MacMillan, D.W.C. *J. Am. Chem. Soc.* **2002**, *124*, 1172.

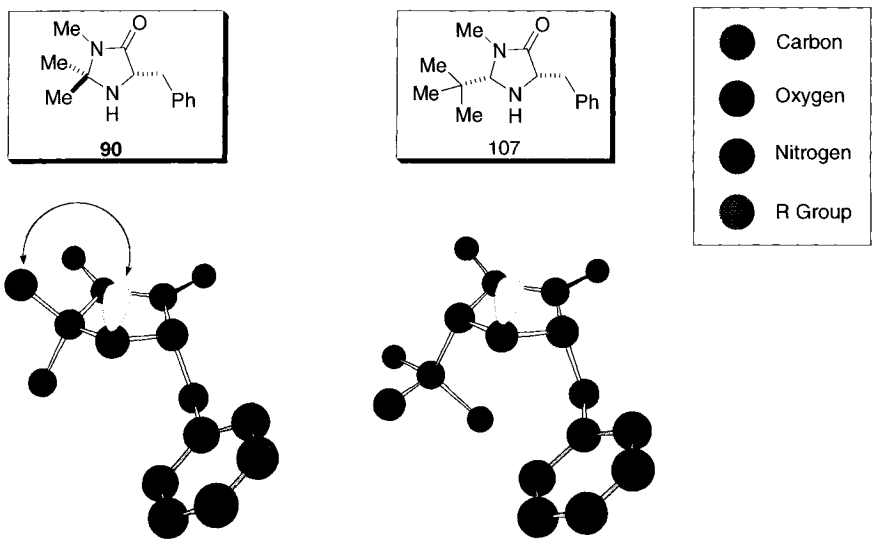

Figure 50. Comparison of Amine Nitrogen Lone Pair Exposure Between Catalyst **90** and **107**. Hydrogen Atoms were Excluded for Clarity.

The replacement with a *tert*-butyl group would not only favour a more reactive amine, but would also better expose the bottom face (as depicted in Figure 51) of the aldehydic system for indole approach. In light of this, the reaction rate was expected to increase. As in the first generation catalyst, substituents were positioned to bias the formation of the *(E)*-iminium and to shield the *re*-face (top face as depicted in Figure 51) from nucleophilic attack as a measure of enantiocontrol.

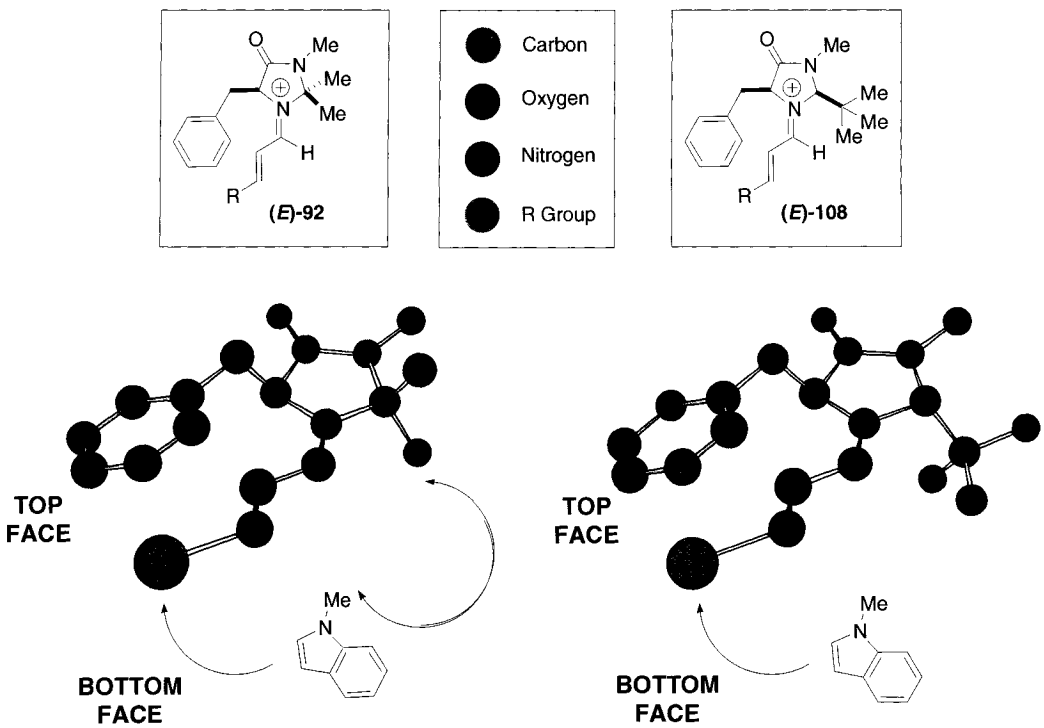

Figure 51. Preferred Route of Indole Approach to *E*-Iminium Generated from First and Second Generation Catalysts. Hydrogen Atoms were Excluded for Clarity.

The new catalyst was used in conjunction with trifluoroacetic acid as a co-catalyst to test a variety of aldehyde substrates. The results are summarized in Table 12.

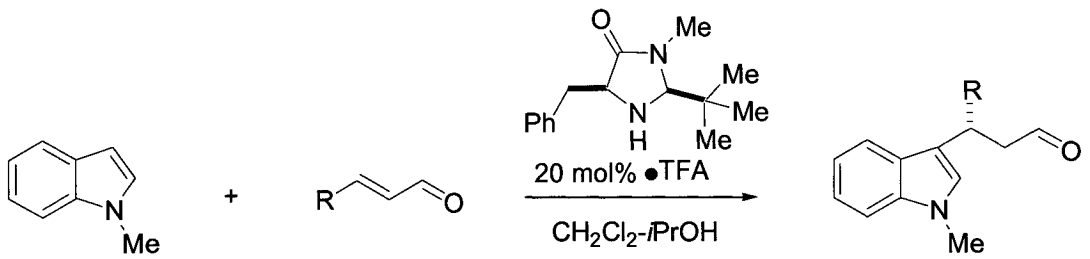

104 **109** **110**

Entry	R	Temp. (°C)	Time (h)	% Yield	% ee
1	Me	-83	19	82	92
2	Pr	-60	6	80	93
3	*i*-Pr	-50	32	74	93
4	Ph	-55	45	84	90
5	CH_2OBn	-83	18	84	96
6	CO_2Me	-83	21	89	91

Table 12. Organocatalyzed Friedel-Crafts Alkylation Using *N*-Methyl Indole and α,β-Unsaturated Aldehydes.

The efforts that MacMillan's group had put towards the development of a new catalyst were rewarded with a marked improvement in reaction rate and enantioselectivity.

5.2.2 Novel Catalyst Development.

Inspired by the developments in the field of organocatalyst, our group has initiated efforts to establish a catalytic process based on iminium activation. As mentioned before, iminium based catalysis involves three processes. The first step being iminium formation, followed by nucleophillic attack of the iminium intermediate, and finally hydrolysis to give the product and regenerate the catalyst (see Scheme 32 for an example in cycloaddition).

It has been suggested that the formation of the iminium intermediate is the rate-limiting step in the catalytic cycle. To address this issue, we envisioned a catalyst with increased amine nucleophilicity to promote iminium formation with α,β-unsaturated aldehydes. This, we believed, could be achieved by exploiting the α-effect.

5.2.2.1 The α-effect

The unusual reactivity of nucleophiles that possess an unshared electron pair onthe position α to the nucleophilic atom, was termed the α-effect by Edwards and Pearson in 1962[30]. For a series of nucleophiles in which the nucleophilic atom is held constant, a linear correlation exits between conjugate acid pK_a and rate constant of the reaction (i.e. nucleophilic attack of a carbonyl group). In other words, a trend could be observed within a series of oxygen nucleophiles, nitrogen nucleophiles and sulfur nucleophiles respectively. However, substrates in which the nucleophilic atom is next to another atom that possesses a lone pair deviate from the described trend. Such substrates display a greater nucleophillicity than expected based on their pK_a value.

Hydrazines, for instance, exhibit an unusual increase in nucleophillicity that is attributed to the α-effect. A better understanding of the matter could be achieved by examining the orbital interactions of substrates that display the α-effect.

---

[30] Edwards, J.O. and Bruice, T.C. *J. Am. Chem. Soc.* **1962**, *84*, 16.

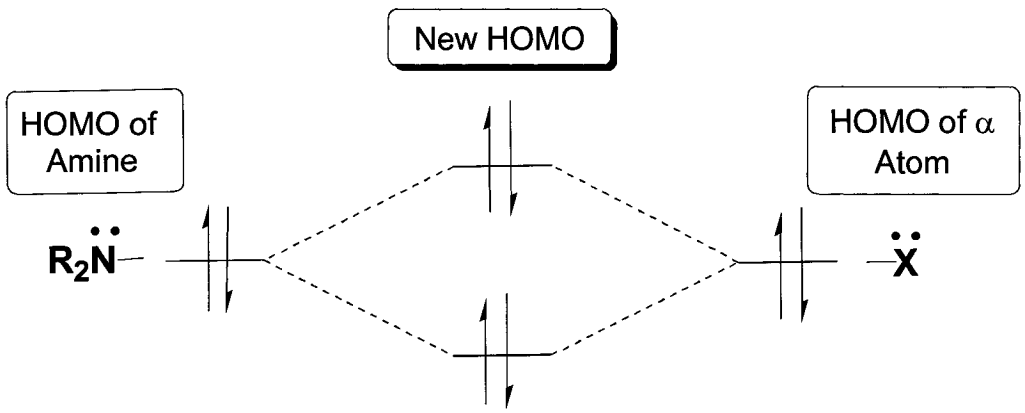

Figure 52. Filled Orbital of Nitrogen Nucleophile Having an X- Substituent With a Lone Pair.

Given that the orbital bearing the nucleophillic lone pair overlaps with the lone pair of the flanking heteroatom, a new molecular orbital would be generated. The new HOMO of this system will be higher in energy relative to the unsubstituted nucleophile. This ultimately translates to enhanced nucleophilicity, since this will tend to lower the gap between nucleophile HOMO and electrophile LUMO.

5.2.2.2 Synthesis of Novel Catalyst.

The idea of improving the kinetics through the α-effect was appealing. We therefore sought to incorporate this principle into our catalyst design as a feature to promote iminium formation.

Thus, we designed an organocatalyst based on hydrazine, in which the nucleophilic nitrogen is flanked by another nitrogen atom satisfying the requirement for the α-effect to occur. Camphor was selected as the backbone for our hydrazine catalyst. This inexpensive and relatively compact chiral compound would serve to impart selectivity to various synthetic transformations. Mathieu Lemay has successfully synthesized a chiral hydrazide catalyst **118** in five steps starting from camphor sulfonic acid.

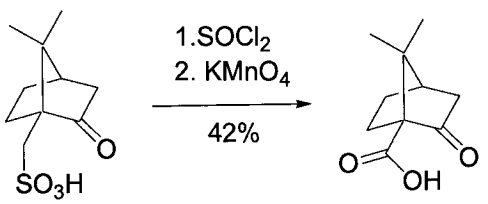

111 **112**

Scheme 37. Synthesis of Ketopinic Acid[31].

Camphor sulfonic acid was converted to ketopinic acid **112**, through oxidation of its sulfonyl chloride derivative. The structure **112** is a key compound in our scheme as it can be condensed with a variety of hydrazines to give a series of hydrazide catalysts. Initial studies led us to focus on benzyl hydrazine that is readily made from a reaction between benzyl bromide and hydrazine monohydrate.

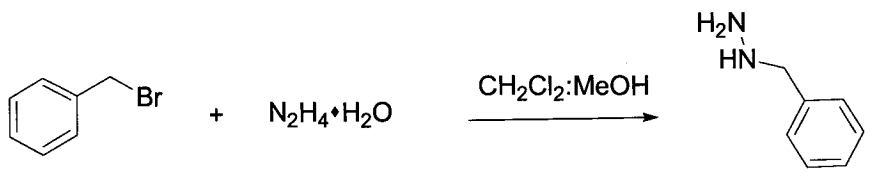

113 **114** **115**

Scheme 38. Preparation of Benzyl Hydrazine.

The catalyst **118**, was then produced in three steps from ketopinic acid and benzyl hydrazine. Cyclization of the hydrazone **116** was achieved by heating at a high temperature while removing the water formed in the reaction with a Dean-Stark apparatus. Reduction of the hydrazone proceeded with sodium cyanoborohydride to give the desired hydrazide catalyst in excellent yield.

---

[31] Bartlett, P.P.; Knox, L.H. *Organic Synthesis. Coll. Vol. 5*, p698.

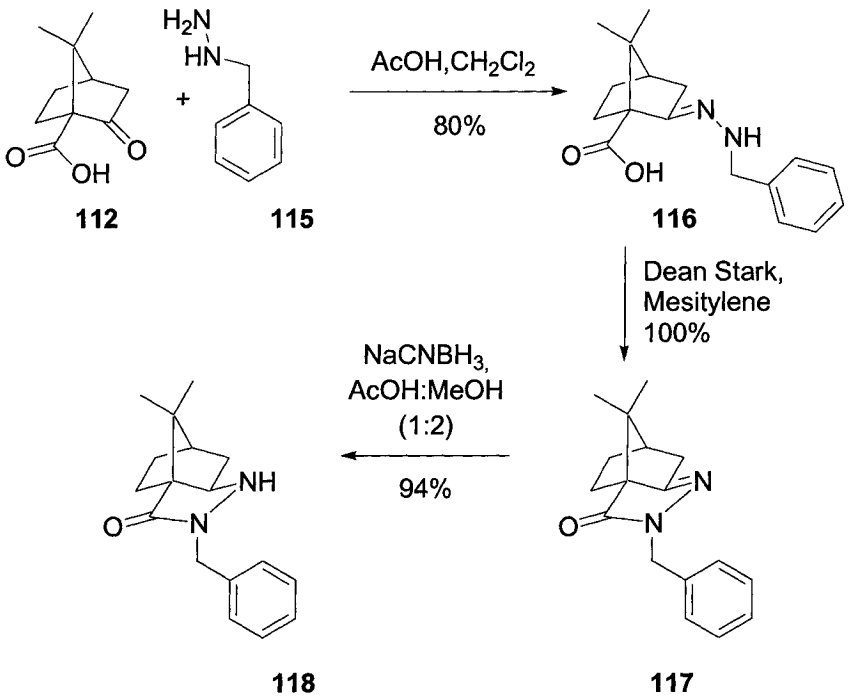

Scheme 38. Formation of Chiral Hydrazide Catalyst from Ketopinic Acid.

5.2.2.3 Application of Hydrazide Catalyst to Diels-Alder Reaction.

Mathieu Lemay first targeted the Diels-Alder reaction to evaluate the efficiency of the catalyst **124**. Conditions were first tested using cinnamaldehyde as the α,β-unsaturated aldehyde component. Using perchloric acid as a cocatalyst in an aqueous solvent at room temperature, produced the cycloaddition products in a 1.9:1 ratio of *exo:endo* isomers. The conversion and enantioselectivity of the *exo* and *endo* isomers were excellent.

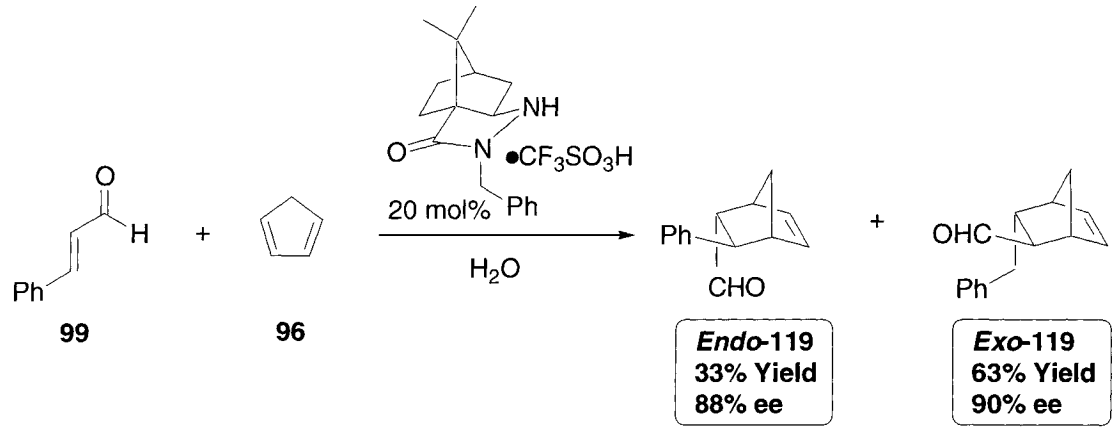

Scheme 39. Applying Chiral Hydrazide Catalyst in the Diels-Alder Reaction.

Semi-empirical calculations (PM3 in Spartan Pro) suggested that the iminium in Figure 53 would arise from the catalyst **118** and cinnamaldehyde. A NOESY experiment further supported this to be the preferred iminium geometry. Dienophile approach from the bottom face of this iminium **120,** as depicted in Figure 53, would provide us with the observed stereochemistry observed for the *endo* and *exo* adducts **119**.

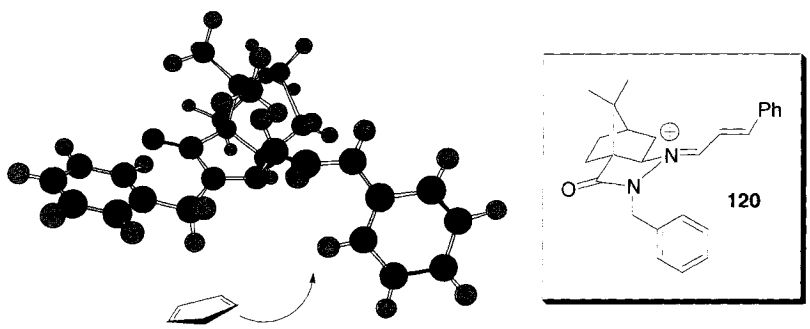

Figure 53. Preferred Iminium Formed by Catalyst **118** and Cinnamaldehyde.

Further NMR studies by Mathieu Lemay, allowed for monitoring of the rate of iminium formation for **118**, which was discovered to be a rapid process compared to MacMillan's catalyst. This information confirmed our notion that the α-effect of the hydrazine moiety would contribute to quicker iminium generation. The finding also suggested that the rate limiting step for our catalytic Diels-Alder reaction is

not formation of the iminium, but rather another process. Efforts towards elucidating the mechanism of the hydrazide catalysis are underway.

With the success of the catalyst **118**, further studies to improve on the catalytic scaffold and to expand reaction scope of hydrazide catalysts were initiated by our group.

CHAPTER 6
HYDRAZIDE CATALYSIS

Our investigation into chiral catalysis mediated by hydrazides has delivered promising results. Mathieu Lemay was triumphant in exploiting the α-effect by means of a novel hydrazide catalyst **114**, to effectively lower the LUMO energy of α,β-unsaturated aldehydes through the generation of an iminium intermediate. The activated aldehyde could then be subjected to an enantioselective Diels-Alder reaction at room temperature. We were motivated by the experimental outcomes to dig further into the realm of hydrazide catalysis by exploring other catalytic structures and other organic transformations.

6.1. New Catalyst Design

Our original catalyst possessed a camphor backbone as a platform for enantioselectivity. We were curious to explore other scaffolds in an attempt to improve the catalyst activity and to learn more about hydrazide catalysis. Our first efforts focused on creating a bicyclic structure, in which a simple cyclopentane ring would replace the camphor unit.

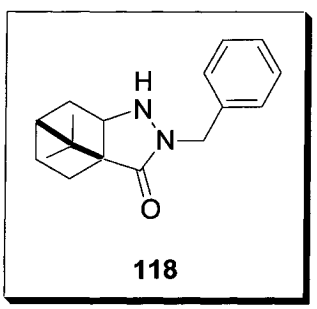

118

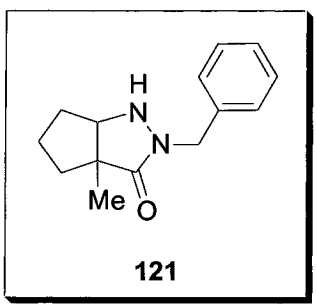

121

Figure 54. Catalyst **121** from Replacement of Camphor Moiety in Catalyst **118** with Cyclopentane.

We hoped that the bicyclic structure would impose enough ring strain to enhance the exposure of the nucleophilic nitrogen lone pair so that iminium formation with aldehyde substrates could proceed with greater ease. The methyl group in **121** could be modified readily to give a series of analogues for us to test structure versus catalyst activity relationships. To evaluate our new catalyst structure, we first decided to make **121** in a racemic fashion. After ensuring that good conversion could be achieved in our targeted Diels-Alder reaction, an asymmetric synthesis would be pursued.

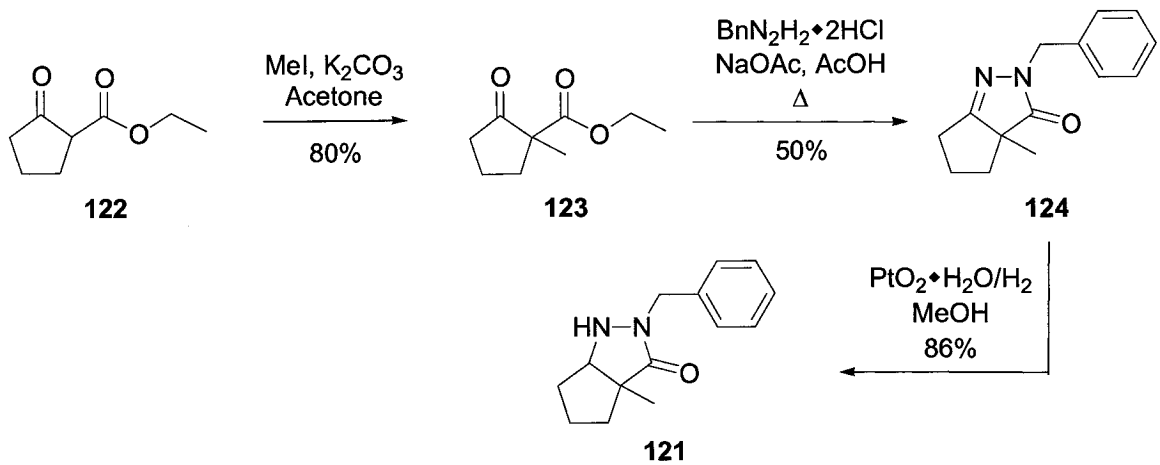

Scheme 39. Racemic Synthesis of Bicyclic Hydrazide Catalyst.

Freshly distilled methyl iodide was used to alkylate the commercially available keto-ester **122**. The difference in pK_a values between the α-hydrogens of the ketone, allowed one to selectively deprotonate the more acidic hydrogen by means of a weak carbonate base. By this method, we were able to methylate at the more substituted position to produced **123**. Refluxing the substituted keto-ester **123** with benzyl hydrazine in acetic acid allowed for two successive steps to occur in one pot. Firstly, a reaction between the ketone and primary nitrogen of the hydrazine produced an imine intermediate. This was followed by the condensation between the hydrazine component and the ester group to furnish the cyclized product **124**. Finally, reduction of the imine proceeded with platinum

oxide under a hydrogen atmosphere to give the catalyst **121** in 69% yield over three steps.

The bicyclic hydrazide catalyst **121** was tested in a Diels-Alder reaction using (*E*)-cinnamaldehyde and cyclopentadiene as the dienophile and diene components respectively. A catalyst loading of 20 mol% was employed along with perchloric acid, which, at the time of experimentation, was the determined to be the optimal co-catalyst. A control experiment was also set up to determine the contribution of background reaction caused by the acid co-catalyst (Table 13, entry 1). The reaction was allowed to proceed for 48 hours before the appropriate work up was ensued. As the aldehydic proton for the starting material and those of the *endo/exo* products were distinguishable by proton NMR, this provided us with a facile method to determine product conversion as well as the *endo:exo* ratio of the adducts from spectral analysis of the crude material. The results of this experiment are summarized in Table 13.

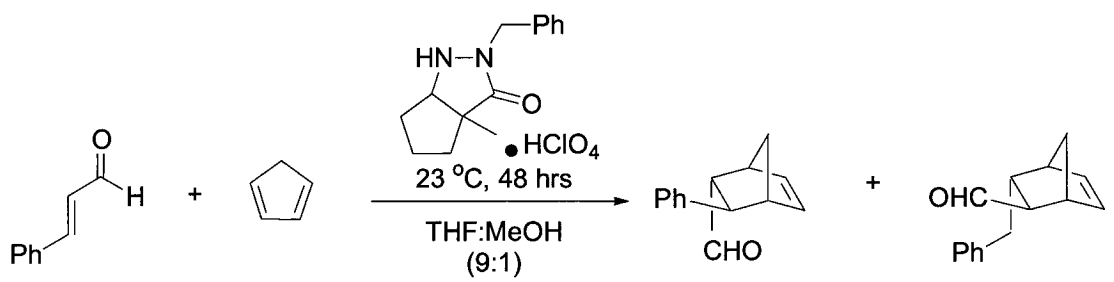

99 *1 eqv.* **96** *4 eqv.* ***Endo*-119** ***Exo*-119**

Entry	Catalyst 127	$HClO_4$	% Conversion	Endo : Exo
1[a]	0 eqv.	0.18 eqv.	7	1.3 : 1
2	0.2 eqv.	0 eqv.	1.4	1.7 : 1
3	0.2 eqv.	0.1 eqv.	8.5	1 : 3.1
4	0.2 eqv.	0.18 eqv.	13.2	1 : 1.9

Table 13. Evaluation of Catalyst **121** in a Diels-Alder Reaction with Cinnamaldehyde and Cyclopentatdiene.

[a] Result from Mathieu Lemay.

Much to our dismay, poor adduct formation was noted for the catalyst **121**. Using 0.2 equivalents of catalyst at all times, the conversion improved, albeit slightly, with increasing amounts of acid cocatalyst (Table 13, entries 2 to 4). A maximum of 0.18 equivalents of $HClO_4$ was used to ensure that the acid catalyzed reaction would not over contribute to adduct formation. Comparing the hydrazide catalyzed reactions to the control experiment (Table 13, entry 1), the product conversion by **121** in the presence and absence of perchloric acid was no better than in the case where only the acid co-catalyst was present. Observing the *endo:exo* ratio of the Diels-Alder adducts resulting from hydrazide catalysis by **121**, seem to reveal a small preference for the *exo* isomer.

The experimental outcome led us to reconsider our catalyst design. The *cis* fusion of the cyclopentane ring was regarded to be a possible limiting factor. A *cis* configuration would facilitate the α-nitrogen to be in resonance with the carbonyl group and thus restricting the desired alpha effect. To resolve this, a six membered ring, which would provide us with a *trans* ring fusion similar to the original catalyst **118**, was the chosen to be the next structure for our study. Efforts towards the synthesis of **128** were consequently pursued.

The synthetic scheme for the racemic production of **121** was flexible enough to accommodate the change from a five membered ring to a six membered ring in the catalytic scaffold. Starting from the cyclohexene keto-ester **125**, selective methylation was accomplished in the same simple and efficient manner as before. Refluxing the alkylated product with benzyl hydrazine provided a bicyclic imine, a result of two successive transformations, in good yield.

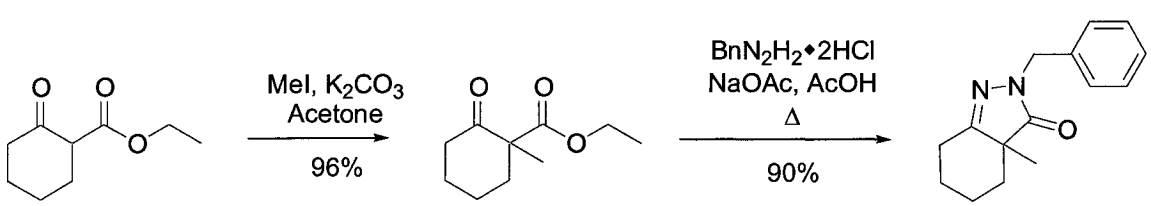

125 **126** **127**

Scheme 40. Towards the Synthesis of Hydrazide Catalyst **128**.

Imine reduction by our usual method with platinum oxide was problematic as the starting material was still predominant after a 24-hour hydrogenation period. There was also indication of the risk of reducing the benzene moiety of **135** to the corresponding cyclohexyl derivative. Therefore, a change of reduction method was necessary. This task was later accomplished by using sodium cyanoborohydride[32] as a reduction agent. A criterion for imine reduction by this method necessitated the imine to be in its protonated form in order for it to be activated towards reduction. The acidic conditions required for imine reduction was satisfied by using a 1:2 mixture of acetic acid to methanol as the solvent for the reaction.

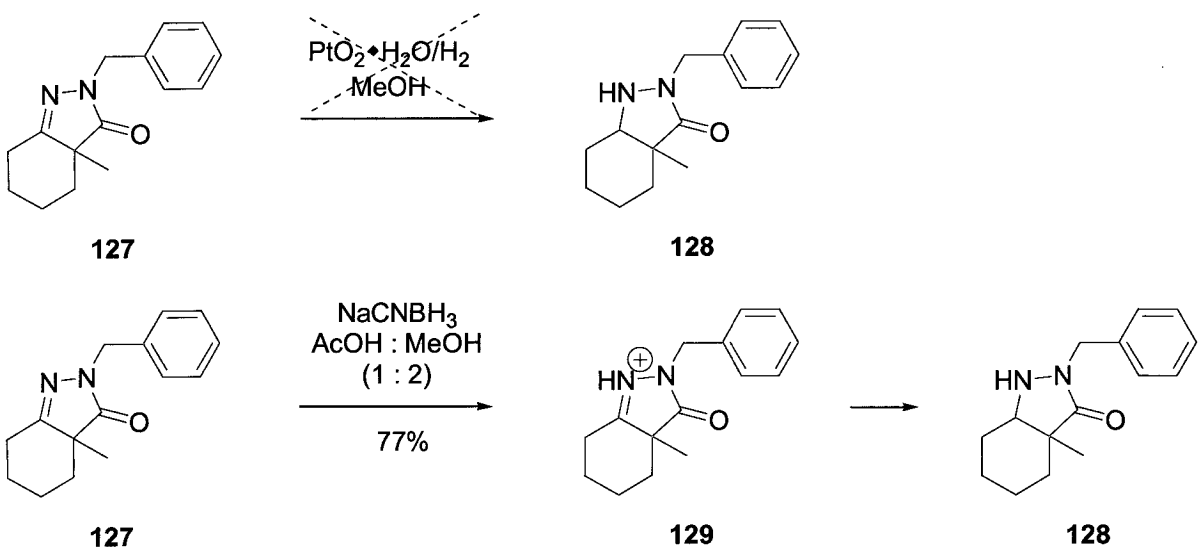

Scheme 41. Methods of Imine Reduction to Generate Hydrazide Catalyst.

[32] Borch, R.F.; Bernstein, M.D.; Durst, D. *J. Am. Chem. Soc.* **1971**, *93*, 2897.

The newly synthesized catalyst was tested with our targeted reaction. Once again, 20 mol% of catalyst was applied to the Diels-Alder reaction between (*E*)-cinnamaldehyde and cyclopentadiene with varying amounts of acid co-catalyst.

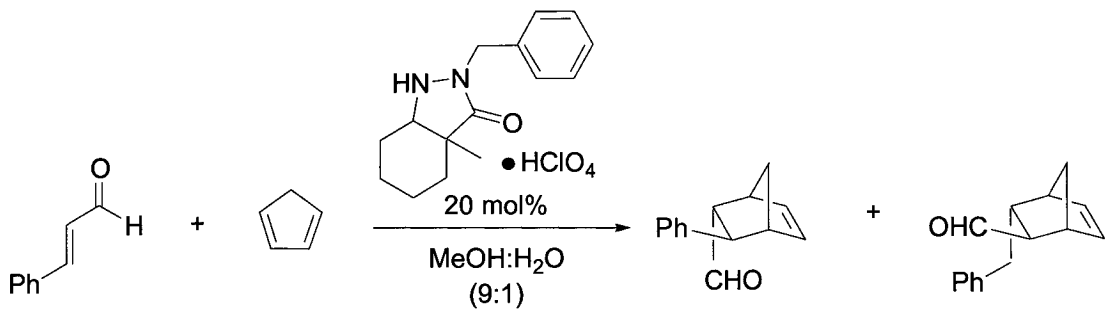

99 **96** ***Endo*-119** ***Exo*-119**

Entry	Catalyst 127	$HClO_4$	% Conversion	Endo : Exo
1[a]	0 eqv.	0.18 eqv.	7	1.3 : 1
2	0.2 eqv.	0 eqv.	3.1	1 : 1.2
3	0.2 eqv.	0.1 eqv.	12.4	1 : 2.1
4	0.2 eqv.	0.18 eqv.	9.7	1 : 2.1

Table 14. Evaluation of Catalyst **128** in a Diels-Alder Reaction with Cinnamaldehyde and Cyclopentatdiene.

[a] Results from Mathieu Lemay.

No obvious trends could be established from the product conversions indicated in Table 14. What can be said is that the hydrazide catalyzed reaction in the presence or absence of perchloric acid was not significant. The conversion in these cases could be largely accounted for by the competing acid catalyzed reaction, which was represented by our control experiment (Table 14, entry 1).

It appears that substituting the camphor moiety of **118** with a simpler cyclic system, resulted in a lost of catalyst activity. Efforts towards catalyst optimization thus concentrated on the camphor catalyst as a base structure with modifications

made to the substitution of the hydrazide moiety. Other members of the Ogilvie group are currently pursuing this work.

6.2 Application of Hydrazide Catalysis to Friedel-Crafts Alkylation.

In chapter 5, the hydrazide catalyst **118** was successfully applied to the Diels-Alder reaction. Indeed, there was evidence that iminium generation effected the lowering of the dienophile LUMO energy to accelerate the reaction. This was also achieved enantioselectively by the chiral catalyst. The MacMillan group has also applied iminium catalysis to the Diels-Alder reaction. In addition to this, the group has also expanded their work to include reactions such as the Friedel-Crafts alkylation showing just how valuable iminium based catalysis can be. We also initiated projects towards determining the scope of our hydrazide catalyst, as such, the Friedel-Crafts reaction was explored.

6.2.1 Friedel-Crafts Alkylation of Pyrroles

Pyrrole is an aromatic heterocycle with substantial π character that makes it susceptible towards electrophilic substitution. Substitution preferentially occurs at the α-position rather then at the β-position. This is the case because the σ-complex generated by electrophilic addition to the carbon adjacent to the heteroatom experiences better stabilization then that derived from a β addition.

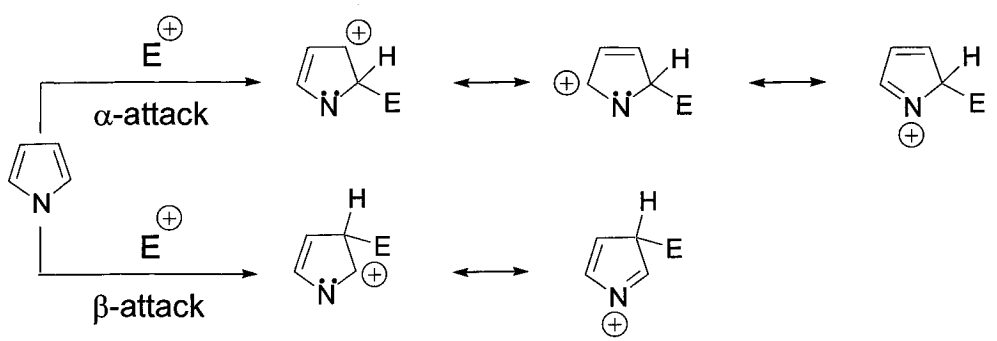

Scheme 42. Electrophilic Substitution in Pyrrole.

Lewis acid mediated alkylation, usually associated with the Friedel-Crafts reactions, is not recommended for pyrroles, as polymerization can result. MacMillan has illustrated that organocatalysis can be a useful method of carrying out the alkylation of pyrroles[33].

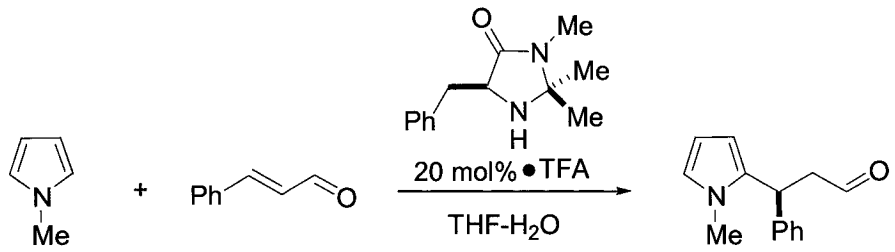

101 **99** **130**

Entry	Temperature (°C)	Time (hr)	Yield (%)	ee (%)
1	23	3	78	81
2	-30	42	87	93

Table 15. Friedel-Crafts Alkylation of *N*-Methyl Pyrrole by *(E)*-Cinnamaldehyde Employing MacMillan's Imidazolidinone Catalyst **90**.

Using MacMillan's study as a model to test for catalyst activity, we subjected the hydrazide catalyst **118** to the Friedel-Crafts alkylation of *N*-methyl pyrrole. Three different Bronsted acids including trifluoroacetic acid, perchloric acid, and triflic acid were evaluated as co-catalyst candidates. Reactions were monitored at room temperature until disappearance of **99** by means of TLC. Table 16 provides an account of the experimental outcome.

[33] Paras, N.A.; MacMillan, D.W.C. *J. Am. Chem. Soc.* **2001**, *123*, 4370.

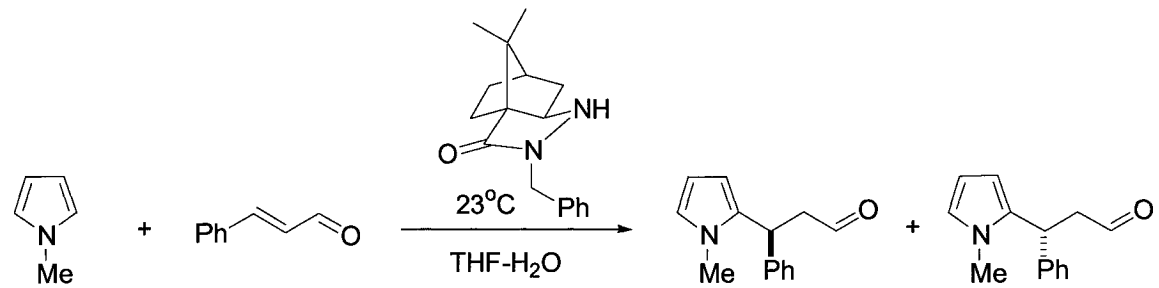

101 **99** ***S*-130** ***R*-130**

Entry	Catalyst Eqv.	Acid	Acid Eqv.	Result by TLC
1	0.2	-	-	No reaction
2	0.2	TFA	0.18	Decomposition
3	-	TFA	-	Decomposition
4	0.2	$HClO_4$	0.18	Decomposition
5	-	$HClO_4$	-	Decomposition
6	0.2	CF_3SO_3H	0.18	Decomposition
7	-	CF_3SO_3H	-	Decomposition

Table 16. Friedel-Crafts Alkylation of *N*-Methyl Pyrrole by *(E)*-Cinnamaldehyde Employing Hydrazide Catalyst **118**.

Monitoring the reactions by TLC proved difficult, as streaking on the TLC plate was noted as early as 5 minutes after reaction commencement. The only exception to this observation was entry 1 (Table 16), in which no reaction resulted since no acid co-catalyst was used. Over the course of time, the reaction mixtures containing acid turned from a pale yellow solution to a prominent burgundy colour. The reactions were allowed to progress for a 4-hour period before work up was ensued. Chromatography of the complex mixture was not pursued. The NMR spectra of the crude materials did not show signs of product formation.

It has been well documented that pyrroles can easily undergo polymerization in the presence of acids[34]. It was indeed likely that polymerization of *N*-methyl pyrrole was interfering with the desired β-alkylation reaction. This postulate was supported by the series of control experiments that were executed with only the presence of acid. Regardless of the acid, each control (Table 16, entries 3, 5 and 7) displayed similar results by TLC as did the reactions containing both acid and hydrazide catalyst (Table 16, entries 2,4 and 6). In fact, repeating the reaction with as little as 0.05 equivalents of TFA along with the usual 20% catalyst loading still resulted in a product mixture that could not be separated on TLC.

Conducting the reaction at low temperatures (-78°C → -5°C) using TFA as the co-catalyst significantly impeded the reaction rate. After a 42-hour period, (*E*)-cinnamaldehyde was still deemed abundant by TLC visualization, accompanied by the familiar streaking on the alumina plate. The same observations were noted for the control experiment with only TFA present.

All this evidence supports the notion that the reactivity of MacMillan's imidazolidinone catalyst **90** is different then that of our hydrazide catalyst **118**, despite the fact that the two are based on the phenomenon of iminium activation. It appears that catalysis by **90**, occurs quickly enough so that polymerization is not an issue. However, when **118** was applied to the Friedel-Crafts alkylation of pyrrole, acid catalyzed polymerization prevailed over the desired reaction.

---

[34] "The acid-catalysed polymerizationof pyrroles and indoles", Smith, G.F. *Adv. Heterocyl. Chem.* **1963**, *2*, 287.

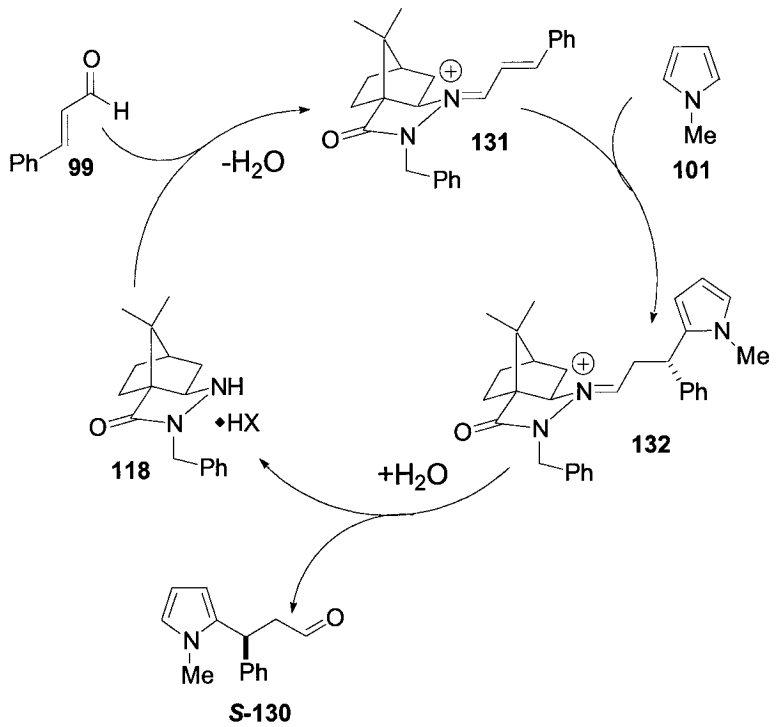

Scheme 43. Hydrazide Catalyzed Friedel-Crafts Alkylation of *N*-Methyl Pyrrole.

Preliminary kinetic studies by Mathieu Lemay have show that iminium formation (Scheme 43, **118**→**131**) is a fast process. Thus we speculated that hydrolysis of **132** to provide the product and regenerate the catalyst was rate limiting. Impeded hydrolysis of **132** would give acid catalyzed polymerization a chance to occur, which appears to be consistent with our experimental results.

6.2.2 Friedel-Crafts Alkylation of Indoles.

Due to the acid sensitivity of pyrrole substrates, we decided to focus our attention on the alkylation of indoles. The indole structure consists of a benzene ring that is fused to the pyrrole framework. As such, indoles, like their pyrrole counterparts, are also reactive towards electrophilic substitution, although the

former are found to be less nucleophilic[35, 36]. This minor contrast between pyrrole and indole reactivity was of great interest to us, as it suggested that acid catalyzed indole polymerization, although possible, would be less overwhelming.

Alkylations of indolic substrates, unlike pyrroles, occur preferentially at the β-position as opposed to the α-position. β-alkylation is favourable as the cation intermediate formed is stabilized by donation of the nitrogen lone pair through resonance without disruption of the benzonoid aromaticity (Scheme 44).

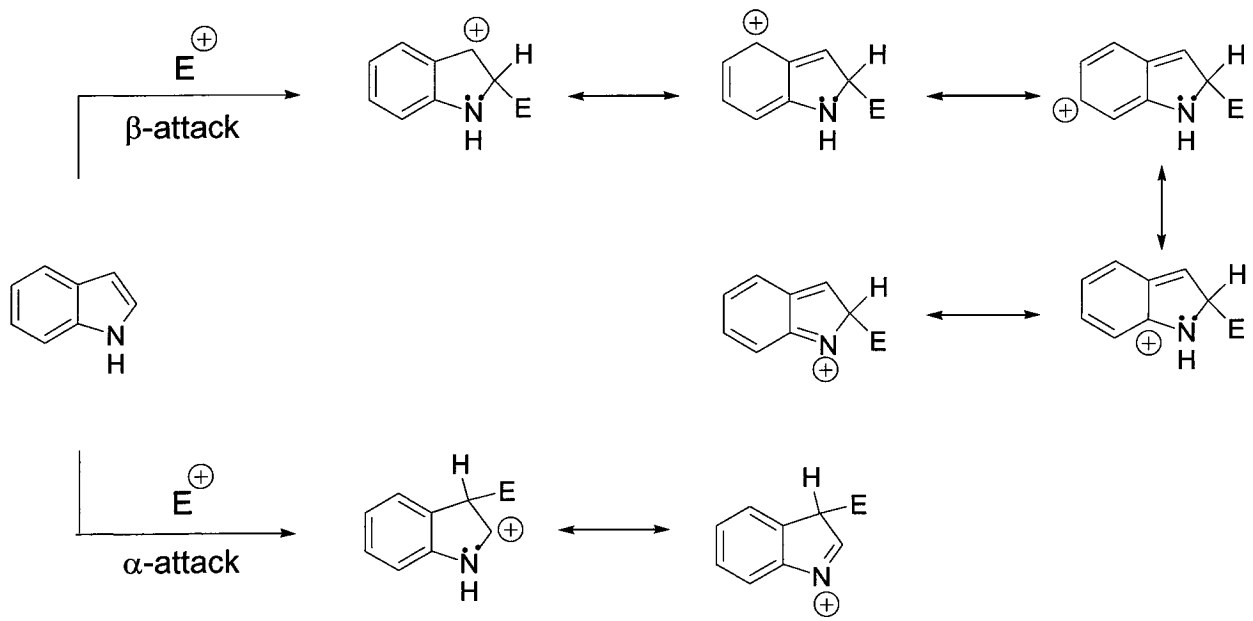

Scheme 44. Electrophilic Substitution in Indole.

[35] " Heterocyclic Chemistry II: Five-Membered Heterocycles ". Gupta, R.R.; Kurmar, M.; Gupta, V. Springer. **1998**.

[36] " Heterocyclic Chemistry. Joule, J.A.; Mills, K. Blackweell Science. **2000**.

Earlier discussion has revealed that a second-generation imidazolidinone catalyst **107** was created by the MacMillan group to effect the enantioselective alkylation of indole. This became a model for us to base our study on.

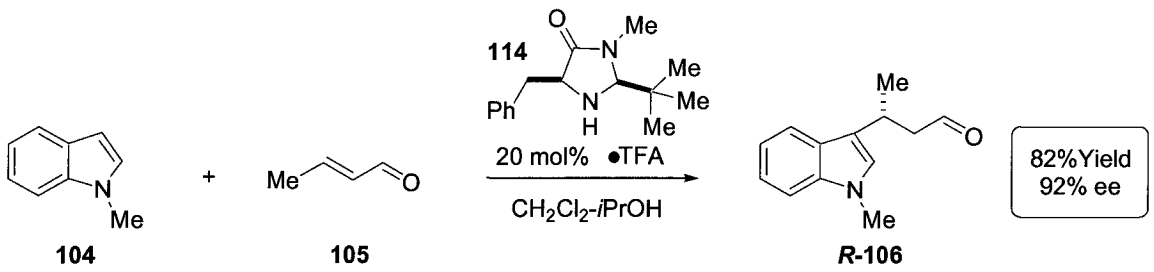

Scheme 45. Imidazolidinone Catalyzed Friedel-Craft Alkylation of *N*-Methyl Indole at -83°C for 19 Hours.

6.2.1 Optimization of Reaction Conditions

We launched our own investigation into this reaction using triflic acid as the co-catalyst as it was recently determined to be the optimal acid for the Diels-Alder reaction. A reaction with conditions similar to that imposed by MacMillan's work, was done as a platform for comparison. In addition to this, a study of binary solvent systems was completed at room temperature, the results of which are disclosed in Table 17.

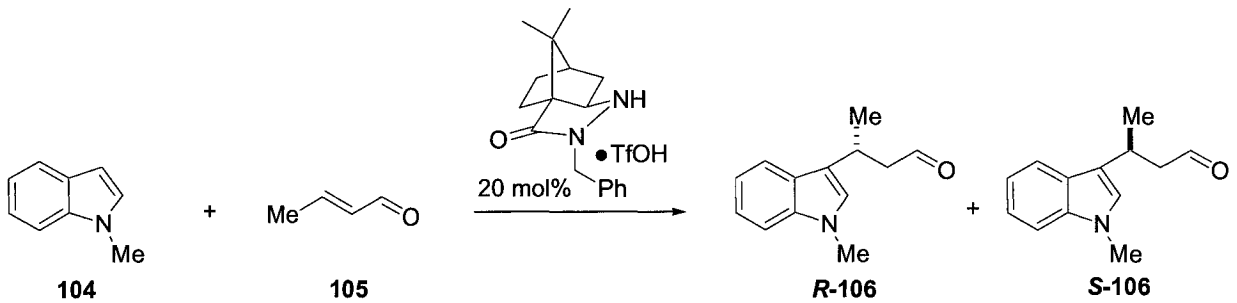

104 105 *R*-106 *S*-106

Entry	Solvent (85:15)	Temperature	Time (hr)	Yield (%)	ee[a] (%)
1	CH_2Cl_2:*i*PrOH	-78°C	72[b]	25	61
2	CH_2Cl_2:*i*PrOH	23°C	50	30	44
3	CH_2Cl_2:MeOH	23°C	50	11	41
4	CH_2Cl_2:H_2O	23°C	3.5	45	48
5	THF:*i*PrOH	23°C	50	36	46
6	THF:MeOH	23°C	50	9	47
7	THF:H_2O	23°C	4	27	49
8	CH_3NO_2:*i*PrOH	23°C	4	23	51
9	CH_3NO_2:MeOH	23°C	4	39	52
10	CH_3NO_2:H_2O	23°C	4	53	39

Table 17. Solvent Study of Hydrazide Catalyzed Friedel-Crafts Alkylation of Indole.

[a] ee determine by reduction of the aldehyde to the corresponding alcohol. Selectivity favours *R* isomer.

[b] Reaction stopped after 72 hours although incomplete.

The results from Table 17 can be summarized by the following observations. The best selectivity was achieved in 61% enantiomeric excess when the reaction was executed at a low temperature (entry 1). The worst yields were obtained when MeOH was present in the reaction (entries 3 and 6) and the best yielding reaction was attained by a mixture of nitromethane/water (entry 10). The alkylation was observed to be a slow process unless water was the co-solvent, where

consumption of **105** was complete in a matter of hours instead of days. Referring to the catalytic cycle of the reaction (Scheme 46), if iminium hydrolysis was indeed the rate determining step, then the addition of water would contribute to enhancing the speed of this process. Investigations into the reaction mechanism are still ongoing.

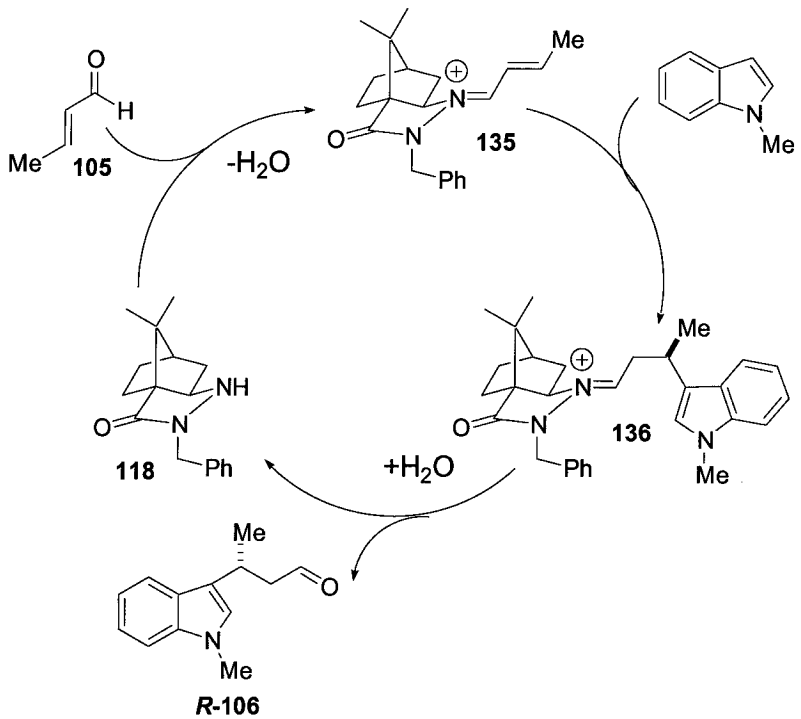

Scheme 46. Hydrazide Catalyzed Friedel-Crafts Alkylation of *N*-Methyl Indole.

Based on the information obtained from our primary solvent scan, we decided that an ideal system would be one that included water to accelerate the reaction rate and one that would also tolerate low temperatures as measure of enantiocontrol. Solvent miscibility needed to be considered here as a biphasic solvent system with water would cause it to freeze out at temperatures below 0°C. Thus, dichloromethane was eliminated as a possible choice of solvent. Finally, a combination of THF and water was selected as the former was characterized by a freezing point of - 108°C. To effectively lower the freezing point of water, *iso*propanol was included to create a tertiary solvent system. A

85:12:3 mixture of THF:*i*PrOH:H_2O was found to be tolerated in the temperature range of -18 °C and -78°C without the formation of water crystals.

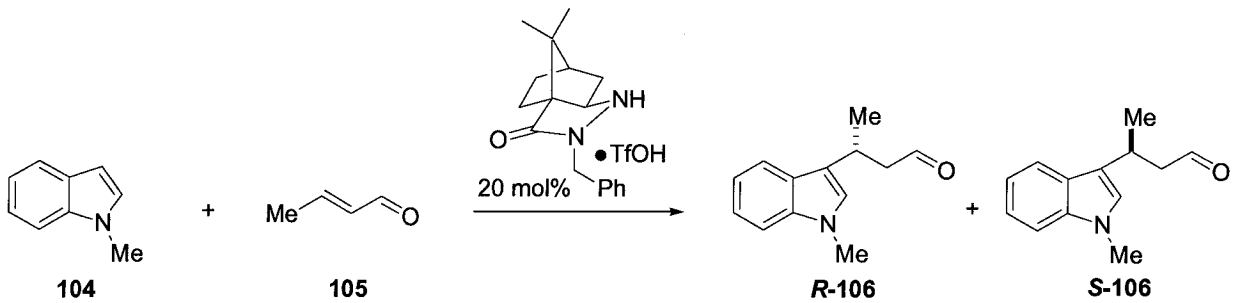

Entry	Solvent (85:12:3)	Temperature	Time (hr)	Yield (%)	ee[a] (%)
1	THF:*i*PrOH:H_2O	23°C	6	32	47
2	THF:*i*PrOH:H_2O	-18°C	54	27	62
3[b]	THF:*i*PrOH:H_2O	-18°C	54	8	1

Table 18. Hydrazide Catalyzed Friedel-Crafts Alkylation of *N*-Methyl Indole in a Tertiary Solvent System.

[a] ee determine by reduction of the aldehyde to the corresponding alcohol. Selectivity favours *R* isomer.

[b]Control experiment with only the acid co-catalyst.

Examining the results in Table 18 show that although reaction rates were improved at room temperature, low temperature reactions were still slow and the yields remained rather low. Further to this, no improvements to the enantioselectivity of the reaction were noted. Conducting the alkylation without the hydrazide **118** present served as a control to evaluate the non-selective acid catalyzed reaction. Non-specific catalysis was found to contribute 8% to the already deficient yield. We thus embarked on a study to ameliorate the productivity of the reaction by adjusting the reaction conditions.

An aqueous mixture of nitromethane had provided the best yield thus far and this became the starting point for us to fine-tune the reaction parameters. Additional analysis of the reaction revealed the formation of a side product that could only be isolated in pure form by using benzene or toluene as an eluant in column chromatography. The structure was elucidated to be **138**, which could arise from acid catalyzed 1,2-addition to the desired Friedel-Crafts product followed by nucleophilic substitution.

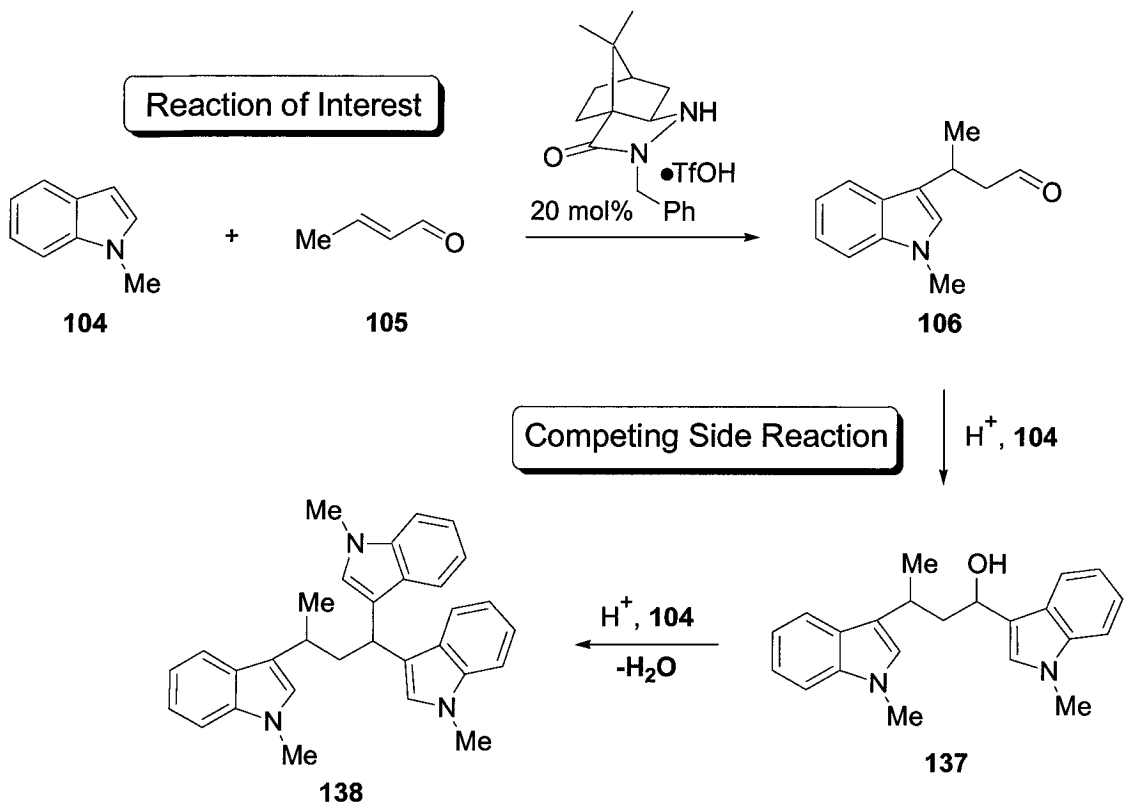

Scheme 47. Proposed Route to Side Product Generation.

This process consumes 3 units of *N*-methyl indole for every unit of **138** formed. Consequently, we witnessed a decrease in yield of the desired reaction since the indole substrate was quickly being depleted by a competing transformation. As further evidence of this, the target reaction was repeated with an excess of indole, which was expected to favour the production of the tri-indole substrate

138 over the mono-alkylated product **106**. Our predictions were confirmed as experiment outcome presented **138** as the major product.

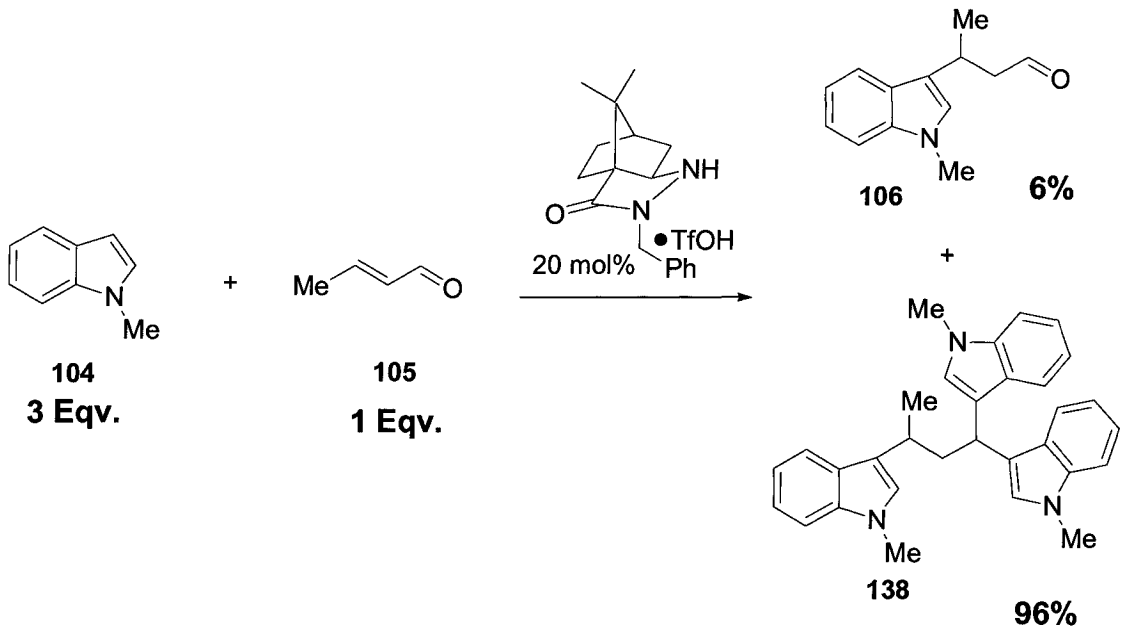

Scheme 49. Friedel-Crafts Alkylation Using *N*-Methyl Indole in Excess.

We reasoned that increasing the equivalents of crotonaldehyde **138** could drive the Friedel-Crafts alkylation is spite of the side reaction. The idea was fruitful as we witness a steady improvement in productivity with increasing amounts of aldehyde. Satisfied with the optimization, we conducted the rest of our experiments with 10 equivalents of crotonaldehyde.

Entry	Aldehyde	Time (hr)	106 Yield	138 Yield
1	3 eqv	3.5	52%	35%
2	6 eqv	3.5	68%	19%
3	10 eqv.	3.5	81%	8%

Table 19. Effects of Aldehyde Equivalents on Product Distribution.

The favourable yields observed with using nitromethane as a solvent prompted us to attempt using this solvent at low temperatures. Selected solvent systems

were also reevaluated to verify if the modified reaction conditions would bring about a global increase in yield.

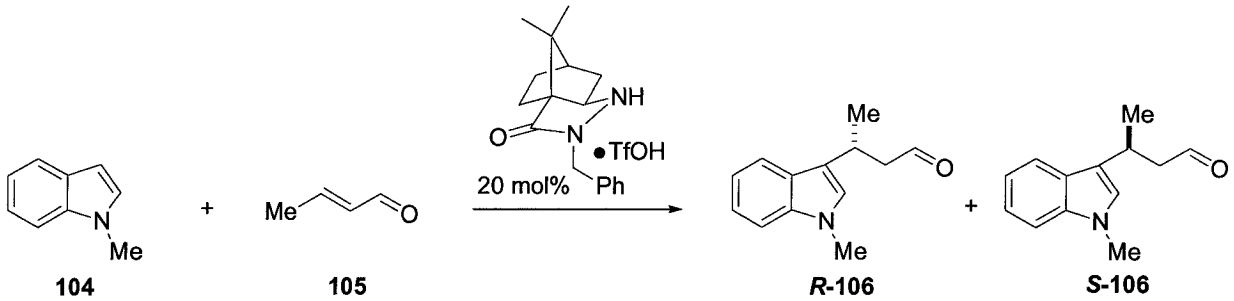

104 105 *R*-106 *S*-106

Entry	Solvent	Eqv.	Temp.	Time (hr)	Yield	ee
1	CH_3NO_3:H_2O	3	23°C	3.5	53%	39%
2	CH_3NO_3:H_2O	10	23°C	3.5	81%	38%
3	CH_3NO_3:*i*PrOH	3	23°C	4	39%	52%
4	CH_3NO_3:*i*PrOH	10	23°C	7	59%	34%
5	CH_3NO_3:*i*PrOH	10	-18°C	24	46%	47%
6	CH_3NO_3:*i*PrOH:H_2O	10	23°C	3.5	76%	33%
7	CH_3NO_3:*i*PrOH:H_2O	10	-18°C	20	62%	47%
8	THF:*i*PrOH:H_2O	3	23°C	6	32%	47%
9	THF:*i*PrOH:H_2O	10	23°C	4	56%	37%

Table 20. Effects of Increased Crotonaldehyde Equivalents on Friedel-Crafts Alkylation of *N*-Methyl Indole.

Unfortunately, the increase in reaction yields mediated by excess aldehyde, was not as effective with solvent systems other than nitromethane and water. In fact, some cases saw a decrease in enantioselectivity (Table 20, entry 4 and 9). A consequent control reaction without the hydrazide catalyst was conducted in aqueous nitromethane. This provided the desired product racemically, in 30% yield. This background reaction was overwhelming and made us skeptical to continue with this solvent system.

6.2.2 Results From Applying a Second Generation Catalyst

Further optimization towards improving the yield and selectivity of catalyst **118** towards the targeted Friedel-Crafts reaction, were abandoned to pursue a second-generation hydrazide catalyst **139** synthesized by Livia Aumand.

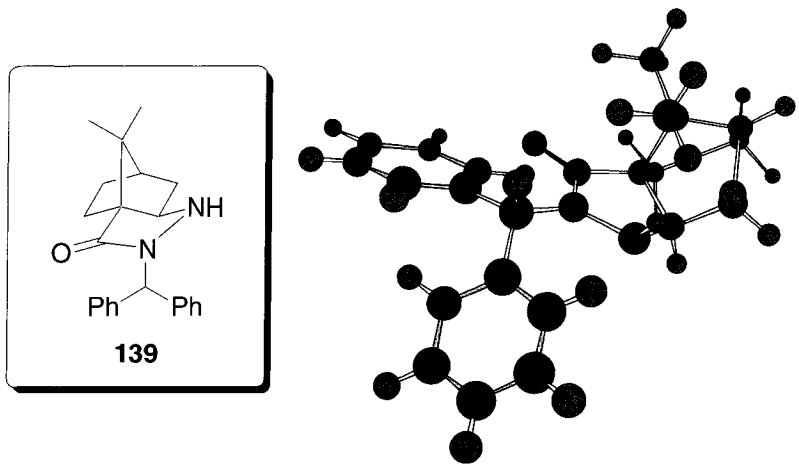

Figure 55. Second Generation Hydrazide Catalyst with Increased Steric Bulk.

The change from benzyl to a biphenyl substituent was done to enhance the steric bias of the catalyst. As a direct result of this, the generation of the iminium from the catalyst and aldehyde substrate should preferably adopt a geometry that would minimize steric interactions.

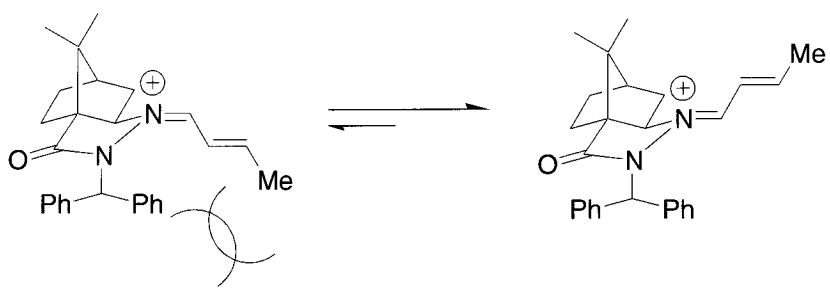

Scheme 49. Steric Contributions Leading to Biased Geometry of Iminium Intermediate.

The new catalyst was evaluated in our targeted Friedel-Crafts transformation, using a tertiary solvent system.

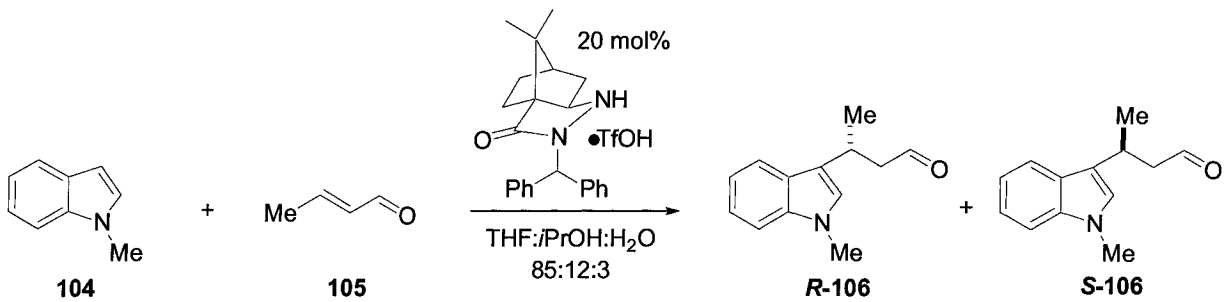

Entry	Temperature	Time (hr)	Yield	ee
1	23°C	4	22%	18%
2	-18°C	48	20%	26%

Table 21. Friedel-Crafts Alkylation of *N*-Methyl Indole Employing the Hydrazide Catalyst **139**.

We were disappointed to see that the revision made to the catalyst was deleterious to both the yield and selectivity of the reaction. The progress of this reaction was notably different to analogous reaction that employed the original catalyst **118**. After an hour, the reaction mixture displayed a purple colour that suggested the occurrence of a side reaction.

The steric effects imposed by the diphenyl substituents could indeed hinder indole approach to the activated aldehyde and therefore affect a lowering in yield and selectivity. As the results were a regression to our initial findings, optimizations to reaction conditions involving **139** were not pursued.

6.3. Conclusions.

Unfortunately, the success of the hydrazide catalysis experienced with the Diels-Alder application has yet to be duplicated in Friedel-Crafts reactions. The difference in selectively between the two transformations can be rationalized by examining the structure of the iminium ion generated by the catalyst and the α.β-unsaturated aldehyde.

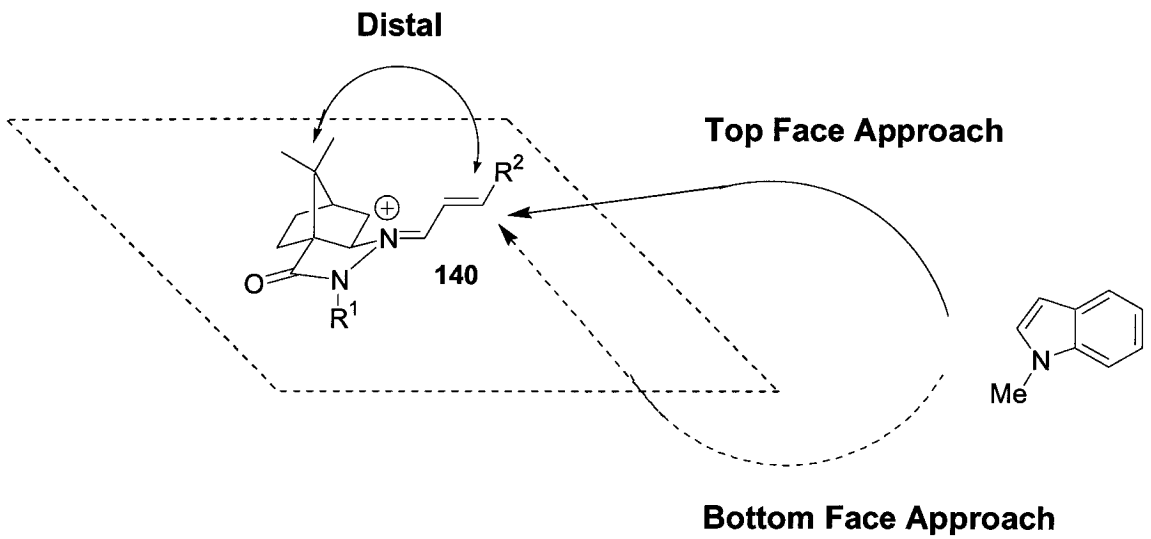

Figure 55. Facial Selectivity of Hydrazide Catalyzed Friedel-Crafts Alkylation of *N*-Methyl Indole.

The gem dimethyl groups of the camphor architecture are key in controlling the facial selectivity of the substrate approach. In an ideal situation, the gem dimethyl substituents would block the top face approach of the nucleophile to impart selectivity. In the case of the Friedel-Crafts alkylation of indole, the substrate reacts at the β-position of the iminium intermediate, which is distant from the control elements. The facial bias of the catalyst framework therefore has minimal effects here. This is different from the Diels-Alder addition, where the diene is drawn closer to catalyst environment since both the α and β carbons of the iminium ion are involved in product formation.

Another marked difference between the two targeted reactions is that the Friedel-Crafts substrates, particularly pyrrole, exhibit greater sensitivity to acid. Consequently the reaction was impeded by different side reactions such as polymerization.

Efforts towards improving the rate of catalysis would be important to help overcome the competing reactions where the Friedel-Crafts alkylation is concerned. Elucidation of the mechanism of hydrazide catalysis will be a necessary component in our strategy to optimize the reaction rate. As mentioned previously, the control elements for facial selectivity of the catalyst are distal from the reactive β-carbon of iminium formed (Figure 55) and thus imparted poor reaction selectivity. To overcome this problem, one could attempt to employ larger substituents so that the facial selectivity can still be sense at β-carbon of **140.**

Hydrazide catalysis is still a relatively new concept in the field. Although much investigation is needed to expand its utility in different organic transformations, preliminary results indicate that it is possible. Indeed, we expect that hydrazide catalysis will play an important role in the field of organocatalysis.

CHAPTER 7
CLAIMS TO ORGINAL RESEARCH

1. Established that a single fluorescence quencher molecule can simultaneously suppress the fluorescence of two fluorescence donor molecules

2. Successfully, completed the proof of principle that a highthroughput screening method based on FRET can be applied to monitor the desymmetrization of *meso* compounds.

3. Synthesized second-generation hydrazide catalysts **121** and **128** and evaluated their efficiency in the Diels-Alder reaction.

4. Applied camphor based hydrazide catalyst in the Friedel-Crafts alkylation of pyrroles and indoles.

CHAPTER 8
EXPERIMENTAL

8.1. General

All reactions were executed in oven-dried glassware. All anhydrous solvents were distilled prior to use: THF over sodium/benzophenone ketyl; CH_2Cl_2 over calcium hydride: DMF over calcium hydride. Diisopropyl amine was distilled over calcium hydride prior to use. (*E*)- cinnamaldehyde and crotonaldehyde were distilled under reduced pressure prior to use. Reagents that were obtained commercially were used as such. Column chromatography was performed using silica gel 60 (230-400 mesh, Merck). ^{1}H NMR and ^{13}C NMR spectra were recorded on Bruker AMX instruments at 300 MHz and 75 MHz respectively. Chemical shifts are reported in ppm δ units relative to chloroform (7.26 ppm for ^{1}H NMR and 77.0 ppm for decoupled ^{13}C NMR) as an internal standard. Melting points were uncorrected. IR spectra were recorded with a Bomen Michaelson 100 FTIR instrument. Mass spectra were recorded at The University of Ottawa Mass Spectrum Centre. Fluorescence data were obtained from a Cary Eclipse fluorescence spectrophotometer, using a quartz cuvette (path length = 1 cm) or a white NUNC 96-wellplate (300 μL capacity). HPLC data was recorded on a Varian Prostar equipped with a Varian Polaris C18 A-5u 250 x 046 mm (pump Model PS210, PDA detector Model 330 and autosampler Prostar 430). Chiral HPLC data were obtained on a Waters 2695 equipped with a Chiralcel Ad-H (4.6 X 250 mm) chiral column and a Waters PDA detector 2996. Room temperature refers to 23 °C.

8.2 Procedures and Characterizations

Compound 33: {1-[4-(5-Dimethylamino-naphthalene-1-sulfonylamino)-butylcarbamoyl]-3-oxo-4-phenyl-butyl}-carbamic acid tert-butyl ester.

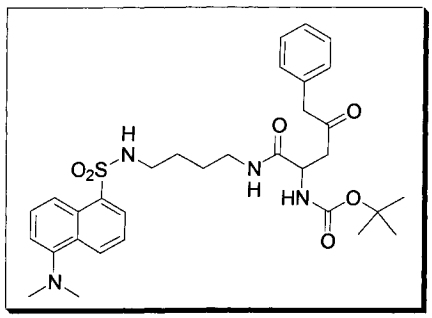

N-(4-aminobutyl)-5-(dimethylamino)naphthalene-1-sulfonamide[37] (1.40 g, 4.35 mmol) was dissolved in 45 mL of DMF in a 100 mL round bottom flask. To this, was added the protected aspartic acid **50** (1.83g, 4.04 mmol) followed by HOBT (1.33 g, 8.71 mmol), DIPEA (3.03 mL, 17.41 mmol) and lastly EDC (1.83 g, 8.71 mmol). The reaction was allowed to stir at room temperature for 18 hours. An excess of water was added to the reaction, which was then extracted three times with EtOAc. The organic layers were combined and washed sequentially with 10 % HCl, saturated $NaHCO_3$ and brine. The organic layer was dried over $MgSO_4$, filtered and concentrated under reduced pressure. The crude product was subjected to silica gel column chromatography using a 2:3 mixture of EtOAc to hexanes as the eluant to give 2.10 g (77 %) of the desired product as a yellow foam. IR (film, cm^{-1}) 3319, 2976, 2940, 1722, 1666, 1571, 1531; ^1H (300 MHz, $CDCl_3$) δ 8.52 (d, J = 8.4 Hz, 1H) 8.29 (d, J = 8.8 Hz, 1H), 8.21 (d, J = 7.1 Hz, 1H), 7.55-7.47 (m, 2H), 7.33-7.23 (br m, 5H), 7.16 (d, J = 7.4 Hz, 1H), 6.47 (br, 1H), 5.61 (br d, J = 8.4 Hz, 1H), 5.12 (br, 1H), 5.08 (s, 2H), 4.43 (br, 1H), 2.97 (m, 3H), 2.80-2.86 (m, 8H), 2.68 (dd, J = 6.1, 17.1 Hz, 1 H), 1.41 (s, 9H), 1.36 (br, 4H); ^{13}C (75 MHz, $CDCl_3$) δ 172.1 (s), 171.1 (s), 155.9 (s), 151.9 (s), 135.7 (s), 135.1 (s), 130.1 (d), 129.6 (d), 128.6 (d), 128.5 (d), 128.3(d), 128.2 (d), 123.4 (d), 119.5 (d), 115.3 (d), 81.0 (s), 67.2 (t), 50.6 (d), 45.5 (q), 42.8 (t), 38.7 (t), 36.1 (t), 28.3 (q), 26.5 (t), 26.4 (t); MS (EI) 626, 518, 418, 171, 108, 91, 79, 41.

[37] Josée Cloutier, Master's Thesis, University of Ottawa, 2004.

Compound 41: {1-[4-(6,10-Dihydro-pyrene-4-sulfonylamino)-butylcarbamoyl]-2-[4-(5-dimethylamino-naphthalene-1-sulfonylamino)-butylcarbamoyl]-ethyl}-carbamic acid tert-butyl ester

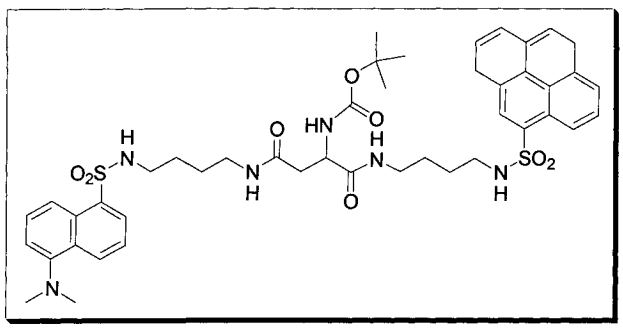

Compound **33** (1.00 g, 1.60 mmol) was stirred in 20 mL of a 4:1:1 mixture of THF:MeOH:H_2O with LiOH (113.9 mg, 3.19 mmol) to give a tan coloured solution. The hydrolysis was continued by stirring at room temperature for 12 hours. Concentrated HCl was added drop-wise until the pH of the solution was slightly acidic as indicated by pH paper. The mixture was then extracted three times with EtOAc. The combined organic phases were washed with brine, dried over $MgSO_4$, filtered and concentrated. The crude material was purified in a silica column using a mixture of EtOH (10%), EtOAc (89%) and acetic acid (1%). The product-containing fractions were concentrated and azeotropic distillation with benzene was done 3 times to remove any traces of acetic acid. 0.611 g (71%) of the acid **40** was isolated and applied to the synthesis of **41** without further purification. The acid **40** (244.0 mg, 0.46 mmol) was stirred in 5 mL of DMF. The amine **36** (208.3 mg, 0.59 mmol), HOBT (122.8 mg, 0.91 mmol) and DIPEA (0.39 mL, 2.27 mmol) were added to the reaction. EDC (174.3 mg, 0.91 mmol) was added last to the mixture, which was stirred for 20 hours at room temperature. 10 % HCl was added to the reaction and this was extracted three times with EtOAc. The combined organic phases were washed sequentially with saturated $NaHCO_3$ and H_2O. The organic layer was dried over $MgSO_4$, filtered and concentrated. The crude material was purified on a silica gel column using EtOAc as an eluant to furnish 207.0 mg of 41 (53 %) as a white foam. IR (film, cm^{-1}) 3437, 2932, 2862, 1659, 1516, 1439, 1388; ^1H (300 MHz, $CDCl_3$) δ 9.08 (d, J = 9.4 Hz, 1H) 8.66 (d, J = 8.3 Hz, 1H), 8.51 (d, J = 8.6 Hz, 1H), 8.46-8.11 (m, 8H), 7.63-7.44 (m, 2H), 7.35-7.11 (m, 2H), 7.00 (br t, J = 5.8 Hz, 1H), 6.75 (br t, J = 5.9 Hz, 1H), 6.32 (br d, J = 7.5 Hz, 1H), 4.25 (br, 1H), 2.94-2.74 (m, 16H), 2.67-2.36 (m, 2H), 1.44-1.24 (m, 17 H); ^{13}C (75 MHz,

$CDCl_3$) δ 171.4 (s), 170.7 (s), 155.6 (s), 152.2 (s), 136.7 (s), 136.6 (s), 134.9 (s), 133.3 (s), 131.5 (s), 130.7 (s), 130.3 (d), 130.2 (s), 130.1 (d), 130.0 (s), 129.8 (d), 129.2 (d), 128.2 (d), 127.6 (d), 127.4 (d), 127.3 (d), 127.2 (d), 125.3 (s), 124.5 (s), 124.3 (d), 124.2 (d), 123.7 (d), 119.9 (d), 115.5 (d), 79.0 (s), 52.0 (d), 45.1 (q), 42.96 (t), 42.93 (t), 42.86 (t), 42.82 (t), 38.54 (t), 38.52 (t), 38.0 (t), 28.0 (q), 26.8 (t), 26.7 (t); MS (ESI, Na^+) 893, 871, 417.

Compound 42: Hexanedioic acid 1-[4-(6,10-dihydro-pyrene-4-sulfonyl-amino)-butylcarbamoyl]-2-[4-(5-dimethylamino-naphthalene-1-sulfonylamino)-butyl- carbamoyl]-ethyl}-amide-2-methyl-4-o-tolylazo-phenyl)-amide

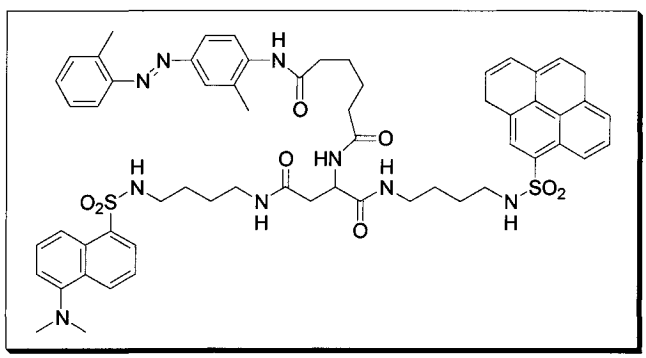

The amide **41** (240.0 mg, 0.276 mmol) was dissolved in 12 mL of CH_2Cl_2 to which 3 mL of TFA was added. This mixture was allowed to stir for 2 hours before the solvent and TFA were removed under reduced pressure. The crude mixture was re-dissolved in EtOAc and extracted with saturated $NaHCO_3$ and then H_2O. The organic layer was filtered through a cotton plug and concentrated under reduced pressure. The crude amine was stirred in 8 mL of DMF along with acid **39** (116.8 mg, 0.331 mmol), HOBT (74.5 mg, 0.551 mmol) and DIPEA (0.24 mL, 1.390 mmol). HBTU (208.9 mg, 0.551 mmol) was added last and the coupling reaction was allowed to proceed for 24 hours at room temperature. EtOAc and H_2O were added to the reaction and a brown precipitate separated from the solution. This precipitate was rinsed with 10 % HCl, saturated $NaHCO_3$ and H_2O. The solid was highly insoluble and attempts to purify it by column chromatography or recrystallization were unsuccessful. The crude product (80 mg) was subjected to preparative HPLC injecting in DMSO solvent and eluting with a gradient of acetonitrile (30 %) and water (70 %) to acetonitrile

(100 %) over a 40 minute run (HPLC solvents were buffered with 0.06 % TFA). Fractions of the peak from 24.0 to 25.0 minutes were collected and concentrated under reduced pressure. To remove any remaining traces of TFA, the produce was added to 4 mL of a 1:1 acetonitrile to ammonia mixture and swirled in a liquid N_2 bath for 15 minutes before subjecting the frozen mixture to lyophilization overnight. This procedure furnished 48.2 mg (16 %) of the desired product. ^1H (500 MHz, DMSO-d_6) δ 9.33 (s, 1H), 9.14 (s, 1H), 8.98 (d, J = 9.3 Hz, 1H), 8.57 (d, J = 8.1Hz, 1H), 8.07 (d, J = 7.1 Hz, 1H), 8.52-8.34 (m, 3H), 8.34-8.51 (m, 3H), 7.92-7.79 (m, 2H), 7.79-7.50 (m, 5H), 7.42 (d, J = 3.3 Hz, 1H), 7.36-7.27 (m, 1H), 7.20-7.16 (m, 1H), 7.05 (t, J = 7.3 Hz, 1H), 6.99 (t, J = 7.6 Hz, 1H), 6.85 (s, 1H), 6.50 (d, J = 7.0 Hz, 1H), 6.31 (d, J = 7.2 Hz, 1H), 4.50-4.37(m, 1H), 2.93-2.60 (m, 10H), 2.59-2.43 (m, 11H), 2.23-2.20 (m, 5H), 2.19-1.99 (m, 3H), 1.67-1.41 (m, 4H), 1.38-1.16 (m, 6H); MS (ESI, Na^+) 1128, 1106, 798, 571, 336.

Compound 43: N-[4-(5-Dimethylamino-naphthalene-1-sulfonylamino)-butyl]-3-[5-(2-methyl-4-o-tolylazo-phenylcarbamoyl)- pentanoylamino]-succinamic acid benzyl ester

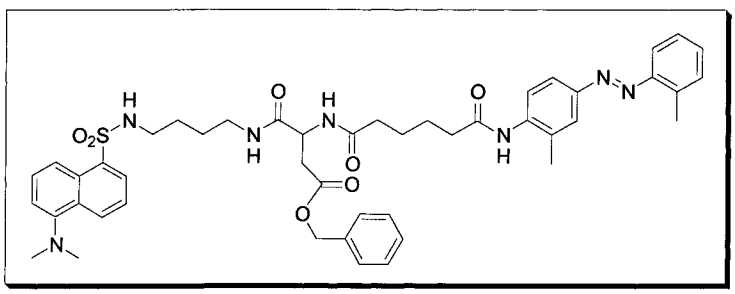

Compound **32** (300.0 mg, 0.479 mmol) was stirred in 12 mL of CH_2Cl_2, to which 3 mL of TFA was added. This mixture was stirred at room temperature for 30 minutes before concentrating under reduced pressure. The crude material was azeotropically distilled with benzene 3 times to remove any traces of excess TFA. The amine was stored as the TFA salt and subjected to a coupling reaction. The amine salt was stirred in 7 mL of DMF with **39** (186.0 mg, 0.526 mmol), HOBT (129.3 mg, 0.957 mmol), and DIPEA (0.29 mL, 2.392 mmol). EDC (183.5 mg, 0.957 mmol) was added last to the reaction. The reaction was stirred for 26 hours and H_2O was added before extracting the mixture 3 times with EtOAc. The

combined organic phases were washed sequentially with 10 % HCl, saturated $NaHCO_3$ and brine. The organic layer was dried over $MgSO_4$, filtered and concentrated under reduced pressure. The crude material was purified by silica gel column chromatography using a mixture of $CHCl_4$:EtOAc:MeOH (50:45:5) as an eluant to furnish 275 mg of **43** (35 %) as an orange coloured solid. IR (film, cm^{-1}), 3284, 3056, 2930, 2867, 1734, 1655, 1638, 1143; ^1H (300 MHz, $CDCl_3$) δ 8.49 (d, J = 8.2 Hz, 1H) 8.26 (d, J = 7.3 Hz, 1H), 8.16 (d, J = 7.1 Hz, 1H), 8.01 (d, J = 8.6 Hz, 1H), 7.81-7.65 (m, 2H), 7.56 (d, J = 7.6 Hz, 1H), 7.46 (t, J = 7.7 Hz, 2H), 7.39-7.17 (m, 8H), 7.17-6.97 (m, 2H), 6.74 (br, 1H), 5.56 (br, 1H), 5.07 (s, 2H), 4.80 (br, 1H), 3.21 (br, 1H), 3.09-2.57 (m, 14H), 2.51-2.15 (m, 7H), 1.86-1.63 (br, 4H), 1.49-1.28 (br, 4H); ^{13}C (75 MHz, $CDCl_3$) δ 171.2 (s), 171.7 (s), 152.3 (s), 151.1 (s), 149.9 (s), 138.7 (s), 138.2 (s), 135.7 (s), 135.6 (s), 134.9 (s), 131.6 (d), 130.0 (d), 130.8 (d), 130.2 (d), 129.9 (s), 129.8 (d), 129.5 (s), 129.0 (d), 128.8 (d), 128.7 (d), 128.6 (d), 126.7 (d), 125.1 (d), 123.6 (d), 123.2 (d), 122.2 (d), 119.1 (d), 115.7 (d), 115.6 (d), 66.9 (t), 49.2 (d), 45.4 (q), 42.8 (t), 38.9 (t), 36.8 (t), 36.7 (t), 35.8 (t), 35.6(t), 26.6 (t), 26.3 (t), 24.8 (t), 18.0 (q), 17.5 (q); M.P. 126 °; C MS (ESI, Na^+) 884, 637, 322, 56.

Compound 45: 3-tert-Butoxycarbonylamino-N-[4-(pyrene-1-sulfonylamino)-butyl]-succinamic acid benzyl ester

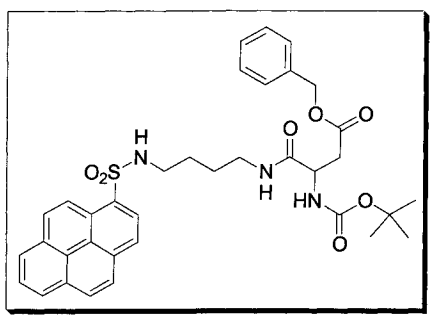

The compound **32,** pyrene-1-sulfonic acid (4-amino-butyl)-amide (150.0 mg, 0.426 mmol), was dissolved in 10 mL of DMF. To this, was added the protected *L*-aspartic acid **50** (165.1 mg, 0.511 mmol) followed by HOBT (115.0 mg, 0.853 mmol), DIPEA (0.29 mL, 1.702 mmol) and lastly EDC (163.2 mg, 0.853 mmol). The reaction was allowed to stir at room temperature for 48 hours. An excess of water was added to the reaction, which was then extracted three times with EtOAc. The organic layers were combined and washed sequentially with 10% HCl, saturated $NaHCO_3$ and brine. The

organic layer was dried over $MgSO_4$, filtered and concentrated under reduced pressure. The crude product was subjected to column chromatography using a 1:1 mixture of EtOAc and hexanes solution as the eluant to give 160 mg (58 %) of the desired product as a tan coloured foam. IR (film, cm^{-1}) 3329, 2975, 2930, 2869, 1732, 166, 1588, 1159; ^1H (300 MHz, $CDCl_3$) δ 8.96 (d, J = 9.4 Hz, 1H) 8.64 (d, J = 8.2 Hz, 1H), 8.31-8.20 (m, 3H), 8.16 (d, J = 8.4 Hz, 2H), 8.07 (d, J = 5.4 Hz, 1H), 8.04 (d, J = 7.1 Hz, 1H) 7.32-7.19 (m, 5H), 6.46 (br t, J = 5.6 Hz, 1H), 5.60 (br d, J = 9.1 Hz, 1H), 5.44 (br t, J = 6.0 Hz, 1H), 5.07 (d, J = 12.3 Hz, 1H), 5.02 (d, J = 12.3 Hz, 1H), 4.41 (br, 1H), 3.20-2.79 (m, 5H), 2.66 (dd, J = 6.2, 16.9 Hz, 1H), 1.39 (s, 9H), 1.35 (br, 4H); ^{13}C (75 MHz, $CDCl_3$) δ 171.2 (s), 171.1 (s), 155.9 (s), 135.7 (s), 135.1 (s), 131.5 (s), 131.2 (s), 130.5 (d), 130.4 (d), 128.9 (d), 128.7 (d), 128.5 (d), 128.3 (s), 127.8 (d), 127.4 (d), 127.3 (d), 127.2 (d), 127.1 (d), 125.6 (s), 124.4 (s), 124.2(d), 123.5 (d), 81.0 (s), 77.6 (s), 67.2 (t), 51.0 (d), 43.2 (t), 39.1 (t), 36.5 (t), 28.7 (q), 26.9 (t); M.P. 124 ° C; MS (CI) 647, 257, 108, 91.

Compound 44: 3-[5-(2-Methyl-4-o-tolylazo-phenylcarbamoyl)-pentanoylamino]-*N*-[4-(pyrene-1-sulfonylamino) -butyl]-succinamic acid benzyl ester

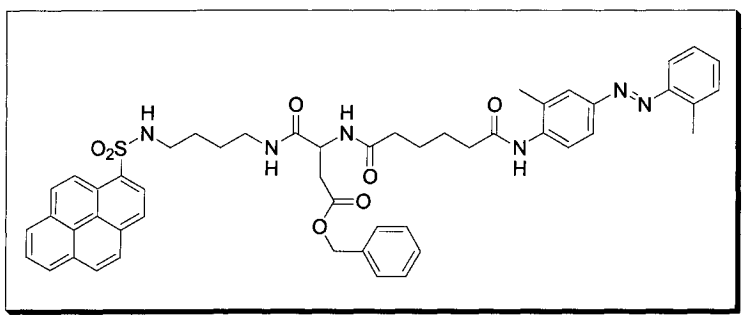

Compound **45** (149.0mg, 0.231 mmol) was stirred in 10 mL of CH_2Cl_2, to which 2mL of TFA was added The reaction was stirred at room temperature for 30 minutes before the mixture was concentrated under reduced pressure. The crude material was distilled azeotropically with benzene three times to remove any traces of excess TFA. The amine salt was stirred in 7 mL of DMF with **39** (105.7mg, 0.299 mmol), HOBT (62.3 mg, 0.461 mmol), and DIPEA (0.20 mL, 1.154 mmol). EDC (88.4 mg, 0.461 mmol) was added last to the reaction. The reaction was stirred for 32 hours before H_2O was added and the mixture

extracted 3 times with EtOAc. The combined organic phases were washed sequentially with 10 % HCl, saturated $NaHCO_3$ and brine. The organic layer was dried over $MgSO_4$ and concentrated under reduced pressure. The crude material was purified by silica column chromatography using a mixture of $CHCl_4$:EtOAc:MeOH (50:45:5) as an eluant to furnish 87 mg (43 %) of **44** as an orange coloured solid. IR (film, cm^{-1}) 3291, 2966, 2928, 2855, 1736, 1642, 1523, 1463, 1157; ^1H (300 MHz, DMSO-d_6) δ 9.37 (s, 1H), 8.99 (d, J = 9.5 Hz, 1H) 8.58 (d, J = 8.2 Hz, 1H), 8.52-8.33 (m, 5H), 8.32-8.05 (m, 4H), 7.88-7.64 (m, 4H), 7.54 (d, J = 7.9 Hz, 2H), 7.47-7.37 (m, 2H), 7.37-7.21 (m, 6H), 5.03 (s, 2H), 4.66-4.51 m, 1H), 2.93-2.50 (m, 9H), 2.43-2.27 (m, 5H), 2.22-2.06 (m, 2H), 1.63-1.47 (m, 4H), 1.38-1.119 (m, 4H); ^{13}C (75 MHz, DMSO-d_6) δ 172.9 (s), 172.3 (s), 170.9 (s), 170.8 (s), 150.9 (s), 149.8 (s), 140.4 (s)), 138.2 (s), 136.9 (s), 134.7 (s), 133.4 (s), 132.4 (s), 132.3 (s), 132.0 (s), 131.9 (s), 131.8 (d), 131.4 (s), 130.8 (d), 130.6 (s), 130.3 (d), 129.2 (d), 128.8 (d), 128.7 (d), 128.0 (d), 127.9 (d), 127.7 (d), 127.5 (d), 127.4 (d), 125.5 (d), 125.4 (d), 125.2 (s), 125.1 (d), 124.3 (d), 124.2 (s), 121.4 (d), 115.9 (d), 66.4 (t), 50.1 (d), 42.9 (t), 38.5 (t), 37.0 (t), 36.2 (t), 35.5 (t), 26.9 (t), 26.5 (y), 25.4(t), 25.3 (t), 18.5 (q), 17.6 (q); M.P. 159 °C; MS (ESI, Na^+) 915, 893, 358, 179, 115, 56.

Compound 51: 2-tert-Butoxycarbonylamino-succinic acid 4-benzyl ester 1-[5-(5-dimethylamino-naphthalene-1-sulfonylamino)-pentyl] ester

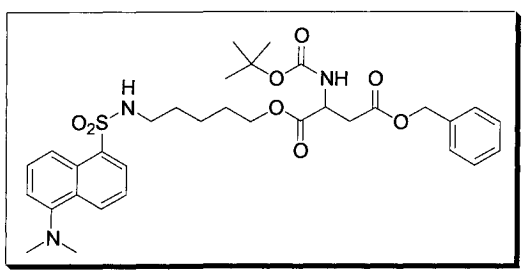

The compound **26,** 5-dimethylamino-naphthalene-1-sulfonic acid (5-hydroxy-pentyl)-amide, (2.40 g, 7.133 mmol), was dissolved in 70 mL of DMF. To this, was added the protected aspartic acid **50** (2.77 g, 8.560 mmol) followed by HOBT (1.927 g, 14.26 mmol), DIPEA (6.2 mL, 35.66 mmol) and lastly EDC (2.733 g, 14.26 mmol). The reaction was allowed to stir at room temperature for 48 hours. An excess of water was added to the reaction, which was then extracted three times with EtOAc. The organic layers were

combined and washed sequentially with 10 % citric acid, saturated $NaHCO_3$ and brine. The organic layer was dried over $MgSO_4$, filtered and concentrated under reduced pressure. The crude product was subjected to column chromatography using a 1:3 mixture of EtOAc and hexanes as the eluant to give 4.1 g (90 %) of the desired product as a yellow coloured foam. IR (film, cm^{-1}) 3309, 2967, 2942, 2868, 2834, 2788, 1738, 1613, 1574, 1504, 1144; ^1H (300 MHz, $CDCl_3$) δ 8.53 (d, J = 8.1Hz, 1H) 8.29 (d, J = 8.8 Hz, 1H), 8.22 (d, J = 7.2 Hz, 1H), 7.5 (t, J = 8.1 Hz, 1H), 7.50 (t, J = 7.9 Hz, 1H) 7.34-7.24 (m, 5H), 7.17 (d, J = 7.4 Hz, 1H), 5.45 (br d, J = 8.5 Hz, 1H), 5.09 (s, 2H), 4.85 (br t, J = 5.3 Hz, 1H), 4.51 (d t, J = 8.6, 4.3 Hz, 1H), 3.93 (t, 6.1 Hz, 2H), 3.03-2.75 (m, 10H), 1.49-1.25 (m, 12H), 1.30-1.00 (m, 3H); ^{13}C (75 MHz, $CDCl_3$) δ 171.4 (s), 171.2 (s), 155.7 (s), 135.7 (s), 135.2 (s), 130.7 (d), 130.1 (s), 130.0 (d), 129.0 (d), 128.9 (s), 128.8 (d), 128.7 (d), 128.5 (d), 123.7 (d), 119.4 (d), 115.7 (d), 80.5 (s), 77.6 (s), 66.7 (t), 65.2 (t), 50.0 (d), 45.5 (q), 42.9 (t), 36.8 (t), 28.9 (t), 28.3 (q), 27.7 (t), 22.5 (t); MS (EI) 641, 524, 235, 171, 91.

Compound 52: 2-tert-Butoxycarbonylamino-succinic acid 4-[5-(10b,10c-dihydro-pyrene-1-sulfonyl- amino)-pentyl] ester 1-[5-(5-dimethylamino - naphthalene-1-sulfonylamino)-pentyl] ester

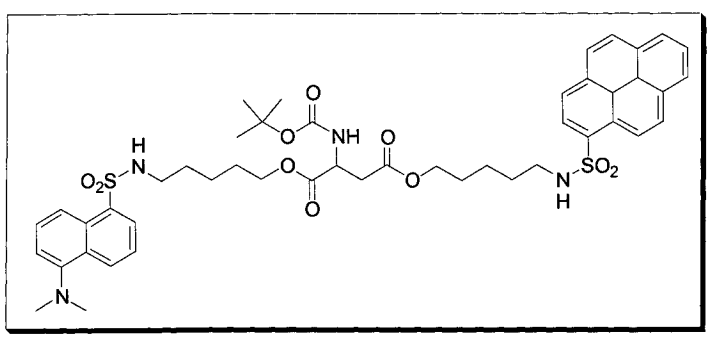

Compound **51** (3.00 g, 4.673 mmol) was stirred in 15 mL of MeOH in a 100 mL round bottom flask equipped with a three-way valve. The apparatus was degassed several times alternating with vacuum and $N_{2\,(g)}$ before 5 mg of Pd/C was added. The mixture was again degassed several times with $N_{2\,(g)}$ before changing to an H_2 (g) atmosphere. The reaction continued for 21 hours at room temperature before work up was pursued. The mixture was filtered through a celite pad using chloroform as an

eluant. The solvent was removed under reduced pressure to provide the crude acid that was used directly without further purification. The crude acid was stirred in 50 mL of DMF at room temperature. The alcohol **27** (1.89g, 5.140 mmol), HOBT (1.26g, 9.346 mmol) and DIPEA (4.0 mL, 23.36 mmol) were incorporated into the mixture. EDC (1.79g, 9.346 mmol) was added last to commence the coupling reaction. After 28 hours 10 % citric acid was added to the reaction and that was extracted three times with EtOAc. The combined organic layers were washed sequentially with saturated $NaHCO_3$, and brine before being dried over $MgSO_4$, filtered, and concentrated under reduced pressure. The crude material was subjected to purification by column chromatography using 5 % MeOH in chloroform as an eluant to furnish 2.55 g of **52** (61%) as an off-white foam. IR (film, cm^{-1}) 3297, 2941, 2868, 1727, 1588, 1503, 1153; ^1H (300 MHz, $CDCl_3$) δ 8.96(d, J = 9.4 Hz, 1H) 8.66 (d, J = 8.2 Hz, 1H), 8.57 (br, 1H), 8.33 (br d, 8.4 Hz, 1H), 8.29-8.15 (m, 6H), 8.12-8.03 (m, 2H), 7.57-7.44 (m, 2H), 7.18 (d, J = 8.0 Hz, 1H), 5.34 (d, J = 8.6 Hz, 1H), 5.29 (br, 1H), 5.14 (br, 1H), 4.45 (dt, 4.7, 8.5 Hz, 1H), 4.10-3.80 (m, 4H), 3.03-2.76 (m, 11H), 2.69 (dd, 4.8, 17.0 Hz, 1H), 1.53-1.30 (m, 17 H), 1.29-1.11 (m, 4H); ^{13}C (75 MHz, $CDCl_3$) δ 171.5 (s), 171.4 (s), 155.8 (s), 135.1 (s), 131.6 (s), 131.3 (s), 130.5 (d), 130.4 (s), 129.9 (d), 128.6 (s), 128.3 (d), 127.8 (d), 127.5 (d), 127.4 (d), 127.3 (d), 127.2 (d), 125.6 (s), 124.4 (s), 124.2 (d), 123.5 (d), 115.9 (d), 80.6 (s), 77.4 (s), 65.7 (t), 65.1 (t), 50.0 (d), 45.6 (q), 42.94 (t), 42.88 (t), 36.8 (t), 29.0 (t), 28.9 (t), 28.3 (q), 27.8 (t), 27.4 (t), 22.7 (t), 22.6 (t); MS (ESI, Na^+) 923, 801, 543, 392,337, 211.

Compound 46: 2-[5-(2-Methyl-4-o-tolylazo-phenylcarbamoyl)-pentanoylamino]-succinic acid 4-[5-(10b,10c-dihydro-pyrene-1-sulfonylamino)-pentyl] ester 1-[5-(5-dimethylamino-naphthalene-1-sulfonylamino)-pentyl] ester

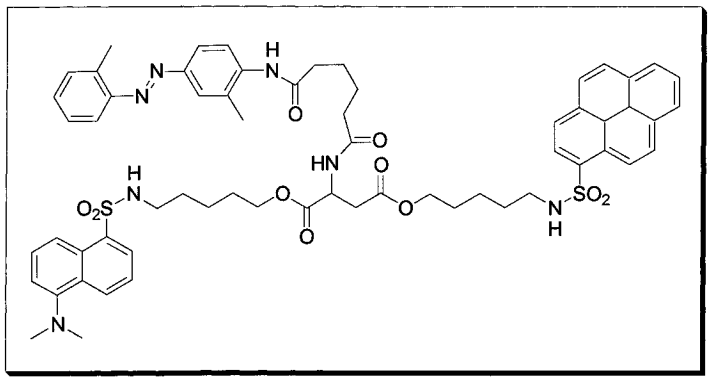

The amide **52** (300.0 mg, 0.333 mmol) was dissolved in 8 mL of CH_2Cl_2 to which 2 mL of TFA was added. This was allowed to stir for 40 minutes before the solvent and TFA were removed under reduced pressure. The sample was azeotropically distilled with benzene twice to remove any traces of TFA. The crude amine salt was stirred in 20 mL of DMF along with the acid **39** (117.6 mg, 0.333 mmol), HOBT (90.0 mg, 0.666 mmol) and DIPEA (0.30 mL, 1.664 mmol). HBTU (252.5 mg, 0.666 mmol) was added last and the coupling reaction was allowed to proceed for 4 days at room temperature. Citric acid was added to the reaction and this was extracted three times with EtOAc. The combined organic extracts were washed with saturated $NaHCO_3$, and H_2O. The organic layer was then filtered through a cotton plug and concentrated under reduced pressure. The crude material was purified by silica gel column chromatography using a 1:1 mixture of EtOAc in $CHCl_3$ as an eluant. 0.378 mg (60 %) of the desired compound was isolated as a dark orange solid. IR (film, cm^{-1}) 3302, 2941, 2867, 1736, 1661, 1519; ^1H (300 MHz, $CDCl_3$) δ 8.98(d, J = 9.4 Hz, 1H) 8.65 (d, J = 8.2 Hz, 1H), 8.50 (d, J = 8.5 Hz, 1H), 8.33 (d, 8.6 Hz, 1H), 8.29-8.11 (m, 6H), 8.10-8.00 (m, 2H), 7.92 (br d, J = 8.3 Hz, 1H), 7.80-7.69 (br, 1H), 7.70-7.54 (m, 3H), 7.48 (t, J = 7.4 Hz, 2H), 7.40-7.21(m, 3H), 7.12 (d, J = 7.5 Hz, 1H), 6.90 (d, J = 8.1 Hz, 1H), 5.87 (br t, J = 4.8 Hz, 1H), 5.79 (br t, J = 5.8 Hz, 1H), 4.89 (dt, 4.7, 8.0 Hz, 1H), 4.08-3.88 (m, 4H), 3.01-2.76 (m, 12H), 2.69 (s, 3H), 2.57-2.31 (m, 4H), 2.23 (s, 3H),1.92-1.70(m, 4H), 1.56-1.15 (m, 12H); ^{13}C (75 MHz, $CDCl_3$) δ 173.7(s), 172.2 (s), 171.6 (s), 171.4 (s), 152.3 (s), 151.1 (s), 149.8 (s), 138.8 (s), 138.3 (s), 135.3 (s), 135.1 (s), 131.6 (s), 131.5

(d), 131.3 (s), 131.0 (d), 130.7 (d), 130.55 (d), 130.46 (d), 130.43(s), 130.2 (s),130.0 (s), 129.8 (s), 129.7 (d), 128.7 (d), 128.3 (s), 127.7 (d), 127.42 (d), 127.35 (d), 127.3 (d), 127.2 (d), 126.8 (d), 125.5 (s), 125.1 (d), 124.4 (d), 124.2 (s), 123.6 (d), 123.5 (d), 123.4 (d), 122.0 (d), 119.2 (d), 115.8 (d), 115.6 (d), 65.8 (t), 65.1 (t), 49.2 (d), 45.8 (q), 43.3 (t), 43.2 (t), 36.7 (t), 36.1 (t), 29.3 (t), 29.2 (t), 28.3 (t), 28.2 (t), 25.4 (t), 23.2 (t), 23.0 (t), 18.4 (q), 18.0 (q), M.P. 66 ° C; MS (ESI, Na^+) 1158, 1136, 851, 481, 353, 82, 56.

Compound 47: 2-[5-(2-Methyl-4-o-tolylazo-phenylcarbamoyl)-pentanoylamino]-succinic acid 4-benzyl ester 1-[5-(5-dimethylamino-naphthalene-1-sulfonylamino)-pentyl] ester

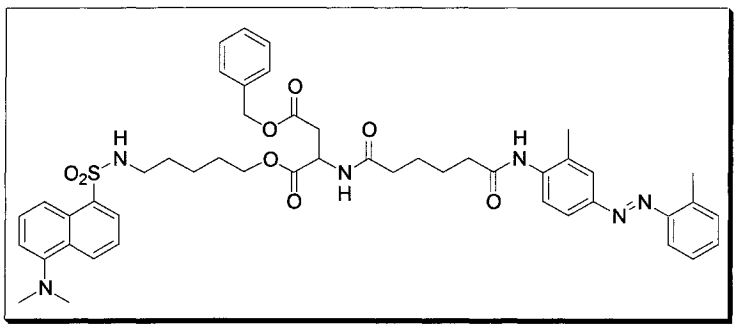

Compound **53** (1.48 g, 2.305 mmol) was stirred in 16 mL of CH_2Cl_2, to which 4 mL of TFA was added. The reaction proceeded at room temperature for 1 hour before the mixture was concentrated under reduced pressure. The crude material was distilled azeotropically with benzene twice to remove any traces of excess TFA. The amine salt was stirred in 20 mL of DMF with **39** (814.6 mg, 2.305 mmol), HOBT (467.3 mg, 3.458 mmol), and DIPEA (1.61 mL, 9.222 mmol). EDC (662.9 mg, 3.458 mmol) was added last to the reaction. The reaction was stirred for 30 hours before H_2O was added and the mixture extracted three times with EtOAc. The combined organic phases were washed sequentially with 10 % HCl, saturated $NaHCO_3$ and brine. The organic layer was dried over $MgSO_4$, filtered and concentrated under reduced pressure. The crude material was purified by silica column chromatography using a 3:2 mixture of EtOAc:hexanes as an eluant. 506.3 mg (25 %) of the product was afforded as an orange solid. IR (film, cm^{-1}) 3297, 2942, 2866, 2788, 1738, 1655, 1521, 1455, 1144; ^1H (300 MHz, $CDCl_3$) δ

8.69 (s, 1H), 8.54 (d, J = 8.5 Hz, 1H), 8.42 (d, J = 8.7 Hz, 1H), 8.23 (dd, J = 1.1, 6.1 Hz, 1H), 8.09(d, 8.4 Hz, 1H), 7.84-7.73 (m, 2H), 7.67-7.50 (m, 4H), 7.46-7.17 (m, 9H), 6.83 (t, J = 5.9 Hz, 1H), 5.13 (s, 2H), 4.84 (dt, 6.4, 7.9 Hz, 1H), 3.91 (t, J = 6.3 Hz, 2H), 2.95-2.79 (m, 10H), 2.70 (s, 3H), 2.51 (br t, J = 6.8 Hz, 2H), 2.40 (s, 3H), 2.30 (br t, J = 6.8 Hz, 2H) 1.87-1.66 (br, 4H), 1.43-1.31 (m, 4H), 1.28-1.13 (m, 2H); ^{13}C (75 MHz, $CDCl_3$) δ 172.9(s), 171.8 (s), 171.0 (s), 170.5(s), 152.3 (s), 151.0 (s), 149.7 (s), 140.2 (s), 138.2 (s), 136.8 (s), 136.6 (s), 131.7 (d), 131.2 (d), 130.6 (s), 130.2 (s), 130.1 (d), 129.2 (d), 128.8 (d), 128.5 (d), 128.2 (d),126.9 (d), 125.2 (d), 123.7 (d), 121.4 (d), 119.9(d), 115.6 (d), 115.5 (d), 66.1 (t), 64.8 (t), 49.0 (d), 44.8 (q), 42.7 (t), 36.3 (t), 36.1 (t), 35.3 (t), 28.9 (t), 27.7 (t), 25.1 (t), 25.0 (t), 22.5 (t), 17.5 (q), 16.8 (q); M.P. 59 °C; MS (ESI, Na^+) 899, 877, 115, 83.

Compound 54: 2-tert-Butoxycarbonylamino-succinic acid 1-methyl ester 4-[6-(pyrene-1-sulfonylamino)-pentyl] ester

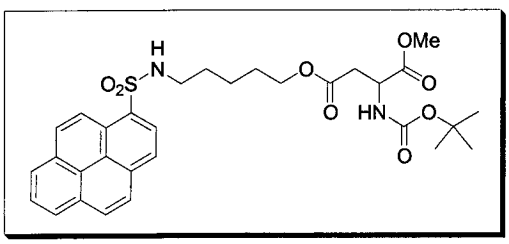

The commercially available aspartic acid derivative **50** (1.00g, 3.093 mmol) was stirred in 20 mL of CH_2Cl_2 at room temperature. Diazomethane was added drop-wise to this until the yellow colour of the reagent persisted. Completion of the methylation was also confirmed by TLC. ^1H NMR of the material was compared to literature results[38] which revealed a pure product that was also achieved in quantitative yield. ^1H NMR (300 MHz, $CDCl_3$,) δ 7.42-7.32 (m, 5H), 5.48 (d, J = 7.9 Hz, 1H), 5.16 (d, J = 12.3, Hz, 1H), 5.12 (d, 12.3 Hz, 1H), 4.67-4.52 (m, 1H), 3.72 (s, 3H), 3.07 (dd, J = 4.5, 17.1 Hz, 1H), 2.89 (dd, J = 4.8, 17.0 Hz, 1H), 1.46 (s, 9H). The solvent was removed under reduced pressure to give a colourless viscous oil. The crude methyl ester (800.0 mg, 2.371 mmol) was stirred in 5 mL of MeOH. The flask was degassed

[38] Englund, E. A.; Gopi, H.N.; Appella, D.H. *Org. Lett.* **2003**, *6*, 213.

with $N_{2\,(g)}$ via a three way valve was attached to the reaction vessel. A small amount of Pd/C was added to the reaction followed by purging with $N_{2\,(g)}$ once again. The reaction was then submitted to an $H_{2(g)}$ atmosphere for 2.5 hours. The reaction was then filtered through a celite pad using chloroform as an eluant. The filtrate was concentrated under reduced pressure and used without further purification. The crude acid was stirred in 20 mL of DMF to which the alcohol **27** (1.045 g, 2.845 mmol), HOBT (760.0 mg, 5.622 mmol) and DIPEA (2.1 ml, 11.85 mmol) were added. EDC (1.077 g, 5.622 mmol) was incorporated last to commence the reaction. The mixture was allowed to stir for 3 days at room temperature before work up was ensued. H_2O was added to the mixture that was extracted three times with EtOAc. The combined organic extracts were washed sequentially with 10% citric acid and saturated $NaHCO_3$. The organic layer was dried over $MgSO_4$, filtered, and concentrated under reduced pressure. The crude material was subjected to purification by silica column chromatography using a 5 % MeOH in $CHCl_3$ solvent system. This procedure furnished 1.19 g (85 %) of product as a fluffy white solid. IR (film, cm^{-1}) 3298, 2957, 1731, 1591, 1499, 1159; ^1H (500 MHz, $CDCl_3$) δ 8.96(d, J = 9.3 Hz, 1H) 8.67 (d, J = 8.2 Hz, 1H), 8.30-8.21 (m, 3H), 8.16 (d, J = 9.2 Hz, 2H), 8.10-8.02 (m, 2H), 5.42 (br d, J = 8.2 Hz, 1H), 5.13 (br, 1H), 4.52 (br, 1H), 3.83 (br, 2H), 3.68 (s, 3H), 2.94-2.79 (m, 3H), 2.68 (dd, J = 4.2, 16.9 Hz, 1H), 1.46-1.30 (m, 13H), 1.24-1.12 (m, 2H); ^{13}C (126 MHz, $CDCl_3$) δ 171.5 (s), 170.7 (s), 155.2 (s), 134.6 (s), 131.1 (s), 130.8 (s), 130.0 (d), 129.9 (d), 127.8 (s), 127.3 (d), 126.89 (d), 126.85 (d), 126.74 (d), 126.67 (d),125.0 (s), 123.9 (s), 123.7 (d), 122.9 (d), 100.0 (s), 80.0 (s), 64.4 (t), 52.6 (q), 49.8 (d), 42.9 (t), 36.6 (t), 29.0 (t), 28.2(q), 27.6 (t), 22.6 (t); MS (EI) 597, 596, 522, 201, 217, 91, 70.

Compound 48: 2-[5-(2-Methyl-4-o-tolylazo-phenylcarbamoyl)-pentanoylamino]-succinic acid 1-methyl ester 4-[6-(pyrene-1-sulfonylamino)-pentyl] ester

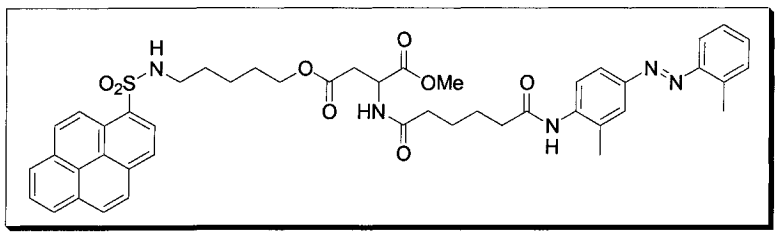

Compound **54** (1.16 g, 1.951 mmol) was stirred in 18 mL of CH_2Cl_2, to which 2 mL of TFA was added. The reaction proceeded at room temperature for 1 hour before the mixture was concentrated under reduced pressure. The crude material was azeotropically distilled with benzene twice to remove any traces of excess TFA. The amine salt was stirred in 30 mL of DMF with **39** (758.4 mg, 2.146mmol), HOBT (527.3 mg, 3.902 mmol), and DIPEA (1.7 mL, 9.755 mmol). EDC (748.0 mg, 3.902 mmol) was added last to the reaction. The reaction was stirred for 4 days before H_2O was added and the mixture three times with EtOAc. The organic combined organic phases were washed sequentially with 10 % citric acid, saturated $NaHCO_3$ and brine. The organic layer was dried over $MgSO_4$ and concentrated under reduced pressure. The crude material was purified by silica column chromatography using gradient of EtOAc (50 %) and hexanes (50 %) to EtOAc (70 %) and hexanes (30%) to provide 774.1 mg (48 %) of **48** as an orange coloured solid. IR (film, cm^{-1}) 3584, 3310, 2950, 2868, 1738, 1590, 1505, 1158, 1143; ^1H (300 MHz, $CDCl_3$) δ 8.94(d, J = 9.4 Hz, 1H) 8.64 (d, J = 8.2 Hz, 1H), 8.34-8.12 (m, 5H), 8.11-8.01 (m, 2H), 7.95 (d, J = 8.3 Hz, 1H), 7.69-7.47 (m, 4H), 7.36-7.12 (m, 3H), 6.70 (d, J = 7.7 Hz, 1H), 5.50 (br t, J = 5.5 Hz, 1H), 4.88 (dt, J = 4.7, 7.8 Hz, 1H), 4.05-3.83 (m, 2H), 3.72 (s, 3H), 2.99-2.74 (m, 4H), 2.66 (s, 3H), 2.54-2.30 (m, 4H), 2.25 (s, 3), 1.87-1.65 (m, 4H), 1.51-1.31 (m, 4H), 1.31-1.15 (m, 2H); ^{13}C (75 MHz, $CDCl_3$) δ 173.3 (s), 171.58(s), 171.4 (s), 151.5 (s), 149.8 (s), 138.7 (s), 138.3 (s), 135.2 (s), 131.6 (d), 131.4 (s), 131.3 (s), 131.0 (s), 130.6 (d), 130.5 (d), 129.3 (s), 128.3 (s), 127.7 (d), 127.42 (d), 127.40 (s), 127.3 (d), 127.2 (d), 126.8 (d),125.6 (s), 125.0 (d), 124.4 (s), 124.2 (d),123.4 (d), 123.1

(d), 122.1 (d), 115.7 (d), 77.6 (d), 65.0 (t), 53.3 (d), 49.3 (q), 43.3 (t), 37.4 (t), 36.9 (t), 36.1 (t), 29.2 (t), 28.2(t), 25.4 (t), 25.0 (t), 23.1 (t), 18.3 (q), 17.9 (q); M.P. 137 °C; MS (ESI, Na^+) 854, 832, 353, 115, 83, 56.

Compound 73: 4-(4-Methoxy-benzyloxy)-butan-1-ol

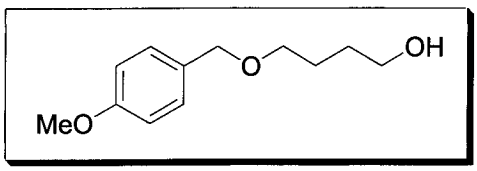

1,4-butandiol (1.50 g, 0.128 moles) was stirred with freshly ground KOH (7.15 g, 0.128 moles) in 80 mL of DMSO at 15 °C. To this, *p*-methoxybenzyl chloride (8.66 mL, 0.068 moles) was added slowly over 1.5 hours via a syringe pump. After the addition, the reaction mixture was stirred for another 30 minutes before work up was started. Saturated NH_4Cl was added to the reaction mixture and this was extracted three times with ether. The combined organic layers were washed with brine, dried over $MgSO_4$, filtered and concentrated under reduce pressure to give the crude material (13.17 g, 0.065 moles) a colorless oil that was used with no further purification. The NMR spectra matched that reported in the literature.[39] ^1H NMR (300 MHz, $CDCl_3$) δ, 7.26 (d, J = 8.4 Hz, 2H), 6.88 (d, J = 8.4 Hz, 2H), 4.45(s, 2H), 3.80 (s, 1H), 3.64 (t, 5.4 Hz, 2H), 3.50 (t, J = 5.7 Hz, 2H), 2.32 (br, 1H), 1.62-1.73 (m, 4H); ^{13}C NMR (75 MHz, $CDCl_3$) δ 159.3 (s), 130.5 (s), 129.5 (d), 113.9 (d), 72.8 (t), 70.1 (t), 55.4 (q), 30.4 (t), 26.9 (t).

Compounbd 74: 4-(4-Methoxy-benzyloxy)-butyric acid[39]

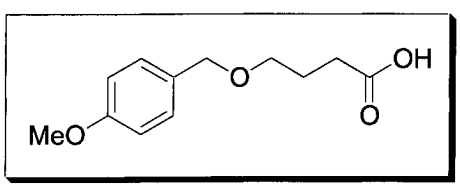

The crude alcohol **73**(4.73 g, 22.50 mmol) was stirred in acetone at -3 °C (NaCl, ice bath). A freshly prepared 2.7 M solution of Jones reagent (25 mL, 67.60 mmol) was added via canula to the reaction flask. The oxidation was allowed to proceed for 3 hours

[39] Hirai, K..; Ooi, H.; Esumi, T.; Iwabuchi, Y. and Hatakeyama, S. *Org. Lett.* **2003**, *5*, 857.

before *iso*propanol was added to quench the reaction. Water was added to the reaction mixture and this was extracted three times with EtOAc. The combined organic extracts were washed with brine, dried over $MgSO_4$, filtered and concentrated under reduced pressure. The crude material was subjected to silica column chromatography using a 2:3 mixture of EtOAc:hexanes that afforded the acid product **74** (4.20g, 83 %) as a colourless oil. FTIR (neat, cm^{-1}) 2941, 2866, 1711, 1612, 1514, 1458, 1362, 1250 cm-1; ^1H NMR (300 MHz, $CDCl_3$): δ 7.25 (d, J = 7.2 Hz, 2H), 6.87 (d, J = 8.7 Hz, 2H), 4.44 (s, 2H), 3.80 (s, 3H), 3.50 (t, J = 6.0 Hz, 2H), 2.47 (t, J = 7.5 Hz, 2H), 1.93 (quint, J = 6.6,13.2 Hz, 2H); ^{13}C NMR (75 MHz, $CDCl_3$) δ 179.6 (s), 159.2 (s), 130.4 (s), 129.3 (d), 113.8 (d), 72.6 (t), 68.7 (t), 55.3 (q), 31.0 (t), 24.8 (t); HRMS (EI) calcd for $C_{12}H_{16}O_4$ (M+): 224.1049, found: 224.1033.

Compound 70: N-Methoxy-4-(4-methoxy-benzyloxy)-N-methyl-butyramide

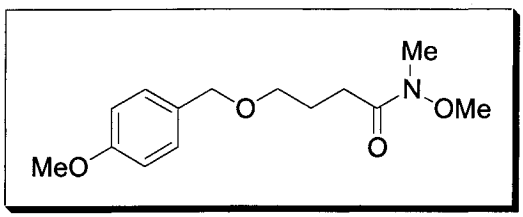

The acid **74** (1.00g, 4.459 mmol) was stirred in 40 mL of DMF at room temperature. To this was added *N, O*-dimethylhydroxylamine (522.0 mg, 5.351 mmol), HOBT (1.21 g, 8.919 mmol), and DIPEA (2.0 mL, 26.76 mmol). EDC (1.71 g, 8.919 mmol) was added last to commence the coupling reaction. The reaction was allowed to proceed for 24 hours. 10 % HCl was added to the reaction and this was extracted three times with EtOAc. The combined organic extracts were washed sequentially with saturated $NaHCO_3$ and brine. The organic layer was then dried over $MgSO_4$, filtered and concentrated under reduced pressure. The crude material was subjected to silica column chromatography using a mixture of 2:3 EtOAc to hexanes as a solvent system to furnished 1.09 g (78 %) of the Weinreb amide **70** as a pale yellow oil. IR (neat, cm^{-1}) 2936, 2858, 1664, 1513, 1247; ^1H (300 MHz, $CDCl_3$) δ 7.22 (d, J = 8.5 Hz, 2 H), 6.84 (d, J = 8.7 Hz, 2H), 4.40 (s, 2H), 3.77 (s, 3H), 3.63 (s, 3H), 3.48 (t, J = 6.2 Hz, 2H), 3.12 (s, 3H), 2.50 (br t, J = 7.3 Hz, 2H), 1.98-1.83 (m, 2H); ^{13}C (75

MHz, $CDCl_3$) δ 159.5(s), 131.0 (s), 129.6 (s), 129.2 (d), 114.1 (d), 72.8 (t), 69.6 (t), 61.6 (q), 55.6 (q), 32.2 (q), 28.9 (t), 25.0 (t); MS (EI) 267, 135, 121, 91, 77, 40.

Compound 69: 3-Hydroxy-2-[2-(4-methoxy-benzyloxy)-ethyl]-5-phenyl-pent-4-enoic acid methoxy-methyl-amide

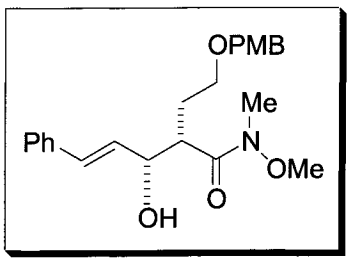

Dry diisopropyl amine (0.115 mL, 0.822 mmol) was stirred in 2 mL of THF at -78 °C. BuLi (0.35 mL, 0.758 mmol), titrated at 2.26 M, was added to the flask and this was allowed to stir for 20 minutes to generate LDA. The Weinreb amide **70** (100.0 mg, 0.374 mmol) was dissolved in 3 mL of THF and added to the stirring LDA over 15 minutes using a syringe pump to generate the enolate. To a solution of (*E*)-cinnamaldehyde (49.0 mg, 0.374 mmol) in 2 mL of THF at -78 °C was added the enolate via a cannula. The reaction continued at -78 °C for 1.5 hours before it was allowed to stir at ambient temperature for an additional 36 hours. The reaction was quenched with saturated NH_4Cl and extracted with EtOAc three times. The combined organic extracts were washed with brine, dried over $MgSO_4$, filtered and concentrated under reduced pressure. Column chromatography afforded 24.0 mg (16 %) of the desired aldol product as a colourless oil. IR (neat, cm^{-1}) 3455, 3001, 2936, 2859, 1659, 1613, 1513; ^1H (300 MHz, $CDCl_3$) δ 7.47-7.10 (m, 8 H), 6.84 (d, J = 8.7 Hz, 2H), 6.59 (d, J = 15.8, 1H) 6.19 (dd, J = 15.8 Hz, 1H), 4.52-4.21(m, 3H), 3.78 (s, 3H), 3.63 (s, 3H), 3.51-3.26 (m, 3H), 3.11 (s, 3H), 2.28-1.82 (m, 2H); ^{13}C (75 MHz, $CDCl_3$) δ 176.5 (s), 159.5(s), 137.1 (s), 131.2 (d), 131.1(s), 130.7 (s), 129.7 (d), 128.9 (d), 127.9 (d), 126.8 (d), 114.1 (d), 74.0 (d), 72.9 (t), 68.0 (t), 62.0 (q), 55.7 (q), 42.9 (d), 32.4 (q), 30.3 (t); MS (EI) 382, 260, 131, 121, 103, 91.

Compound 116: (*S*)-(+)-2-(Benzyl-hydrazono)-7,7-dimethyl-bicyclo[2.2.1] heptane-1-carboxylic acid.

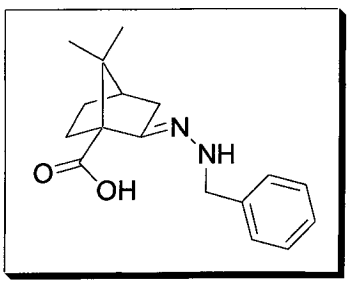

(*S*)-(+)-ketopinic acid (3.36 g, 18.4 mmol) and benzylhydrazine (3.38 g, 27.7 mmol) were stirred in anhydrous dichloromethane (100 ml) at room temperature until the reaction was deemed complete by TLC (15 hours). The solvent was removed under reduced pressure and the crude product was purified by silica gel chromatography using 30% EtOAc in hexanes as an eluant to provide 5.28g of the desired compound as a pale yellow oil (100 %). [α]D = +53.7 (*c* 1.10, CHCl3); IR (neat, cm^{-1}) 3282, 1742; ^{1}H NMR (500 MHz, CDCl3) δ 7.34-7.24 (m, 5H), 4.31 (s, 2H), 2.39 (ddd, J=12.3, 12.1, 4.2 Hz, 1H), 2.32 (ddd J=17.1, 3.7, 3.7 Hz,1H), 2.08-2.01 (m, 1H), 1.97 (t, J=4.38 Hz, 1H) 1.78 (d, J=17.1 Hz, 1H), 1.72-1.67 (m, 1H), 1.30-1.24 (m, 1H), 1.21 (s, 3H), 0.79 (s, 3H); ^{13}C NMR (125 MHz, CDCl3) δ172.7 (C), 159.3 (C), 138.2 (C), 128.6 (CH), 128.2 (CH), 127.6 (CH), 59.3 (C), 55.0 (CH2), 51.4 (C), 44.3 (CH),32.6 (CH2), 32.1 (CH2), 28.1 (CH2), 19.9 (CH3), 19.6 (CH3); MS (EI) 268.2 (M+); HRMS (EI)calcd. for C17H22N2O2 (M+) 286.1681 found 286.1692.

Compound 117: (*S*)-(+)-3-Benzyl-10,10-dimethyl-3,4-diaza-tricyclo [5.2.1.01,5]dec-4-en-2-one.

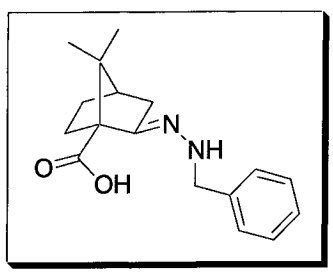

The compound **116** (3.43 g, 11.9 mmol) was stirred in 40 mL of mesitylene and refluxed in a Dean-Stark apparatus to remove the water generated. The reflux proceeded until consumption of the starting material was complete as judged by TLC. The cooled reaction mixture was directly loaded onto a silica column and was purified by flash chromatography first using 100% Hexanes as the eluant to remove the mesitylene, and then using 30 % EtOAc in hexanes to furnish 2.56g of the desired compound as a white solid (80%). Mp 90-92 °C; [α]D = +28.0 (*c*

1.04, CHCl3); IR (film, cm^{-1}) 1690, 1630; ^{1}H NMR (500 MHz , CDCl3) δ 7.30-7.20 (m, 5H), 4.79 (s, 2H), 2.53 (ddd, J=17.5, 3.6, 3.6 Hz, 1H), 2.26 (ddd, J=12.0, 4.3, 4.3 Hz, 1H), 2.21 (t, J=4.32 Hz, 1H), 2.13-2.06 (m, 2H), 1.64 (ddd, J=13.4, 9.5, 4.5 Hz, 1H), 1.45 (ddd, J=13.3, 9.5, 4.3 Hz, 1H), 1.19 (s, 3H), 0.87 (s, 3H); ^{13}C NMR (125 MHz, CDCl3) δ 174.4 (C), 173.5 (C), 137.1 (C), 128.4 (CH), 127.7 (CH), 127.3 (CH), 63.6 (C), 49.7 (C), 49.1 (CH), 47.8 (CH2), 31.8 (CH2), 26.9 (CH2), 25.2 (CH2), 19.1 (CH3), 18.5 (CH3);
MS (EI) 268.2 (M+); HRMS (EI) calcd.for C17H20N2O (M+) 268.1576; found 268.1589.

Compound 118: *(S)*-(+) -3-Benzyl-10,10-dimethyl-3,4-diaza-tricyclo[5.2.1.01,5]decan-2-one (5).

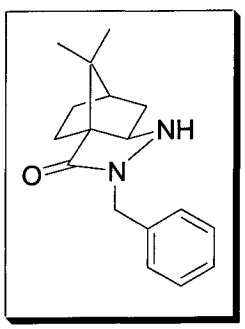

The compound **117** (1.50 g, 5.60 mmol) was stirred in 30 mL of a 2:1 solution of acetic acid to methanol. To this was added sodium cyanoborohydride (3.51 g, 56.00 mmol) and the reaction mixture was then stirred at room temperature for 16 hours. The reaction was quenched by the addition of 2N NaOH solution. This was then extracted three times with ether and the combined organic extracts were washed with brine and dried over $MgSO_4$. The product was concentrated under reduced pressure and purified by flash chromatography using 40% EtOAc in hexanes as an eluant to provide 1.14g of **118** as a white solid (75%). Mp 113-115 °C; [α] D = +12.6 (*c* 1.03, CHCl3); IR (neat) 3210, 1656 cm-1; ^{1}H NMR (500 MHz, CDCl3) δ 7.30-7.22 (m, 5H), 4.68 (d, J=14.3 Hz, 1H), 4.41 (d, J=14.0 Hz, 1H), 3.48 (dd, J=8.3, 4.7 Hz, 1H) 2.14 (dt, J=11.6, 4.8 Hz, 1H), 1.97 (ddd, J=12.9, 7.6, 3.4 Hz, 1H), 1.90-1.82 (m, 2H), 1.62 (dd, J=13.1, 8.4 Hz, 1H), 1.27 (ddd, J=11.9, 9.1, 2.7 Hz, 1H), 1.22-1.17 (m, 1H), 1.08 (s, 3H), 1.05 (s, 3H); ^{13}C NMR (125 MHz, CDCl3) δ 170.6 (C), 135.9 (C), 128.6 (CH), 128.3 (CH), 127.7 (CH), 65.2 (CH), 58.3 (C), 51.1 (C), 47.9 (CH2), 46.7 (CH), 36.3 (CH2), 28.6 (CH2), 26.6 (CH2), 20.9 (CH3), 20.2

(CH3); MS (EI) 270.2 (M+); HRMS (EI) calcd. for C17H22N2O (M+) 270.1732; found 270.1723.

Compound 123: 1-Methyl-2-oxo-cyclopentanecarboxylic acid ethyl ester

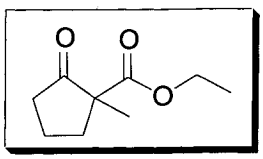

Ethyl 2-oxocyclopentane-carboxylate (5.00g, 32.01 mmol) and K_2CO_3 (17.70 g, 0.128 moles) were stirred in acetone at room temperature. Distilled MeI (4.0 mL, 63.97 mmol) was added drop-wise to the reaction. The mixture was then refluxed for 1.5 hours. H_2O was added to the reaction mixture and this was extracted three times with ether. The combined organic extracts were dried over $MgSO_4$, filtered and concentrated under reduced pressure. This provided 4.14 g (77 %) of crude product which, by comparison of the ^1H NMR with litterature results[40], was deemed quite pure and thus further purification was not pursued. ^1H NMR (300 MHz, $CDCl_3$) δ 4.07 (qd, J = 7.2, 1.5 Hz, 2H), 2.49-2.15 (m, 3H), 2.06-1.71 (m, 3H), 1.22 (s, 3H), 1.16 (t, J = 7.1 Hz, 3H).

Compound 124: 2-Benzyl-3a-methyl-3a,4,5,6-tetrahydro-2H-cyclopentapyrazol-3-one

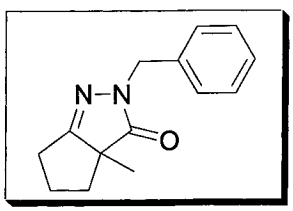

The compound **123** (100.0 mg, 0.588 mmol), benzyl hydrazine dihydrochloride (137.5 mg, 0.705 mmol) and NaOAc (212.0 mg, 2.585 mmol) were dissolved in 5 mL of AcOH. The mixture was refluxed for 40 hours before work up was pursued. Saturated $NaHCO_3$ was added to the reaction mixture and this was extracted with EtOAc. The EtOAc layer was washed with brine, dried over $MgSO_4$, filtered and concentrated under reduced pressure. Purification on a silica column using a 1:3 mixture of EtOAc and hexanes provide 67 mg (50 %) the imine as a white solid. IR (neat, cm^{-1}) 3440, 2976, 2928, 2872, 2365, 1692, 1455;

---

[40] Overberger, C.G. and Shalati, M.D. *Eur. Polym. J.* **1983**, *19*, 1055.

^1H (300 MHz, $CDCl_3$) δ 7.36-7.20 (m, 5H), 4.86 (d, J = 15.2 Hz, 1H), 4.66 (d, J = 15.2 Hz, 1H) 2.63-2.49 (m, 1H), 2.42-2.08(m, 3H), 1.85-1.72 (m, 1H), 1.66-1.52 (m, 1H), 1.37(s, 3H); ^{13}C (75 MHz, $CDCl_3$) δ 178.8 (s), 175.6(s), 137.3 (s), 128.6 (d), 127.9(d), 127.5 (d), 55.2 (s), 47.8 (t), 29.8 (t), 24.5 (t), 22.6 (t), 18.4 (q); MS (EI) 230, 139, 91, 77.

Compound 121: 2-Benzyl-3a-methyl-hexahydro-cyclopentapyrazol-3-one

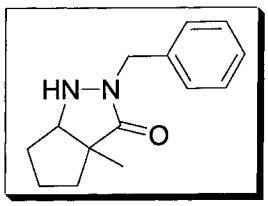

The imine **124** (168.0 mg, 0.736 mmol) was stirred in 6 ml of MeOH in a 25 mL round bottom flask to which a three way valve was attached. The solution was degassed with $N_{2(g)}$ before $PtO_2 \bullet H_2O$ (18.0 mg, 0.074 mmol) was added. The reaction was degassed once again with $N_{2(g)}$ before finally switching to a $H_{2(g)}$ atmosphere. The reduction proceeded for 1 hour. The reaction was passed through a celite pad using $CHCl_3$ as an eluant. The organic solvent was then removed under reduced pressure and the crude product subjected to silica column chromatography using a solvent system of 1:1 EtOAc and hexanes. This procedure furnished 166.0 mg (86 %) of the pure product as a colourless oil. IR (neat, cm^{-1}) 3500, 3216, 3064, 3032, 2925, 2867, 2236, 1667, 1454; ^1H (300 MHz, $CDCl_3$) δ 7.42-7.03 (m, 5H), 4.62 (d, J = 14.5 Hz, 1H), 4.41(d, J = 14.5 Hz, 1H), 4.10 (br, 1H), 3.39 (br d, J = 6.3 Hz, 1 H) 2.32-2.02 (m, 1H), 2.01-1.74 (m, 1H), 1.76-1.35 (m, 4H), 1.24(s, 3H); ^{13}C (75 MHz, $CDCl_3$) δ 176.0 (s), 136.2 (s), 129.2 (d), 128.6 (d), 128.2 (d), 66.6 (d), 53.0 (s), 48.5 (t), 37.7 (t), 34.2 (t), 24.4 (t), 21.4(q); M.P. 86 °C; MS (EI) 230, 139, 91, 77.

Compound 123: 1-Methyl-2-oxo-cyclohexanecarboxylic acid ethyl ester

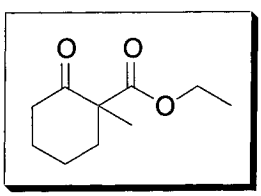

Ethyl 2-cyclohexanone-carboxylate (5.00g, 29.38 mmol) and K_2CO_3 (16.24 g, 0.1175 moles) were stirred in 50 mL of acetone. Distilled MeI (3.66 mL, 58.75 mmol) was added drop-wise to the reaction. The mixture was then refluxed for 18.5 hours. H_2O was added to the reaction mixture and this was extracted three

times with ether. The combined organic extracts were dried over $MgSO_4$, filtered and concentrated under reduced pressure. This provided 5.22 g (96%) of crude product which, by comparison of the ^1H NMR with litterature results[40], was deemed quite pure and thus further purification was not pursued. ^1H NMR (300 MHz, $CDCl_3$) δ 4.13 (qd, J = 7.2, 2.0 Hz, 2H), 2.51-2.31 (m, 3H), 2.06-1.86 (m, 1H), 1.46-1.31 (m, 1H), .1.21 (s, 3H), 1.19 (t, J = 7.1 Hz, 3H).

Compound 127: 2-Benzyl-3a-methyl-2,3a,4,5,6,7-hexahydro-indazol-3-one

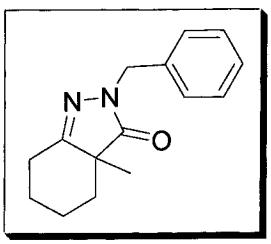

The compound **126** (1.00 g, 5.428 mmol), benzyl hydrazine dihydrochloride (1.27 g, 6.512 mmol) and NaOAc (1.11 g, 13.57 mmol) were dissolved in 50 mL of AcOH. The mixture was refluxed for 46 hours before work up was pursued. The AcOH was removed by azeotropic distillation with toluene. The crude material was redissolved in EtOAc and extracted with saturated $NaHCO_3$. The aqueous layer was extracted with EtOAc twice more before the combined organic extracts were washed with brine. The organic phase was dried over $MgSO_4$, filtered and concentrated under reduced pressure. Purification on a silica column using a 1:3 mixture of EtOAc and hexanes provided 1.18 g (90 %) of the imine as an off-white solid. IR (film, cm^{-1}) 2952, 1702, 1450, 1404; ^1H (300 MHz, $CDCl_3$) δ 7.40-7.16 (m, 5H), 4.89(d, J = 15.2 Hz, 1H), 4.74 (d, J = 15.2 Hz, 1H) 2.51(dd, J = 3.8, 9.7 Hz, 1H), 2.24 (td, J = 13.3, 5.4 Hz, 1H), 2.11-1.95 (m, 2H), 1.78-1.53 (m, 2H), 1.45-1.30 (m, 2H), 1.37 (s, 3H); ^{13}C (75 MHz, $CDCl_3$) δ 179.1(s), 167.9 (s), 137.3 (s), 128.6 (d), 127.8(d), 127.5 (d), 49.1 (s), 47.9 (t), 35.5 (t), 29.1 (t), 27.2 (t), 21.0 (t), 18.0 (q); MS (EI) 243, 242, 174, 106, 91, 77.

Compound 128: 2-Benzyl-3a-methyl-octahydro-indazol-3-one

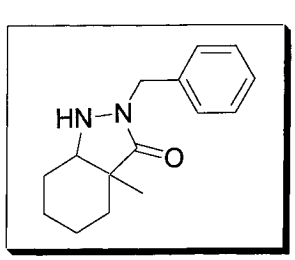

Compound **127** (100.0 mg, 0.413 mmol) was stirred in a solvent mixture consisting of 3 mL of MeOH and 1.5 mL AcOH. To this was added $NaCNBH_3$ (259.0 mg 4.126 mmol. The reaction was stirred for 39 hours. The reaction

mixture was poured into a beaker containing 50 mL of a 2N NaOH solution and stirred for 15 minutes. The mixture was then extracted with EtOAc three times. The combined organic extracts were then washed with brine, dried over $MgSO_4$, filtered and concentrated. The crude material was subjected to silica column chromatography using a 1:1 mixture of EtOAc and hexanes as the eluant to afford 77.8 mg (77 %) of the desired product as a colourless oil. IR (neat, cm^{-1}) 2952, 1702, 1450, 1404; ^1H (300 MHz, $CDCl_3$) δ 7.42-7.03 (m, 5H), 4.61(d, J = 14.9 Hz, 1H), 4.54 (d, J = 13.9 Hz, 1H), 3.17-2.93 (br, 1H), 3.06 (t, J = 5.6 Hz, 1H), 1.80-1.57 (m, 2H), 1.58-1.23 (m, 6H), 1.14 (s, 3H); ^{13}C (75 MHz, $CDCl_3$) δ 177.3 (s), 136.5 (s), 129.2 (d), 1.28.6 (d), 128.1 (d), 61.3 (d), 48.6 (t), 43.5 (s), 30.7 (t), 25.7 (t), 22.3 (t), 21.7 (t), 20.4 (q); MS (EI) 245, 244, 174, 153, 106, 91.

8.3. Procedure for Enantioselective Diels-Alder Reaction

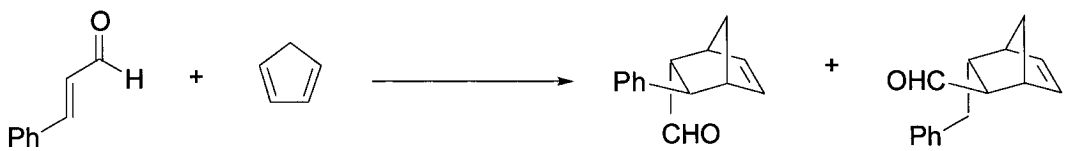

107 **106** ***Endo*-125** ***Exo*-125**

General Procedure, Table 10: 20 mol % of the catalyst **121** (17.4 mg, 7.566 X 10^{-5} moles) was stirred in 3.4 mL of a 9:1 mixture of MeOH to H_2O. To this, (*E*)-cinnamaldehyde (50.0 mg, 0.378 mmol) was added followed by the introductioin of $HClO_4$ from a titrated stock of 0.3604 M, and enough H_2O to achieve a 0.1M solution with respect to the aldehyde component. Lastly, freshly distilled cyclopentadiene (100.0 mg, 3.027 mmol) was added to the reaction, which was allowed to stir at room temperature for 48 hours. H_2O was added to the reaction that was extracted three times with ether. The combined organic extracts were washed sequentially with saturated $NaHCO_3$, H_2O, and brine. The

organic layer was dried over $MgSO_4$, filtered and concentrated. The crude material was then stirred in a mixture of 4 mL $CHCl_3$, 2 mL H_2O and 2 mL TFA for 2 hours. Saturated NH_4Cl was carefully added to the stirring mixture to quench the excess acid. This was extracted with ether three times. The combined ether layers were washed with saturated $NaHCO_3$ was dried over $MgSO_4$, filtered and concentrated. A ^1H NMR of the crude product was used to determine the % conversion and the *endo:exo.*

The same procedure was repeated for catalyst **128.**

8.4 Procedure for Friedel-Crafts Alkylation

General Procedure: The hydrazide catalyst was stirred in 1 ml of solvent and TfOH was added by weight via a microsyringe. The solution was stirred for 10 minutes before adding crotonaldehyde **105**. After stirring for 15 minutes the indole component **106** was added, and the alkylation was allowed to proceed for the time and temperature indicated in Tables 17-21. The reaction was then passed through a pad of silica using ether as an eluant. The filtrate was concentrated and subjected to silica column chromatography using benzene as the eluant to furnish the desired product **106**. To determine the ee%, reduction of the aldehyde **106** to the corresponding alcohol was done using approximately 10 mg **106**, which was stirred in 1 mL of EtOH with excess $NaBH_4$ for 15 minutes. The reaction was quenched with saturated $NaHCO_3$ and the mixture was extracted with CH_2Cl_2. The organic layer was passed through a pad of silica and concentrated under reduced pressure. The resulting alcohol was subjected to chiral HPLC analysis using a Chiracel AD-H column and a solvent system of 3.5:96.5 *i*PrOH to hexanes in a 35 minute run. The retention time for the *S* isomer was 24.69 minutes and that of the R isomer was 27.08minutes.

Table 17: The general procedure was followed using 0.2 equivalents of the catalyst **118** (17.6 mg, 7.623 X 10^{-5} moles), 3 equivalents of crotonaldehyde (80.0 mg, 1.143 mmol), 0.18 equivalents of TfOH (10.0 mg, 6.663 X 10^{-5} moles) and 1 equivalent of N-methyl indole (50.0 mg, 0.381 mmol). The following table discloses the reaction conditions and results.

Entry	Solvent (85:15)	Temperature	Time (hr)	Yield (%)	ee[a] (%)
1	CH_2Cl_2:*i*PrOH	-78°C	72[b]	25	61
2	CH_2Cl_2:*i*PrOH	23°C	50	30	44
3	CH_2Cl_2:MeOH	23°C	50	11	41
4	CH_2Cl_2:H_2O	23°C	3.5	45	48
5	THF:*i*PrOH	23°C	50	36	46
6	THF:MeOH	23°C	50	9	47
7	THF:H_2O	23°C	4	27	49
8	CH_3NO_2:*i*PrOH	23°C	4	23	51
9	CH_3NO_2:MeOH	23°C	4	39	52
10	CH_3NO_2:H_2O	23°C	4	53	39

Table 18: The general procedure was followed using 0.2 equivalents of the catalyst **118** (17.6 mg, 7.623 X 10^{-5} moles), 3 equivalents of crotonaldehyde (80.0 mg, 1.143 mmol), 0.18 equivalents of TfOH (10.0 mg, 6.663 X 10^{-5} moles) and 1 equivalent of N-methyl indole (50.0 mg, 0.381 mmol). The following table discloses the reaction conditions and results.

Entry	Solvent (85:12:3)	Temperature	Time (hr)	Yield (%)	ee[a] (%)
1	THF:*i*PrOH:H_2O	23°C	6	32	47
2	THF:*i*PrOH:H_2O	-18°C	54	27	62
3[b]	THF:*i*PrOH:H_2O	-18°C	54	8	1

Table 19, Entry 1: The general procedure was followed using 0.2 equivalents of the catalyst **118** (14.0 mg, 5.178 X 10^{-5} moles), 3 equivalents of crotonaldehyde (53. 0 mg, 0.155 mmol), 0.18 equivalents of TfOH (6.7 mg, 4.465 X 10^{-5} moles) and 1 equivalent of N-methyl indole (33.0 mg, 0.252 mmol). A 85:15 mixture of CH_3NO_2:H_2O was used as the solvent.

Table 19, Entry 2: The general procedure was followed using 0.2 equivalents of the catalyst **118** (14.0 mg, 5.178 X 10^{-5} moles), 6 equivalents of crotonaldehyde (105.0 mg, 1.498 mmol), 0.18 equivalents of TfOH (6.7 mg, 4.465 X 10^{-5} moles) and 1 equivalent of N-methyl indole (33.0 mg, 0.252 mmol). A 85:15 mixture of CH_3NO_2:H_2O was used as the solvent.

Table 19, Entry 3: The general procedure was followed using 0.2 equivalents of the catalyst **118** (14.0 mg, 5.178 X 10^{-5} moles), 10 equivalents of crotonaldehyde (175.0 mg, 2.497 mmol), 0.18 equivalents of TfOH (6.7 mg, 4.465 X 10^{-5} moles) and 1 equivalent of N-methyl indole (33.0 mg, 0.252 mmol). A 85:15 mixture of CH_3NO_2:H_2O was used as the solvent.

Entry	Aldehyde	Time (hr)	106 Yield	138 Yield
1	3 eqv	3.5	52%	35%
2	6 eqv	3.5	68%	19%
3	10 eqv.	3.5	81%	8%

Table 20, Entry 3: The general procedure was followed using 0.2 equivalents of the catalyst **118** (14.0 mg, 5.178 X 10^{-5} moles), 10 equivalents of crotonaldehyde (175.0 mg, 2.497 mmol), 0.18 equivalents of TfOH (6.7 mg, 4.465 X 10^{-5} moles) and 1 equivalent of N-methyl indole (33.0 mg, 0.252 mmol). The following table discloses the reaction conditions and results.

Entry	Solvent	Eqv.	Temp.	Time (hr)	Yield	ee
1	CH_3NO_3:H_2O	3	23°C	3.5	53%	39%
2	CH_3NO_3:H_2O	10	23°C	3.5	81%	38%
3	CH_3NO_3:*i*PrOH	3	23°C	4	39%	52%
4	CH_3NO_3:*i*PrOH	10	23°C	7	59%	34%
5	CH_3NO_3:*i*PrOH	10	-18°C	24	46%	47%
6	CH_3NO_3:*i*PrOH:H_2O	10	23°C	3.5	76%	33%
7	CH_3NO_3:*i*PrOH:H_2O	10	-18°C	20	62%	47%
8	THF:*i*PrOH:H_2O	3	23°C	6	32%	47%
9	THF:*i*PrOH:H_2O	10	23°C	4	56%	37%

Table 21: The general procedure was followed using 0.2 equivalents of the catalyst **139** (12.0 mg, 5.178 X 10^{-5} moles), 10 equivalents of crotonaldehyde (121.0 mg, 1.726 mmol), 0.18 equivalents of TfOH (4.7 mg, 3.132 X 10^{-5} moles) and 1 equivalent of N-methyl indole (23.0 mg, 0.175 mmol). The following table discloses the reaction conditions and results.

Entry	Temperature	Time (hr)	Yield	ee
1	23°C	4	22%	18%
2	-18°C	48	20%	26%

8.5 Procedure for FRET Experiments

Section 3.1.2. Figure 20 and 21: Stock solutions of **26** (3.4 mg, 1.01X10 $^{-5}$ moles) and **27** (3.7 mg, 1.00 X 10^{-5} moles) were prepared by dissolving the appropriate amounts of each compound with CH_2Cl_2 in 10 mL volumetric flasks to give a final concentration of approximately 1.00 X 10^{-3} M. A set of solutions, with varying amounts of the donor molecules **26** and **27**, were prepared by adding the specified volume of stock solutions via a 1 mL volumetric pipette to a

10 mL volumetric flask and completing the volume with CH_2Cl_2.. The solutions were made in triplicates for better accuracy in the analysis.

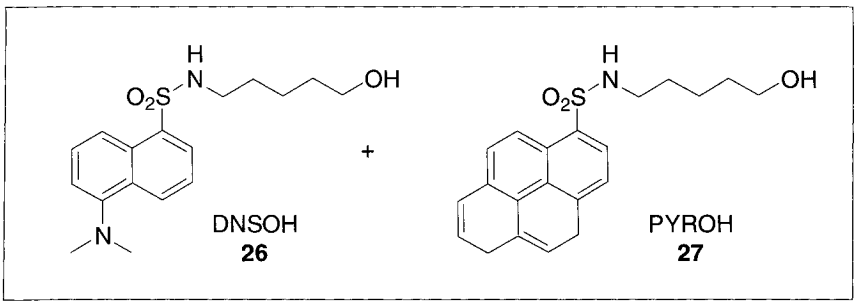

Solution	Vol. DNSOH (mL)	Vol. PYROH (mL)
1	0	1
2	0.1	0.9
3	0.2	0.8
4	0.3	0.7
5	0.4	0.6
6	0.5	0.5
7	0.6	0.4
8	0.7	0.3
9	0.8	0.2
10	0.9	0.1
11	1	0

The solutions were transferred to a quartz cuvette (path length = 1 cm) and subjected to analysis via a spectrofluorometer using the Cary Eclipsed Simple Read program. An excitation wavelength of 370 nm, was used to scan for each fluorescent donor. The fluorescent emission of DNSOH (**26**) was measured at 500nm using an excitation/ emission slit width of 2.5 nm/5 nm. The fluorescence emission of PYROH (**27**) was measured at 400 nm using an excitation/ emission slit width of 2.5 nm/2.5 nm. The results are recorded below. Average results were calculated for each donor and plotted with the concentrations of the respective donor molecules to produce Figure 20.

	DNSOH					PYROH				
Soln.	**Conc. (M)**	**Trial 1**	**Trial 2**	**Trial 3**	**AVER.**	**Conc. (M)**	**Trial 1**	**Trial 2**	**Trial 3**	**AVER.**
1	0,00E+00	8.2	9.3	7.9	**8.5**	1,00E-04	305.7	351.7	361	**339.5**
2	1,00E-05	71.4	63.3	64.1	**66.3**	9,00E-05	258.4	286	319.1	**287.8**
3	2,00E-05	138.1	122	122.6	**127.6**	8,00E-05	224	265.9	286.7	**258.9**
4	3,00E-05	207.4	185.5	177.4	**190.1**	7,00E-05	203.2	238.4	244.6	**228.8**
5	4,00E-05	265.6	235.8	230.7	**244**	6,00E-05	172.1	195.7	213.2	**193.7**
6	5,00E-05	320.8	309.6	314.9	**315.1**	5,00E-05	141.9	167	180.7	**163.2**
7	6,00E-05	387.9	364.4	359.1	**370.5**	4,00E-05	111.9	136.3	153.7	**134**
8	7,00E-05	447	398.1	420.2	**421.8**	3,00E-05	87.9	100.2	112.8	**100.3**
9	8,00E-05	512.2	464.1	491.8	**489.4**	2,00E-05	58	68.8	77.4	**68.1**
10	9,00E-05	615.3	549.4	578.6	**581.1**	1,00E-05	29.7	30.3	39.3	**33.1**
11	1,00E-04	695.5	638.7	626.6	**653.6**	0,00E+00	0.2	0.2	0.3	**0.2**

To evaluate the donor fluorescence response in the presence of free quencher molecules, a 2.50 X $^{-3}$ M stock solution of GBC methyl ester (25 mg, 5.00 X 10^{-5} moles) was prepared in a 20 mL volumetric flask using CH_2Cl_2 as a solvent. Each solution from the three sets was spiked with 0.2 ml of the stock GBC solution such that an equimolar solution of acceptor to donors was created. The solutions were subjected to fluorescence analysis as before, this time using excitation/ emission slit widths of 5 nm/ 5 nm for the detection of both DNSOH and PYROH. An average data set was calculated and plotted with the respective donor concentrations to produce Figure 21.

	DNSOH					PYROH				
Soln.	**Conc. (M)**	**Trial 1**	**Trial 2**	**Trial 3**	**AVER.**	**Conc. (M)**	**Trial 1**	**Trial 2**	**Trial 3**	**AVER.**
1	0,00E+00	2.8	7.5	10.4	**6.9**	1,00E-04	879.7	998.3	1000	**959.3**
2	1,00E-05	65.1	65.4	64.7	**65.1**	9,00E-05	789	923.7	1000	**904.2**
3	2,00E-05	132	120.5	120	**124.4**	8,00E-05	713.6	828.2	872.9	**804.9**
4	3,00E-05	187.2	173.6	178.6	**179.8**	7,00E-05	602.5	714.1	787.2	**701.3**
5	4,00E-05	249.3	242.7	241.4	**244.5**	6,00E-05	512.7	641.7	704.6	**619.6**
6	5,00E-05	294.3	295.8	308.2	**299.4**	5,00E-05	407.6	524.5	574.8	**502.3**
7	6,00E-05	383	344.5	346.5	**358**	4,00E-05	362.7	409.7	473	**415.1**
8	7,00E-05	439	409.6	422.8	**423.8**	3,00E-05	272.2	313.7	380.5	**322.2**
9	8,00E-05	500..3	460	488	**428.2**	2,00E-05	184.1	205.7	255.2	**215**
10	9,00E-05	600.9	524.6	576.5	**567.3**	1,00E-05	93.9	109.1	129.3	**110.7**
11	1,00E-04	627.9	581.9	600.8	**603.5**	0,00E+00	1.3	2.6	1.2	**1.7**

Chapter 3 Figures 27-31: Stock solutions of DNSBOC **32**, PYRBOC **35**, DPG amide **42**,DG amide **43**, and PG amide **44** were prepared in the volumetric flasks in CH_2Cl_2 solvent as indicated below.

Analyte	Amount	Moles	Volume	Conc.
DPG Amide	0.0209 g	1.89E-05	25 mL	7.55E-04 M
DNSBOC	0.0318 g	7.55E-05	50 mL	7.55E-04 M
DG Amide	0.0325 g	3.78E-04	50 mL	7.55E-04 M
PYRBOC	0.0342 g	7.55E-05	100 mL	7.55E-04 M
PG Amide	0.0337 g	3.78E-04	50 mL	7.55E-04 M
Int. Stand. 141	0.0567 g	1.89E-04	50 mL	3.78E-03 M

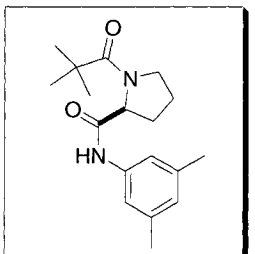

Internal Standard
141

A series of 34 solutions were created from varying amounts of the stock solutions as per table below to mimic the *pseudo*- hydrolysis of **42**. A 1 mL volumetric pipette was used to measure the specified volumes of stock solutions to a 5 mL volumetric flask. 0.2 mL of a 1.89 X 10^{-4} M stock solution of **141** was also

included in each solution as an internal standard for concentration determination by HPLC. CH_2Cl_2 was used to complete the volume of each solution to 10 mL.

Selective to DNS	Volume (X 10^{-1}mL)				
Solutions	DPG AMIDE	DNSBOC	PG AMIDE	PYRBOC	DG AMIDE
1	10	0	0	0	0
2	9	1	9	0	0
3	8	2	8	0	0
4	7	3	7	0	0
5	6	4	6	0	0
6	5	5	5	0	0
7	4	6	4	0	0
8	3	7	3	0	0
9	2	8	2	0	0
10	1	9	1	0	0
11	0	10	0	0	0

Selective to PYR	Volume (X 10^{-1}mL)				
Solutions	DPG AMIDE	DNSBOC	PG AMIDE	PYRBOC	DG AMIDE
12	10	0	0	0	0
13	9	0	0	1	9
14	8	0	0	2	8
15	7	0	0	3	7
16	6	0	0	4	6
17	5	0	0	5	5
18	4	0	0	6	4
19	3	0	0	7	3
20	2	0	0	8	2
21	1	0	0	9	1
22	0	0	0	10	0

Non Selective	Volume (X 10^{-1}mL)				
Solutions	DPG AMIDE	DNSBOC	PG AMIDE	PYRBOC	DG AMIDE
DNSBOC Varied PYRBOC Held Constant at 50%					
23	5	0	0	5	5
24	4	1	1	5	5
25	3	2	2	5	5
26	2	3	3	5	5
27	1	4	4	5	5
28	0	5	5	5	5
PYRBOC Varied DNSBOC Held Constant at 50%					
29	5	5	5	0	0
30	4	5	5	1	1
31	3	5	5	2	2
32	2	5	5	3	3
33	1	5	5	4	4
34	0	5	5	5	5

Each of the 34 solutions were transferred to a 1 mL quartz cuvette (path length = 1 cm) and evaluated for fluorescence by means of a spectrophotometer. The solutions were scanned using excitation/emission slits of 5 nm/5 nm at wavelengths of 315 nm, 340 nm and 370 nm. The fluorescence emission intensities of the dansyl and pyrene moieties were measured at 500 nm and 400 nm respectively and recorded as an average of three readings using the Cary Eclipsed Advanced Read Program.

Selective to DNS	DNSBOC			PYRBOC		
Solutions	315 nm	340 nm	370 nm	315 nm	340 nm	370 nm
1	30.2705	19.7878	22.963	17.3378	16.637	9.991
2	103.2668	46.3485	88.7375	21.4926	19.3663	12.1434
3	152.5273	58.7578	134.996	23.8045	19.0809	13.4936
4	182.4178	61.4051	163.1286	26.1414	18.962	15.0973
5	234.8092	77.8284	211.1333	30.7777	22.0005	17.5997
6	260.2271	77.054	234.7187	30.204	19.2773	16.9014
7	246.6073	64.5901	224.2452	28.228	15.6498	15.9687
8	257.7504	65.7868	232.5158	29.1294	16.0623	16.2456
9	260.1212	62.0442	232.2532	26.7761	13.3723	14.8513
10	290.1287	67.8257	260.6541	29.5495	14.7142	16.3123
11	322.0327	75.1381	291.3709	34.9016	17.3574	19.843

Selective to PYR	DNSBOC			PYRBOC		
Solutions	315 nm	340 nm	370 nm	315 nm	340 nm	370 nm
12	32.313	24.6056	25.56	18.0813	20.0494	10.6692
13	31.8674	19.9042	26.4607	314.7412	314.0501	180.4529
14	31.4521	15.4229	26.1866	503.8903	420.7467	284.7527
15	31.0095	13.7351	26.1537	587.5537	451.2336	331.7255
16	30.3129	12.0361	25.9152	666.6309	466.579	381.3638
17	29.232	10.4966	25.7356	695.6978	438.3674	397.6349
18	28.7602	9.3746	24.9327	711.9838	417.8508	411.2344
19	26.7166	8.1757	23.6043	685.6526	369.4687	398.6454
20	28.2089	8.1501	24.6277	757.8318	399.9711	438.8103
21	25.9629	6.9658	22.9138	687.1608	342.2206	396.1201
22	25.8643	6.7322	22.8317	699.2155	322.4926	394.2672

Non Selective	DNSBOC			PYRBOC		
Solutions	315 nm	340 nm	370 nm	315 nm	340 nm	370 nm
DNSBOC Varied, PYRBOC Held Constant at 50%						
23	28.2874	9.6988	23.9698	654.0065	398.9246	364.5547
24	64.5862	18.4587	55.7261	567.9985	329.5576	319.4476
25	89.2037	23.3797	80.4615	515.3461	267.2965	291.1137
26	120.8144	30.6397	108.2609	461.8586	237.8781	264.1086
27	136.593	33.066	125.3815	421.8265	207.422	243.0826
28	153.34	34.1757	142.3004	391.3443	174.9776	225.7845
PYRBOC Varied, DNSBOC Held Constant at 50%						
29	245.5259	74.5361	225.1516	30.763	20.2279	17.6455
30	222.7037	64.0067	202.6041	149.4903	94.1151	85.4752
31	195.61	51.0504	180.8295	264.8724	130.2688	135.8645
32	17.4391	43.0476	160.9711	295.0114	153.6865	169.9337
33	167.7773	40.3233	153.179	360.6424	180.2126	206.8815
34	158.992	37.0562	147.3698	415.5569	196.372	242.9615

The concentration of the fluorescence donors, DNSBOC **32** and PYRBOC **35**, were verified by HPLC by correlating the area under the curve (AUC) of the given donor peak to that of the internal standard by the following formula:

X = Unknown Concentration
A = 1.54 X 10^{-4}M

$$\text{Analyte Concentration X} = \left[\frac{\text{AUC}_X \text{ Analyte}}{\text{AUC}_A \text{ Internal Standard}}\right] \div \text{Signal Ratio}_A * A$$

The signal ratio$_A$ is the given by the peak area ratio of the analyte and internal standard when both are at the same concentration **A** (arbitrarily chosen to be 1.54 X 10^{-4} M). Solutions containing equimolar amounts of the internal standard and donors were prepared to determine the respective signal ratios disclosed in the following table.

Analyte	AUC	AUC Int. Std.	Signal Ratio
DNSBOC	1556627	5404430	0.288
PYRBOC	1759796	2306010	0.7631

With a method to verify the actual concentration of DNSBOC and PYRBOC established, each of the 33 *pseudo*-hydrolysis solutions were subjected HPLC analysis using a gradient system of 50%B→100%B (Solvent A = H_2O, Solvent B = Acetonitrile, 35 min. run). The HPLC corrected concentrations were subsequently calculated and compared to the theoretical concentrations to furnish Figures 27 to 31.

Selective to DNS							
	Int. Stand.	DNSBOC			PYRBOC		
Sol.	AUC	AUC	[THEOR] (M)	[HPLC] (m)	AUC	[THEOR] (M)	[HPLC] (M)
1	8791627	0	0.00E+00	0.00E+00	0	0	0
2	9237296	315416	1.51E-05	1.79E-05	0	0	0
3	7337134	367946	3.02E-05	2.63E-05	0	0	0
4	7871407	693703	4.53E-05	4.62E-05	0	0	0
5	8355770	1001772	6.04E-05	6.29E-05	0	0	0
6	6652833	1042966	7.55E-05	8.22E-05	0	0	0
7	8806535	1589675	9.06E-05	9.46E-05	0	0	0
8	7082125	1467413	1.06E-04	1.09E-04	0	0	0
9	4878860	1129902	1.21E-04	1.21E-04	0	0	0
10	7121486	1882731	1.36E-04	1.39E-04	0	0	0
11	9292413	2706699	1.51E-04	1.53E-04	0	0	0

Selective to PYR							
	Int. Stand.	DNSBOC			PYRBOC		
Sol.	AUC	AUC	[THEOR] (M)	[HPLC] (m)	AUC	[THEOR] (M)	[HPLC] (M)
12	8057854	0	0	0	0	0.00E+00	0.00E+00
13	9720587	0	0	0	838119	1.51E-05	1.71E-05
14	10441479	0	0	0	1725150	3.02E-05	3.27E-05
15	10256468	0	0	0	2617979	4.53E-05	5.06E-05
16	10824144	0	0	0	3486711	6.04E-05	6.38E-05
17	10644818	0	0	0	4363650	7.55E-05	8.12E-05
18	9669364	0	0	0	4756833	9.06E-05	9.75E-05
19	11981551	0	0	0	6608819	1.06E-04	1.09E-04
20	7521799	0	0	0	4870300	1.21E-04	1.28E-04
21	8142964	0	0	0	5743828	1.36E-04	1.40E-04
22	8660126	0	0	0	6786155	1.51E-04	1.55E-04

Non Selective							
	Int. Stand.	DNSBOC			PYRBOC		
Sol.	AUC	AUC	[THEOR] (M)	[HPLC] (m)	AUC	[THEOR] (M)	[HPLC] (M)
DNSOH Varied, PYROH Held Constant at 50%							
23	8264616	0	0.00E+00	0.00E+00	3355992	7.55E-05	8.05E-05
24	6989534	222884	1.51E-05	1.67E-05	2683766	7.55E-05	7.61E-05
25	6102129	327817	3.02E-05	2.82E-05	2431815	7.55E-05	7.90E-05
26	11441989	1017455	4.53E-05	4.66E-05	4506208	7.55E-05	7.80E-05
27	10180722	1211743	6.04E-05	6.24E-05	4016202	7.55E-05	7.82E-05
28	10161831	1487391	7.55E-05	7.67E-05	4147367	7.55E-05	8.09E-05
PYROH Varied, DNSOH Held Constant at 50%							
29	10656622	1489550	7.55E-05	7.33E-05	0	0.00E+00	0.00E+00
30	8507953	1233333	7.55E-05	7.60E-05	657871	1.51E-05	1.53E-05
31	8408347	1254765	7.55E-05	7.82E-05	1352764	3.02E-05	3.19E-05
32	8293700	1184402	7.55E-05	7.49E-05	1954894	4.53E-05	4.67E-05
33	9626209	1410630	7.55E-05	7.68E-05	3038031	6.04E-05	6.25E-05
34	8290825	1204134	7.55E-05	7.61E-05	3209000	7.55E-05	7.67E-05

Chapter 3 Figures 24-25, Schemes 11-12: Using a volumetric pipette, 1.0 ml of the indicated stock solutions was transferred to a 10 mL volumetric flask to which CH_2Cl_2 was added to complete the volumes. The diluted solutions were analyzed by a fluorescence spectrometer in a 1 mL quartz cuvette using the Cary Eclipse Scan Program. The excitation wavelength was 370 nm and the emission intensities were measured at 500 nm and 400 nm for dansyl and pyrene respectively.

Analyte	Amount	Moles	Volume	Conc.
DPG Amide	0.0209 g	1.89E-05	25 mL	7.55E-04 M
DNSBOC	0.0318 g	7.55E-05	50 mL	7.55E-04 M
DG Amide	0.0325 g	3.78E-04	50 mL	7.55E-04 M
PYRBOC	0.0342 g	7.55E-05	100 mL	7.55E-04 M
PG Amide	0.0337 g	3.78E-04	50 mL	7.55E-04 M

Chapter 3 Figures 33-38: Stock solutions of DNSOH **26**, PYROH **27**, DPG ester **46**,DG ester **47**, and PG ester **48** were prepared in the volumetric flasks in dichloroethane solvent as indicated below.

Analyte	Amount	Moles	Volume	Conc.
DPG Ester	0.0858 g	1.51E-04	50 mL	1.51E-03 M
DNSOH	0.0508 g	1.51E-04	100 mL	1.51E-03 M
DG Ester	0.1324 g	1.51E-04	100 mL	1.51E-03 M
PYROH	0.0558 g	1.51E-04	100 mL	1.51E-03 M
PG Ester	0.1256 g	1.51E-04	100 mL	1.51E-03 M
Int. Stand. **141**	0.0456 g	1.51E-04	100 mL	1.51E-03 M

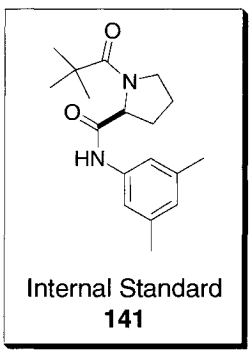

Internal Standard
141

A series of 55 solutions were created from varying amounts of the stock solutions as per table below to mimic the *pseudo*- hydrolysis of **46**. A 1 mL volumetric pipette was used to measure the specified volumes of stock solutions to a 10 mL volumetric flask. 1.0 mL of a 1.51 X 10^{-3} M stock solution of **141** was also included in each solution as an internal standard for concentration determination

by HPLC. Dichloroethane was used to complete the volume of each solution to 10 mL.

Selective to DNS	Volume (X 10^{-1} mL)				
Solutions	DPG ESTER	DNSOH	PG ESTER	PYROH	DG ESTER
1	10	0	0	0	0
2	9	1	9	0	0
3	8	2	8	0	0
4	7	3	7	0	0
5	6	4	6	0	0
6	5	5	5	0	0
7	4	6	4	0	0
8	3	7	3	0	0
9	2	8	2	0	0
10	1	9	1	0	0
11	0	10	0	0	0

Selective to PYR	Volume (X 10^{-1} mL)				
Solutions	DPG ESTER	DNSOH	PG ESTER	PYROH	DG ESTER
12	10	0	0	0	0
13	9	0	0	1	9
14	8	0	0	2	8
15	7	0	0	3	7
16	6	0	0	4	6
17	5	0	0	5	5
18	4	0	0	6	4
19	3	0	0	7	3
20	2	0	0	8	2
21	1	0	0	9	1
22	0	0	0	10	0

Non Selective	Volume (X 10^{-1} mL)				
Solutions	DPG ESTER	DNSOH	PG ESTER	PYROH	DG ESTER
DNSBOC Varied PYRBOC Held Constant at 50%					
23	5	0	0	5	5
24	4.5	0.5	0.5	5	5
25	4	1	1	5	5
26	3.5	1.5	1.5	5	5
27	3	2	2	5	5
28	2.5	2.5	2.5	5	5
29	2	3	3	5	5
30	1.5	3.5	3.5	5	5
31	1	4	4	5	5
32	0.5	4.5	4.5	5	5
33	0	5	5	5	5
PYRBOC Varied DNSBOC Held Constant at 50%					
34	5	5	5	0	0
35	4.5	5	5	0.5	0.5
36	4	5	5	1	1
37	3.5	5	5	1.5	1.5
38	3	5	5	2	2
39	2.5	5	5	2.5	2.5
40	2	5	5	3	3
41	1.5	5	5	3.5	3.5
42	1	5	5	4	4
43	0.5	5	5	4.5	4.5
44	0	5	5	5	5

Random	Volume (X 10^{-1} mL)				
Solutions	DPG ESTER	DNSOH	PG ESTER	PYROH	DG ESTER
45	8	1	1	2	2
46	3	4	4	3	3
47	1	8	8	1	1
48	0	7	7	3	3
49	3	1	1	6	6
50	7	2	2	1	1
51	5	3	3	2	2
52	6	1	1	3	3
53	8	1	1	1	1
54	5	4	4	1	1
55	1	3	3	6	6

Each of the 55 solutions were transferred to a 1 mL quartz cuvette (path length = 1 cm) and evaluated for fluorescence by means of a spectrophotometer. The solutions were scanned using excitation/emission slits of 5 nm/10 nm at wavelengths of 370 nm. The fluorescence emission intensities of the Dansyl and Pyrene moieties were measured at 500 nm and 400 nm respectively and recorded as an average of three readings using the Cary Eclipsed Advanced Read Program. The same solutions (200 μL) were also loaded on a white NUNC polypropylene wellplate and analyzed with an excitation wavelength of 370 nm and excitation/emission slits of 10nm/10nm. Emission readings at 500 nm for dansyl and 400 nm for pyrene were recorded as an average of triplicate readings using the Cary Eclipse Advanced read program.

Selective to DNS	DNSOH		PYROH	
Solutions	Cuvette	Wellplate	Cuvette	Wellplate
1	44.0547	9.7265	15.9684	12.8081
2	121.0947	56.2629	18.9497	12.8065
3	179.2611	95.7625	21.1784	12.0668
4	251.3923	144.9266	25.3966	13.8375
5	327.8307	185.6216	28.6885	13.5309
6	372.0904	224.9375	29.7967	13.5894
7	430.7535	256.9481	33.1456	13.6072
8	493.0274	301.9453	36.0546	14.4387
9	537.4014	336.0919	37.4054	14.7436
10	568.5362	370.4471	37.9129	14.4477
11	676.1298	420.01	44.306	14.6019

Selective to PYR	DNSOH		PYROH	
Solutions	Cuvette	Wellplate	Cuvette	Wellplate
12	42.5834	7.3249	15.34	12.3614
13	41.6096	8.4973	91.5164	17.3237
14	46.7067	10.6997	177.221	23.9157
15	47.9479	11.2583	246.1138	27.1401
16	49.0675	12.2815	318.8051	33.7293
17	50.1458	12.9743	385.5395	36.6007
18	51.303	14.2921	448.8086	44.6067
19	53.7297	15.8595	510.7813	50.6438
20	57.6952	16.3088	579.0946	52.6342
21	56.3681	18.4931	615.7754	59.4655
22	56.2374	19.4321	664.6812	64.8956

Non Selective	DNSOH		PYROH	
Solutions	Cuvette	Wellplate	Cuvette	Wellplate
DNSOH Varied, PYROH Held Constant at 50%				
23	51.9905	14.8633	406.536	39.3941
24	87.5735	37.4483	405.1956	40.3948
25	118.0011	57.5141	373.8258	38.484
26	150.1998	77.1369	387.1697	39.7745
27	177.1184	94.3972	370.1458	39.2669
28	209.1524	111.7029	367.2767	38.2212
29	246.5165	136.929	362.825	38.9651
30	257.7754	149.7557	347.7546	39.2399
31	282.7866	172.5854	336.8652	39.0114
32	327.2216	187.6388	359.2958	38.7383
33	353.6964	211.8984	345.0793	38.3766
PYROH Varied, DNSOH Held Constant at 50%				
34	371.8581	210.0703	30.5912	13.6533
35	365.2417	204.7948	69.2207	16.0333
36	342.1836	208.6748	94.6587	18.6945
37	358.4055	207.6188	135.1575	20.7766
38	365.3381	208.8094	167.7866	23.7284
39	340.6315	206.6098	191.5166	26.3795
40	351.7723	203.9689	227.7039	28.6103
41	345.8692	203.1949	253.6991	31.0085
42	346.7969	200.262	282.1945	33.122
43	297.9546	184.686	260.3319	32.6473
44	345.1861	198.6246	340.4235	36.6321

Random	DNSOH		PYROH	
Solutions	Cuvette	Wellplate	Cuvette	Wellplate
45	108.5554	52.4144	159.8503	23.1471
46	288.5159	168.8404	226.1239	28.1195
47	516.5078	316.1415	100.1851	18.3902
48	484.5878	278.0317	217.9197	27.357
49	112.8639	54.1381	418.8655	43.1424
50	188.6665	93.8811	101.3296	18.4369
51	235.9303	131.7393	161.4061	23.8122
52	116.8092	52.3606	246.805	28.9755
53	120.4616	58.0983	503.1655	49.9715
54	299.3883	163.0916	99.5744	18.715
55	239.683	133.6192	429.4581	45.754

The concentration of the fluorescence donors, DNSOH **26** and PYROH **27**, were verified by HPLC by correlating the area under the curve (AUC) of the given donor peak to that of the internal standard by the following formula:

X = Unknown Concentration
A = 1.54 X 10^{-4}M

$$\text{Analyte Concentration X} = \left[\frac{AUC_X \text{ Analyte}}{AUC_A \text{ Internal Standard}}\right] \div \text{Signal Ratio}_A * A$$

The signal $ratio_A$ is the given by the peak area ratio of the analyte and internal standard when both are at the same concentration **A** (arbitrarily chosen to be 1.54 X 10^{-4} M). Solutions containing equimolar amounts of the internal standard

141 and donors were prepared to determine the respective signal ratios disclosed in the following table.

Analyte	AUC	AUC Int. Std.	Signal Ratio
DNSOH	1208425	4097410	0.29492
PYROH	4065819	4869920	0.83488

With a method to verify the actual concentration of DNSOH and PYROH established, each of the 55 *pseudo*-hydrolysis solutions were subjected HPLC analysis using a gradient system of 30%B→100%B (Solvent A = H_2O, Solvent B = Acetonitrile, 35 min. run). The HPLC corrected concentrations were subsequently calculated and compared to the theoretical concentrations to furnish Figure **33**.

Selective to DNS							
	Int. Stand.	**DNSOH**			**PYROH**		
Sol.	**AUC**	**AUC**	**[THEOR] (M)**	**[HPLC] (m)**	**AUC**	**[THEOR] (M)**	**[HPLC] (M)**
1	7188525	0	0.00E+00	0.00E+00	0	0	0
2	9109946	178450	1.51E-05	1.00E-05	0	0	0
3	12510541	623389	3.02E-05	2.55E-05	0	0	0
4	8074080	596948	4.53E-05	3.79E-05	0	0	0
5	9844312	997001	6.04E-05	5.19E-05	0	0	0
6	10987682	1485014	7.55E-05	6.92E-05	0	0	0
7	9764139	1565788	9.06E-05	8.21E-05	0	0	0
8	8493270	1505279	1.06E-04	9.07E-05	0	0	0
9	8725590	1858836	1.21E-04	1.09E-04	0	0	0
10	9706005	2008774	1.36E-04	1.06E-04	0	0	0
11	7069517	1703524	1.51E-04	1.23E-04	0	0	0

Selective to PYR							
	Int. Stand.	DNSOH			PYROH		
Sol.	AUC	AUC	[THEOR] (M)	[HPLC] (m)	AUC	[THEOR] (M)	[HPLC] (M)
12	7188525	0	0	0	0	0.00E+00	0.00E+00
13	9275735	0	0	0	393144	1.51E-05	7.67E-06
14	6397323	0	0	0	748388	3.02E-05	2.12E-05
15	8607718	0	0	0	1379303	4.53E-05	2.90E-05
16	9026225	0	0	0	1881796	6.04E-05	3.77E-05
17	3926003	0	0	0	1331199	7.55E-05	6.13E-05
18	11512286	0	0	0	4282623	9.06E-05	6.73E-05
19	6027153	0	0	0	2953860	1.06E-04	8.86E-05
20	8898608	0	0	0	4782291	1.21E-04	9.72E-05
21	9698191	0	0	0	6254199	1.36E-04	1.17E-04
22	7607426	0	0	0	5269473	1.51E-04	1.25E-04

Non Selective							
	Int. Stand.	DNSOH			PYROH		
Sol.	AUC	AUC	[THEOR] (M)	[HPLC] (m)	AUC	[THEOR] (M)	[HPLC] (M)
DNSOH Varied, PYROH Held Constant at 50%							
23	7622511	0	0.00E+00	0.00E+00	2680373	7.55E-05	6.36E-05
24	9056507	100054	7.55E-06	5.66E-06	2662360	7.55E-05	5.32E-05
25	5552426	150728	1.51E-05	1.39E-05	1966939	7.55E-05	6.41E-05
26	6540705	230479	2.27E-05	1.80E-05	2184595	7.55E-05	6.04E-05
27	7015111	341638	3.02E-05	2.49E-05	2610171	7.55E-05	6.73E-05
28	9072057	551913	3.78E-05	3.11E-05	3055623	7.55E-05	6.09E-05
29	10017651	739535	4.53E-05	3.78E-05	3371375	7.55E-05	6.09E-05
30	8894778	687952	5.29E-05	3.96E-05	2866865	7.55E-05	5.83E-05
31	5725898	555466	6.04E-05	4.97E-05	2134920	7.55E-05	6.74E-05
32	6167142	633938	6.80E-05	5.26E-05	2080650	7.55E-05	6.10E-05
33	5829995	797164	7.55E-05	7.00E-05	2070660	7.55E-05	6.42E-05
PYROH Varied, DNSOH Held Constant at 50%							
34	5777872	1084494	7.55E-05	9.61E-05	0	0.00E+00	0.00E+00
35	3741541	468368	7.55E-05	6.41E-05	132786	7.55E-06	6.42E-06
36	8368578	935656	7.55E-05	5.72E-05	527319	1.51E-05	1.14E-05
37	6800287	778095	7.55E-05	5.86E-05	642103	2.27E-05	1.71E-05
38	11249369	1107264	7.55E-05	5.04E-05	1604709	3.02E-05	2.58E-05
39	3624811	449106	7.55E-05	6.34E-05	712005	3.78E-05	3.55E-05
40	7126273	755567	7.55E-05	5.43E-05	1587504	4.53E-05	4.03E-05
41	10934744	1192793	7.55E-05	5.59E-05	2678885	5.29E-05	4.43E-05
42	5681983	806953	7.55E-05	7.27E-05	1769460	6.04E-05	5.63E-05
43	6624766	909939	7.55E-05	7.03E-05	2169384	6.80E-05	5.92E-05
44	9877299	1238545	7.55E-05	6.42E-05	3574414	7.55E-05	6.55E-05

Random							
	Int. Stand.	DNSOH			PYROH		
Sol.	AUC	AUC	[THEOR] (M)	[HPLC] (m)	AUC	[THEOR] (M)	[HPLC] (M)
45	5486633	122917	1.51E-05	1.15E-05	660577	3.02E-05	2.18E-05
46	5170136	493210	6.04E-05	4.88E-05	1106436	4.53E-05	3.87E-05
47	6070473	1429597	1.21E-04	1.21E-04	462718	1.51E-05	1.38E-05
48	3441650	831130	1.06E-04	1.24E-04	743661	4.53E-05	3.91E-05
49	7885607	216037	1.51E-05	1.40E-05	3332467	9.06E-05	7.64E-05
50	9054604	451337	3.02E-05	2.55E-05	502867	1.51E-05	1.00E-05
51	11037582	592034	4.53E-05	2.75E-05	1376040	3.02E-05	2.25E-05
52	3755433	93013	1.51E-05	1.27E-05	768864	4.53E-05	3.70E-05
53	5691550	140724	1.51E-05	1.27E-05	2719959	1.06E-04	8.64E-05
54	4203769	386550	6.04E-05	4.71E-05	312643	1.51E-05	1.35E-05
55	4176354	342925	4.53E-05	4.20E-05	1892643	9.06E-05	8.20E-05

Chapter 3 Schemes 13-17: Using a volumetric pipette, 1.0 ml of the indicated stock solutions was transferred to a 10 mL volumetric flask to which dichloroethatne was added to complete the volumes. The diluted solutions were analyzed by a fluorescence spectrometer in a 1 mL quartz cuvette using the Cary Eclipse Scan Program. The excitation wavelength was 370 nm and the emission intensities were measured at 500 nm and 400 nm for dansyl and pyrene respectively.

Analyte	Amount	Moles	Volume	Conc.
DPG Ester	0.0858 g	1.51E-04	50 mL	1.51E-03 M
DNSOH	0.0508 g	1.51E-04	100 mL	1.51E-03 M
DG Ester	0.1324 g	1.51E-04	100 mL	1.51E-03 M
PYROH	0.0558 g	1.51E-04	100 mL	1.51E-03 M
PG Ester	0.1256 g	1.51E-04	100 mL	1.51E-03 M

APPENDIX

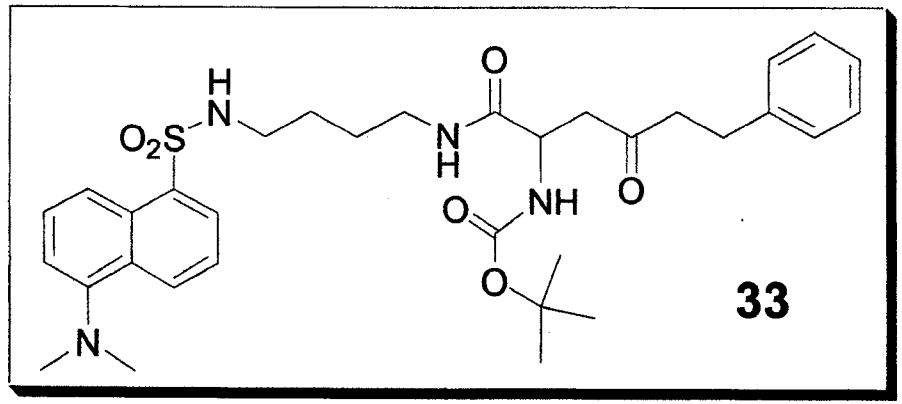
H
N
O_2S
N
H
O
O
NH
O
O
N
33

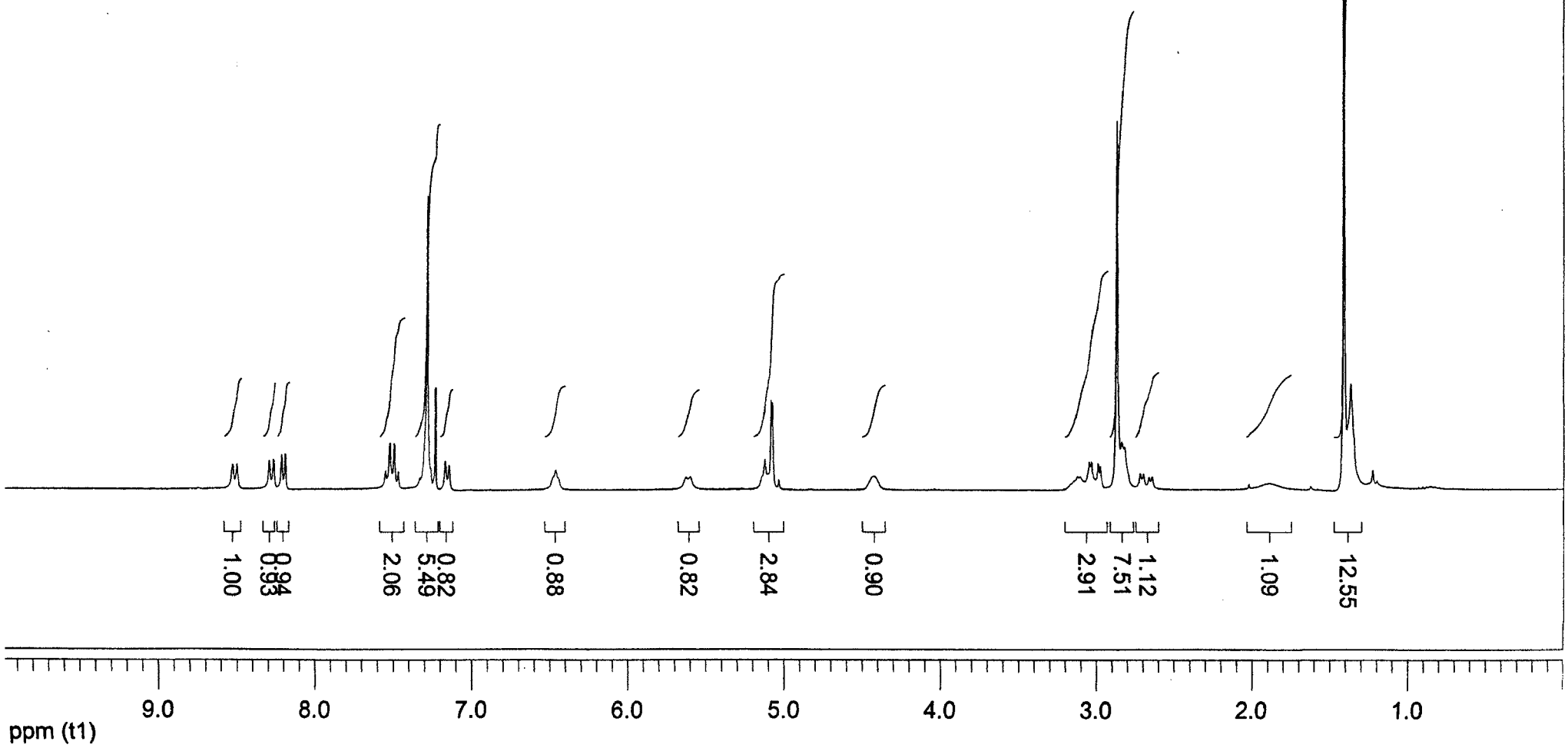
1.00
0.93
0.94
2.06
5.49
0.82
0.88
0.82
2.84
0.90
2.91
7.51
1.12
1.09
12.55
9.0
8.0
7.0
6.0
5.0
4.0
3.0
2.0
1.0
ppm (t1)

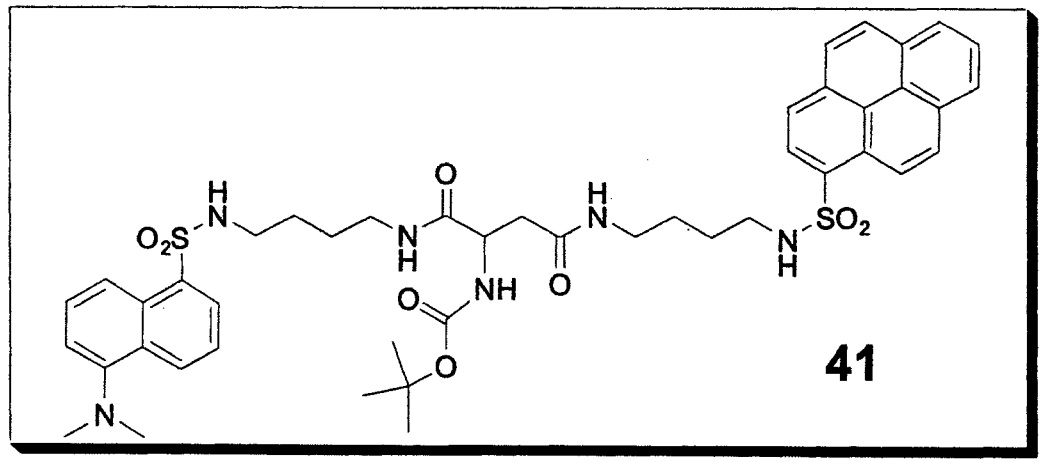
41

1.00
1.11
1.20
7.88
1.80
2.60
0.65
0.64
0.67
0.92
3.73
15.73
2.02
2.68
16.03
9.0
8.0
7.0
6.0
5.0
4.0
3.0
2.0
1.0
ppm (t1)

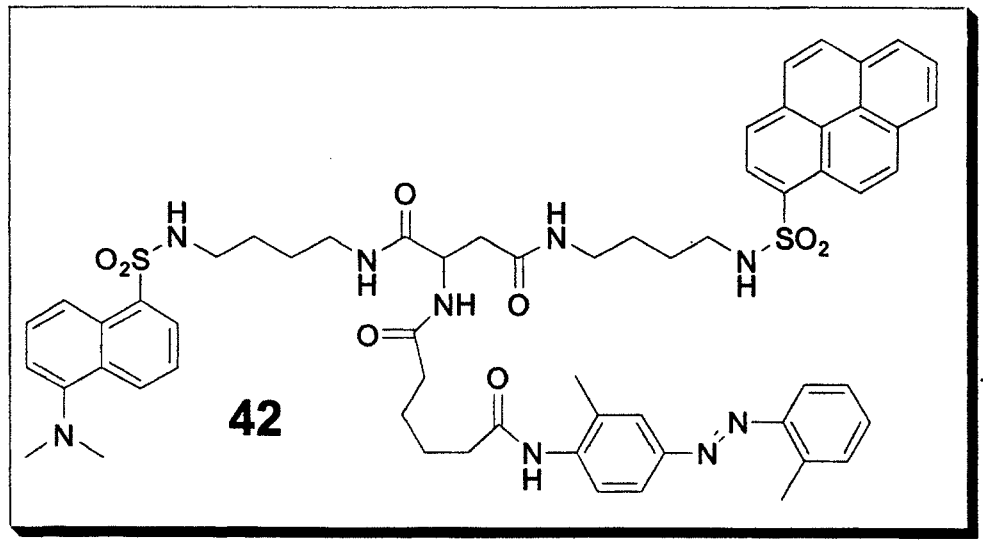

42

1.11 1.09 1.25 1.25 4.10 3.13 2.20 2.08 5.66 1.55 1.83 1.19 1.20 0.99 1.89 11.00 13.41 5.27 3.77 4.75 7.22

5.0

ppm (t1)

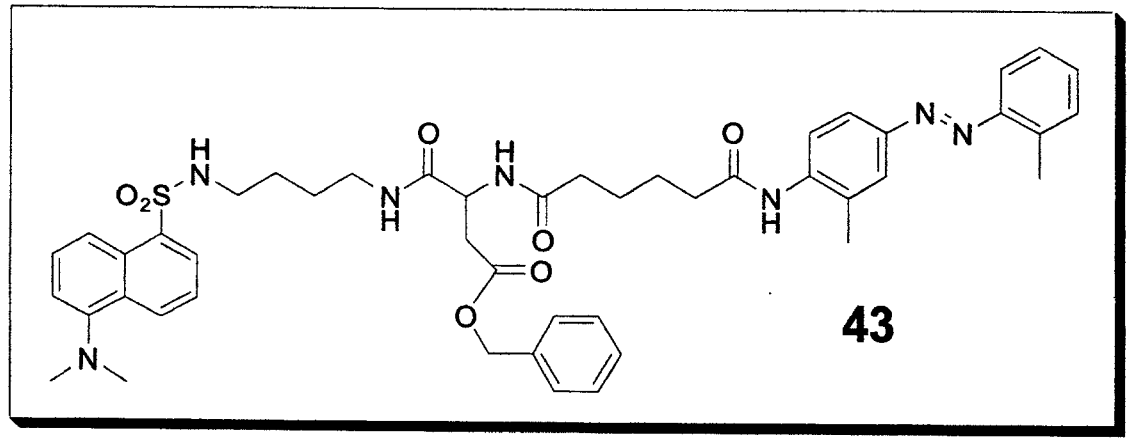

43

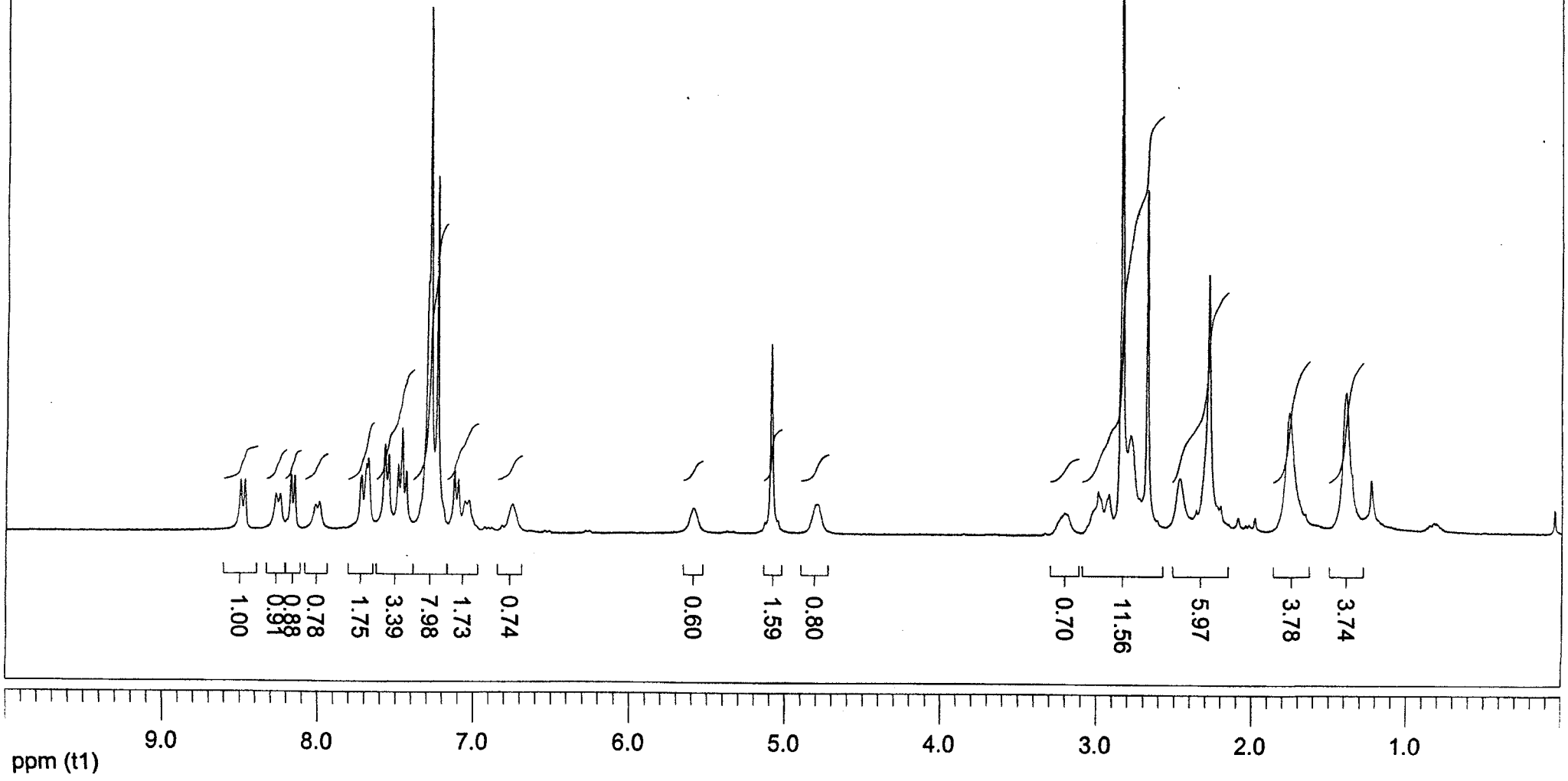
1.00
0.89
0.88
0.78
1.75
3.39
7.98
1.73
0.74
0.60
1.59
0.80
0.70
11.56
5.97
3.78
3.74
9.0
8.0
7.0
6.0
5.0
4.0
3.0
2.0
1.0
ppm (t1)

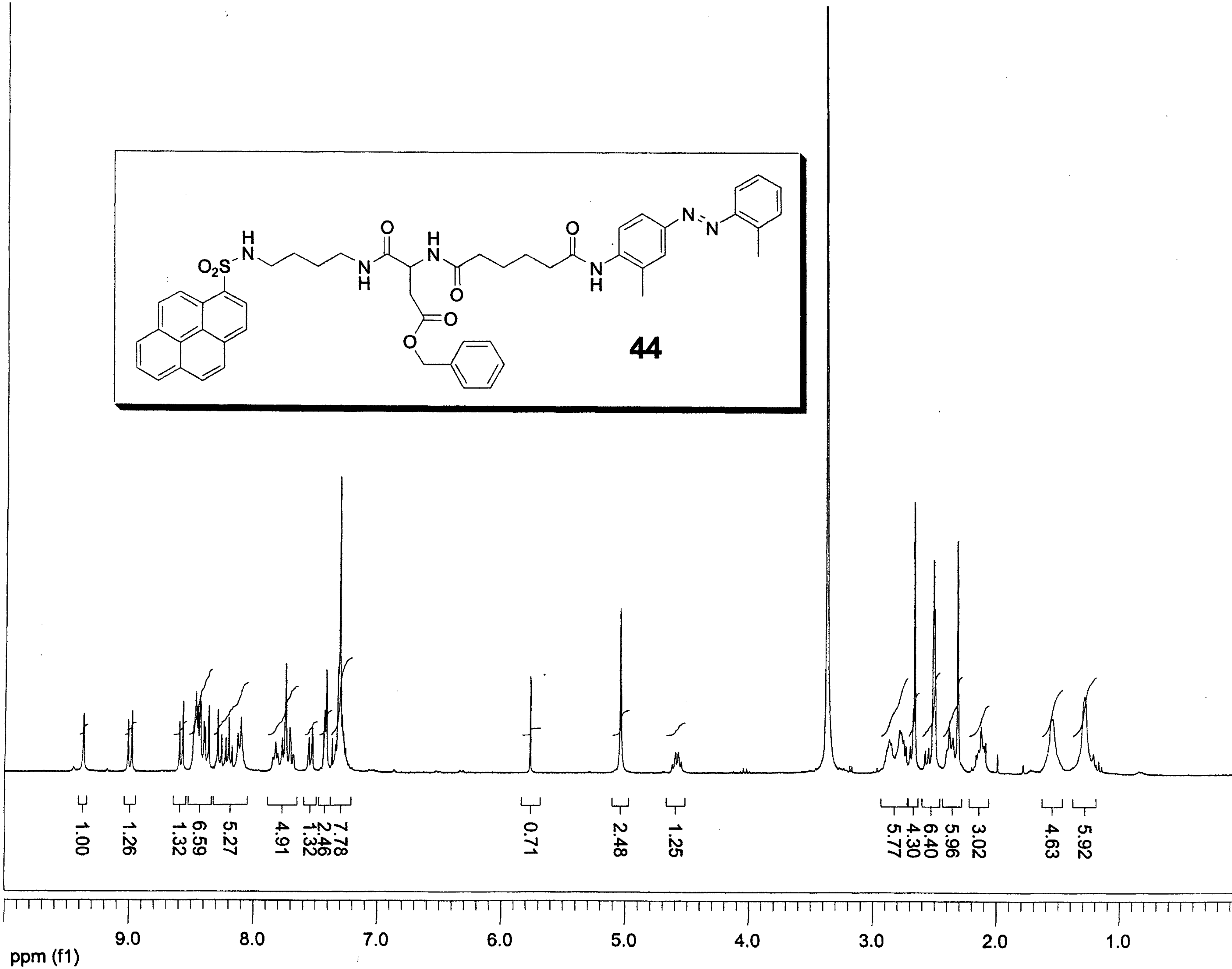

44
1.00
1.26
1.32
6.59
5.27
4.91
1.32
2.46
7.78
0.71
2.48
1.25
5.77
4.30
6.40
5.96
3.02
4.63
5.92
9.0
8.0
7.0
6.0
5.0
4.0
3.0
2.0
1.0
ppm (f1)

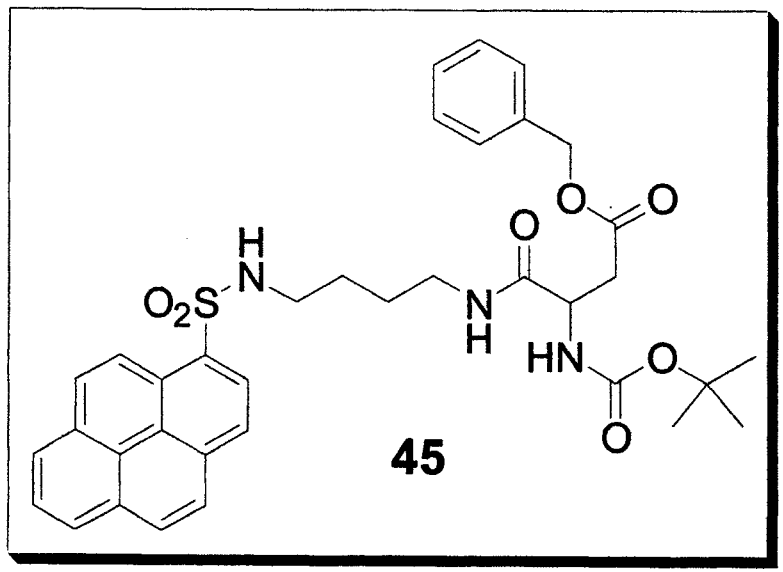
O
O
O
HN
O_2S
NH
HN
O
O
O
45

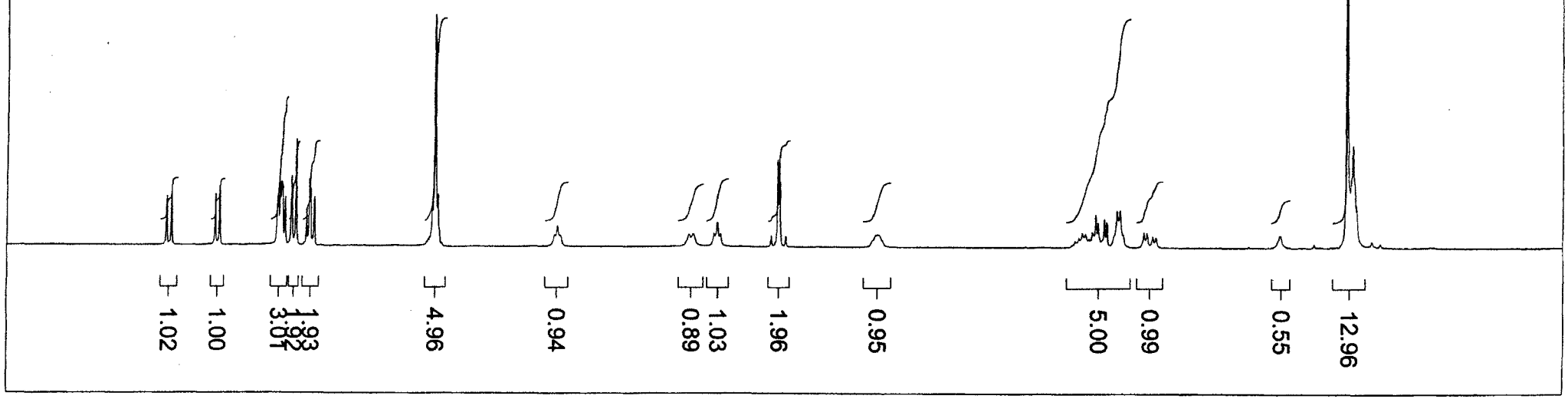
1.02
1.00
3.01
1.93
4.96
0.94
0.89
1.03
1.96
0.95
5.00
0.99
0.55
12.96

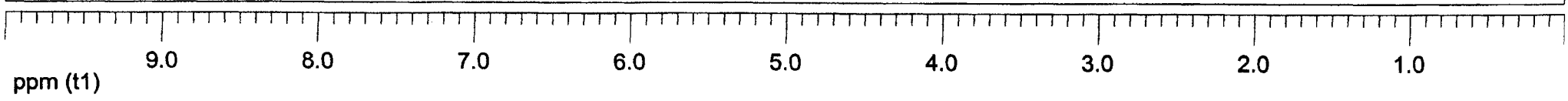
9.0
8.0
7.0
6.0
5.0
4.0
3.0
2.0
1.0
ppm (t1)

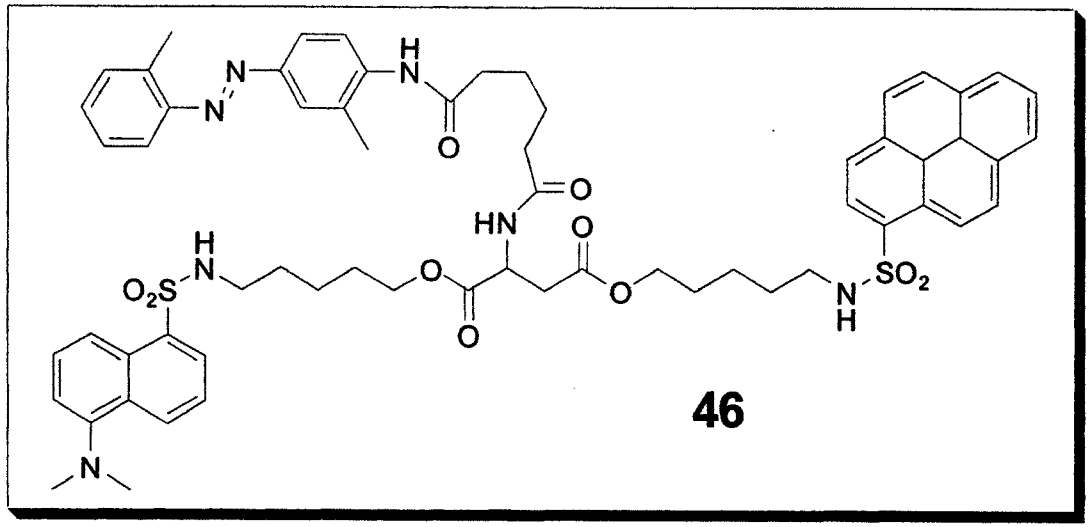

46

1.00
1.01
1.01
1.09
6.05
2.17
0.91
1.00
2.91
2.02
3.16
1.02
0.95
0.91
0.91
0.98
4.44
11.93
2.84
4.07
2.97
1.29
3.89
12.64
9.0
8.0
7.0
6.0
5.0
4.0
3.0
2.0
1.0
ppm (f1)

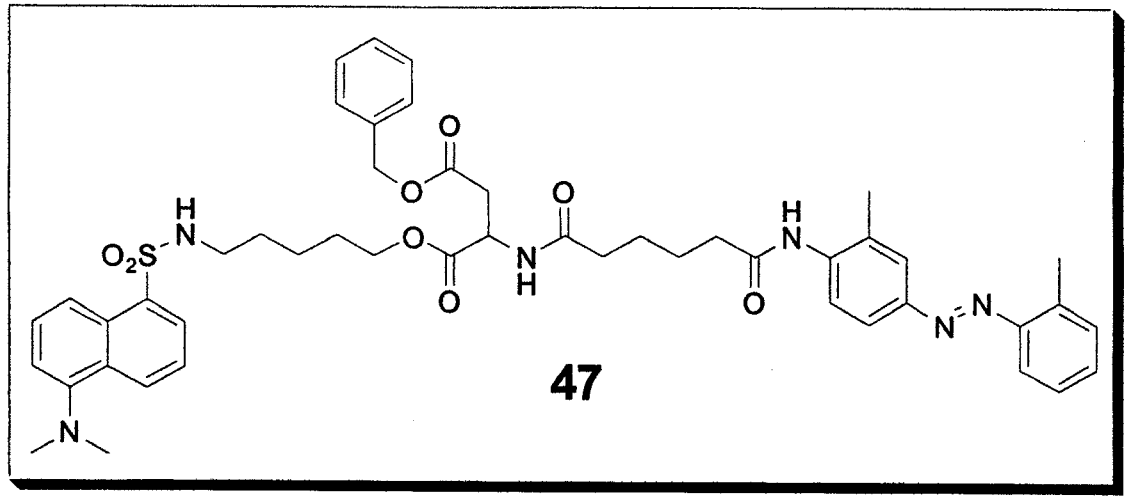

47

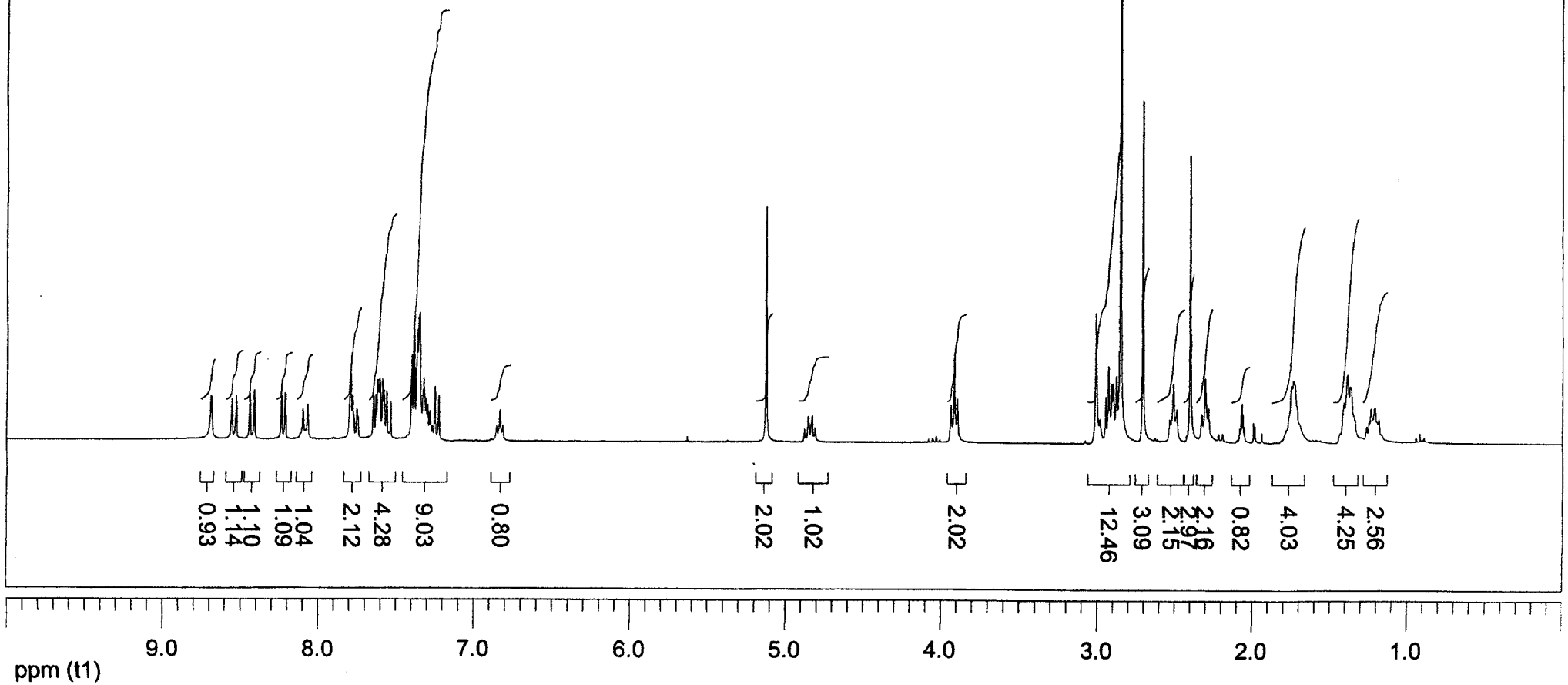
0.93
1.14
1.10
1.09
1.04
2.12
4.28
9.03
0.80
2.02
1.02
2.02
12.46
3.09
2.15
0.82
4.03
4.25
2.56
9.0
8.0
7.0
6.0
5.0
4.0
3.0
2.0
1.0
ppm (t1)

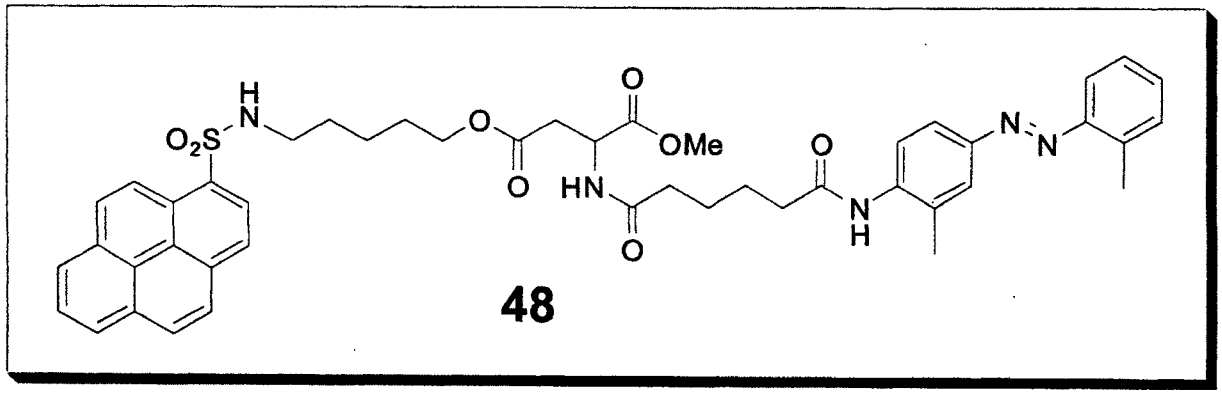
HN
O_2S
O
O
OMe
O
HN
O
O
N
H
N
N

48

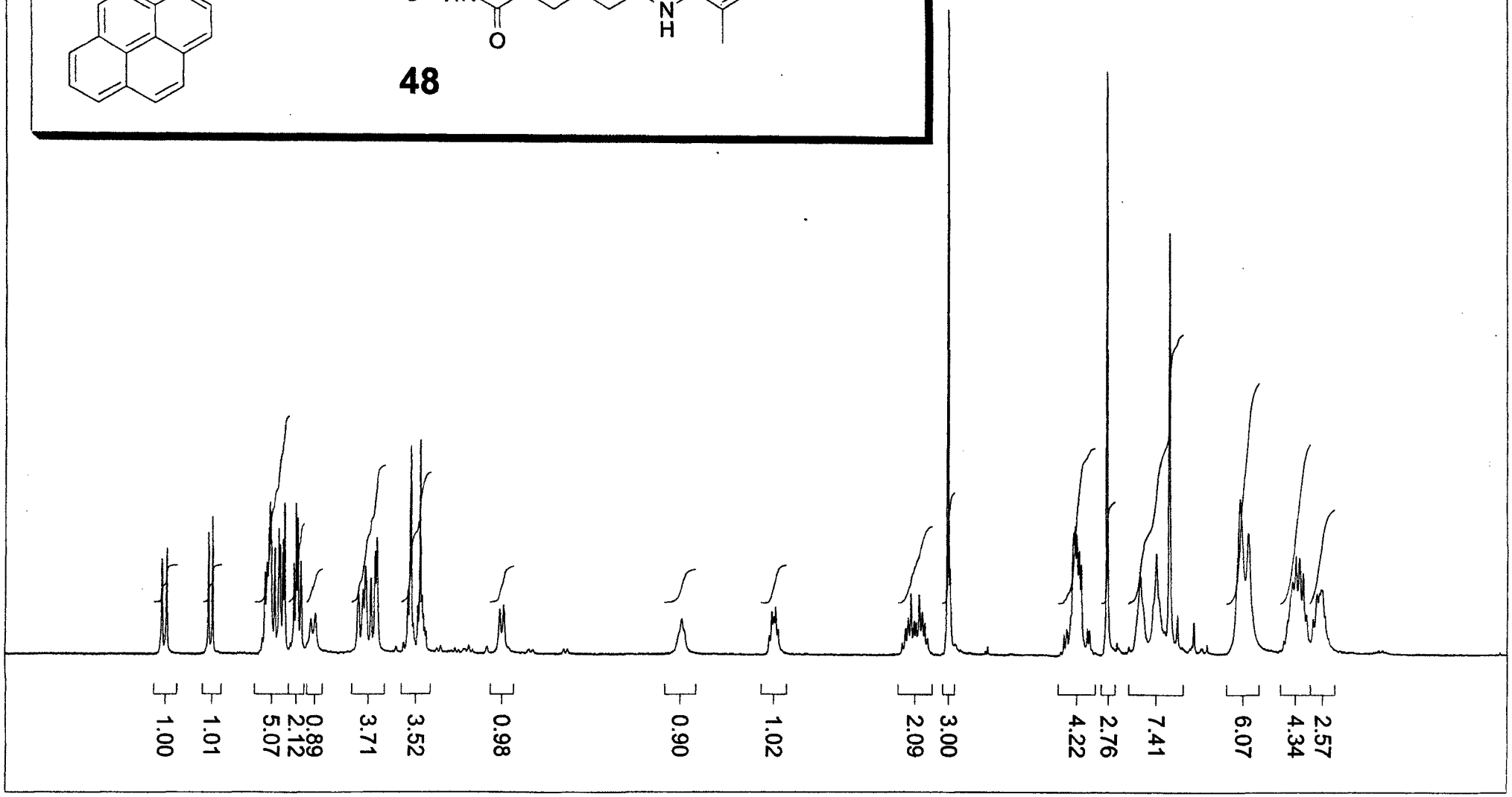
1.00
1.01
5.07
2.12
0.89
3.71
3.52
0.98
0.90
1.02
2.09
3.00
4.22
2.76
7.41
6.07
4.34
2.57
9.0
8.0
7.0
6.0
5.0
4.0
3.0
2.0
1.0
ppm (t1)

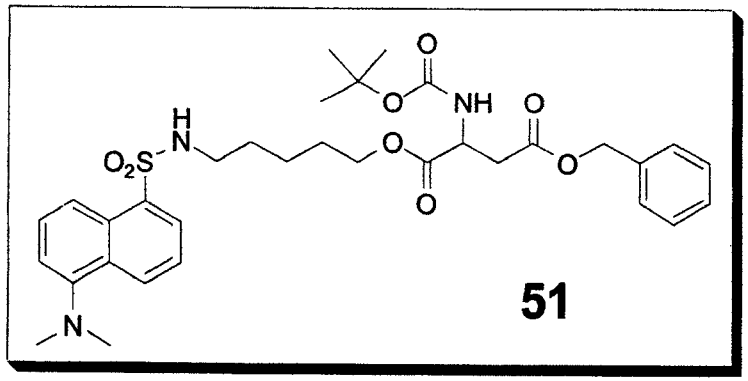

51

1.00 1.04 1.06 2.22 5.38 0.82 0.89 2.23 0.90 0.93 2.01 1.24 9.05 14.18 3.12

9.0 8.0 7.0 6.0 5.0 4.0 3.0 2.0 1.0

ppm (t1)

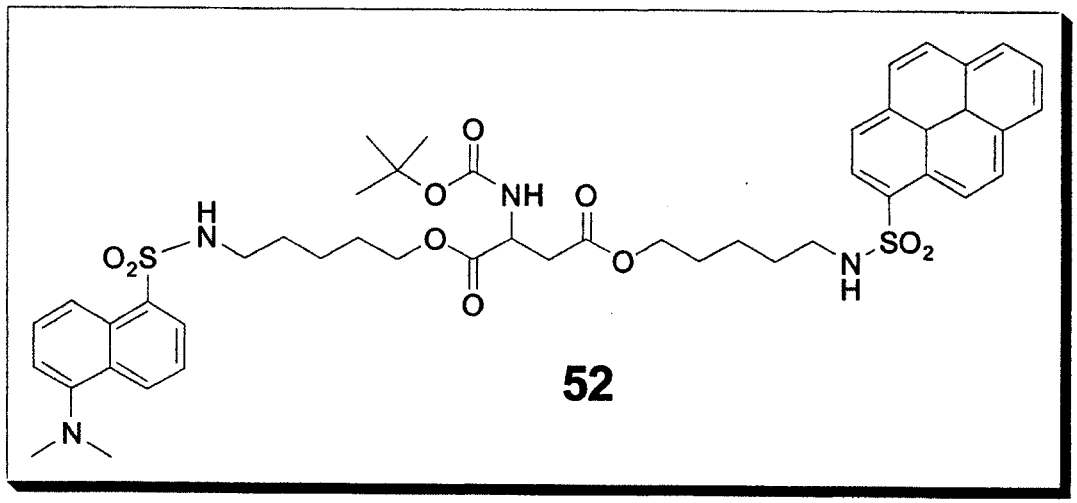

52

1.00
1.05
0.89
7.10
2.11
2.04
1.63
0.93
1.08
0.86
1.06
4.37
11.53
1.08
18.61
4.53
9.0
8.0
7.0
6.0
5.0
4.0
3.0
2.0
1.0
ppm (t1)

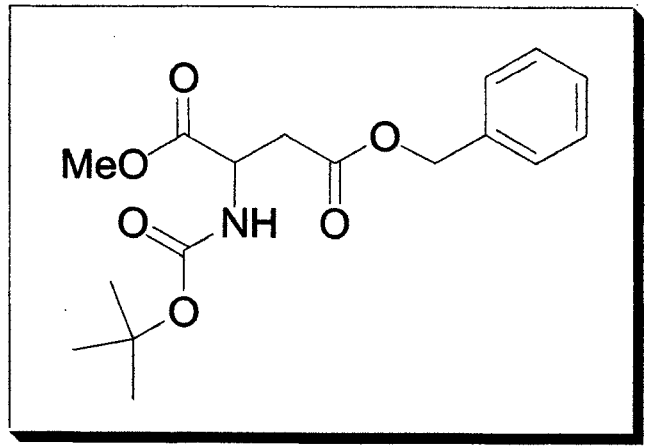

3.13 0.56 1.38 0.61 2.00 1.38 6.18

7.0 6.0 5.0 4.0 3.0 2.0 1.0

ppm (t1)

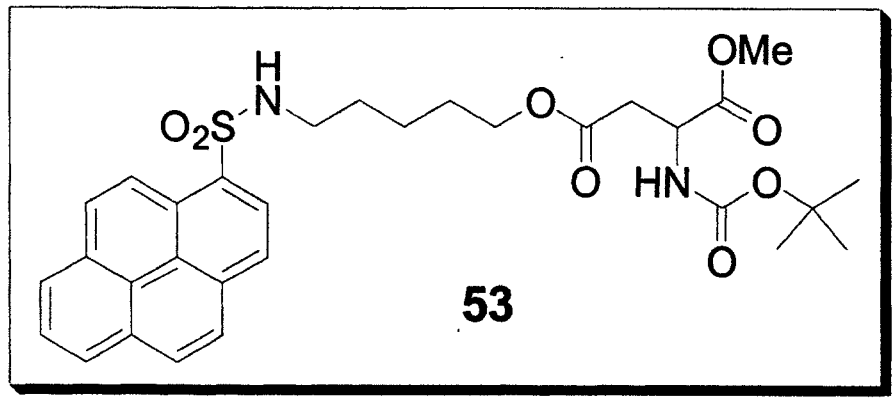

53

1.00 1.00 3.08 2.04 3.04 0.85 0.81 0.86 2.00 3.08 3.02 0.95 13.77 2.22

9.0 8.0 7.0 6.0 5.0 4.0 3.0 2.0 1.0

ppm (t1)

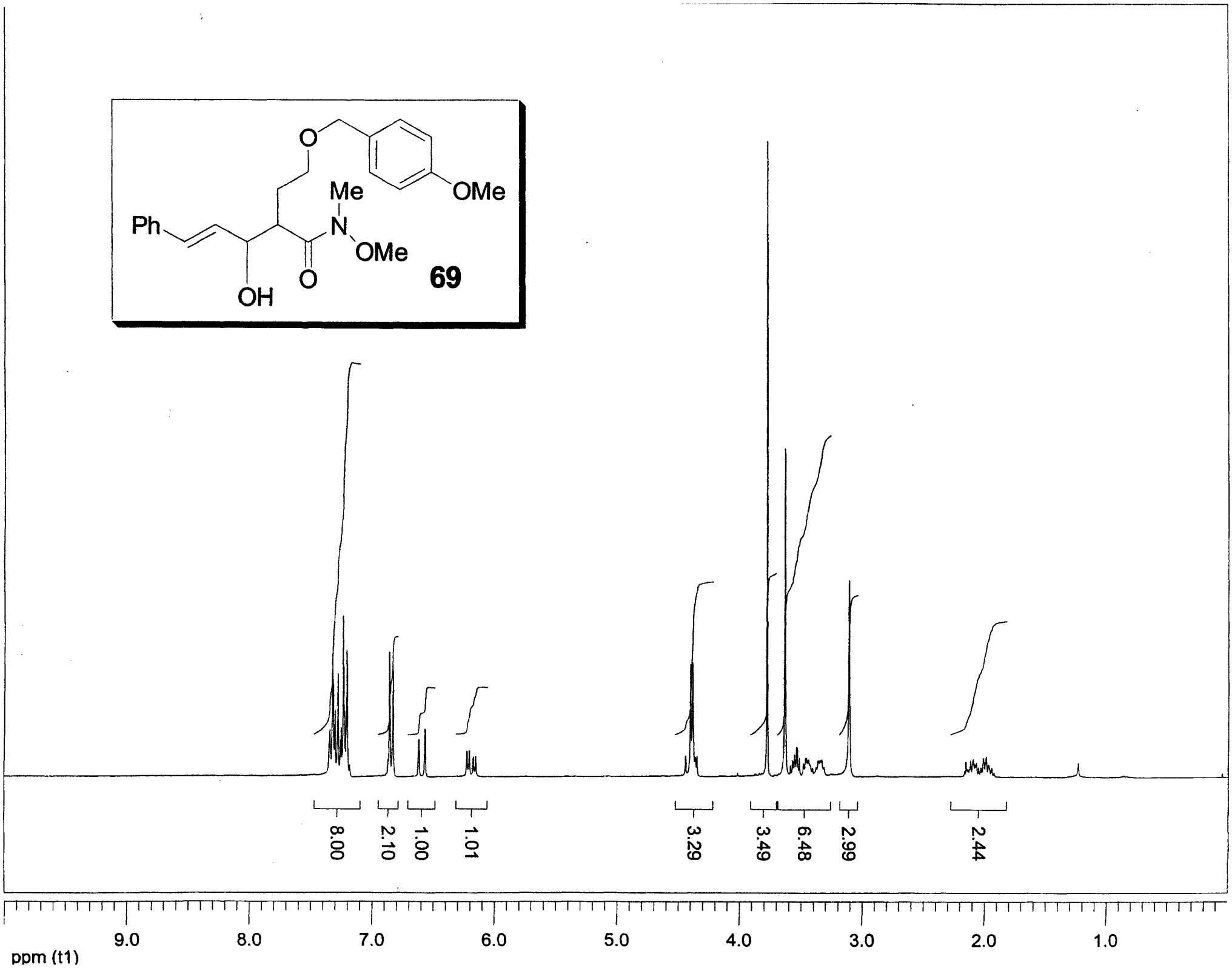
O
Me
OMe
Ph
N
OMe
O
OH
69
8.00
2.10
1.00
1.01
3.29
3.49
6.48
2.99
2.44
9.0
8.0
7.0
6.0
5.0
4.0
3.0
2.0
1.0
ppm (t1)

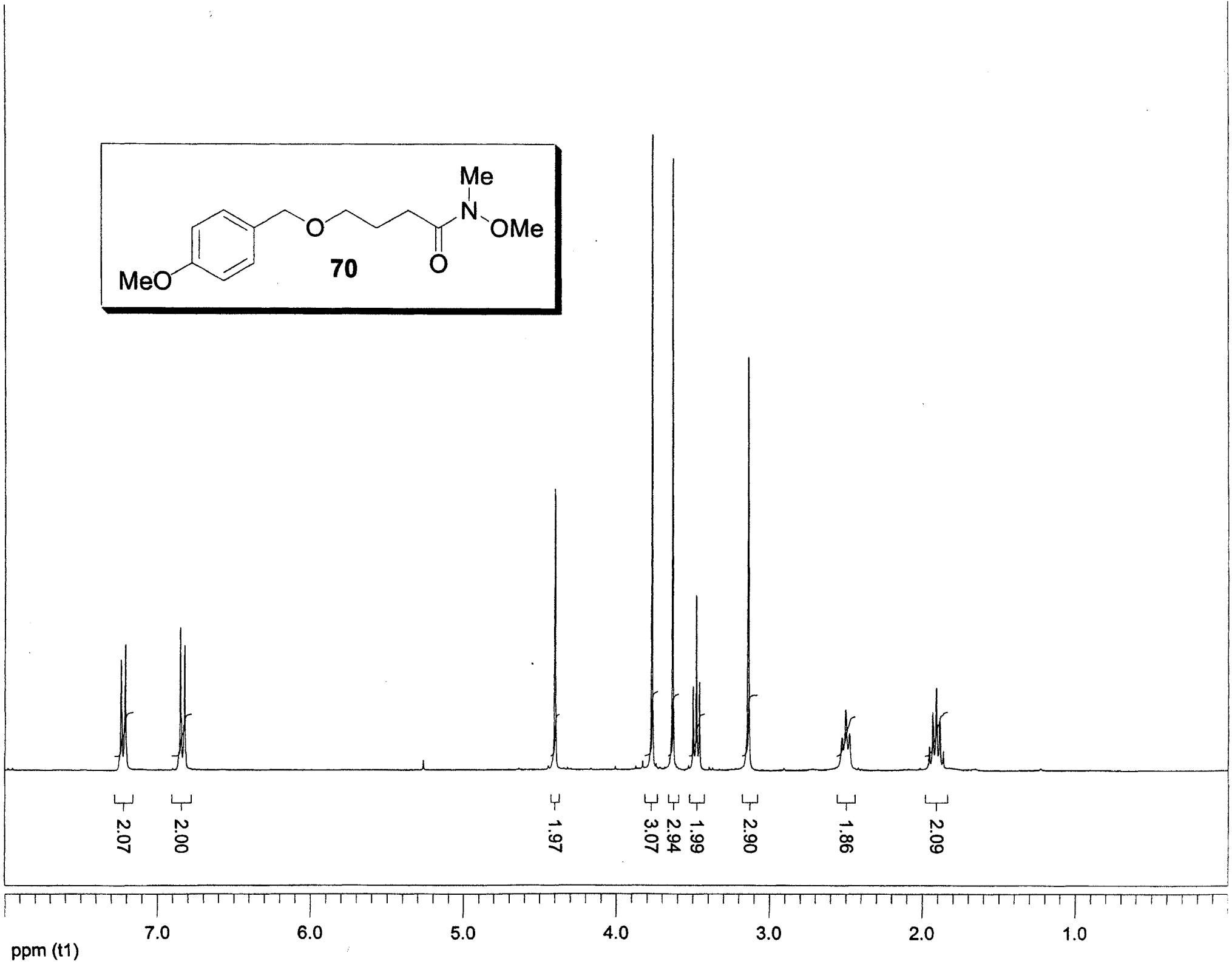
Me
N
OMe
O
O
MeO
70
2.07
2.00
1.97
3.07
2.94
1.99
2.90
1.86
2.09
7.0
6.0
5.0
4.0
3.0
2.0
1.0
ppm (t1)

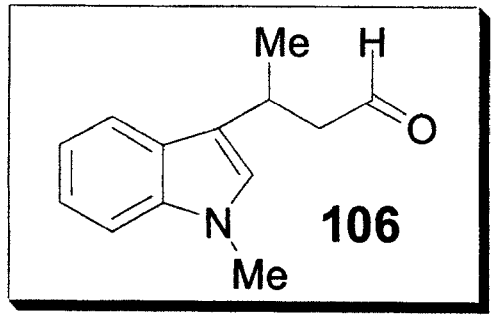

106

1.00 1.12 3.28 0.99 4.24 2.12 3.25

9.0 8.0 7.0 6.0 5.0 4.0 3.0 2.0 1.0

ppm (t1)

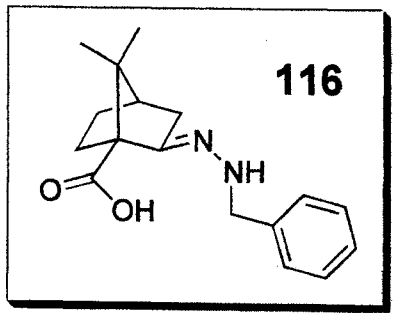
116
N
NH
O
OH

5.55
2.00
2.00
1.03
0.97
1.01
4.07
2.94
9.0
8.0
7.0
6.0
5.0
4.0
3.0
2.0
1.0
ppm (t1)

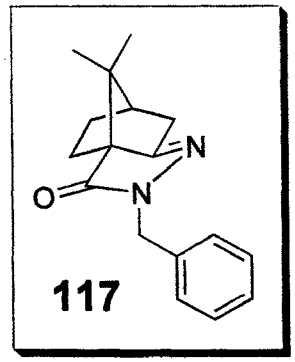
N
O
N

117

4.96
2.01
0.99
2.01
2.04
1.00
1.00
3.02
3.00
9.0
8.0
7.0
6.0
5.0
4.0
3.0
2.0
1.0
ppm (t1)

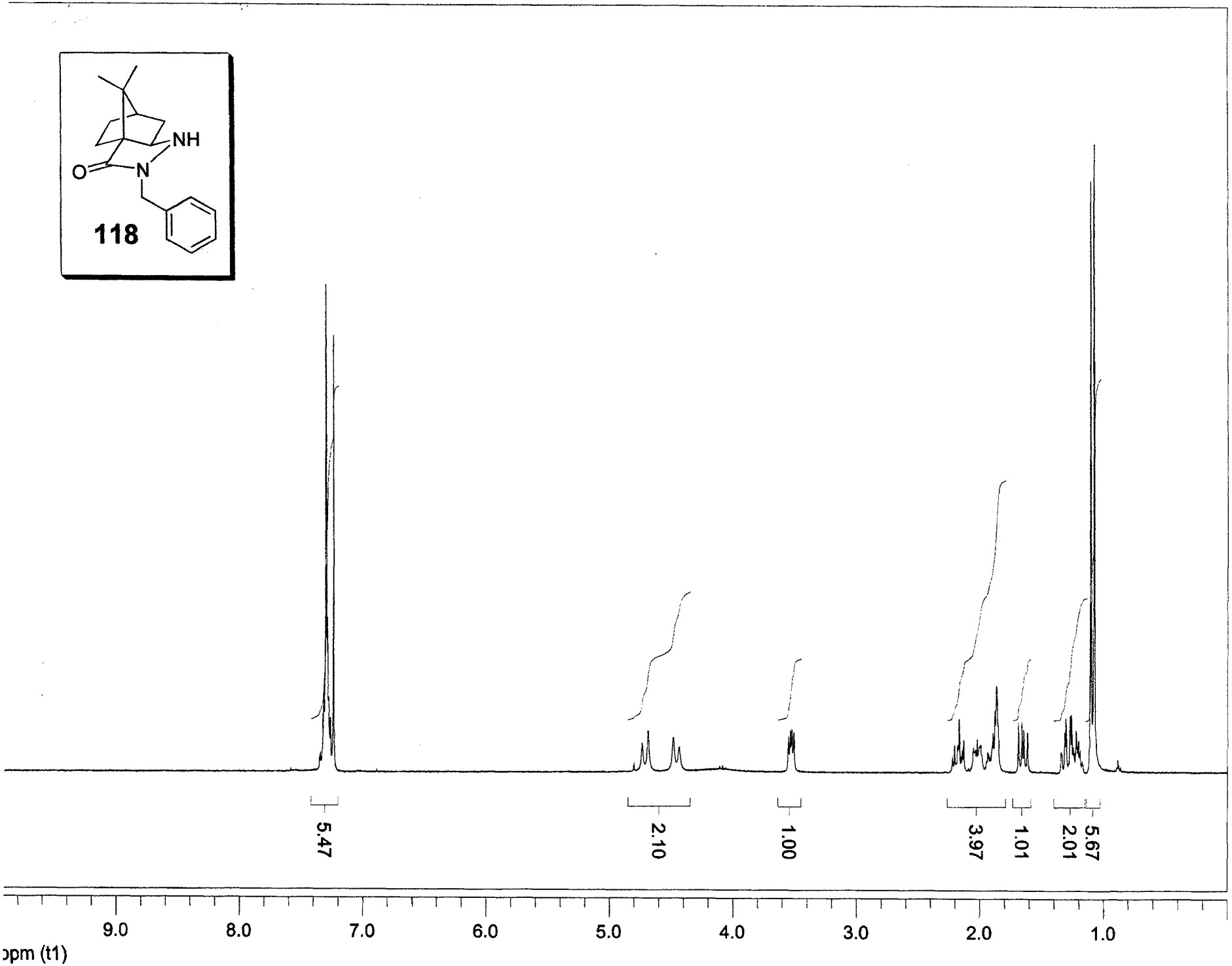
NH
O
N
118
5.47
2.10
1.00
3.97
1.01
2.01
5.67
9.0
8.0
7.0
6.0
5.0
4.0
3.0
2.0
1.0
ppm (t1)

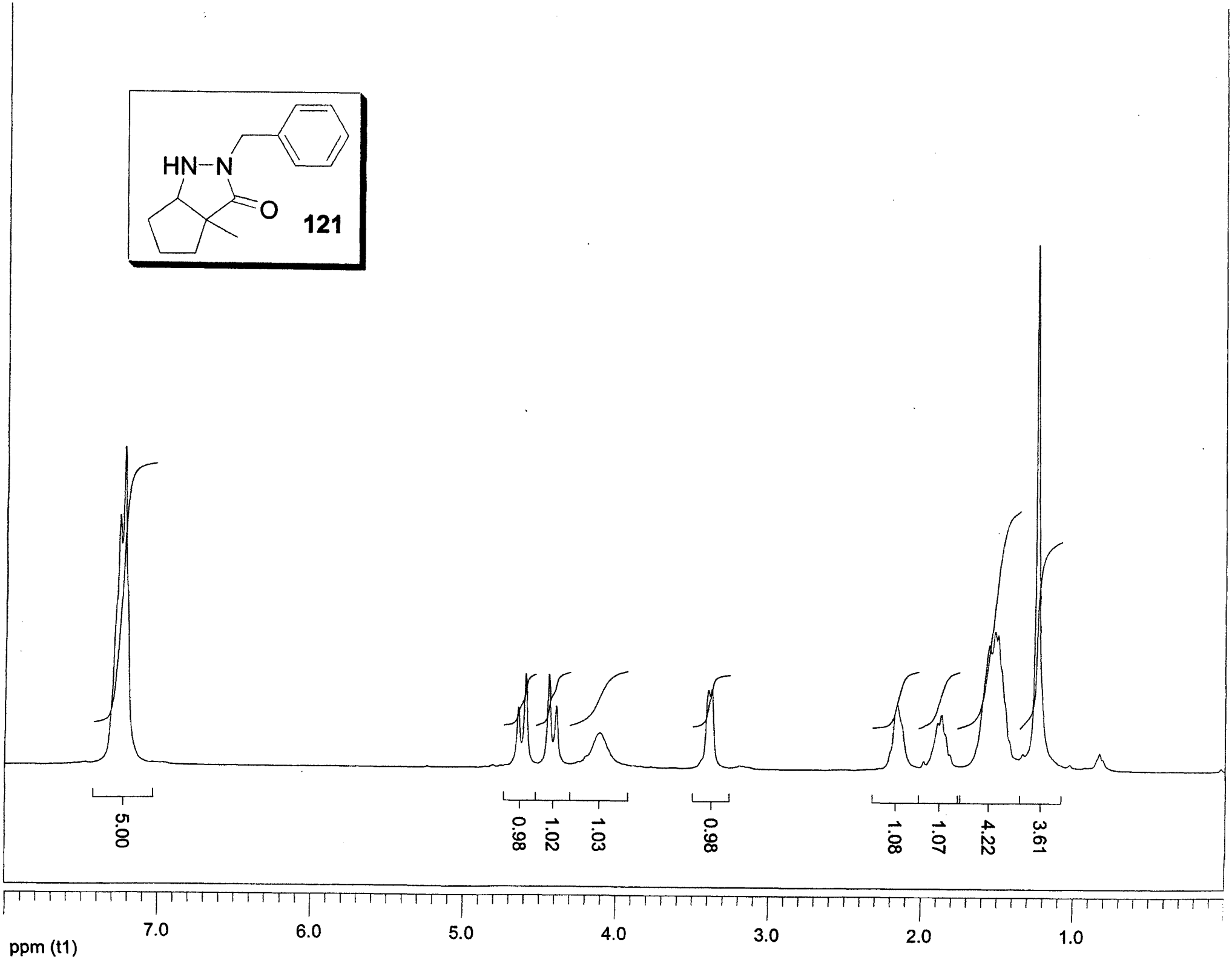
HN–N
O
121
5.00
0.98
1.02
1.03
0.98
1.08
1.07
4.22
3.61
7.0
6.0
5.0
4.0
3.0
2.0
1.0
ppm (t1)

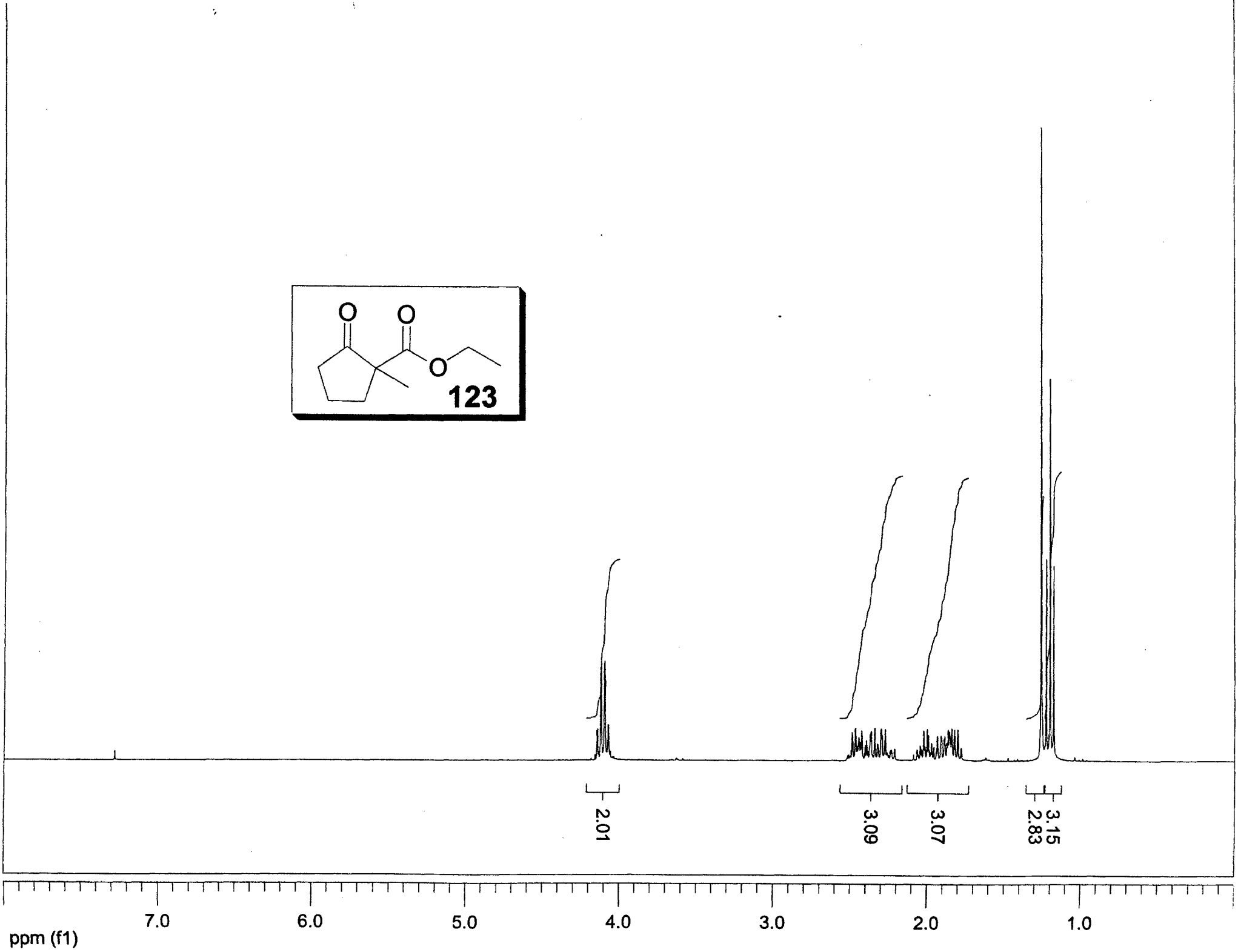
123
2.01
3.09
3.07
2.83
3.15
7.0
6.0
5.0
4.0
3.0
2.0
1.0
ppm (f1)

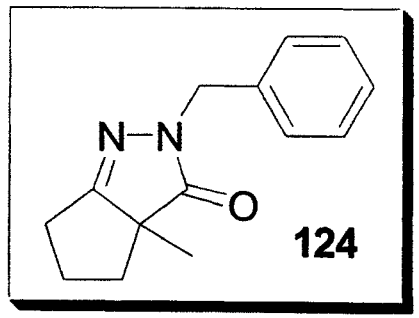
N–N
O
124

5.08
0.99
1.00
1.00
3.17
1.18
1.06
3.05
7.0
6.0
5.0
4.0
3.0
2.0
1.0
ppm (f1)

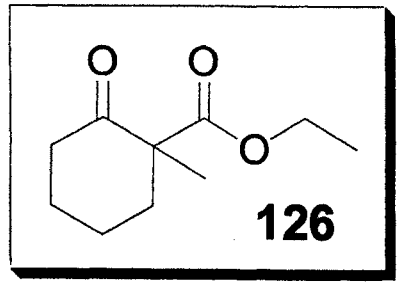
O
O
O
126

2.00
2.98
1.09
3.11
1.06
3.42
7.0
6.0
5.0
4.0
3.0
2.0
1.0
ppm (t1)

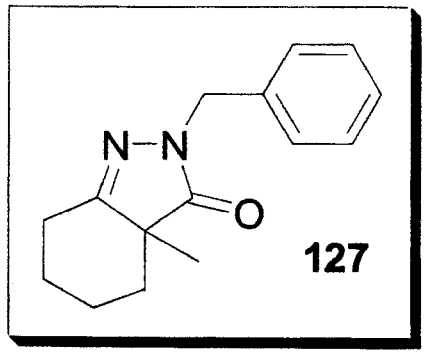
N–N
O
127

5.00
0.96
1.00
0.93
0.95
1.93
2.19
1.78
3.18
7.0
6.0
5.0
4.0
3.0
2.0
1.0
ppm (f1)

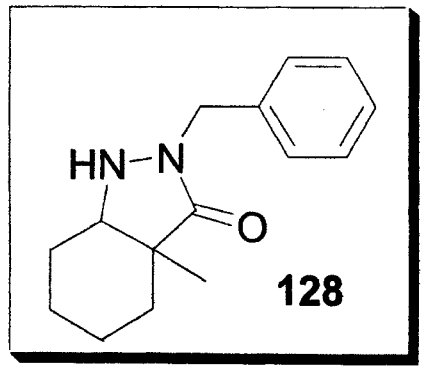

128

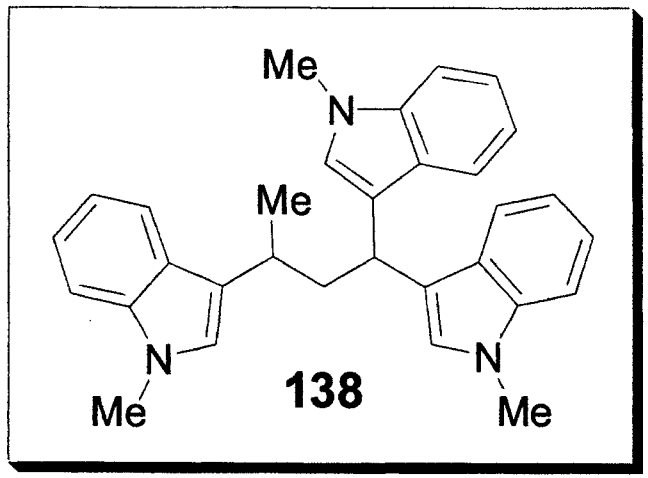

1.00 1.77 6.87 2.91 0.88 1.82 0.32 0.87 8.68 0.94 0.89 0.88 2.61

7.0 6.0 5.0 4.0 3.0 2.0 1.0

ppm (f1)